SYNTHETIC CONTROL OF LIGHT ABSORPTION IN CONJUGATED POLYMERS

By

PENGJIE SHI

A DISSERTATION PRESENTED TO THE GRADUATE SCHOOL
OF THE UNIVERSITY OF FLORIDA IN PARTIAL FULFILLMENT
OF THE REQUIREMENTS FOR THE DEGREE OF
DOCTOR OF PHILOSOPHY

UNIVERSITY OF FLORIDA

2011

To my parents

ACKNOWLEDGMENTS

I would like to take this opportunity to express my appreciation to those who helped me in one way or another on conducting my research and the writing of this dissertation.

I would like to first thank my advisor Dr. John R. Reynolds for his continuous and generous guidance throughout my six-year study. I have to admit that it was a highly challenging and difficult time for me to grow from an inexperienced student into a successful polymer chemist. On many occasions, when I was about to give up my synthesis and project, it was his wise insight and creative inspiration which saved my research. The work presented in this dissertation would not have been possible without his support and advice. Moreover, he dedicates himself to creating an excellent environment for our study, handles the research group as a warm family, and educates us well for our future. I am very grateful for the time he put in reviewing my research reports, publications, oral presentations, and dissertation, and also for his consideration for my well being.

I extend these thanks to the professors who have made great contributions to my study at the University of Florida, especially my supervisory committee for their support and invaluable discussions: Prof. Kenneth B. Wagener, Prof. Kirk S, Schanze, Prof. Michael J. Scott and Prof. W. David Wei in the Chemistry Department, and Prof. Jiangeng Xue in the Material Science and Engineering Department.

I gratefully acknowledge the help and advice from many members in the Reynolds' group: Dr. Emilie Galand, Dr. Christian B. Nielsen, Dr. Stefan Ellinger, Dr. Timothy Steckler, Dr. Genay Jones, Dr. Robert Brookins, Dr. Ryan Walzack, Dr. Aubrey Dyer, Dr. Svetlana Vasilyeva, Dr. Chad Amb, Dr. Dan Patel, Dr. Jianguo Mei, Dr. Pierre

Beaujuge, Dr. Mike Craig, Dr. Andy Spring, Dr. Fengjun Deng, Dr. Leandro Estrada, Dr. Eric Shen and Dr. David Liu. I can still remember the moment when Dr. Galand taught me how to perform column chromatography, and Dr. Nielsen showed me the titration of n-BuLi. Special thanks to Dr. Mei, who helped me not only scientifically but also in my everyday life throughout my unpleasant chemistry routine. I also owe thanks to those who are in the group and still working on their PhDs: Romain Stalder, Frank Arroyave, Unsal Koldemir, Egle Puodziukynaite, Coralie Richard, Justin Kerszulis, Caroline Grand, Natasha Teran and Jimmy Deininger. My life in Florida could not have been so happy and pleasant without their support and friendship.

I would also like to thank my collaborators who have contributed to the projects I have carried out during my study at the University of Florida. The work on broadly absorbing black-to-transmissive switching electrochromic polymers was conducted in collaboration with Dr. Jianguo Mei, Dr. Chad Amb, Dr. Aubrey Dyer, Dr. Svetlana Vasilyeva, Dr. David Liu, Eric Knott, and Emily Thompson. I wish to point out that the repeatability study in this work would not be so perfect without Dr. Dyer being so demanding of my synthetic capabilities. The project on fast switching water soluble electrochromic polymers was conducted in collaboration with Dr. Chad Amb, Dr. Aubrey Dyer, Dr. Mike Craig and Justin Kerszulis. This project would never have been completed without Dr. Chad's understanding and intuition. It was an enjoyable time to receive his phone calls from Michigan. I am looking forward to visiting his house and going fishing with him on his little boat. Chapter 5 on diketopyrrolopyrrole-based copolymers for organic solar cells was conducted in collaboration with Prof. Franky So, Dr. Jianguo Mei, Dr. Jegadesan Subbiah and Tzung-Han Lai. Here, Prof. Franky So

deserves a lot of credit for his wise advice and generous hospitality. Moreover, I still feel guilty to ask Tzung-Han to walk from the Material Science and Engineering Department to the Chemistry Department under the Florida sunshine in the summer time and discuss the project with me again and again. I really appreciate his patience and professionalism.

I also have to thank my undergraduate advisor Prof. Caiyuan Pan at the University of Science and Technology of China, who built my enthusiasm in polymer science and engineering, as well as those colleagues who helped and supported me during my stay in the lab: Dr. Yugang Li, Dr. Baoqing Zhang, Dr. Yezi You, Dr. Chunyan Hong, Dr. Xiang Yu and Dr. Bin Luan.

I give my special thanks to my friends Prof. Pierre Audebert, Dr. Xian Chen, Dr. Seoung Ho Lee, Dr. Kai Lang and his wife Yidan Jiang, Dr. Ruowen Wang, Dr. Yan Chen, and Dr. Huaizhi Kang. Without their support, I would have never made it through these six years.

Finally, I would like to say “thanks” to my parents Jinghuai Shi and Jinlan Wang, who are always supporting and encouraging me all the time. I know that they are willing to sacrifice everything for my growing up and being successful.

TABLE OF CONTENTS

page

LIST OF TABLES

LIST OF FIGURES

LIST OF ABBREVIATIONS

AFM	Atomic force microscopy
BTD	2,1,3-Benzothiadiazole
CV	Cyclic voltammetry
DOT	3,4-Dioxythiophene
DPV	Differential pulse voltammetry
DMF	Dimethylformamide
EC	Electrochromic
ECD	Electrochromic device
ECP	Electrochromic polymer
EtHx	2-Ethylhexyl
Fc/Fc^{+}	Ferrocene/Ferrocenium
FET	Field effect transistor
GPC	Gel permeation chromatography
HOMO	Highest occupied molecular orbital
ICBA	Indene-C_{60} bisadduct
ITO	Indium tin oxide
IR	Infrared Spectrum
J_{sc}	Short current density
LED	Light emitting diode
LUMO	Lowest occupied molecular orbital
M_n	Number average molecular weight
M_w	Weight average molecular weight
NMR	Nuclear magnetic resonance
OPVs	Organic photovoltaics

OFET	Organic field effect transistor
PCE	Power conversion efficiency
PCBM	[6,6]-Phenyl-C61-butyric acid methyl ester fullerene
PDI	Polydispersity index
ProDOT	Propylenedioxythiophene
PSC	Polymer solar cell
p-TSA	*p*-Toluenesulfonic acid
PV	Photovoltaic
SCE	Saturated calomel electrode
TGA	Thermogravimetric analysis
TLC	Thin layer chromatography
UV	Ultraviolet spectrum
Vis	Visible spectrum
V_{oc}	Open circuit voltage

Abstract of Dissertation Presented to the Graduate School
of the University of Florida in Partial Fulfillment of the
Requirements for the Degree of Doctor of Philosophy

SYNTHETIC CONTROL OF LIGHT ABSORPTION IN CONJUGATED POLYMERS

By

Pengjie Shi

December 2011

Chair: John R. Reynolds
Major: Chemistry

Conjugated polymers with alternating single and double carbon-carbon bonds along polymer backbones have become a unique branch in the family of polymeric materials. Researchers are especially interested in the optoelectronic properties of conjugated polymers, due to their capabilities in light weight and inexpensive organic electronic devices, such as photovoltaics, light emitting diodes, field-effect transistors and electrochromic devices. This dissertation focuses on the use of chemistry as a basis for optimization of these properties. In particular, the investigations involve development of new synthetic routes and methods to produce conjugated polymers with controlled absorption profiles, energy level distributions, band gaps and solubility, as well as evaluation of their use in electrochromic and photovoltaic applications.

In a first instance, a synthetic methodology is devised for the synthesis of black-to-transmissive switching electrochromic polymers. By introducing the random Stille polymerization method, which can be used to combine multiple monomers, adjust their relative ratios and control the monomer sequence distribution, a random black-to-transmissive electrochromic conjugated polymer (ECP) has been synthesized with a broad absorption across the entire visible region, and the reproducibility of the

polymerization was examined in detail. Black-to-transmissive ECPs were reproduced in batches with highly repeatable absorption spectra, number average molecular weights and polydispersity index. Moreover, successful characterization and device work enhance the probability that this polymer may be used for commercial electrochromic windows and displays.

In a second project, the synthesis of a blue-to-transmissive ECP and a black-to-transimissive ECP, which are functionalized with carboxylate ester groups, was accomplished. Basic hydrolysis of the carboxylate ester side chains affords the polymer salts with water solubility, allowing thin films to be formed by spray-casting from the polymer/water solutions. Upon subsequent neutralization of the thin-films, the resulting polymer acid films are ready to be redox switched in a KNO_3/water electrolyte solution and show a dramatic improvement in the switching speed compared with their ester derivatives at the sub-second switching time scale.

A third project extended the random polymerization to improve the light-harvesting efficiency of conjugated polymers by broadening their absorption spectra. Diketopyrrolopyrrole-based conjugated copolymers were synthesized with a broad absorption from 350 to 800 nm, except for a small absorption gap between 550 to 650 nm. Further exploring the external quantum efficiency, photoluminescence quenching effect with fullerene, photovoltaic prosperities and polymer:fullerene film morphology of these random copolymers has provided a fundamental understanding of how polymer light absorption, side chains, stacking ability, and energy levels influence the performance of solar cell materials with thiophene and benzodithiophene as donors and diketopyrrolopyrrole as an acceptor.

CHAPTER 1
INTRODUCTION

1.1 *π*-Conjugated Polymers

Conjugated organic polymers have received considerable interest due to the combination of physical properties of polymers or macromolecules (low density, processibility, solubility, mechanical properties, flexibility *etc.*) with the optoelectronic properties of semiconductors. These properties qualify conjugated organic polymers as a special category of unique and novel materials with numerous attractive applications, such as photovoltaic devices (OPVs),[1,2] organic field-effect transistors (OFETs),[3,4] organic light-emitting diodes (OLEDs),[5,6] electrochromic devices (ECDs)[7,8] and chemical sensors.[9,10] Besides their interesting applications, one of the most desirable aspects of *π*-conjugated organic polymers is the easy fine-tuning and optimization of their physical and optoelectronic properties via modification of their chemical structures, such as polymer backbones and pendant groups. Moreover, the potential of being manufactured into large area and flexible devices by low cost printing and patterning techniques (spray casting, inkjet printing and roll-to-roll printing) has dramatically stimulated the development of these organic semiconducting materials.[11-15]

To a chemist, especially a polymer synthesis chemist in this field, the necessary skills include not only his/her synthetic capabilities in looking for efficient, scalable and consistent methods to produce polymer batches with highly reproducible properties, but also the ability to understand the structure-property relationships of the materials, as well as the working principles of the optoelectronic devices. Therefore, this chapter will introduce the unique electronic structures of organic conducting polymers, followed by a detailed discussion of the energy level variation with changes in the chemical structures.

After that, band gap control, as an important aspect in this field, will be addressed. In this synthesis-oriented dissertation, several polymerization methods to achieve the final target materials will also be described. Finally, the processing and patterning of conjugated polymers, as well as the selected applications which lead the eventual goal of polymer synthesis, will be discussed.

1.1.1 Conjugated Polymers Electronic Structures

Attempts to understand the electronic behavior of conjugated polymers started with the synthesis of the simplest form of conjugated polymer-- polyacetylene (PA) -- in the late 1950s. However, not until two decades later was the key breakthrough in the synthesis of iodine-doped high conductivity PA (~ 10^3 S•cm^{-1}) disclosed by Hideki Shirakawa, Alan J. Heeger and Alan G. MacDiarmid.[16-19] Subsequent discussions of the theory of soliton excitations and doping effects in polyacetylene initiated the development of modern applications in organic conjugated materials, and the field of conducting polymers was born.[20-22]

Here, the analysis of the electronic structure of π-conjugated systems starts with polyacetylene. Considering a linear PA with an infinite chain length at the Hückel molecular orbital (HMO) level, there is a slight split of the energy levels as the number of repeat units increases, the overall spread in energy distribution for each orbital set becomes larger. As more and more repeat units are joined together, the overlapping of the π-orbitals spans a much wider range of energy level, and the energy gap (band gap, E_g) between the highest occupied molecular orbital (often referred to as the HOMO level) and the lowest unoccupied molecular orbital (referred to as the LUMO level) becomes smaller and smaller. For an infinite conjugation chain length, each of the

orbital sets contains an infinite number of nearly continuous energy levels, and thus is called a band.

At the theory level, the band structures of PA consist of a valence band (VB) filled with electrons and an empty conduction band (CB). With all equal bond lengths in the HMO model, the two bands are degenerate at the zone edge and produce a zero band gap. However, in contrast, the structure of PA shows a long and a short bond alternation (1.45 and 1.35 Å, respectively) with a band gap about 1.5 eV. The geometrical distortion and the opening of a band gap are due to the electron-electron repulsions, which cause a Jahn-Teller distortion, also recognized as a Peierls distortion in condensed matter physics. Considering the distortion effect, the two degenerate ground states of PA, which are caused by the delocalization of π-electrons along the polymer backbone, will not interconvert, and strictly speaking they are not resonance structures (Figure 1-1a). In fact, the more symmetrical intermediate form with a zero band gap does not exist in the real world.[23] Figure 1-1b shows a simplified model with the buildup of energy bands in a conjugated polymer as described above. It is worth mentioning that this simple approach can be applied to many other conjugated polymer systems. More detailed and accurate theoretical calculations of energy levels for polyacetylene, polycyclopentadiene, polypyrrole, polyfuran and polythiophene have been reported by Salzner *et al*.[24]

One of the well accepted guidelines to distinguish metals, semiconductors and insulators is the size of the band gap. More specifically, when the E_g is about 0 eV, the material is considered to be a metal. Due to the disappearance of the energy barrier between VB and CB, there is a high probability of finding electrons in the conduction

band of this type material. On the other hand, when the E_g rises to the range between 0 and 3 eV, the material is identified as a semiconductor. In this case, the electrons are tightly bonded in the valence band, and very few of them can be found in the conduction band. A direct influence over this phenomenon is the conductivity of semiconductors, which falls in the range of 10^{-8} to 10^{2} S•cm^{-1} compared to > 10^{3} S•cm^{-1} for metals. Based on the E_g and conductivity values, π-conjugated polymers are classified as semiconductors. Eventually, a further increase of the band gap to higher than 3 eV, affords insulators, which have no electrons in the CB.

a)

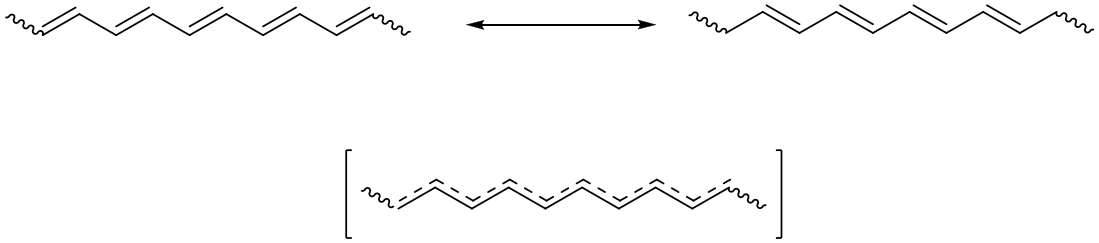

b)

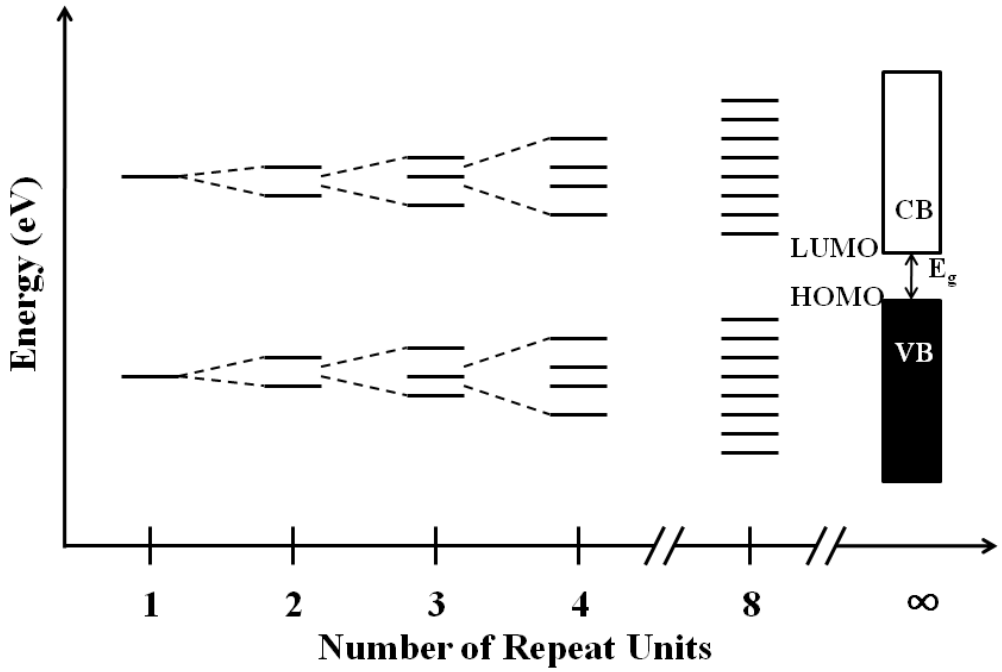

Figure 1-1. Band structures of polyacetylene. a) The degenerate PA. b) Simplified band structures illustrating the buildup of energy bands in a conjugated polymer.

1.1.2 Energy Level Distribution

Band gap is the most widely used terminology in this field, and it has a great influence on the optoelectronic properties of the conjugated polymers including the conductivity and the spectral absorption and emission. The energy level distributions, on the other hand, have a large influence on the redox properties and the stability of the polymers, and thus the final applications. Here, the change of polymer properties based on the change of polymer energy levels will be discussed using several common homopolymers, for example, polythiophene (PTh), polypyrrole (PPy), poly(3,4-ethylenedioxythiophene) (PEDOT), poly(3,4-propylenedioxythiophene) (PProDOT), and poly(3-hexylthiophene) (P3HT).

As shown in Figure 1-2, polythiophene shows a HOMO level at -5.3 eV. The relative high HOMO level means that PTh can be easily oxidized (p-doping) chemically and electrochemically. However, considering the air stability threshold at -5.2 eV, PTh actually shows an excellent environmental stability (stable toward oxygen and moisture in the air) in both its neutral and doped states, and the polymer is an extensively studied material for applications such as transistors, conductors, sensors and solar cells.[25-27] By replacing the sulfur atom with a nitrogen atom in the aromatic ring, polypyrrole shows much higher HOMO and LUMO energy levels at -4.6 eV and -2.2 eV, respectively. Clearly, the high energy levels cause the polymer to have a low resistance to oxidation and a high resistance to reduction. In other words, PPy is a good material for p-type doping; however, it cannot be n-type doped. With a band gap of about 2.4 eV, PPy films are yellow/green color in their neutral form and are sensitive to air and oxygen. [28-30]

Moreover, the HOMO level of PEDOT is observed at -4.6 eV, which is 0.7 eV higher than that of PTh. The raised energy level can be attributed to the electron

density- donating effect of the oxygen atoms in the 3- and 4- positions of the thiophene ring. With the ethylenedioxy bridge, EDOT monomer has become one of the most electron-rich aromatic rings in the thiophene family, and it is widely used as a repeat unit in conjugated polymers. In fact, EDOT can be easily electropolymerized, whereas thiophene is more difficult to polymerize by this route. Compared with PTh, PEDOT can be oxidized easily, but is more difficult to n-dope than PTh.[31-33] More interestingly, with a band gap of 1.6 eV, polymer PEDOT shows a saturated blue color in its neutral state and becomes highly transparent in the fully oxidized state.

Similar to PEDOT, the family of poly(3,4-propylenedioxythiophene) derivatives, PProDOT, has been shown to exhibit varied properties relative to PEDOT due to a slight change in the substituent bridge. PProDOT shares a similar oxidation potential (HOMO level) to that of the PEDOT, but a larger band gap (1.9 eV) compared with PEDOT at 1.6 eV. In its neutral state, the polymer thin film shows a purple color, and can be converted into a highly transmissive state upon full oxidation.[34] It is worth mentioning that the alkyl chain on the propylenedioxy bridge has afforded the polymer with considerable processability in organic solvents such as toluene, THF and chloroform. In this dissertation, several donor monomers based on the ProDOT unit have been synthesized and utilized in the synthesis of electrochromic polymers, as will be described in Chapter 3 and 4.

Another interesting case in this discussion is regioregular poly(3-hexylthiophene), which was first reported by Rieke, and then by the McCullough group.[35-39] The HOMO energy level of P3HT (-5.4 eV) is 0.1 eV lower than that of PTh, and the band gap is around 2.1 eV.[40] The lowered HOMO energy level has increased the stability of the

polymer thin films, while also opening a larger potential window between the HOMO level of P3HT and the LUMO level of PCBM (a potential increase of the open circuit voltage) in the bulk heterojunction (BHJ) solar cell. Actually, P3HT has become the most investigated conjugated polymer in the field of BHJ solar cells.

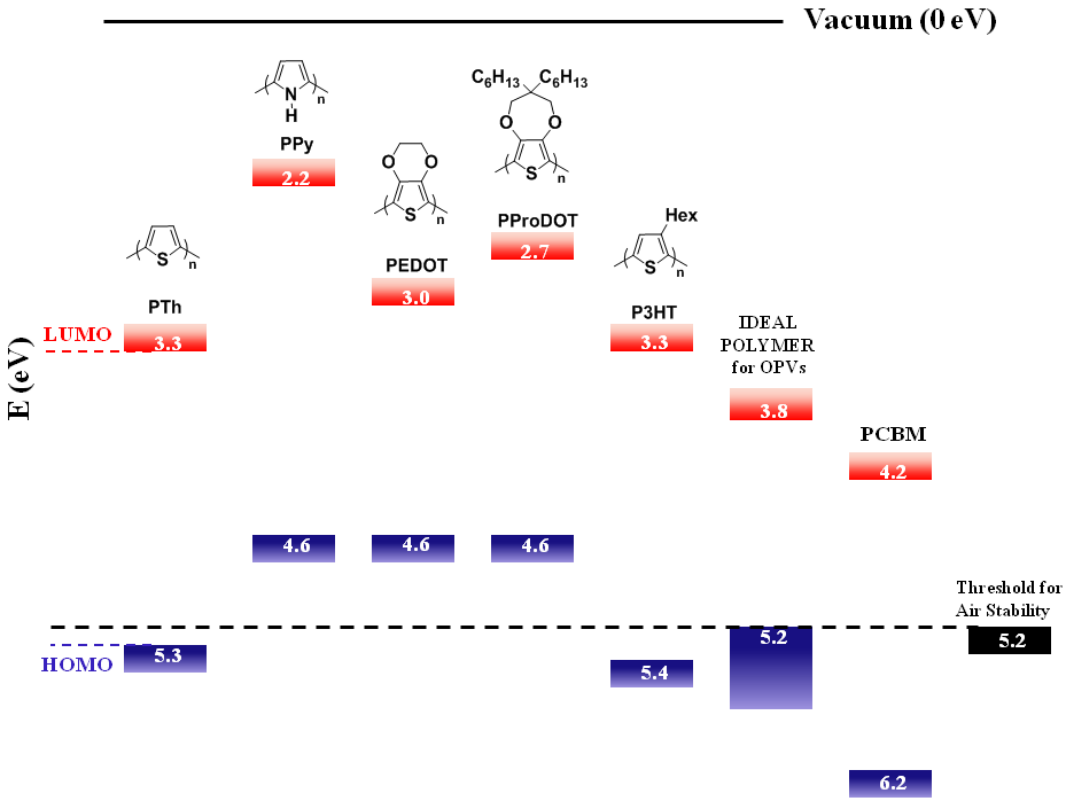

Figure 1-2. Energy levels of PTh, PPy, PEDOT, PProDOT, P3HT and an 'ideal donor polymer' for organic photovoltaics (designed to be integrated in BHJ solar cells employing PCBM as an acceptor). Black dashed lines indicate the thresholds for air stability (5.2 eV).[57] In all cases orbital energies are given based on the assumption that the energy of SCE is 4.7 eV *vs*. vacuum[41] and Fc/Fc^+ is +0.38 V *vs*. SCE (i.e. 5.1 eV relative to vacuum). Reported energy levels can be different depending on the method of determination.

Based on the discussion above, it is obvious that the HOMO energy level needs to be relatively high in order to achieve a good p-type doping character in conjugated polymers. In the application of electrochromic devices, it is important that this type of material be oxidized easily by electrochemical methods and achieve a stable full

oxidized state in the potential windows of the electrolyte solutions. On the other hand, the ideal donor polymers for BHJ solar cells should have HOMO levels as low as possible for a larger V_{oc}, and thus a higher power conversion efficiency (more detailed discussion will be presented in Section 1.6.2).

1.1.3 Solubility of Conjugated Polymers

Due to the nature of their intrinsic chemical structure, conjugated polymers were considered to be insoluble 'hard rocks' for a long time. This is especially true in the earlier stages of the field in the early 1980s, since none of these conducting polymers (for example, PA, PPy, polyfuran, PTh, polyaniline and PEDOT) is soluble in common organic solvents. Moreover, from the polymerization to the purification, characterization and processing of the polymers, the solubility of conjugated polymers is the only issue that orients the entire preparation procedure. Thus, improving their solubility and the processability in organic or even aqueous solutions has become an important factor in the synthesis of conjugated polymers.

The first effort was the synthesis of poly(3-alkylthiophene). When prepared by chemical or electrochemical methods, polythiophene cannot be dissolved or processed in solutions. Although iodine doped PTh has shown a high conducting property (0.1 $S \bullet cm^{-1}$), the lack of processability and environmental stability has dramatically limited the further usage of this material.[42-44] To solve that problem, Kaeriyama reported the synthesis of soluble conducting PThs by electrochemical polymerization of thiophenes having a long alkyl group (hexyl, octyl, dodecyl and octadecyl).[45] As expected, the electrochemically polymerized poly(3-alkylthiophene) can be prepared in organic solutions, which were then used to determine their molecular weight and to cast films. In the meantime, Elsenbaumer reported the synthesis and characterization of a series of

irregular P3ATs which can form highly conducting, environmentally-stable complexes with electron acceptor dopants.[46,47] Their synthesis approach was achieved by nickel catalysed Grignard coupling of the 2,5-diiodo-3-alkylthiophene using THF and 2-methyltetrahydrofuran as the reaction solvents. One of the important finding of that study was that homopolymers of 3-alkylthiophenes incorporating alkyl groups equal to or greater than butyl in size are readily soluble at room temperature in common organic solvents such as THF, toluene, xylene and methylene chloride.

From the chemistry stand point, fine tuning of the solubility of conjugated polymers can be easily achieved by introducing solubilizing side chains onto the polymer backbone. Generally, there are two types of functional groups to be utilized- alkyl groups (linear or branched), which improve the polymer solubility in organic solvents; and ionic groups (sulfonate, carboxylate, phosphonate and ammonium), which make the polymers water soluble. One special case is poly(3,4-ethylenedioxythiophene):poly(styrenesulfonate) (PEDOT:PSS), which is a mixture of positively charged PEDOT and negatively charged PSS. These polymer salts can be dispersed in water and processed into thin films. In terms of the chemical control of the molecule structure, the selection of the side groups is mostly guided by the processability and applications of the polymers.

1.2 Band Gap Engineering

Band gap control has always been an essential synthetic consideration in the field of conducting polymers. In the early stages, conducting polymers and their doped forms were considered as potential alternatives for metals. Preparation of conjugated polymers with low or zero band gaps and thus high intrinsic conductivity was the primary goal.[48-50] After that, the discovery of the fact that conjugated polymers can be

applied in a series of electronic and photonic devices such as OPVs, OLEDs and FETs as semiconductors, has dramatically changed the situation. Band gap engineering has focused on a precise control in the size of the energy gap and has always been involved in the control of optical properties, energy level distribution, and charge transport properties.[51]

1.2.1 Methods of Band Gap Control in Conjugated Polymers

In the previous discussion, polyacetylene was demonstrated to have a band gap of 1.5 eV due to the bond length alternation (BLA), which results from Peierls distortion (Section 1.1.1). As a matter of fact, this effect has been the major contribution to the opening of an energy gap between VB and CB for all the conjugated polymers. Without doubt, band gap control can be achieved by tuning the bond length alternations on the molecule level *via* chemical modifications.

Moreover, conjugated polymers based on aromatic systems show a non-degenerate ground state. In Figure 1-3a, the aromatic and quinoid forms of PTh are not energetically equivalent. In this case, the aromatic form is more energetically favored than the quinoid form, and π-electrons are more localized in the aromatic rings. As a result, the single bond character of the C-C bond between two aromatic rings is actually increased, leading to a large bond-length alternation. This resonance effect is recognized as E_{Res} in the band gap contribution (Figure 1-3b). Introduction of a fused ring system is a direct way to reduce the aromatic stabilization energy. For example, when polyisothionaphthene adopts its quinoid form (Figure 1-3a), the loss of aromaticity on the thiophene ring is retrieved by the formation of benzene ring. This transition of aromaticity dramatically decreases the energy barrier between the aromatic form and

the quinoid form, and reduces the band gap of the polymer (1.0 eV compared with 2 eV of PTh).[52]

a)

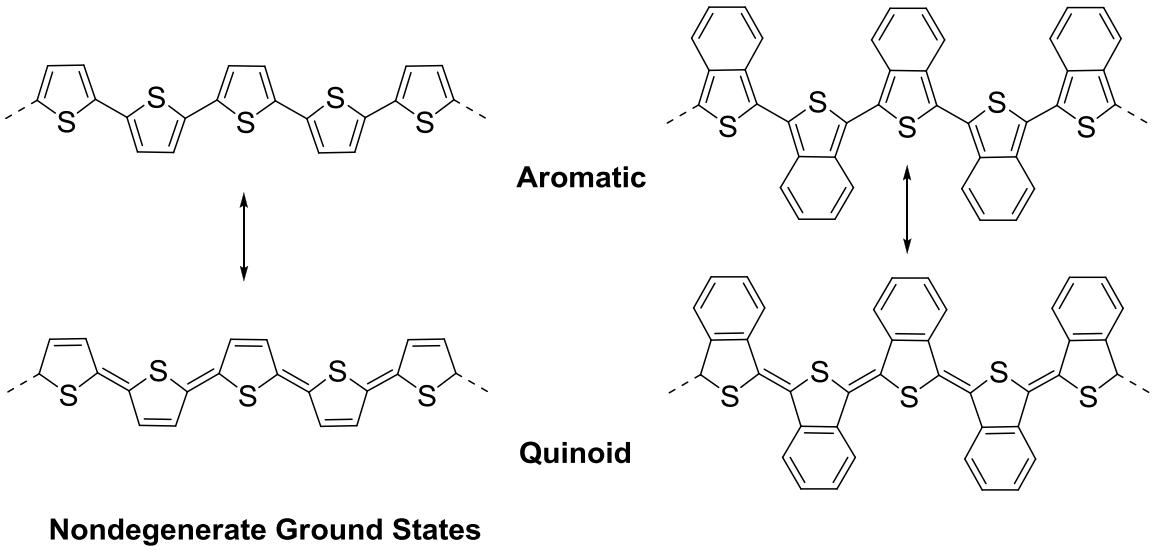

b)

$$E_g = E_{BLA} + E_{Res} + E_{Sub} + E_{\theta} + E_{Int}$$

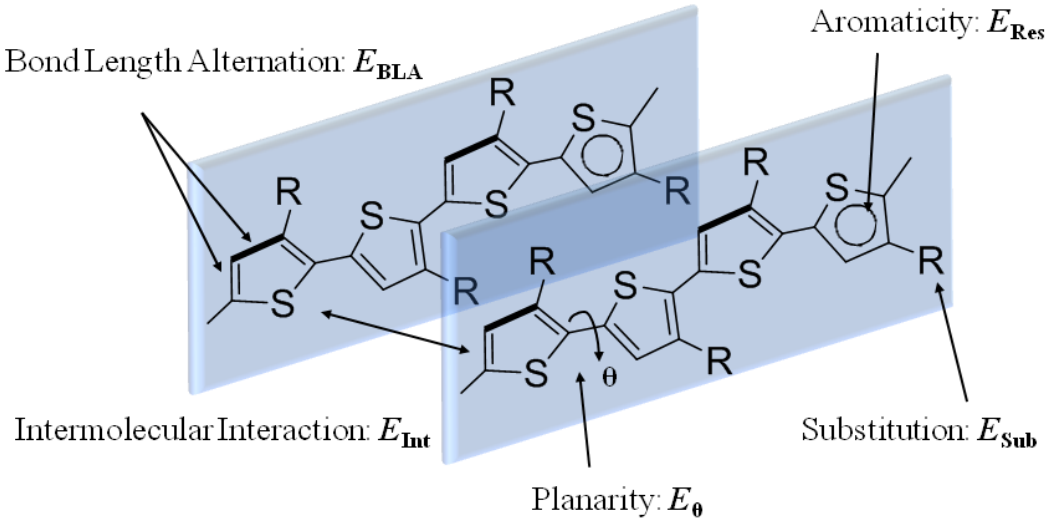

Figure 1-3. Structural factors in the origin of band gap. a) Aromatic and quinoid structure of polythiophene and polyisothionaphthene. b) Schematic illustration of structural factors in the band gap control of conjugated polymers using regioregular poly(3-alkylthiophene) (P3AT) as an example. (Adapted and modified with permission from Ref. 51)

Another aspect in band gap tuning comes from the substituents on the polymer backbone (E_{Sub}). Although most of the side chains are intentionally introduced to increase the solubility of the conjugated polymers, they still have the ability to influence the electron density of the conjugated systems, especially for substituents with non-neglectable electron-donating and electron-withdrawing effects. Furthermore, the torsion angle (θ) between two adjacent aromatic rings is also an important parameter in evaluating the conjugation length and thus the band gap. The delocalization of the electrons requires a continual overlapping of the π orbitals. A planar molecular geometry favors the delocalization of π electrons and thus decreases the band gap. The last contribution comes from the intermolecular interactions (E_{Int}). Clearly, strong π-π interactions between two adjacent polymer chains will help the electron distribution and reduce the band gap.

In fact, all the factors in the band gap control will interact with each other, resulting in a complicated overall contribution to the band gap and the energy levels of the conjugated polymers. Changing one of the parameters may cause a series of changes to the rest. For example, increasing the size of the substituents (R group in Figure 1-3b) can potentially cause more steric hindrance between the adjacent rings as well as between adjacent polymer chains. The overall effect will include an increase in the rotational disorder and a decrease in the intermolecular interaction.

1.2.2 The Donor-Acceptor Approach in Band Gap Control

As a powerful synthetic tool in controlling the band gaps of conjugated polymers, the “donor-acceptor” (DA) approach was first introduced by Havinga *et al*.,[53-55] and utilized to achieve narrow and low band gap polymers. The donor represents an electron-rich unit and the acceptor shows a strong electron affinity. The interaction

between the donors and the acceptors in the polymer backbone will potentially increase the delocalization of the electrons, reducing the bond length alternation and thus the band gap. Figure 1-4 shows the hybridization process of the HOMOs and LUMOs of a D-A system. The formed complex has broader valence and conduction bands and a small HOMO-LUMO separation in between. This concept has served as a basis for structure modification of many conjugated systems. By carefully selecting the structures of the donors and acceptors and their respective electron donating and withdrawing strengths, conjugated polymers with controlled energy levels and band gaps have been synthesized and applied in applications such as OPVs,[56-59] OFETs,[60,61] and OLEDs.[62] Another area is electrochromics, which will be discussed in detail later in this dissertation.

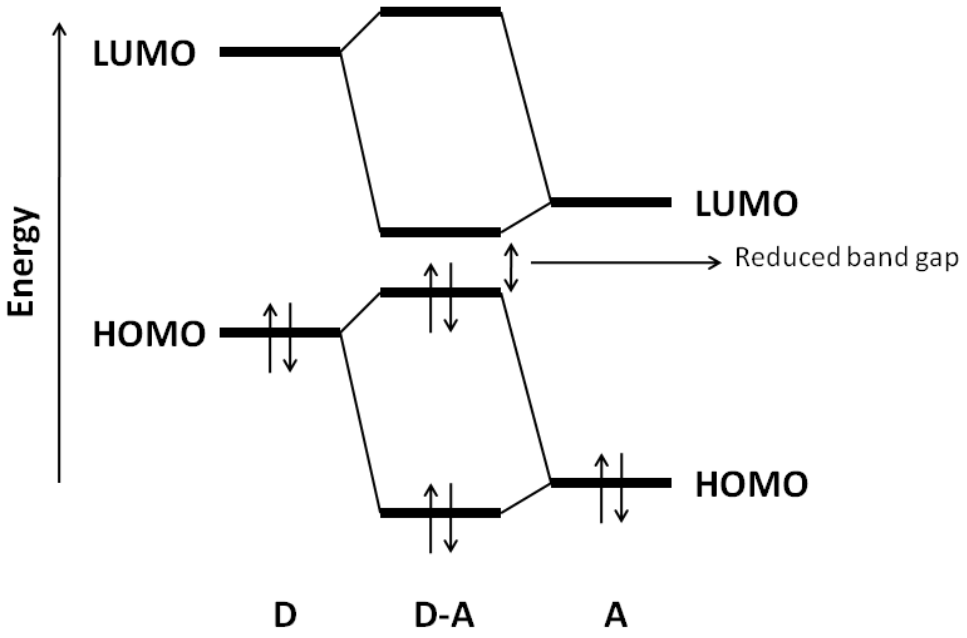

Figure 1-4. Illustration of the donor-acceptor concept. Hybridization of the HOMOs and the LUMOs of the donor-acceptor fragment yields a compressed band gap. (Adapted with permission from Ref. 55)

1.3 Polymer Synthesis

During the past three and a half decades, considerable knowledge (theoretical and experimental) has been gained in the field of organic conjugated polymers. This section will place the role of synthesis in perspective, with a general introduction to oxidative polymerization, metal mediated polymerization and Knoevenagel condensation, with a particular focus on random polymerization.

1.3.1 Oxidative Polymerizations

Oxidative polymerization was one of the earliest polymerization methods for producing π-conjugated polymers. The polymerization usually proceeds by either chemical or electrochemical oxidation. Both methods aim to produce the radical cation intermediate by oxidizing the monomers and the polymer fragments. The radical cation then couples with another radical cation to form a dication, or with a neutral species to form a new radical cation, which can be oxidized into a dication. The rearomatization into a neutral form involves the the loss of two protons. Eventually, polymers are formed after repeated oxidation-coupling cycles. Compared with other polymerization methods, oxidative polymerizations are rather inexpensive, convenient, and able to produce high quality conjugated polymers under certain conditions.

In an electrochemical oxidative polymerization, the polymer films are grown directly on the anode. The quality of the polymerization and thus the polymer films depends on the applied potential, the monomer structure, the electrode material, current density, temperature, solvent and many other factors.[63] One major drawback of this polymerization is that the formed polymers can be irreversibly over-oxidized and can decompose on the electrode during the electrochemical switches, since the polymers usually have lower oxidation potentials than the monomers. In some cases, they also

produce undesirable crosslinks and prevent control of the regioregularity of the unsymmetrical monomers.

Unlike electrochemical polymerization, chemical oxidative polymerization is usually accomplished with a chemical oxidant (such as $FeCl_3$ or $SbCl_5$) in organic solutions.[64-66] It is worth mentioning that the polymerization produces the oxidized polymers, and an extra reduction process with hydrazine or ammonium hydroxide is necessary in order to obtain the neutral polymers. On the other hand, the propagation of the polymerization can be limited by the solubility of the oxidized polymers, which are less soluble than the neutral polymers and tend to precipitate out of the solution.[67] There are also other disadvantages for this polymerization. For example, the metal ions can be easily trapped in the polymer network;[68] and the polymerization process is difficult to repeat, leading to low reproducibility of the final products.

Oxidative polymerization, ether electrochemical or chemical, requires monomers with low oxidation potentials, and this dramatically limits application in more complicated conjugated systems. More efficient, reproducible and controllable polymerizations are indeed needed.

1.3.2 Transition Metal Mediated Polymerizations

The development of organometallic chemistry, especially in the area of transition metal mediated cross-coupling reactions, has stimulated the growth of conjugated polymer research for 20 years. With the ability to form carbon-carbon single bonds directly from 'activated' sp^2 carbons, many cross-coupling reactions provide an opportunity to build polymer backbones with an extended single-double bond alternation, which is the key structure of conjugated polymers. Most of these reactions are coupling reactions of aromatic halides with aromatic organotin, organozinc,

organoboron, organomagnesium and organolithium derivatives, namely Stille, Negishi, Suzuki-Miyaura, Kumada–Corriu coupling, respectively.[69] However, they are not just limited to aromatic systems. Interestingly, these reactions share a similar catalytic cycle, which contains a transition metal catalyzed oxidative addition, a transmetallation with an organometallic nucleophile, and a reductive elimination of the transition metal. Other useful reactions may include the Heck and the Sonogashira reactions, which are specifically used to build double bond and triple bond linkages.

The Stille coupling reaction[70,71] is perhaps the most effective cross-coupling reaction in the synthesis of conjugated polymers due to its mild reaction conditions and high resistance to the surrounding chemical environment.[72,73] This coupling reaction involves two types of starting materials: organic tin compounds and aryl halides (Figure 1-5). In the case of a polymerization, the starting materials are usually difunctionalized aromatic rings. Since Stille polymerization is the dominant polymerization method used in this dissertation, the discussion here will be more complete and detailed.

Figure 1-5 shows a catalytic cycle of a typical Stille coupling reaction. Except for the similar three-step mechanism (oxidative addition, transmetalllation and reductive elimination), an important consideration is the change to Pd(0) from Pd(II) catalysts, which consumes two equivalent organostannane monomers, and changes the stoichiometry of the reactive functional groups. Given the fact that the high molecular weight polymers are restricted by the precise stoichiometric control of the functional groups (or the monomers) in a step growth polycondensation, this imbalance of the monomers needs to be corrected at the beginning of the reaction or by using Pd(0) catalysts.

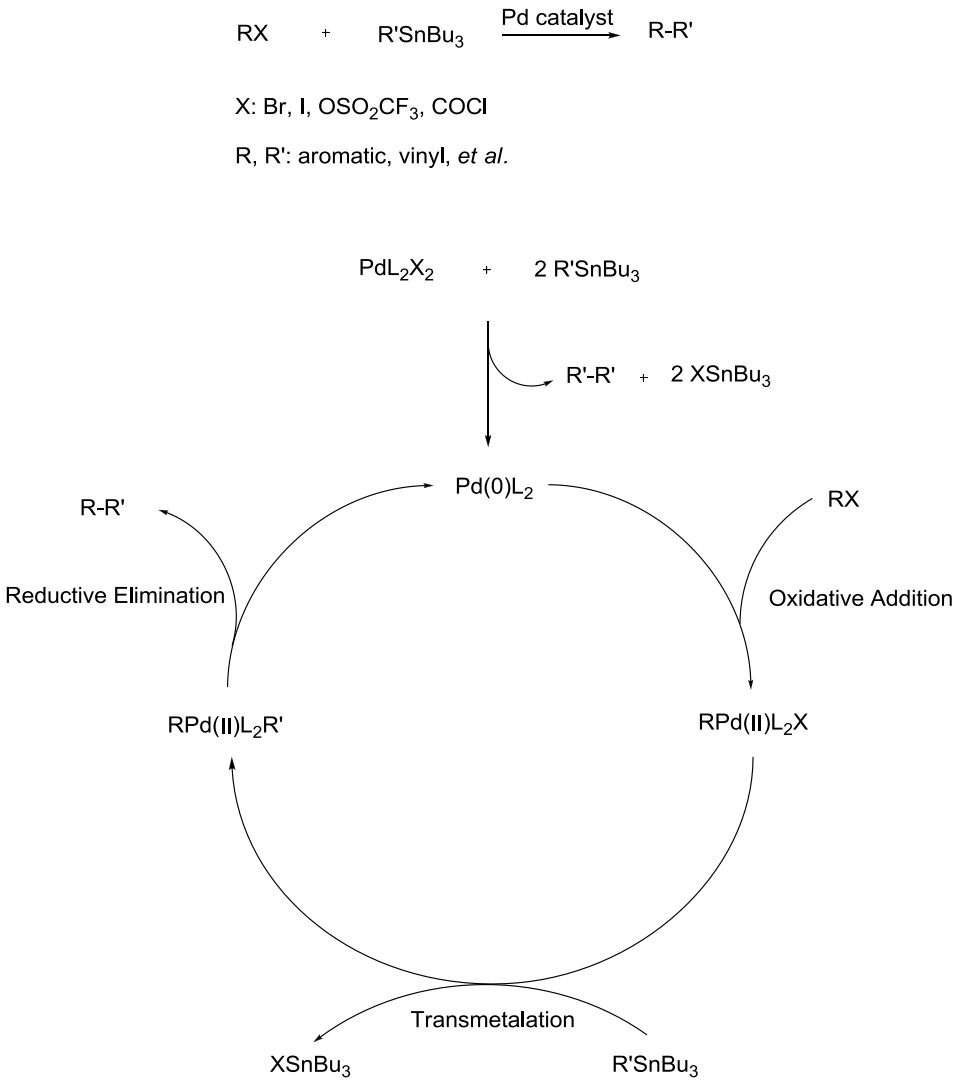

Figure 1-5. General reaction scheme and mechanism of the Stille Reaction.

Generally, the monomers in a Stille polymerization are electron-deficient halides (bromide or iodide) and electron-rich organotin compounds. It is believed that an aromatic system with better electron affinity favors the oxidative addition of the Pd(0) catalyst; and a system, which is strongly electron donating, activates the C-Sn bond in the transmetalation step.[71] Between the two types of halide monomers, it is also well known that diiodo monomers always show a higher reactivity than dibromo monomers.[72] Moreover, the organotin compounds are usually made by lithiation of the aromatic rings,

followed by addition of trimethyltin chloride or tributyltin chloride (Figure 1-6). For some cases, the lithiation reagents (*e.g.* n-BuLi) may react with the original functional groups on the aromatic rings, changing the reaction to another pathway.[74] To solve this problem, a new method of introducing the trialkyltin groups onto the aromatic system based on a Stille reaction of hexamethylditin and aromatic bromide is established in this dissertation (Chapter 4). One other problem in the synthesis of ditin monomers is the purification. While some of the ditin monomers can be purified by vacuum distillation and recrystallization, most of them are high boiling oils. Purification with triethylamine treated silica gel can reduce the decomposition of the tin compounds only to a relatively low point, but cannot totally eliminate it. This lack of purification options can become a major issue in applying Stille polymerizations, especially in large scale production, and thus needs more investigation in the future.

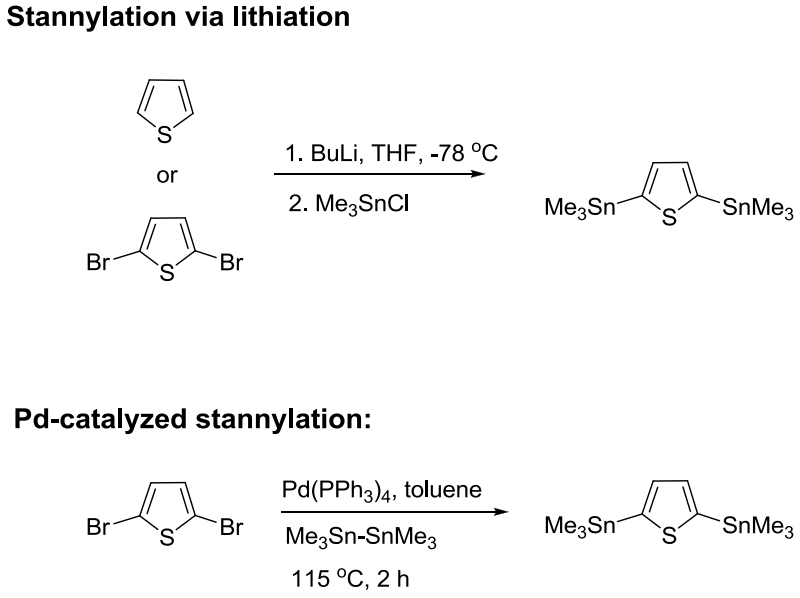

Figure 1-6. Examples of the synthesis of aromatic tin compounds.

Except for the reactivity of the monomers, the choice of catalysts and ligands also plays an important role in the Stille polymerization. Here, $PdCl_2(PPh_3)_2$, $Pd(PPh_3)_4$, and

$Pd_2(dba)_3$ are commonly used catalysts in the polymerization.[75,76] Clearly, the first two catalysts are not stable in air; and the use of these two catalysts does not require extra ligands. Compared with the first two Pd catalysts, $Pd_2(dba)_3$ shows much better stability in air, however, it becomes very unstable when mixed with the ligands. The amount of Pd used in the reaction is usually 2 mol % equivalent relative to the tin monomer. For a typical reaction using $Pd_2(dba)_3$ as a catalyst, 4 equivalent of the ligand (for each Pd) should be used. These ligands can be triphenylphosphine (PPh_3), tri(o-tolyl)phosphine ($P(o\text{-tolyl})_3$), triphenylarsine ($AsPh_3$) and tri(2-furyl)phosphine (TFP). Interestingly, the 'weak' ligands such as $AsPh_3$ and TFP have shown a large rate acceleration in the Stille reactions.[72,77] The reactivity of the ligand can be roughly evaluated as $AsPh_3$ > TFP > $P(o\text{-tolyl})_3$> PPh_3. Despite the reactivity, TFP associated $Pd_2(dba)_3$ catalyst is surprisingly stable, and faster rates are obtained with 2 equivalent of the ligand for each Pd.

In some cases, additives are used together with the catalysts and the ligands to improve the reaction time and the molecular weight. For example, when 1 equivalent of CuO was added to the Stille polymerization of distannyl-alkyldithienopyrroles and 4,7-bis(5-bromo-4-alkylthiophen-2-yl)benzothiadiazole, the molecular weight of the polymers was observed to increase 4-5 times.[78] Reported reactions based on CuO additive can also be found in other works.[79,80] CuI is also an optional choice for the additive.[81-83] When the salt is added, it reacts with organostannanes to form organocopper intermediates, which yield a much faster transmetalation with the Pd(II) species.[84] The effect of these additives is believed to highly depend on the solvent. In highly polar solvents like DMF and N-methyl-2-pyrrolidone (NMP), which can dissolve

the salts very well, the effect can be dramatic. However, these highly polar solvents can also make the polymers precipitate out before they reach a high molecular weight. Clearly, the solvent or solvent mixture needs to be carefully selected to achieve a satisfactory polymerization result.

The ideal solvent for a Stille polymerization should be a good solvent for the monomers, the catalysts/ligands, the additives and the final polymers. It is even better if they can stabilize the catalysts and fulfill the reaction temperature requirements. The most commonly used solvents in this type of polymerization are toluene, xylene, chlorobenzene, THF, DMF, NMP, dioxane, and chloroform. A high boiling point solvent, such as toluene, xylene, and chlorobenzene, can be easily applied to high temperature Stille polymerizations and used to dissolve a large variety of conjugated polymers. THF and dioxane have shown some interesting results in stabilizing the Pd catalysts. DMF and NMP are needed to dissolve the Cu salt additives. They can also act as coordinating ligands to the Pd center to accelerate the polymerizations.[85] Mixed solvent systems, such as toluene/DMF and THF/DMF, have also been investigated and have shown some promising results.[86-88]

Eventually, it is important to remind scientists that the organotin compounds have been demonstrated to be highly toxic, and will cause serious health and environmental problems.[89] Tin compounds need to be handled with extreme caution and tin waste need to be kept separate for disposal.

The Suzuki polymerization, which uses boronic acid or esters as the organometallic species to react with the aryl halides, uses much less toxic materials than Stille polymerization. Generally, Suzuki coupling requires a base to activate the

boron-containing reagents for transmetalation.[90] The choice of the base and the solvent mixture has immediately increased the complexity of the polymerization; in other words, optimization of the reaction conditions is usually more time consuming than Stille coupling.

Compared with organotin compounds, organoboron reagents for Suzuki coupling can be synthesized by versatile chemical reactions.[91-93] However, these monomers usually present low stabilities in the presence of acid and base (Figure 1-7). This problem becomes even worse during polymerizations, because the constant decomposition of boronic monomers changes the stoichiometric balance of the monomers and lowers the molecular weights of the polymers.[94] More detailed discussion of Suzuki polymerizations can be found in Robert Brookins' dissertation.[95]

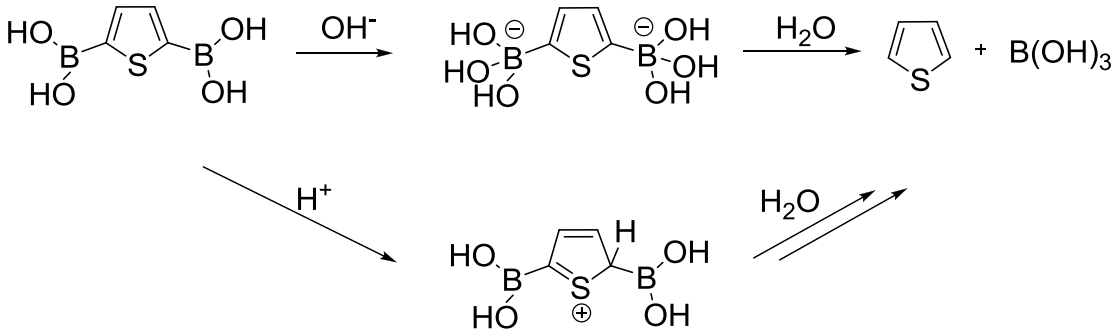

Figure 1-7. Deboronation of boron monomers. (Adopted and modified with permission from Ref. 95)

1.3.3 Other Polymerization Methods in the Synthesis of Conjugated Polymers

Except for the synthesis of conjugated polymers *via* the formation of C-C single bonds from sp^2 carbons, there are other useful methods, such as Wittig and Knoevenagel coupling, which are able to build carbon-carbon double bonds (vinylene linkage) by a polycondensation. Figure 1-8 shows an example of Wittig polycondensation in the synthesis of poly(*p*-phenylene vinylene) (PPV) based

conjugated polymers. The reaction can be processed in mild conditions. Although several different conditions have been reported in order to favor one of the geometries (*cis* or *trans*), there is still no absolute control of the double bond configuration.[96-98]

Wittig Polycondensation:

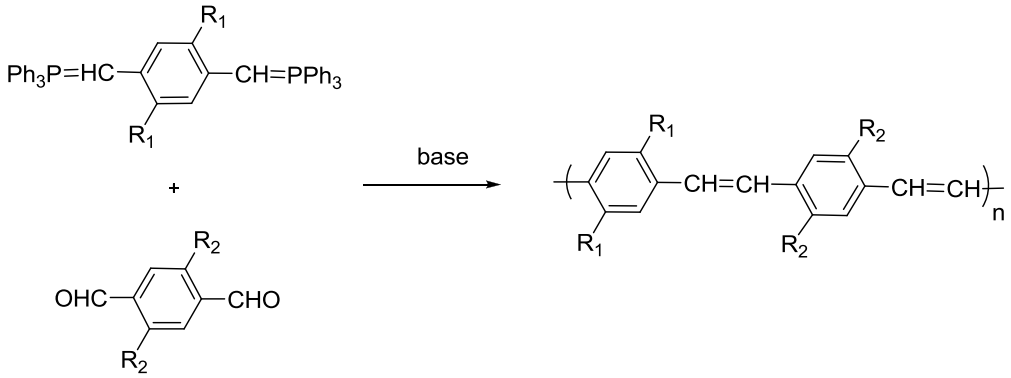

Knoevenagel Polycondensation :

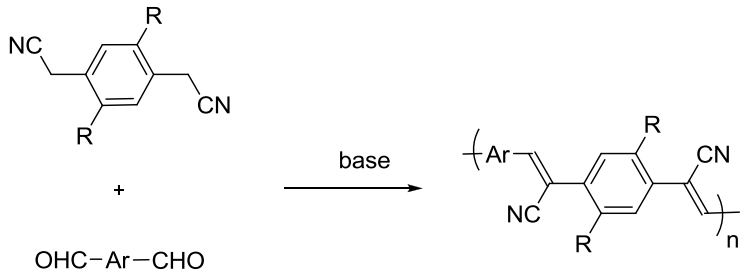

Figure 1-8. Examples of typical Wittig and Knoevenagel polycondensations.

The Knoevenagel condensation was first used to produce CN-PPV derivatives from xylylene dinitrile and an aromatic dialdehyde. The reaction involves nucleophilic addition of a carbanion to the aldehyde under basic conditions, and then the formation of a double bond between two aromatic rings by the elimination of water (Figure 1-8).[99] By changing the structures of the aromatic systems, the Knoevenagel polycondensation can be applied to the synthesis of various cyanovinylene linked conjugated polymers. Previous work reported by our group involved a detailed study of the synthesis and

characterization of donor-acceptor cyanovinylene polymers with narrow band gaps based on thiophene, EDOT, ProDOT and alkyloxy benzene.[100-103]

1.3.4 Random Polymerization

Random polymerization, as a useful methodology in polymerization, is designed to incorporate two or more monomer units in the synthesis of statistical copolymers with irregular monomer sequences. In the field of conjugated polymers, this method is broadly used to combine multiple monomers, adjust their relative ratio and control the monomer sequence distribution, in order to achieve the desired energy level distribution, band gaps, optical properties and interchain interactions.

Some useful random polymerization constructions, which use Stille polymerization as a model and can be applied to other transition metal mediated cross-coupling reactions or to a variety of polymerization methods by one skilled in the art, will now be introduced. In order to reduce the complexity of the discussion, the functional group reactivities are assumed to be independent of their positions. In Figure 1-9, the Stille polymerization of single monomer Bu_3Sn-**A**-Br with two different functionalities will produce a homopolymer. Furthermore, the polymerization of two monomers Bu_3Sn-**A**-Br and Bu_3Sn-**B**-Br will produce a truly random copolymer, in which the probability of finding **A** or **B** at a particular point in the polymer backbone is equal to the mole fraction of that monomer residue in the chain. More complicated systems can be easily achieved by adding a third, fourth and more monomers with the same type of functionality. There is no absolute formula for the amounts of added monomers.

On the other hand, in the polymerization of difunctional monomers with the same functionality, the sum of the monomers with organotin functional groups must be equal to the sum of the monomers with bromo groups. A direct polymerization of Bu_3Sn-**A**-

$SnBu_3$ and Br-**B**-Br will produce a polymer with strict alternation of **A** and **B** repeat units. When a third monomer Br-**C**-Br is incorporated in the polymerization, the reaction produces a random copolymer, in which any **A** unit must be bonded to ether a **B** unit or a **C** unit, while **B** and **C** cannot be next to each other or themselves. Looking at a bigger picture of this polymer, it is a truly random copolymer with -(**AB**)- and -(**AC**)- as repeat units. Moreover, the blending of two distinct types of monomers will generate a random polymer with a more complicated sequence. In here, any **A** or **B** unit can be connected to each other or to a **C** unit, but cannot be next to itself; only **C** units are able to be linked to each other (Figure 1-9). It should be noted that the polymer structure of this polymerization is not correlated to the polymer sequence due to its complexity.

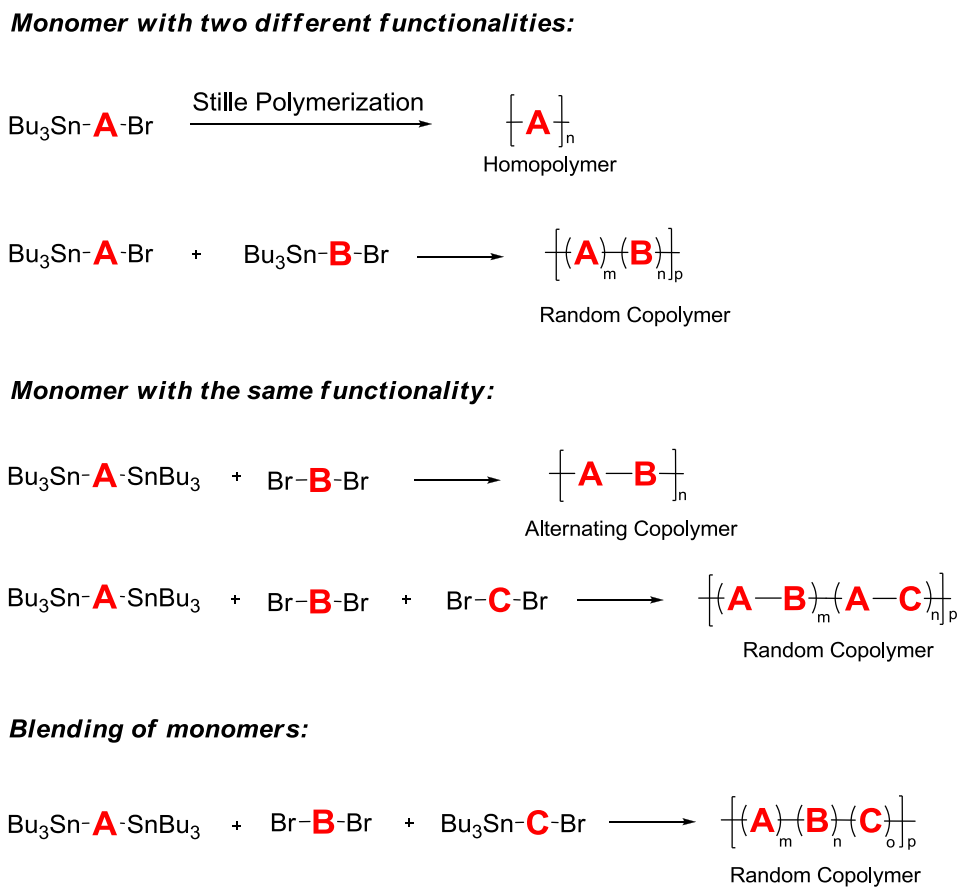

Figure 1-9. Schematic illustration of random polymerization with monomer alternation sequence *via* Stille polymerization.

In this field, many interesting polymers have been produced by random polymerization. Wang *et al.*[104] reported the synthesis of a white light emitting copolymer *via* a random Suzuki polymerization. By incorporating 4,7-bis(4-(*N*-phenyl-*N*-(4-methylphenyl)-amino)phenyl)-2,1,3-benzothiadiazole (OMC) as an orange dopant unit in the main chain of polyfluorene (PF) as the blue host (Figure 1-10), the copolymer emitted white light with simultaneous blue (λ_{max} = 421 nm/445 nm) and orange emission (λ_{max} = 564 nm) in a single layer device.

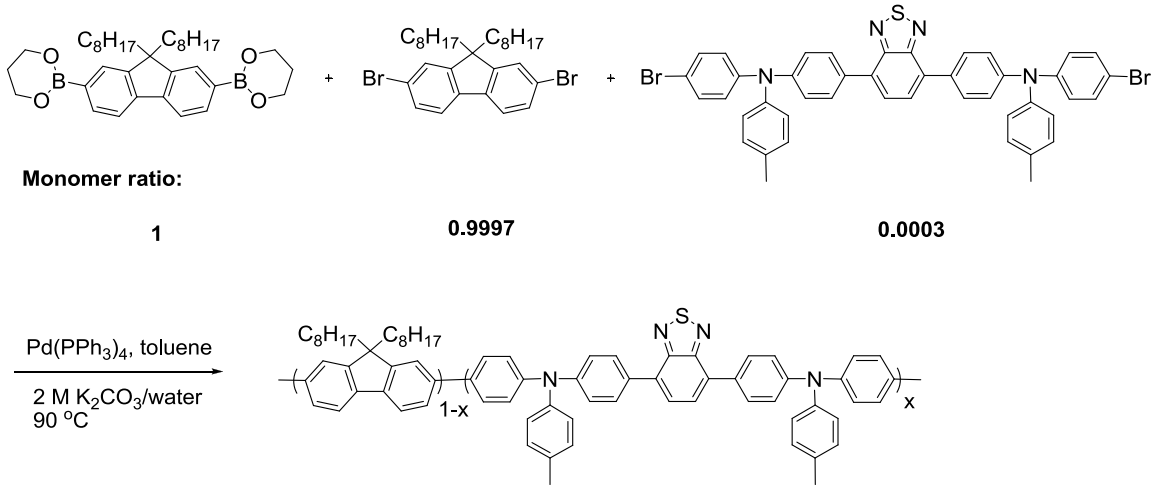

Figure 1-10. Synthesis of random copolymer for white organic light-emitting diodes. (Adopted and modified with permission from Ref. 104)

Yu *et al.*[105] prepared a series of copolymers based on thieno [3,4-b]thiophene, thiophene and 3-hexylthiophene units *via* a random Stille polymerization (Figure 1-11). By controlling the ratio of the monomers in the copolymer composition, the optoelectronic properties of the copolymers could be fine tuned. For example, by increasing the thienothiophene composition, the HOMO levels of the copolymers increased with a decrease of the LUMO levels, leading to smaller band gaps (from polymer D to polymer A). Polymer C showed a number average molecular weight as high as 132 kDa, and a polymer/PCBM solar cell PCE about 1.93%, which is higher

than that of PTTD and P3HT OPVs prepared using similar conditions (0.73% and 1.39%, respectively).

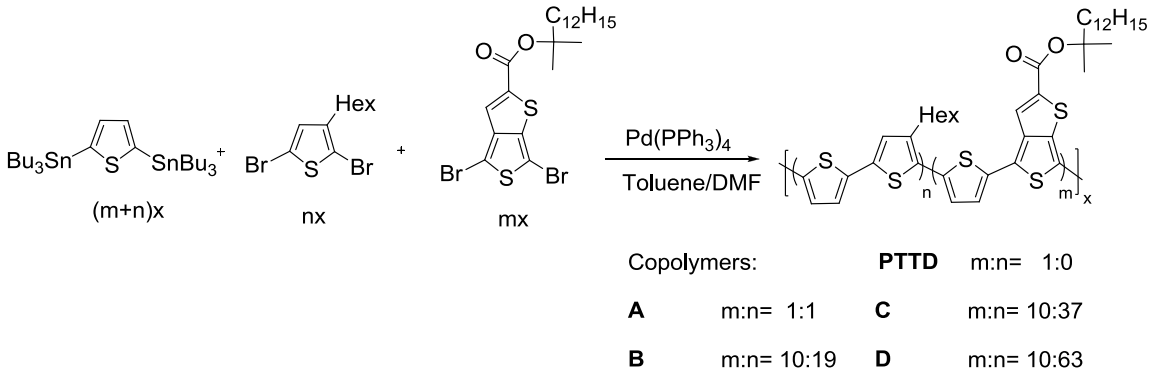

Figure 1-11. Synthesis of random copolymer for OPVs (Adopted and modified with permission from Ref. 105).

Besides these well-established polymerization methods, an important feature in the synthesis of conjugated polymers is the ability to prepare the polymers in batches with a reproducible molecular weight (MW) and PDI range, the same purity level after purification, and thus the same optoelectronic properties and device performance.

In one case, McGehee and Fréchet *et al.*[106] pointed out that the molecular weight of regioregular P3HT had a profound effect on both the morphology and the charge transport property of the polymer thin films. They showed that with an increase in MW from 3.2 to 36.5 kDa, the corresponding field-effect mobility of the transistor increased from 1.7×10^{-6} to 9.4×10^{-3} $cm^2 V^{-1} s^{-1}$, an increase of four orders of magnitude. A further study on the morphology of the films confirmed that the improvement in the mobility occurred because the longer polymer chains brought neighboring grains together, thereby minimizing the grain boundaries and favoring the charge transport.[107,108]

In another report, Janssen *et al.*[109] demonstrated the synthesis of two PDPP3T polymers with distinct MW and PDI *via* Suzuki polymerization under different conditions (Figure 1-12). Surprisingly, both the hole and electron mobilities of the two polymers remained about the same (μ_h = 0.04, μ_e = 0.01 $cm^2\ V^{-1}\ s^{-1}$ for high MW polymer and μ_h = 0.05, μ_e = 0.008 $cm^2\ V^{-1}\ s^{-1}$ for low MW polymer, respectively), and were independent of the polymer molecular weight. In spite of the similarity in the mobilities, the two polymers showed a dramatic difference in their OPV performance. When blended with $PC_{71}BM$, the high molecular weight PDPP3T (M_n = 54 kDa) provided a PCE up to 4.7% with V_{oc} of 0.65 V, J_{sc} of 11.8 mA cm^{-2}, and FF of 0.6, while the low MW polymer (M_n = 10 kDa) only showed a PCE of 2.7% with V_{oc} of 0.68 V, J_{sc} of 6.3 mA cm^{-2}, and FF of 0.63. The reduced short circuit current and efficiency in the low MW polymer were mainly due to the more corrugated morphology of the blending film, which limited the interaction between the polymer and PCBM.[110-112]

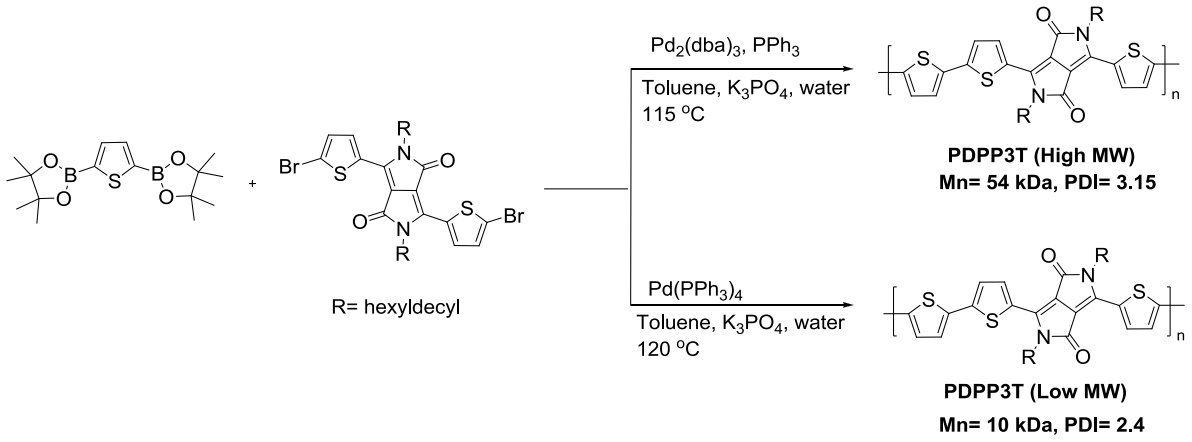

Figure 1-12. Synthesis and structure of PDPP3Ts with distinct molecular weights by Suzuki polymerization. (Adopted and modified with permission from Ref. 109).

1.4 Synthetic Control of Polymer Spectral Absorption

Combining theory with practical experience in chemical reactions, this section will address how the polymer spectral absorption (color) is controlled by synthetic modifications in real cases. It is worth mentioning that the colors of these materials are not driven only by the wavelength of the absorption (energy), but also by the intensity of the absorption band. This is especially true in the case of donor-acceptor conjugated polymers, which will mostly present dual optical transitions with distinct absorption intensities. This discussion will begin with polymers with one absorption band in the visible region, and then move to the D-A copolymers with complex absorption profiles.

As one of the simplest conjugated polymers, the electrochemically polymerized polythiophene film, which can reflect or transmit visible light, shows a red color due to its neutral state π-π^* absorption transition from 620 nm to below 350 nm, which essentially covers the entire visible spectrum except for the red region.[113-115] In the case of PEDOT, combining the electron donating effect of the oxygen atoms directly linked to the 3 and 4 positions of the thiophene rings, with a sulfur-oxygen interaction of adjacent EDOT rings, which dramatically reduces torsion angles and forces the polymer backbones to adopt a more planar conformation than that of PT, the band gap is reduced.[116] The neutral PEDOT film has a single absorption band with λ_{max} at 610 nm and is blue in color due to the lack of absorption in the range of 350-500 nm.[117,118] Moreover, by replacing the ethylene bridge of EDOT with a propylene bridge and adding substituents (for example, -CH_2OEtHx) on the central carbon, a thin film of the new polymer PProDOT(CH_2OEtHx)$_2$ showed a blue shift of the absorption band (λ_{max}= 581 nm) compared with that of PEDOT, and an increase of the band gap, probably due to a limited effective conjugation length and reduced interchain interactions induced by the

bulky substituents. A red-purple color was observed, since the polymer film transmits part of the blue (400-450 nm) and most of the red regions (650-700 nm).[119]

On the other hand, compared with PT, the bulky acyclic side chains (*e.g.* -OEtHx) of the 3,4-dialkyloxythiophenes will directly generate strong steric repulsions to the adjacent rings, resulting in a decrease of the effective conjugation length and an increase of the band gap. A thin film of polymer poly{3,4-di(2-ethylhexyloxy)thiophene} shows an orange color with absorption maximum at 483 nm (Figure 1-13).[120,121] Randomly incorporating the dimethoxythiophene into the polymer backbone reduces the steric effect and lowers the band gap. The reduced band gap leads to a red shift of the absorption, which affords the copolymer a red color (λ_{max}= 525 nm).

Furthermore, conjugated polymers with dual optical transitions can be obtained *via* the donor-acceptor approach,[122-124,130] which provides an elegant method of modifying the spectral characteristics of the polymers by controlling the strength of the electron-rich and electron-deficient moieties, as well as their feed ratios. One particular example is the synthesis of conjugated polymers with the color green- a color state that requires an efficient absorption in the blue and red regions with a window of transmission in the green region of the visible spectrum. In 2004, the Wudl group reported the synthesis of bithiophene-thienopyrazine copolymer PDDTP (Figure 1-14a), which gave the necessary two band absorption with a transmission window at 550 nm. By absorbing strongly in the blue (below 500 nm) and red (above 600 nm) region, the polymer film was able to reflect a saturated green color.[125]

In a similar approach, Toppare *et al.*[126] reported another green-colored copolymer based on 4,7-di(2,3-dihydro-thieno[3,4-b][1,4]dioxin-5-yl)benzo[1,2,5]thiadiazole (BDT)

(Figure 1-14b). The electropolymerized donor-acceptor polymer PBDT was investigated as a possible candidate for electrochromic applications. The insoluble polymer film was revealed to be a neutral state green electrochromic material, which had a highly transmissive sky blue oxidized state.

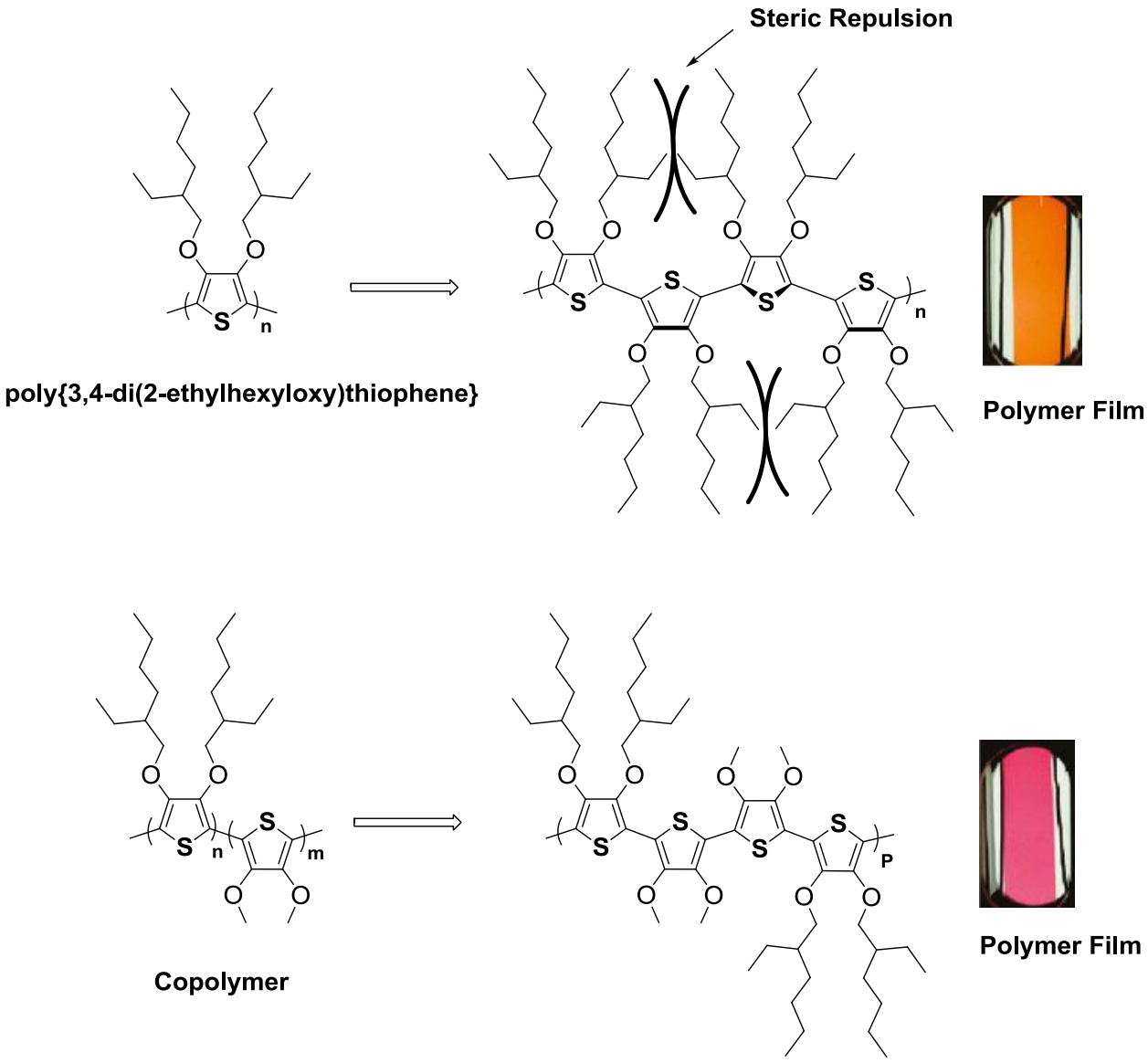

Figure 1-13. Structures of poly{3,4-di(2-ethylhexyloxy)thiophene} and a random copolymer of di(2-ethylhexyloxy)thiophene and dimethoxythiophene. Steric repulsions between side chains in the first polymer decrease the effective conjugation length, and shift the absorption band to the blue region. Photographs are of the polymers in their neutral states. (Adopted and modified with permission from Ref. 121).

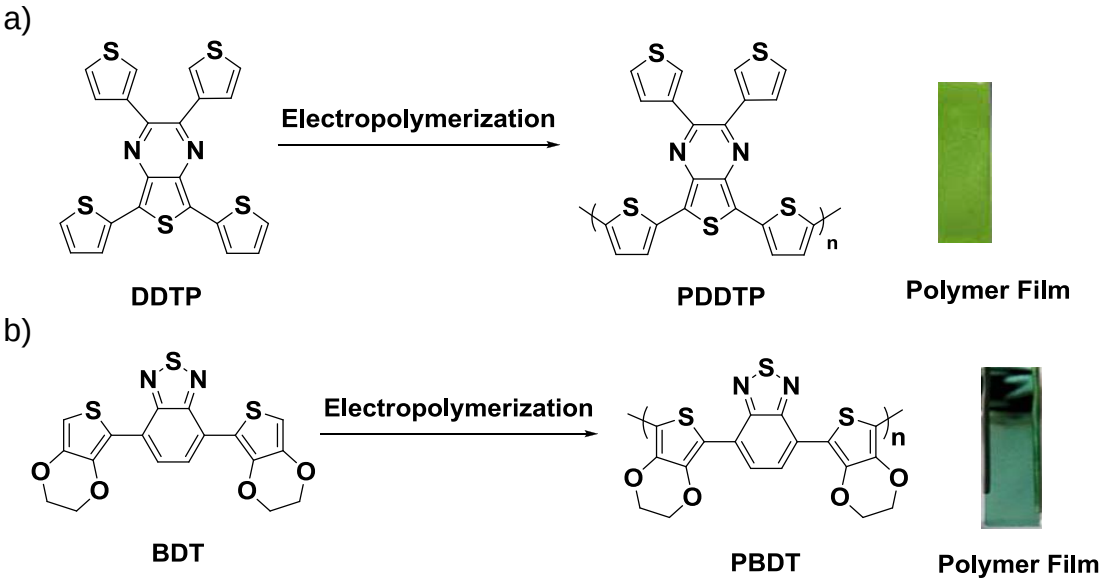

Figure 1-14. Electrochemical polymerization of a) DDTP and b) BDT. Photograph are of the polymers in its neutral state. (Adopted and modified with permission from Ref. 125 and 126, respectively).

In the mean time, our group developed a series of solution processable green-to-transmissive conjugated polymers using ProDOP, thiophene or EDOT as donors and BTD as an acceptor (Figure 1-15a and b).[127,128] In this systematic study, it was shown that the polymer absorption spectra (both absorption wavelength and intensity) can be controlled by tuning the feed ratios of the donors and acceptors. With more and more donor moieties in the polymer main chain, the high energy absorption band shows a red-shift as well as an increase in the intensity, while the low energy absorption moves to shorter wavelength with lower intensity (Figure 1-15b). This has caused a 'merging' effect of the two optical transitions and provided an opportunity to make conjugated copolymers that absorb broadly and evenly over the entire spectrum. In one instance, a polymer was prepared by copolymerization of a ProDOT-BTD-ProDOT trimer with ProDOT in a 1:4 molar ratio. The polymer film showed an inklike black color in its neutral state and was highly transmissive in the oxidized state (Figure 1-15c). More

discussion of the D-A effect in the polymer absorption spectral engineering can be found in Pierre Beaujuge's dissertation[129] and subsequent publication.[130]

a)

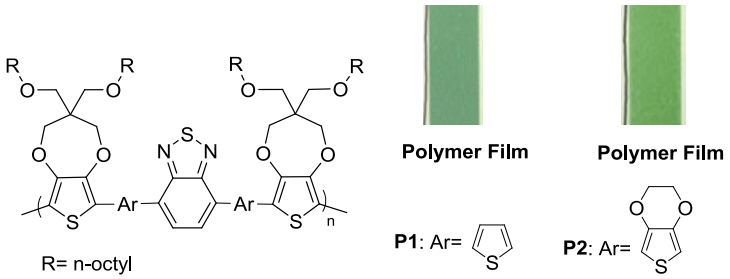

b)

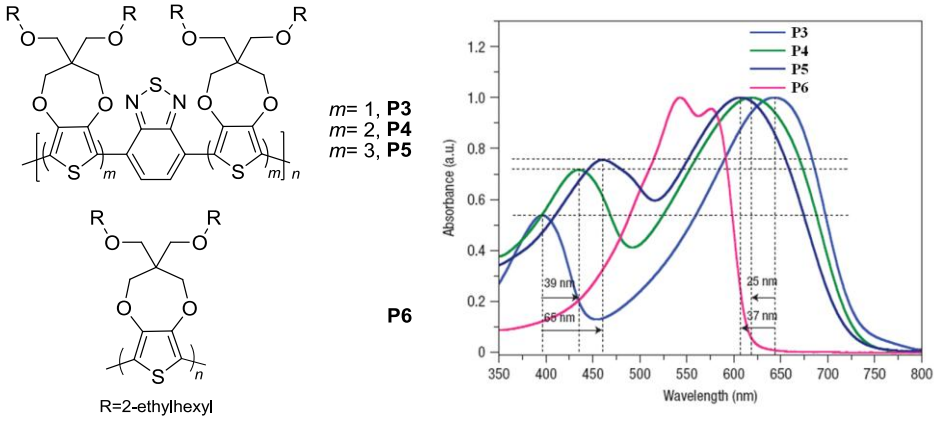

c)

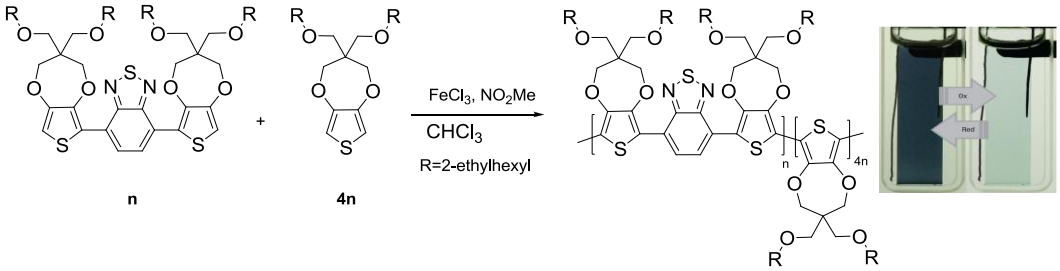

Figure 1-15. Spectral engineering of green- and black-to-transmissive conjugated polymers. a) Molecular structures for the DA copolymers **P1** and **P2**. Photographs are of the polymers in their neutral states (Adopted and modified with permission from Ref. 127. Copyright 2008 Wiley-VCH.) b) Molecular structures for the copolymers **P3**-**P6**. The solution optical absorption spectra of polymers in toluene show a 'merging' effect of the dual optical transition with increasing the donor ratio. c) Synthesis of inky black copolymer. Photographs are of the polymers switched from their neutral colored state to oxidized transmissive state. (Adopted and modified with permission from Ref. 128. Copyright 2008 Nature Publishing Group)

1.5 Processing and Patterning of Conjugated Polymers

"Improved device uniformity and reliability, as well as the development of low cost high-throughput material processing and patterning techniques, are critical to enable organic electronics to mature into a robust and manufacturable technology."[131]

Reviewing the history of conjugated polymers, the interest in these materials has changed from simply pursuing high conductivity of solid polymers to manufacturing complex organic electronic devices,[132,133] which usually require processing of the materials from their solutions into solid films. Consequently, this change has involved two important aspects of the field: the synthesis and characterization of soluble conjugated polymers and the processing of these materials into devices. While the synthesis and characterization of these soluble polymers is essential in understanding fundamental structure-property relationships, only the incorporation of these materials in device structures and subsequent testing will demonstrate the practical usage and the commercial applicability of materials. This section briefly introduces some common processing and patterning techniques available for soluble polymers.

Spin coating[134] is a procedure to produce uniform thin films on hard flat substrates. Specifically, by rotating the substrate, most of the polymer fluid on top of the substrate will spin off the edges of the substrate by centrifugal force and remain as a thin layer of the polymer (0.01-1 μm). The thickness of the polymer films can be controlled by the rotation speed and time, the polymer concentration and the solvent. This method has been broadly utilized in the processing of films for polymer light-emitting devices and photovoltaics in research laboratories and academia, but is rarely used in high volume manufacturing because of its low cost efficiency and waste considerations.

Spray casting[135] is used to cast materials with homogeneous microstructures *via* the deposition of polymer solution droplets onto a substrate. The process can be easily achieved by utilizing a common pressurized airbrush sprayer. Moreover, this technique can be applied to a variety of substrates with all kinds of shapes or even soft and flexible substrates. Although the spray cast films are relatively rough (average roughness on the order of several tens to hundreds of nanometers) compared with the spin coat films, spray casting is still a simple and rapid processing method with few special requirements to obtain films with thicknesses in the range of 50 nm to several micrometers. Spray coating has become one of the most straightforward approaches for processing soluble conjugated polymers in ECDs applications.[136,137] On the other hand, one disadvantage of spray casting is the relatively low process yield (70%) due to overspray and material 'blasted' off the top surface.

Screen printing[138] is a more realistic method for processing and patterning organic electronic devices and has been utilized for the fabrication of solar cells, LEDs and OFETs.[139-141] In screen printing, the films are sequentially deposited through a mask on a large area substrate to obtain a pattern with a resolution on the 100 μm scale. This versatile and comparatively simple technique offers obvious advantages in terms of materials and production costs, and is appropriate for fabricating organic electronics on an industrial scale.

Inkjet printing[142] is suitable for printing with low-viscosity, soluble organic semiconductors.[143,144] This technique uses printheads, which use piezoelectric or thermal inkjet technology, to deposit materials on substrates. Since the printheads do not make direct contact with the substrates, it is considered a non contact method and

can be utilized on a varity of substrates. Moreover, a higher resolution is achievable by this method (35 to 40 µm wide), compared with screen printing (> 100 µm wide). As with the screen printing method, inkjet printing has been commonly used to prepare active layers for organic electronic devices. For example, Aernouts *et al.*[145] has reported the use of inkjet printing for depositing P3HT:fullerene blends thin films. The resulting organic films are used as the active layer for solar cells with power conversion efficiency of 1.4%.

Slot die[146] is a coating technique for applying material solutions on a substrate to form thin films. Generally, material solutions are forced out from a reservoir through a slot by pressure, and transferred to a moving substrate. Since all of the coating fluid is applied to the substrate via the control of a positive displacement pump and the slot in the die exit, slot die coating is more efficient and cleaner than spin coating. This process has been successfully applied to many types of conjugated polymer solutions such as water based PEDOT:PSS inks and organic solvent based P3HT:fullerene blends.[147,148]

1.6 Selected Applications of Conjugated Polymers

1.6.1 Electrochromic Devices

Electrochromic devices (ECDs) are electrochemical cells, in which the electrochromic material exhibits a reversible change in its absorption/transmission or reflection upon an electrochemical redox reaction. Although many types of materials have been studied and utilized in the ECDs (metal oxides, organic molecules and inorganic complexes), conjugated polymers have gained more and more attention due to their better processability, faster switching speed and greater color variability.[149] Two types of dual polymer ECDs, which are used in the characterization of black-to-transmissive ECP in Chapter 3, will be introduced.

An absorptive/transmissive (window type) ECD switches reversibly between a highly absorptive (colored) state and a highly transmissive (bleached) state. As shown in Figure 1-16a, films of two complementary electrochromic materials are deposited on the electrodes with a layer of electrolyte sandwiched between. More specifically, the substrates can be glass or flexible plastic materials. The working and counter electrodes, as well as the electrolyte, must be transparent to allow light to pass through the polymers. In this instance, the anodically coloring material is a minimally color-changing polymer (N-alkyl substituted poly(3,4-propylenedioxypyrrole), MCCP).[150] When a positive potential is applied to the electrode with cathodically coloring electrochromic polymer, the device is switched from its colored state to a highly transmissive state.

An absorptive/reflective (display type) ECD is operated in a way that the light cannot pass through the device, but is reflected back. Depending on the reflective materials used in the device construction, this type of ECD can either be a specular reflective device[151-153] or a diffuse reflective device.[154-157] It is worth noting that the reflected light passes through the active layer (the working electrode with ECPs) twice before it reaches the human eye. As shown in Figure 1-16b, the diffuse reflective device is constructed similarly to the window-type device. In Figure 1-16b, TiO_2 particles are dispersed in the electrolyte and used as the diffuse reflective material. When one side of the electrochromic polymer is oxidized and appears to be highly transmissive, the device shows the white appearance of TiO_2 on the transmissive side, but a colored appearance of the ECP on the other side.

a)

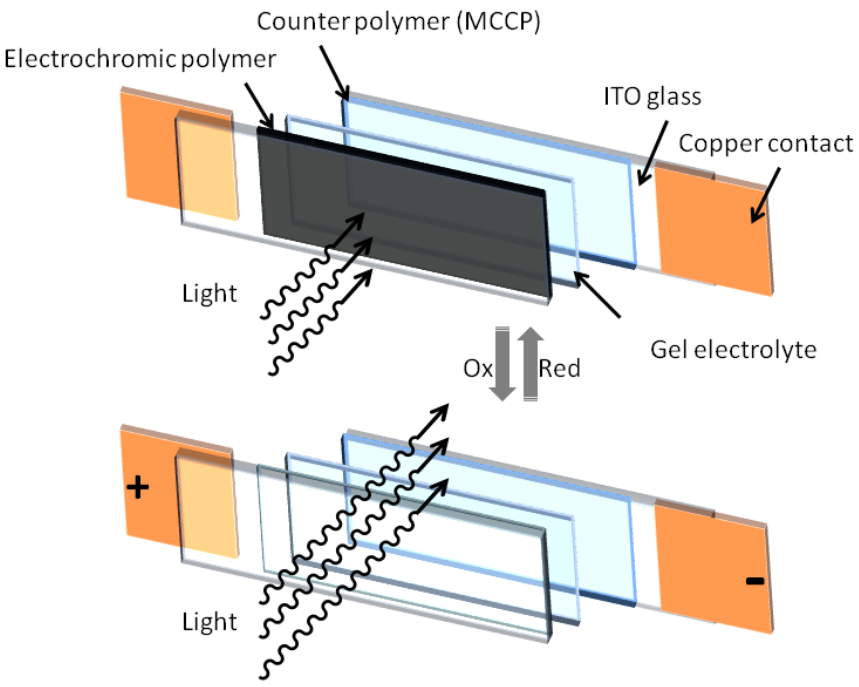

b)

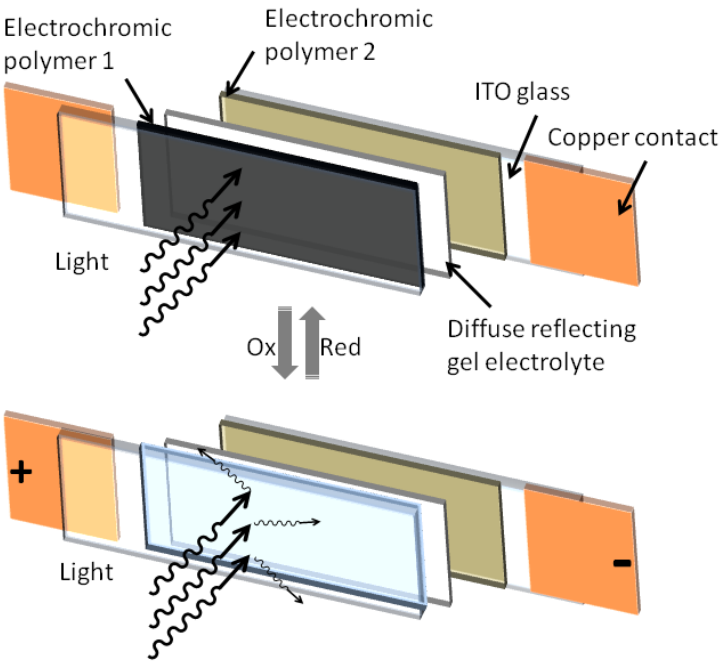

Figure 1-16. Schematic demonstration of a typical a) absorptive/transmissive window-type electrochromic device. Light can pass through the device after the front ECP is oxidized and a minimally color changing polymer (MCCP) is used as a counter electrode . b) An absorptive/reflective electrochromic device using TiO_2 particles as diffuse reflective materials. Light is reflected upon oxidation of the front ECP layer.

1.6.2 Photovoltaic Cells

Organic photovoltaics (OPVs), as potential replacements for silicon-based solar cells, have gained considerable attention over the past decade due to their low cost, light weight and flexibility. Along with the improvement of the efficiency from less than 1% up to 11% (PCE of 11.5% in a DSSC with the ruthenium based sensitizer),[158] several different device configurations have been developed, including dye-sensitized solar cells (DSSCs),[159,160] bulk heterojunction solar cells (BHJ)[161-165] and organic-inorganic hybrid solar cells.[166] This section will focus on polymer/fullerene BHJ solar cells, since they are the only conformation used in characterizing the DPP based copolymers in Chapter 5. Moreover, without an extensive summary of the principles and all of the factors that affect the power conversion efficiency (PCE), the discussion below will address only the most basic components in the synthesis of conjugated polymers for solar cell application.

First reported by Heeger and coworkers,[167] the polymer/fullerene BHJ solar cell has become one of the most investigated branches in the OPV family owing to the conjugated polymer's tunable structures and thus controlled band gaps, energy level distributions and processabilities. Figure 1-17 demonstrates a typical polymer/fullerene BHJ solar cell construction. The active layer, which contains interpenetrating networks of conjugated polymers and fullerene derivatives (*e.g.* [6,6]-phenyl-C_{61}-butyric acid methyl ester, $PC_{61}BM$), is sandwiched between two electrodes. The cathode Al and the anode ITO are used to collect the dissociated charges, and PEDOT:PSS is spin-coated from aqueous solution on ITO to facilitate hole-extraction. Figure 1-18 shows the structures of the conjugated polymers and PCBM derivatives that will be discussed below.

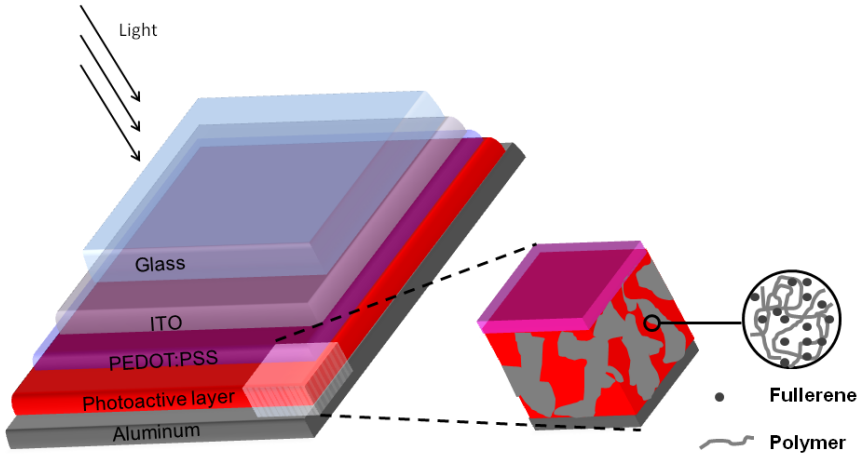

Figure 1-17. Schematic demonstration of a typical polymer/PCBM BHJ solar cell. Photoactive layer based on polymer/PCBM blend comprises interconnected morphology, which is enriched by either the donor polymers or the acceptor PCBM. Interpenetrating interfaces of polymer/PCBM favor carrier generation and carrier transport efficiency.

Among all the homo-conjugated polymers, regioregular poly(3-hexylthiophene) (RR-P3HT) is perhaps the most successful and well investigated polymer in BHJ solar cells. As discussed in Section 1.1.2, RR-P3HT shows HOMO-LUMO levels at -5.2 and -3.3 eV, respectively, with an optical band gap of 1.9 eV. Nowadays, the BHJ solar cell with the structure of ITO/PEDOT:PSS/P3HT:indene-C_{60} bisadduct (ICBA) (1:1, w/w)/Ca/Al, has shown a PCE as high as 6.48% with V_{oc} of 0.84 V, J_{sc} of 10.61 mA cm^{-2} and FF of 0.727.[168] In this report, the key factors for achieving high V_{oc} and FF, and thus high performance are the use of indene-C_{60} bisadduct (Figure 1-18) instead of $PC_{61}BM$, the optimization of the donor (P3HT)/acceptor (ICBA) ratio, the solvent annealing, and the thermal annealing. More specifically, the raised LUMO energy level of ICBA (0.17 eV higher than that of PCBM) contributes significantly to the expansion of energy difference between the HOMO of the donor polymer P3HT and the LUMO of the acceptor fullerene, thereby causing an increase in the V_{oc}. The annealing treatment

favors the formation of a more uniform distribution of P3HT/ICBA and a better interpenetrating network. Actually, the processing techniques for optimizing the film morphology in the study of P3HT solar cells have become guidelines in all polymer/PCBM BHJ solar cell designs. However, despite the respectable V_{oc} and excellent FF, the overall performance has been limited by the rather small photocurrent due to the relatively wide band gap of P3HT, which restricts the absorption below 650 nm, while an essential part of solar energy is located in the red and infrared region. Consequently, this concern leads to a new direction: preparation of low band gap donor-acceptor conjugated polymers with efficient light harvesting property for organic solar cells.

The poly(thieno[3,4-b]thiophene-co-benzodithiophene) (PTB) family is a series of D-A copolymers with benzodithiophene derivatives as donors and thienothiophene derivatives as acceptors (Figure 1-18).[161,169-171] As two members in this low band gap family, PTBF0 and PTBF1 show absorption onsets at 780 and 737 nm with optical band gaps at 1.59 and 1.68 eV, respectively. While PTBF0 gives a PCE of 5.1% with J_{sc} of 14.1 mA cm^{-2}, V_{oc} of 0.58 V, and FF of 0.624, the fluorinated PTBF1 shows a dramatic increase of the V_{oc} (0.74 V) and FF (0.689) and thus a PCE (7.2%) due to the lowered HOMO level and better nanoscale morphology induced by the fluorine atom.[171] A further optimization of the solar cell processing conditions improves the PCE up to 7.4%.[170] Compared with P3HT solar cells above, it is obvious that the dramatic increase in PCE comes from the increase of J_{sc}, which is related to the polymer absorption in the visible and near-IR region. It is worth mentioning that 1,8-diiodooctane (DIO) is used to improve the miscibility between the polymer and PCBM and thus the film morphology.

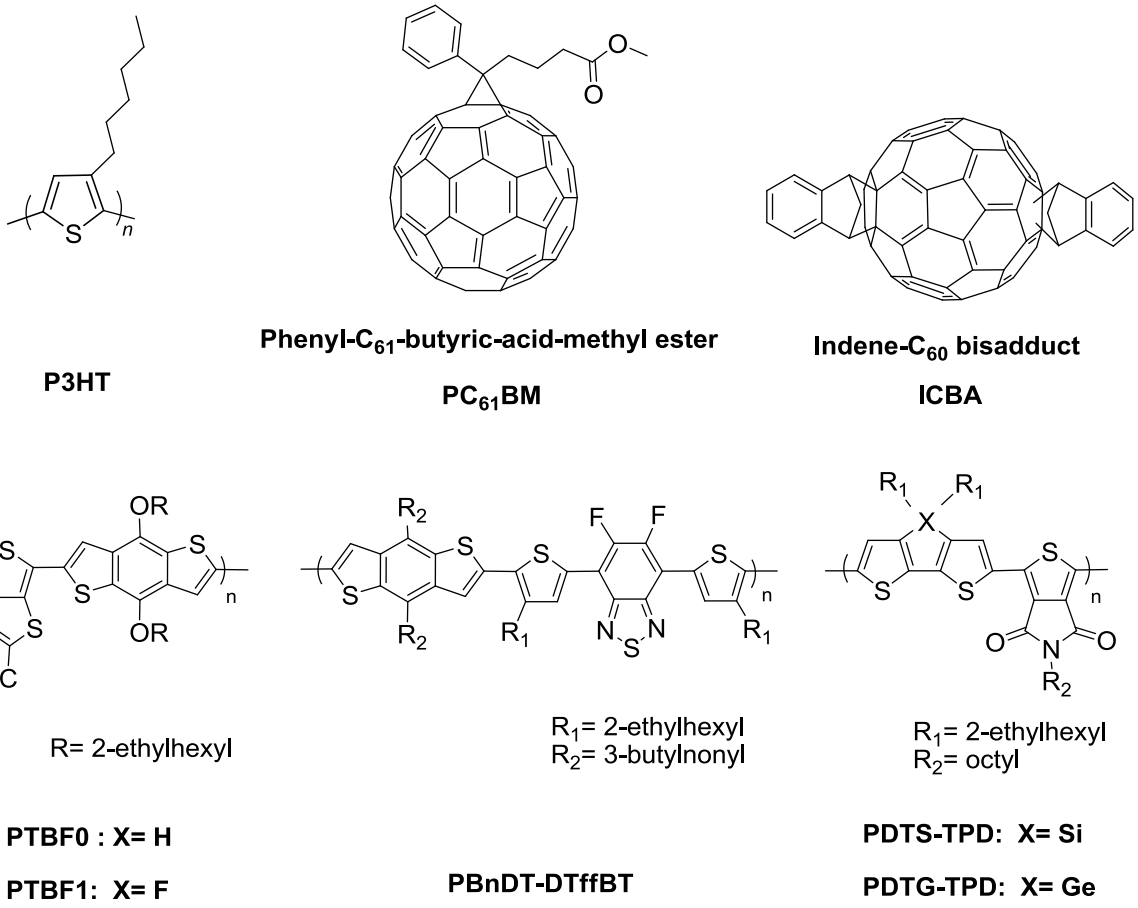

Figure 1-18. Representative conjugated polymers with high power conversion efficiency and fullerene derivatives.

In another case, polymer PBnDT-DTffBT (Figure 1-18),[172] which is a D-A copolymer using benzodithiophene and 5,6-difluoro-4,7-dithien-2-yl-2,1,3-benzothiadiazole (DTffBT) as repeat units, shows a PEC of 7.2% with J_{sc} of 12.9 mA cm^{-2}, V_{oc} of 0.91 V, and FF of 0.61. Clearly, the introduction of electron-withdrawing fluorine atoms into the polymer backbone has lowered both the LUMO (-3.33 eV) and HOMO levels (-5.54 eV) of the polymer and afforded a high V_{oc}. Moreover, an optimized film morphology, which was possibly facilitated by the F atoms, was observed and caused a noticeable increase of the J_{sc} and FF.

Furthermore, our group has reported a comparison result of two polymers, PDTS-TPD (a copolymer of dithienosilole and N-octyl-thienopyrrolodione) and PDTG-TPD (a copolymer of dithienogermole and N-octyl-thienopyrrolodione).[173] By simply changing the Si atom into a Ge atom, while keeping all the other groups the same, the inverted solar cell of PDTG-TPD (glass/ITO/ZnO/Polymer:PCBM/MoO_3/Ag) showed a PCE of 7.3%, compared with 6.6% for PDTS-TPD. Although the V_{oc} of the DTG-based polymer solar cell decreased to 0.85 V (0.89 V for PDTS-TPD), the increase of J_{sc} (12.6 *vs.* 11.5 mA cm^{-2} for PDTS-TPD) and FF (0.68 *vs.* 0.65 for PDTS-TPD) has raised the PCE to a significant level. This is possibly due to the slightly red-shifted absorbance of the DTG analogue and the difference in intermolecular packing.

Clearly, recent developments in the synthesis of new materials for OPVs have brought solar power conversion efficiencies above 7% or even higher than 8% with a few classified structures. The understanding of the structure-property relationships of the conjugated polymers, as well as the optimization of the operating conditions of solar cells, is still the key to further improve the PCEs. Especially, fine-tuning of the light absorption, the HOMO-LUMO levels and the film morphologies as a function of polymer structures, as well as polymer structural details, purity levels, molecular weights, ending groups as a function of chemistry control, are the most important points for a synthetic chemist.

1.7 Thesis of This Dissertation

As discussed in this chapter, during the past four decades the synthesis and characterization of π-conjugated polymers has generated great attention and success. The applications of these organic semiconducting materials extends from energy producing devices (solar cells), to low energy consumption devices (light emitting

diodes and field-effect transistors), to bistable devices (electrochromics). However, most of these materials and devices are currently limited to the research laboratory; the commercialization of these polymeric materials is not yet developed. This is largely due to synthetic difficulties and the lack of deep understanding in the structure-property relationship of conjugated polymer. These issues lead to the themes of this work: understanding the impact of structural parameters in controlling the polymers' optical and electronic properties; utilizing basic organic and polymer chemistry knowledge in the search for new synthetic routes and methods to prepare conjugated polymers, in which band gap, energy levels and light absorption are finely controlled for different applications; and finally, accessing water soluble and processable conjugated polymers, which minimize environmental impact and processing costs.

Chapter 2 describes briefly the techniques employed for the work presented in this dissertation. The purification of the polymers as well as the importance of the polymerization repeatability and reproducibility are also discussed in Chapter 2. In Chapter 3, a new synthetic methodology is devised for the synthesis of black-to-transmissive switching electrochromic polymers. By introducing the random Stille polymerization method, which has prove to be an efficient, scalable and more consistent polymerization process in producing conjugated polymers, random black-to-transmissive electrochromic polymers has been synthesized in batches with a highly repeatable absorption spectra, number average molecular weight (M_n) and PDI. Moreover, successful characterization and device work enhance the potential of this polymer to be used for electrochromic devices. Based on the work in Chapter 3, the study in Chapter 4 is an extension of the random methodology to the synthesis and

characterization of water soluble and processable conjugated electrochromic polymers, WS-ECP-Blue and WS-ECP-Black, with the goal of improving the polymer electrochromic switching rate and the ability of polymers to be utilized in large area spraying in an environmentally friendly aqueous solution. Along with the synthetic details and structure characterizations, a complete comparison of the electrochromic behaviors of organic and water soluble polymers is given in Chapter 4. Chapter 5 targets understanding the structural influences in the performance of solar cell materials with diketopyrrolopyrrole as a conjugated core. Although the same synthetic methodology has been applied to expand the absorption spectra of DPP-based conjugated polymers, a fundamental understanding in the balance of polymer solubility, stacking ability, light absorption, and energy levels is the key to this chapter. Finally, Chapter 6 gives a summary of the work presented in this dissertation and provides suggestions for the future research.

CHAPTER 2
EXPERIMENTAL METHODS AND CHARACTERIZATIONS

2.1 General Synthetic Methods

All chemical reagents and dehydrated solvents were commercially available and used without further purification unless otherwise noted. All reactions were carried out with oven-dried glassware and dry solvents (the purification of solvents can be found in reference 174) in an argon atmosphere unless otherwise stated. For column chromatography, Whatman Purasil silica gel (230-400 Mesh, pore diameter 6 nm) was used. Detailed synthesis and purification procedure for specific compounds is available in the experimental section of Chapter 3-5.

2.2 Purification of Polymeric Materials

The purification of polymeric materials has become an essential part of the synthesis procedure. In order to achieve high performance in applications such as OPVs, OLEDs and ECDs, the impurities arising from a polymerization must be thoroughly eliminated; otherwise they will act as defect sites in devices. In a Stille polymerization used in the synthesis of mostly the polymers in this dissertation, the impurities may include: 1) the toxic tin halides produced during the transmetallation step in the polymerization; 2) palladium catalysts as well as ligands; 3) low molecular weight small molecules, oligomers and polymers due to the decomposition and oxidative homocouplings of organotin compounds. A step-by-step process to eliminate all these impurities will be introduced in this section. It is worth mentioning that this process can be applied not only to the polymers from the Stille polymerization, but also other types of polymerizations such as Suzuki, Negishi, GRIM and oxidative polymerization. For each different polymerization, the procedure may change slightly.

A general procedure for the purification may include the addition of a palladium scavenger, precipitation of the polymers, filtration and Soxhlet extraction. Following the completion of the polymerization, diethylammonium diethyldithiocarbamate (D-DDC) is added directly into the polymer solution, and then the solution mixture is stirred for 1 h at 50°C under an argon atmosphere (experimental details are available for DPP based copolymers in Chapter 5). D-DDC is used as a scavenger to coordinate with the palladium catalyst, allowing the palladium to dissolve into the methanol solution during precipitation of the polymers in the following step. The amount of the D-DDC added to the polymer reaction solution depends on how much of the catalyst is used (usually 10 times the catalyst amount). After cooling to room temperature, the reaction mixture is then pipetted into methanol, causing precipitation of the polymer. The amount of the methanol used here should be 20 times the polymerization solution volume. By this process, most of the palladium catalyst, tin-halides and small molecules should remain in solution and be removed by a subsequent filtration process. However, there is still a chance of small amounts of these impurities being trapped in the polymer network. In light of this, the following Soxhlet extraction is crucial.

Soxhlet extraction is a continuous solid-liquid extraction, generally used to collect the desired compounds from a solid material by recycling a small volume of warm solvent. In this case, the process is reversed, as the desired compounds are the pure polymers, and the low molecular weight impurities are extracted (Figure 2-1a). Thus, the extraction solvents and the extraction sequence must be carefully designed to fulfill this purification purpose. Usually, the Soxhlet extraction of a conjugated polymer starts with methanol, which is a poor solvent for polymers but a good solvent for the residual

catalysts, tin halides and other small molecules. Then, hexane is used to remove low molecular weight oligomers and polymers. Sometimes, extraction with acetone is also applied in between due to its higher solubility for the catalysts. Finally, extraction with chloroform will dissolve the pure polymer into the solution while filtering the polymer solution through the extraction thimble. The extract is concentrated and precipitated into methanol again to yield the solid polymer. Sometimes, chloroform is not able to dissolve the final polymer and so becomes an intermediate extraction solvent, with chlorobenzene employed as the final solvent.

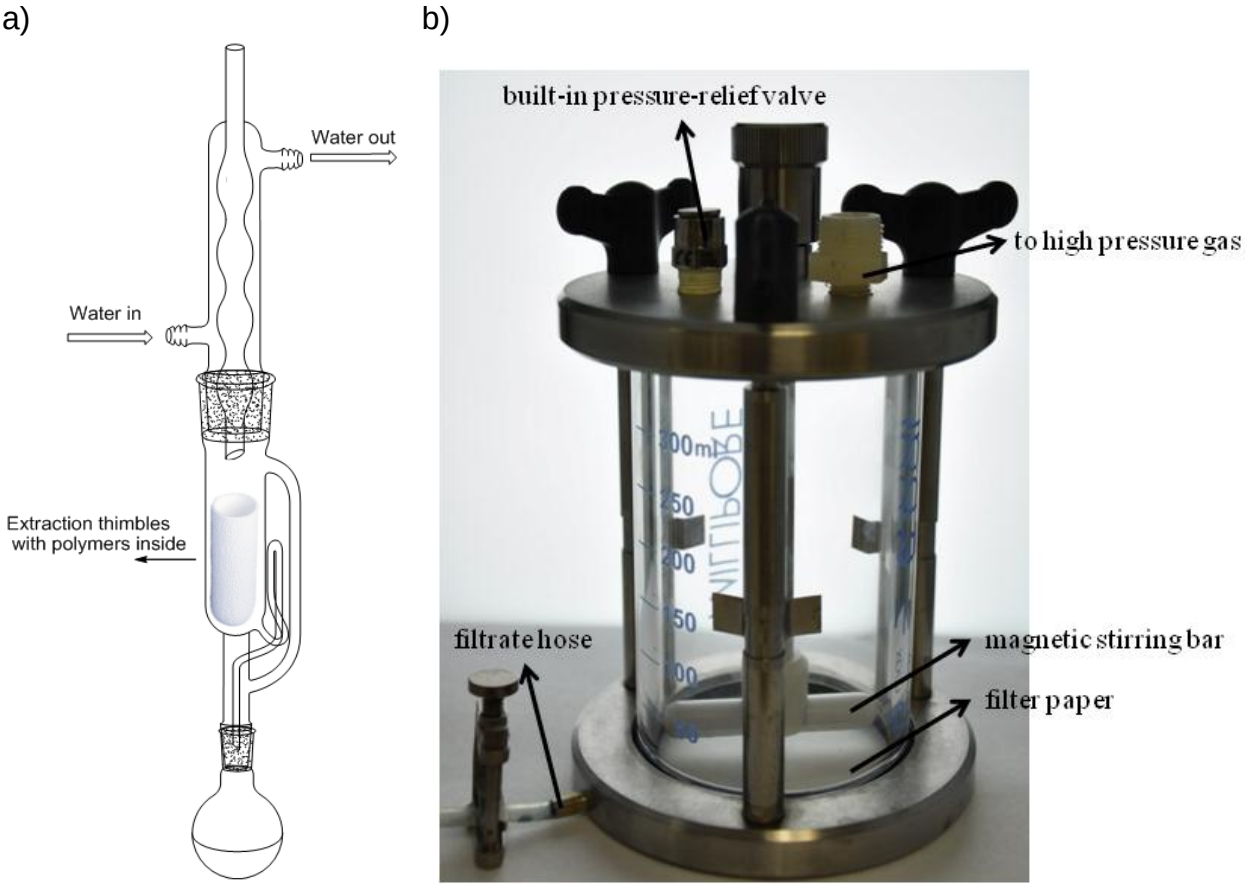

Figure 2-1. Demonstration of polymer-purification methods. a) Soxhlet extraction and b) 'Slurry' filtration.

Table 2-1 shows comparative results of samples before and after Soxhlet extraction. These samples were received having been precipitated once without further purification treatments. Samples with ID 'BASF-Black' were synthesized by the Stille polymerization, and samples with ID 'BASF-Magenta' were synthesized by the Grignard-Metathesis (GRIM) polymerization. As we can see, due to the loss of low molecular weight fractions (20-30 wt% of the samples), the polymers show higher number average molecular weights with lower PDIs after the extraction. Moreover, the optical properties of the polymers are also changed. For example, polymer **BASF-Black 2266-70** shows a reduced absorption intensity in the short wavelength region after the extraction (Figure 2-2). It is worth noting that these samples were synthesized by our collaborators in BASF. More importantly, the polymerization scale of these samples is tremendously large compared to our laboratory production (usually less than 300 mg each time). This is especially true for sample **BASF-Black JB-1**, which was prepared at the 28 g level. The success of these scale-up reactions has brightened the prospect that conjugated polymers will become commercially available and be applied in realistic optoelectronic devices.

Table 2-1. GPC results of polymer samples before and after the Soxhlet extraction.

Sample ID	M_n (kDa)	M_w (kDa)	PDI	Amount
BASF-Black JB-1 (*)	7.0	12.0	1.7	27.5 g
BASF-Black JB-1 (**)	10.2	15.0	1.5	21 g
BASF-Black 2266-70 (*)	8.0	14.0	1.7	11.5 g
BASF-Black 2266-70 (**)	10.0	15.5	1.6	9.5 g
BASF-Magenta 2181-100 (*)	20.0	35.0	1.8	10 g
BASF-Magenta 2181-100 (**)	23.0	39.0	1.7	7.3 g

* Samples before Soxhlet extraction. ** Samples after Soxhlet extraction.

Although the difference in absorbance is too small to be perceived by the naked eyes, other indicators are present to suggest the loss of low molecular weight material.

One example is disappearance of the strong smell of tin compounds after the extraction, and the decrease in the tendency to delaminate under repeated electrochemical switching. Delamination is usually caused by the presence of defects associated with a large amount of small molecules in the polymer film or at the polymer/substrate interface. As these small molecules are removed by the solvent during the switching, voids are created. This change of the material packing density makes the polymer matrix collapse and separate from the substrate. After eliminating the small molecules using Soxhlet extraction, the pure polymer will tend to form homogenous films with fewer defects, avoiding the phenomena described above.

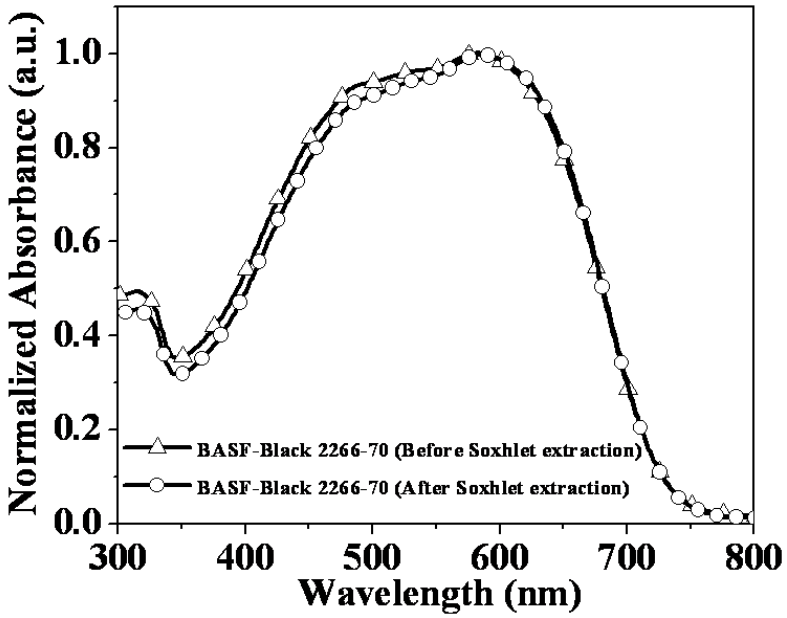

Figure 2-2. Solution absorption change of polymer **BASF-Black 2266-70** after soxhlet extraction in chloroform.

In spite of the positive effects in the purification of conjugated polymers, the Soxhlet extraction is a slow process. Depending on the quality and quantity of the sample, it usually takes 2-10 days to purify one sample, as the process relies on repeated passive extraction. Recently, a much faster purification method called ‘Slurry’

was introduced to the group by Dr. Mike Craig. The extraction time can be reduced to less than a day using this technique. As shown in Figure 2-1b, by stirring the polymer solid dispersion with extraction solvents (the same solvents used in the Soxhlet extraction) in a Millipore stirred cell, the extraction process is accelerated. Furthermore, a high pressure filtration of the mixture combined with concurrent stirring is also believed to reduce the risk of filter papers being blocked by the polymer particles, which is also a concern when using Soxhlet extraction thimbles. However, this process involves the use of more solvents than a typical Soxhlet extraction since it is not a recycling process. The recovery of organic solvents needs to be considered in the practical use of this purification process in the future. A typical procedure of using 'Slurry' is shown in Chapter 3, Section 3.8.

2.3 A Brief Discussion of Polymerization Repeatability and Reproducibility

The repeatability and reproducibility of a polymerization are important parameters. Repeatability refers to replication of results by an individual researcher, whereas reproducibility is replication of results by other operators. A reproducible process with a low batch-to-batch variability is extremely important for transferring the synthesis from the academic lab to industrial production. Clearly, it is meaningless to continue scientific research, which cannot be repeated or reproduced by other groups.

A detailed repeatability study of the Stille random polymerization is demonstrated in Section 3.2.4. Considering the particularity of the polymerization, which follows a step-growth mechanism, the stoichiometric control of the bifunctional monomers becomes one of the most crucial factors. For instance, factors such as the impurities in the monomers, human errors in the weighing step and unsuccessful transferring of the chemicals into the reaction vessel, resulting in inaccurate monomer ratios, will reduce

the repeatability of the polymerization. According to the results in Section 3.2.4, the Stille polymerization shows a great tolerance to various batches of monomers, catalysts and solvents. Polymers, which were produced with the same monomer ratio, exhibited consistent molecular weights and optical properties.

Moreover, the reproduction of **ECP-3** (see Chapter 3 for **ECP-3** details) on a large scale was accomplished by the BASF team. Sample **BASF-Black JB-1** and **BASF-Black 2266-70** have number average molecular weights similar to that of **ECP-3** after the Soxhlet extraction. However, there is a detectable deviation of the solution absorption spectra between the samples (Figure 2-3). For example, **BASF-Black 2266-70** shows a lower absorption intensity in the range of 450-600 nm compared with **EPC-3**. Although the reason for the variability of the polymerization is still unknown, the reproducibility of the polymers is considered to be successful since this small change in the absorption spectra cannot be distinguished by the human eye.

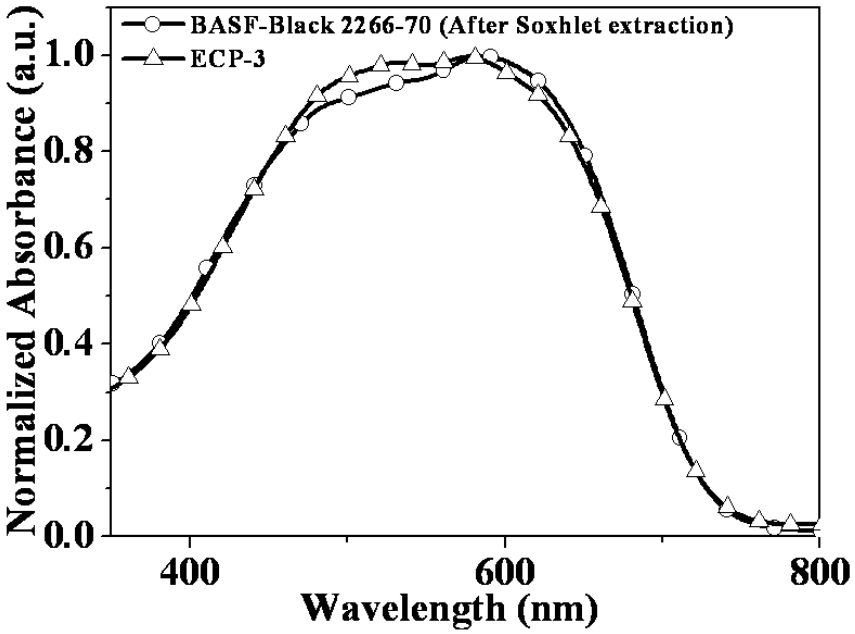

Figure 2-3. Solution absorption of polymers **BASF-Black 2266-70** and **ECP-3** in chloroform.

2.4 Materials Characterization

2.4.1 Structural Characterization

Proton NMR (300 MHz) and ^{13}C NMR (75 MHz) spectra were recorded on a Mercury 300 spectrometer using deuterated chloroform as solvent and tetramethylsilane as internal reference. High-resolution mass spectrometry was performed by the Spectroscopic Services at the Department of Chemistry of the University of Florida with a Finnigan MAT 96Q mass spectrometer. Elemental analyses were performed by Robertson Microlit Laboratories, Inc., Atlantic Microlab, Inc. or the University of Florida, Department of Chemistry spectroscopic services.

2.4.2 Polymer Molecular Weight Characterization

Gel permeation chromatography (GPC) was performed using a Waters Associates GPCV2000 liquid chromatography system with its internal differential refractive index detector (DRI) at 40°C, using two Waters Styragel HR-5E columns (10 μm PD, 7.8 mm i.d., 300 mm length) with HPLC grade THF as the mobile phase at a flow rate of 1.0 mL min^{-1}. Injections were made at 0.05-0.07 % w/v sample concentration using a 220.5 μL injection volume. Retention times were calibrated against narrow molecular weight polystyrene standards (Polymer Laboratories; Amherst, MA).

2.4.3 Thermal Characterization

Polymer thermal stability was assessed by thermogravimetric analysis (TGA) on a TA Instruments TGA Q1000 Series using high-resolution dynamic scans under nitrogen. The TGA samples (3-4 mg) were typically heated to 50°C to equilibrate to a constant mass, and then heated at a heating rate of 50°C/min with resolution number of 4.00 and sensitivity value of 1.00. The final temperature is set to be 650°C.

2.4.4 Electrochemical Characterization

Electrochemistry is a powerful tool to evaluate the electronic properties of conjugated polymers, providing information such as the onsets of oxidation and reduction (HOMO and LUMO energy levels), half-wave potentials and electrochemical bandgaps. Electrochemistry was performed using a three-electrode cell with a platinum wire or a platinum flag as the counter electrode, a silver wire quasi-reference electrode or Ag/Ag^+ reference electrode calibrated using a 5 mM solution of Fc/Fc^+ in 0.1 M electrolyte solution, and a platinum button or ITO-coated glass slide (7 × 50 × 0.7 mm, 20 Ω /cm^2) as the working electrode. The ITO electrodes were purchased from Delta Technologies, Ltd. All potentials were reported *vs*. Fc/Fc^+. An EG&G Princeton Applied Research model 273 potentiostat was used under the control of CorrWare II software from Scribner and Associates. The electrolyte solutions were prepared from dry lithium bistrifluoromethanesulfonimidate (LiBTI) electrolyte dissolved in freshly distilled propylene carbonate (PC) or KNO_3 in water, and bubbled with argon for 20 minutes before the experiments.

Two different electrochemistry methods were used in this dissertation- cyclic voltammetry (CV) and differential pulse voltammetry (DPV).[175,176] Detailed discussions of these two methods can be found in dissertations from Jennifer. A. Irvin, Christopher A. Thomas and Emilie M. Galand.[177-179] Since all electrochemical measurements reported in this dissertation will be referenced versus the Fc/Fc^+ redox couple, the conversion of the energy levels to the vacuum level were recalibrated by using -5.1 eV as the oxidation potential of ferrocene *vs.* vacuum. It is worth mentioning that -4.8 eV is also commonly used as the Fc oxidation potential. The debate of which number is the true value can be found in the dissertation of Barry C. Thompson[180] and reference 181.

2.4.5 Optical Spectra Characterization

Absorption spectra were obtained using a Varian Cary 500 Scan UV-vis/NIR spectrophotometer and quartz crystal cells (1 cm x 1 cm x 5.5 cm, Starna Cells, Inc.). ATR-IR measurements were performed on a Perkin-Elmer Spectrum One FTIR outfitted with a $LiTaO_3$ detector.

2.4.6 Spectroelectrochemistry

As one of the most basic tools to evaluate the electrochromic behavior of ECPs, spectroelectrochemical measurements were performed to obtain absorption or transmittance changes upon oxidation and reduction of polymer thin-films. By progressively applying an electrical bias to a polymer film, the formation of polarons and bipolarons in the polymer chains will generate a series of continuous changes in the film absorption spectra. Figure 2-4a gives the result of a typical spectroelectrochemical experiment. In this case, the blue-colored polymer film was gradually oxidized (p-doping) in a 0.1 M LiBTI/PC solution. The depletion of the dual absorption band in the visible region (350-400 and 500-800 nm, respectively), as well as the rise of electronic absorptions at longer wavelengths due to polaron (λ_{max}= 1000 nm) and bipolaron carriers (λ_{max}> 1600 nm), afford a highly transmissive oxidized state of the polymer film.

2.4.7 Colorimetry

To evaluate the color changes of the ECPs occurring on electrochemical switching (on the basis of the “Commission Internationale de l’Eclairage” 1976 *L*a*b** color standards), *in situ* colorimetric measurements were performed using a Minolta CS100 Colorimeter in transmission mode with a GraphicLite LiteGuard II standard D50 light source. The light source and the sample to be measured were placed in a color viewing booth. The interior of the light booth is coated with a standard gray neutral 8 (GTI

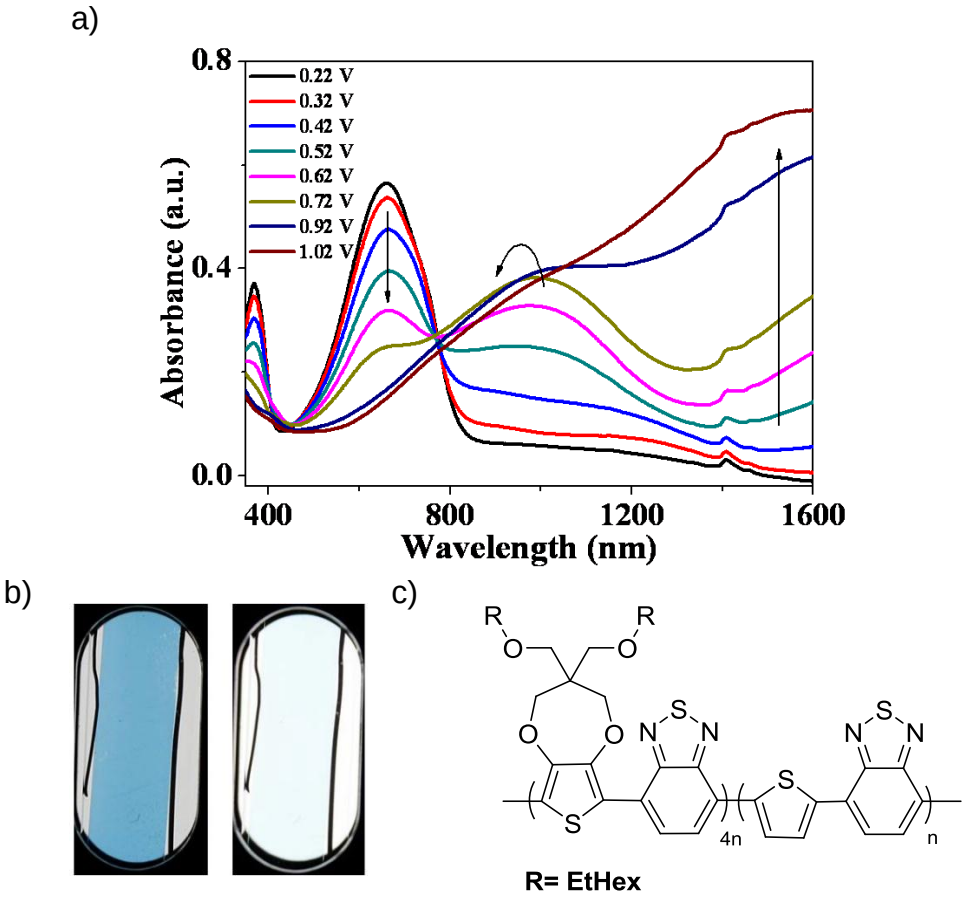

Figure 2-4. Demonstration of spectroelectrochemical series for a blue-to-transmissive electrochromic polymer film. a) A typical spectroelectrochemistry data plot. The films were spray-cast onto ITO-coated glass from toluene (1 mg/mL). Electrochemical oxidation of the films was carried out in 0.1 M LiBTI/PC supporting electrolyte using a silver wire as a reference electrode, and a platinum wire as the counter electrode. All potentials given are referenced *vs.* Fc/Fc^{+}. b) Photographs of the film held at 0.22 V (left) and 1.02 V (right). c) Structure of the polymer.

Graphic Technology, Inc.) matte latex enamel (equivalent to Munsell N8) to allow for accurate assessment of color of the sample during measurement. Photography was performed in the same light booth using ether a Nikon D90 at a exposure time of 1/40~1/25 sec, f-stop of f/5.3, ISO sensitivity of 200 or 400, and focal length of 75~80 mm, or a Canon EOS REBEL XSi at a exposure time of 1/125~1/60 sec, f-stop of f/4~f/5.6, ISO sensitivity of 200, and focal length of 18~55 mm. The photograph file-type

was JPEG and the files were cropped to contain only the polymer film to exclude extraneous background using Adobe Photoshop. No additional alterations to the photography files were performed.

2.4.8 Morphology Characterization

Atomic force microscopy was used to characterize donor-acceptor blend surface morphologies in bulk-heterojunction solar cells (Chapter 5). Data were acquired as tapping mode height image on a Veeco Innova scanning probe microscope (SPM) with a Nanodrive controller and MikroMasch NSC-15 AFM tips. The instrument was a sample scanning instrument, whereby the tip remains stationary while the sample was scanned. In tapping mode, the tip was oscillated at ~300 MHz (resonant frequency of tips used), and the tip oscillation amplitude was damped by the surface being probed until the oscillation amplitude reached a specified set point. The sample was then scanned and the height of the sample constantly adjusted by the piezoelectric scanner to maintain the specified set point.[182]

2.5 Electrochromic Devices

2.5.1 Transmissive/Window Type Devices

The window-type device was constructed using ITO/glass (25 x 37.5 x 1.1 mm, 8-12 Ω, Delta Technologies, Ltd.) coated with the electrochromic polymer at one electrode and the minimally color-changing polymer, PProDOP-N-C18, at the other. The polymer was spray-cast from methylene chloride or toluene. The gel electrolyte was comprised of LiBTI dissolved in propylene carbonate to a concentration of 0.5 M followed by the addition of 1.1 g of poly(methyl methacrylate) (PMMA, M_n~1, 000 kDa) per 10 mL of electrolyte. A layer of the gel was spread onto one of the polymer-coated ITO electrodes

and the device was assembled using 3M tape as a spacer and epoxy as a sealant on the outer edges of the glass. The device schematic is shown in Chapter 1.

2.5.2 Reflective/Display Type Devices

The reflective device was constructed using ITO/glass (25 x 37.5 x 1.1 mm, 8-12 Ω, Delta Technologies, Ltd.) coated with the electrochromic polymer. The polymer was spray-cast from toluene to an optical density such that the absorption at λ_{max} was ~ 0.8 a.u.. The gel electrolyte was comprised of LiBTI dissolved in propylene carbonate to a concentration of 0.5 M, followed by the addition of 1.1 g of PMMA per 10 mL of electrolyte. Titanium dioxide (Acros) was added to the gel and stirred until the gel was an opaque white. A layer of the gel was spread onto one of the polymer-coated ITO electrodes and the device was assembled using double-sided tape as a spacer and epoxy as a sealant on the outer edges of the glass. The device schematic is shown in Chapter 1.

2.6 Photovoltaic Devices

Before device fabrication, the ITO coated glass substrates were cleaned with acetone, isopropyl alcohol and DI water. The ZnO-PVP composite was spin-coated onto the cleaned ITO substrate at 3000 RPM, and then annealed at 200°C for 40 mins. The **PDPP3T**:$PC_{71}BM$ (1:1) mixture was dissolved in chlorobenzene with 5% v/v 1,8-diiodoctane (DIO) (Chapter 5). The polymer **P3** and **P4**:$PC_{71}BM$ solution was prepared in the same way at a concentration of 20 mg/mL. The mixture solution was spin coated onto ZnO films to an optimum thickness of 105 nm. Then the film was annealed at 70°C for 40 min. A 5 nm layer of molybdenum oxide (MoO_3) and a 100nm layer of silver were thermal evaporated at 1×10^{-6} Torr. Devices were encapsulated before measurements.

Photocurrent-voltage (*J*-*V*) characterization was performed with a Keithley 4200 semiconductor characterization system and a Newport Thermal Oriel 94021 1000W solar simulator (4 in. by 4 in. beam size). The light intensity was determined by an ORIEL 91150V monosilicon reference cell calibrated by Newport Corporation. EQE measurement was conducted using a Xe DC arc lamp as light source, an ORIEL 74125 monochromator, a Keithley 428 current amplifier, an SR 540 chopper system and an SR830 DSP lock-in amplifier from SRS. The generated EQE spectrum was integrated with an A.M. 1.5 G spectrum to compare with the measured short circuit current values. A PerkinElmer LS55 fluorescence spectrometer and Lambda 750 UV/VIS spectrometer were used for photoluminescence and absorption experiments.

CHAPTER 3
BROADLY ABSORBING BLACK-TO-TRANSMISSVIE SWITCHING ELECTROCHROMIC POLYMERS USING HIGHLY REPRODUCIBLE STILLE METHODS

3.1 Electrochromic Polymers

Compared to inorganic metal oxides (*e.g.* tungsten oxide),[183-185] small molecule organic electrochromes (*e.g.* viologen derivatives)[149,186] and electrodeposited *π*-conjugated polymers films (*e.g.* polythiophene and polypyrrole), solution-processable *π*-conjugated polymers have offered great advantages in the field of non-emissive electrochromic devices (ECDs). More specifically, these advantages may include good processability, mechanical flexibility, high optical contrast, rapid redox switching and long-term stability.[13,187,188] In addition, the utilization of *π*-conjugated polymers as electrochromic materials has significantly improved the development of applications such as low-cost organic electronic displays, smart windows, electronic paper and rear view mirrors.[7,189,190] As one of the major research aspects in the Reynolds' group, we focus on the synthesis and characterization of soluble *π*-conjugated polymers, which can be easily oxidized or reduced and show two or more distinct colored states based on redox activities.

Generally, all of the *π*-conjugated electroactive polymers possess electrochromic behavior. For example, electrochemically polymerized polythiophene undergoes a red to blue switch upon the oxidation of the polymer films, which corresponds to the bleaching of the *π*-*π** transition in the visible region with simultaneous emergence of polaron and bipolaron infrared optical transitions tailing into the red region.[114,115,191] On the other hand, a red to black-green color switch is also observed by reducing the polymer film from its neutral state to its reduced form.[192] In addition, unsubstituted

polypyrrole yields a yellow to brown-black switch on successful p-doping,[193] and the switching colors of its *N*-alkyl and *N*-phenyl derivatives are not significantly affected by successive structural modifications at the nitrogen position.[194] Although various interesting switching colors have been attained by these conjugated polymers and their derivatives (mainly based on side chain modifications), and the structure-property relationships have been successfully investigated, it is almost impossible to reach the practical utility of ECDs by using these types of electrochromic materials, which can only be switched between two or more distinct and highly colored states. This triggers new questions for the materials scientists: what kind of polymeric electrochromic materials do we really want and how can we achieve them?

On the other hand, electrochromic materials that can be switched between a strongly colored state and a highly transmissive or near transparent state would find much broader applicability, such as in transmissive window-type devices and reflective display-type devices. Moreover, considering the existing print and spray techniques, the target polymers must have considerable solubility in either regular organic solvents (toluene, THF and chlorinated solvents) or water. Other important requirements may include: 1) stable chemical structures (backbones and side chains), which cannot be decomposed easily by a serious of chemical treatments, as well as by UV and visible light; 2) suitable HOMO energy levels, which may ensure the polymers' stability in air during processing and provide high device stabilities; on the other hand, high HOMO values allow for low oxidation potentials and stable oxidized states (no or low degradation after thousands of redox switches); 3) high molecular weights (usually higher than 10,000 Da), where the polymers' optical properties are saturated.

Keeping the important requirement discussed above in mind, the Reynolds' group has been dedicated to fulfill this extensive program by the synthesis and characterization of conjugated polymers for electrochromic applications. With the invention of a neutral yellow to cathodic transmissive conjugated polymer (ECP-yellow, Figure 3-1), the field of electrochromic polymers has now reached an important milestone.[136,195] During the past few years, a series of polymeric electrochromes which are colored (yellow,[195] red and orange,[120] magenta/purple,[119,196] blue,[197] green and cyan,[127,128]) in the neutral state and highly transmissive in the oxidized state, have been investigated by our group (Figure 3-1). Based on this successful work, the full color palette is now complete, allowing a large variety of colors for transmissive and reflective electrochromic applications. However, there are only two reports of black-to-transmissive electrochromic polymers.[128,198] This is due to the complexity in producing a polymer absorption spectrum which absorbs evenly over the entire visible spectrum (400-750 nm) in the fully neutralized state, while effectively bleaching out over the same region in the fully oxidized state.

Recently, we presented our first black-to-transmissive switching ECP based on the donor-acceptor approach.[128] By varying the relative contribution of donor and acceptor moieties in the polymer backbone, the two-band absorption in the visible spectrum could be controlled. In addition, using a particular feed ratio of two different monomers, the discrete absorption bands merged into a broad absorption across the entire visible region. The spray-cast polymer thin film exhibited a deep black neutral state and attained a highly transmissive state when fully oxidized. Due to the synthetic complexity of the polymer, which involved the synthesis and chromatographic separation of donor-

acceptor-donor trimers, and which may limit reproducible large-scale production of the material, we wanted to develop a method that would lead to polymer batches with highly reproducible absorption spectra and an efficient, scalable and consistent polymerization process.

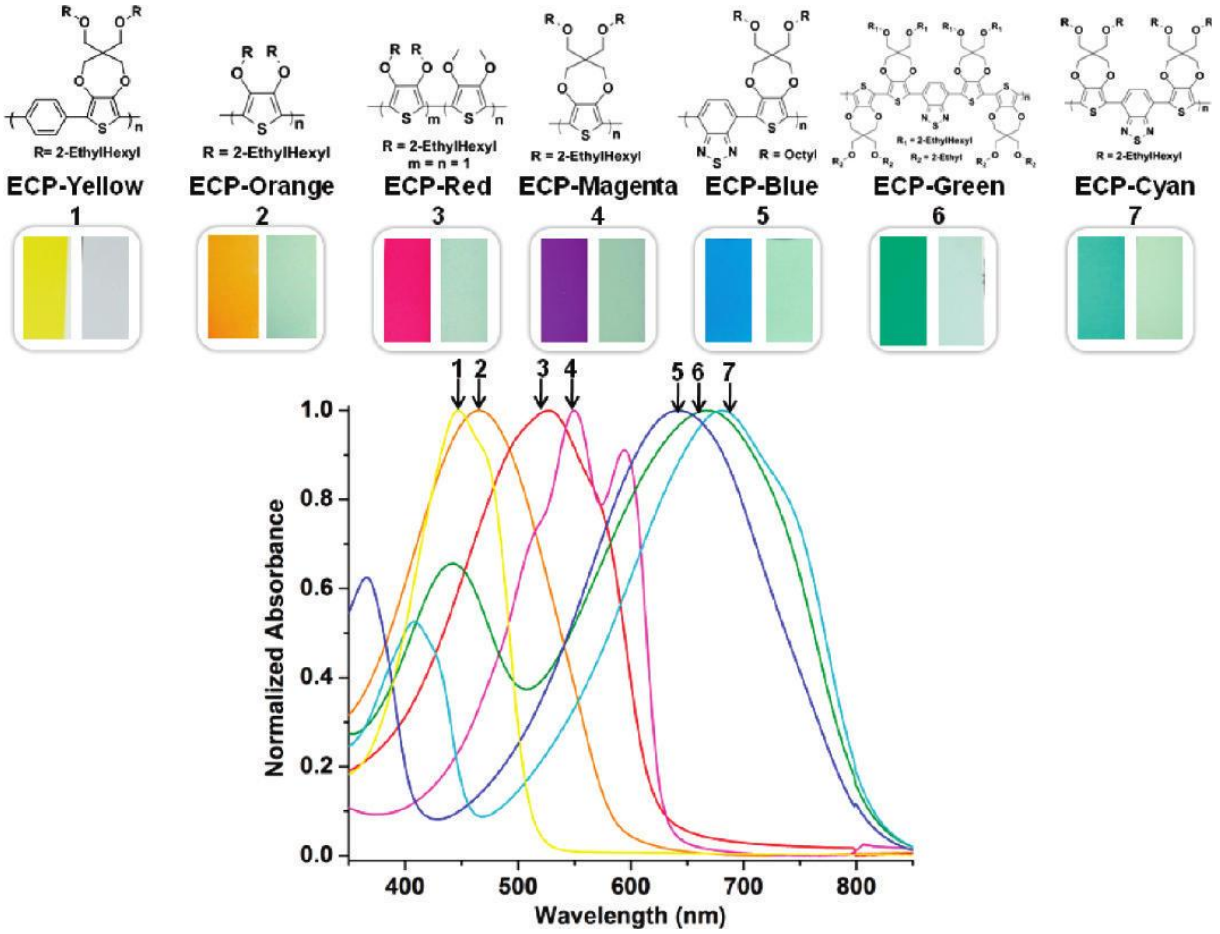

Figure 3-1. Repeat unit structures and photographs of spray-cast polymer films in the neutral colored, and oxidized transmissive states and normalized absorption spectra of polymer films of **P1**-**P7**. (Adapted with permission from Ref.121 and Ref. 136 Copyright 2011 American Chemical Society)

In order to achieve this goal, a transition-metal mediated random coupling polymerization was chosen. In the specific instance demonstrated here, we used a Stille polymerization; however, the method can also be applied to many other transition-metal mediated reactions, including Suzuki, Negishi, and Kumada couplings. Under the most

common Stille polymerization conditions, two monomers (typically an aryl distannane and an aryl dihalide) are cross-coupled using a palladium catalyst to produce polymers with alternating Ar-Ar´ couplings.[199-201] In this approach, we desired to incorporate a random mixture of donor and acceptor heterocycles in order achieve a black ECP by utilizing more than two monomers in the polymerizations. In order to simulate the ratio of electron-rich to electron-poor heterocycles determined in our previous work, we chose to randomly polymerize both 2,5-dibromo- and 2,5-tributylstannyl-2-ethylhexyloxy-substituted 3,4-propylenedioxythiophene (ProDOT-$(CH_2OEtHx)_2$) with 4,7-dibromo-2,1,3-benzothiadiazole (BTD) in different feed ratios (Figure 3-2).[202]

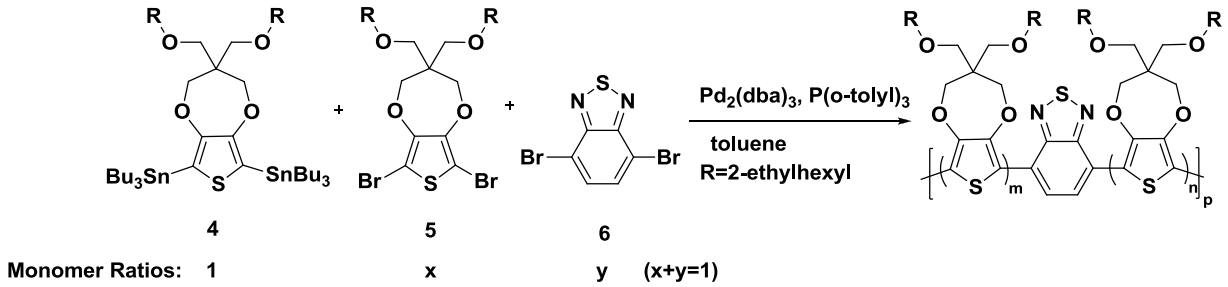

Figure 3-2. Reaction scheme for the Stille polymerization of three monomers.

In this chapter, several random broadly absorbing copolymers were produced with number average molecular weights between 10 to 18 kDa and polydispersities ranging from 1.3 to 1.6 after Soxhlet extraction. Polymers from successive repeated experiments showed highly reproducible absorption spectra as well as matched M_n and PDI. The polymer **ECP-3** was utilized as an example to demonstrate the electrochromic properties of these polymers. The thin film of **ECP-3** showed a transmittance change ($\Delta\%T$) as high as 42% (%*T* from 36% to 78%) at the 1 s switch time as well as a high continuous switching stability (18,000 cycles, 1.5 s switch time). Successful

characterization and application study indicate that these polymers have high potential for use in electrochromic devices.

3.2 Polymer Synthesis and Characterization

3.2.1 Monomer Syntheses and Purification

Figure 3-3 shows the synthesis of the monomers: 6,8-bis(tributylstannyl)-3,3-bis((2-ethylhexyloxy)methyl)-3,4-dihydro-2H-thieno[3,4-b][1,4]dioxepine (compound **4**), 6,8-dibromo-3,3-bis((2-ethylhexyloxy)methyl)-3,4-dihydro-2H-thieno[3,4-b][1,4]dioxepine (compound **5**) and 4,7-dibromobenzo[c][1,2,5]thiadiazole (compound **6**). Starting from commercially available 3,4-dimethoxythiophene **1**, ProDOT intermediate compound **2** with a propylenedioxy bridge was synthesized via transetherification with 2,2-bis(bromomethyl)propane-1,3-diol in 80% yield after column chromatography. Occasionally, in order to achieve a white crystalline solid of compound **2**, an additional recrystallization step using a hexane/THF (5:1) mixture as the solvent was applied. The subsequent reaction of compound **2** with 2-ethylhexan-1-ol under basic conditions in DMF afforded ProDOT-$(CH_2OEtHx)_2$ (compound **3**) as a colorless oil in 78% yield. Compared with the previously reported procedure for making compound **3**,[119] which required formation of the 2-ethylhexan-1-olate sodium salt precursor before adding the ProDOT intermediate, the procedure used here was modified into one *in-situ* reaction by adding all the reagents at once (Section 3.8 for experimental details). Moreover, the reaction time was reduced to one day instead of two days by monitoring the progress of the reaction using TLC and the reaction yield was improved from 70% to 78% after purification. A high purity level of compound **3** is crucial for the next step in the synthesis of di-tributyltin substituted ProDOT-$(CH_2OEtHx)_2$ (compound **4**) due to the complexity of the purification of **4**.

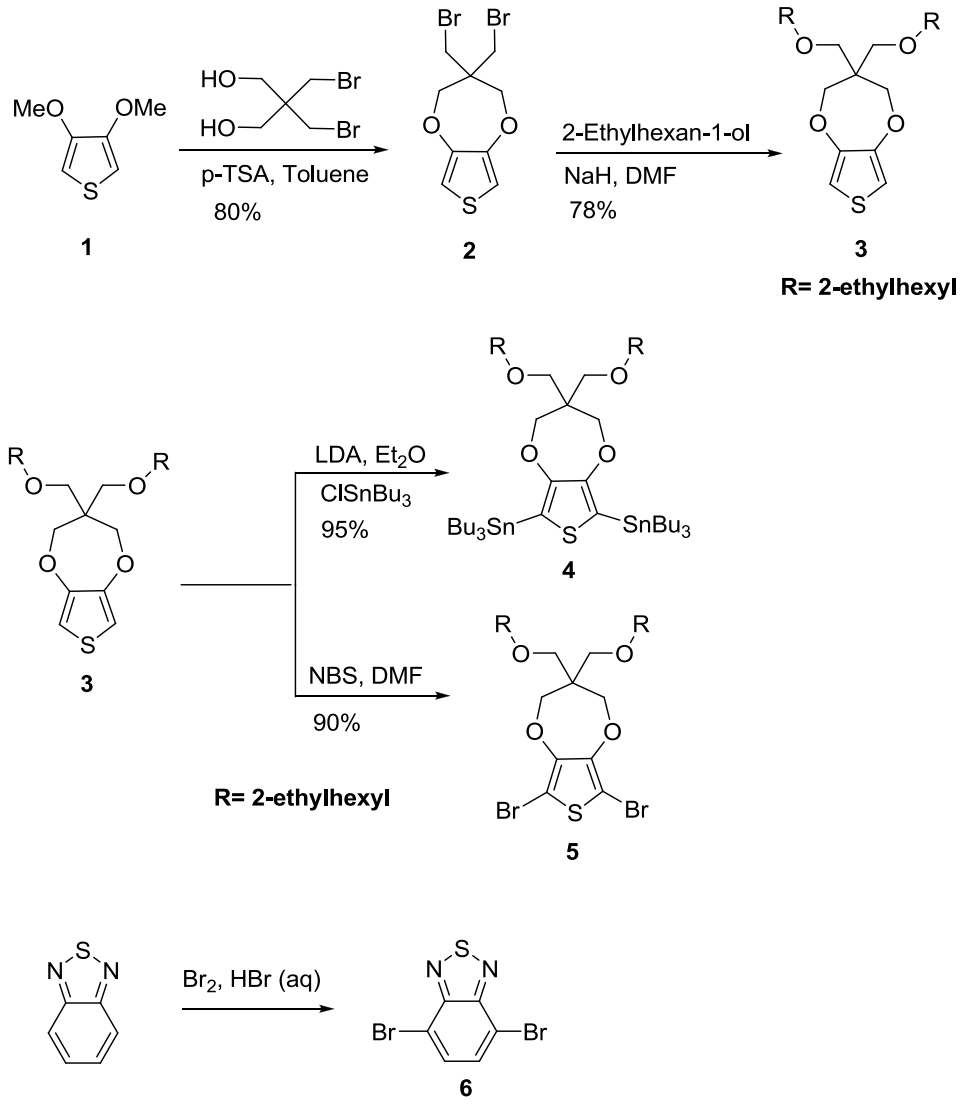

Figure 3-3. Reaction scheme for the synthesis of ditin compound **4** and dibromo compounds **5** and **6** for random Stille polymerization.

The first attempt at making compound **4** was carried out in THF, and *n*BuLi was used as a deprotonation agent. This process involved the formation of an aromatic dilithium salt at room temperature. However, at such a high temperature (25°C), the solvent THF was decomposed by *n*BuLi[204] and the resulting impurities could not be separated from the crude product mixture. The proposed reaction is shown in Figure 3-4. Ethylene and the acetaldehyde lithium enolate were formed during the decomposition of THF via a reverse [3+2] cycloaddition,[205] where the later enolate ion was a much

weaker nucleophile than *n*BuLi, and could not react with the protons on the 2 and 5 position of thiophene rings.[206-208] After quenching with tributyltin chloride, the enolate was converted to an organotin compound, which could not be separated from compound **4**.

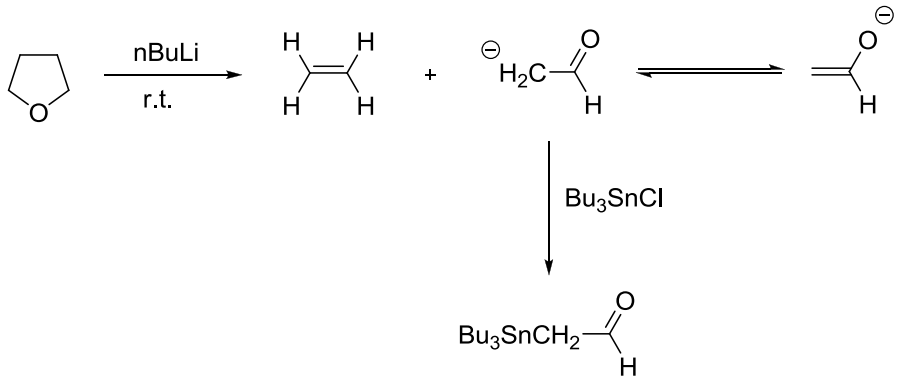

Figure 3-4. Proposed reaction scheme for the impurities in the synthesis of compound **4** using THF as a solvent.

In order to avoid this situation and improve the reaction yield, diethyl ether was used instead of THF, and fresh LDA, which was made by reacting diisopropylamine with *n*BuLi, was used as an alternative deprotonation agent. Using the conditions described in Section 3.8, no decomposition of the solvent or the starting material was observed. After flash column chromatography with hexane as an eluent on treated silica gel (washed with neat triethylamine, then hexane), compound **4** was achieved in 95% yield. It is worth mentioning that compound **4** decomposed in the column, even though the silica gel was treated. The monotin compound could be observed under ^{1}H NMR after silica gel purification, and was estimated to comprise 2% of the total composition of the product; on the other hand, the crude NMR showed no trace of monotin compound or unreacted starting material compound **3**. This observation provided a motivation for searching for new purification methods such as neutral or basic alumina filtration

instead of flash column, since most of the impurities in this reaction was stannanamine, which should be readily absorbed by alumina.

The preparation of compounds **5** and **6** was performed under traditional bromination conditions using NBS and bromine, respectively. The difficulty of purifying compound **5** was reduced by using highly pure compound **3** and recrystallized NBS as starting materials, affording a high reaction yield of about 90%. However, the purification of compound **6** is more challenging as the recrystallization of the crude product does not eliminate the light yellow impurities. Column chromatography was always applied in order to achieve a white crystalline compound **6**, but this process consumed a large amount of solvent because of the low solubility of compound **6** in hexane, which is the only proper eluent for this separation (more polar eluent will extract the impurities and wash them out). A more efficient and low cost chromatography technique solved this problem. As shown in Figure 3-5, the impure solid mixture was dispersed on top of silica gel in an addition funnel. Then hexane was refluxed, condensed and dripped on the crude product. The extracted materials were passed through the silica gel, and the impurities were absorbed by stationary phase (silica gel). Eventually, pure compound **6** was recovered in the round bottom flask. By recycling the solvent hexane, a large scale purification of **6** can be achieved in a cost-effective manner.

It is necessary to emphasize the importance of obtaining a high purity level of monomer compounds **4**, **5** and **6**. Because the Stille polymerization is a step-growth polymerization, a high conversion is required in order to achieve high molecular weight polymers. Without considering the reaction time, which is assumed to be infinite in this case, the stoichiometric control of the bifunctional monomers becomes the only factor

that can affect the number average degree of polymerization (X_n). In other words, the existing non-functional and monofunctional monomers, the impurities, and inaccurate weighing of the starting materials may cause a deviation from stoichiometric balance of the functional groups, thereby lowering the polymer molecular weight and expanding the polydispersity index.

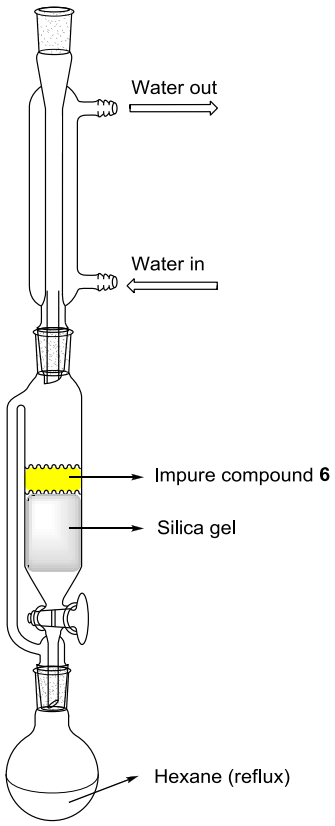

Figure 3-5. Demonstration of purifying compound **6** by recycling the eluent hexane. The condensed hexane will drip on the impure compound **6**; extract the pure compound, which passes through the silica gel. The impurities are absorbed by the silica gel.

3.2.2 Random Stille Polymerization with Multi Monomers

As described in the general introduction (Chapter 1, Section 1.3.4), to produce a random step growth polymerization, a minimum of three monomers is required when using bifunctional monomers bearing the same reaction functionality. In this case, we

chose ditin compound **4** and two dibromo compounds **5** and **6** to simulate the ratios of donors and acceptors. As long as the number of -Br functionality equals that of the –$SnBu_3$ functionality, the Stille polymerization will proceed without any difficulty. Moreover, judging by the reactive sites as well as the chromophore cores of the monomers, where monomer **4** and **5** are sharing the same core unit structure (ProDOT-$(CH_2OEtHx)_2$, Figure 3-2), there will always be an odd number of ProDOT units between any two BTD units in the same polymer backbone.

The polymerization was accomplished using Stille polymerization with $Pd_2(dba)_3$/P(o-tolyl)$_3$ as the catalyst system and toluene as the solvent. Five polymerizations with different donor-acceptor ratios were carried out in order to determine optimal ratio to produce a polymer absorbing broadly and evenly across the entire visible region. Before being characterized, all the polymers were purified via a Soxhlet extraction process to remove any unreacted monomer, low molecular weight oligomers and polymers as well as palladium catalyst. The polymers are highly soluble in common organic solvents such as chloroform, DCM, THF and toluene (> 10 mg/mL). Table 3-1 shows the GPC results and elemental analysis results for these polymers. All the polymers had number average molecular weights (M_n) from 10.5 to 14.4 kDa, except for **ECP-1** at around 9.7 kDa. Due to the successful elimination of low molecular weight materials by Soxhlet extraction, the PDI of the polymers ranges from 1.3 to 1.6, which is lower than the PDI of a typical step-growth polymerization. The low PDI also indicates that all the chains in the same polymer have similar conjugation lengths and thus the same optical and electronic properties. Furthermore, a good agreement of the

elemental analysis results with the calculated values confirmed that the monomers were polymerized according to the ratios predetermined.

Table 3-1. GPC estimated molecular weights in THF and elemental analysis of the polymers (Adapted with permission from Ref. 202 Copyright 2010 WILEY-VCH Verlag GmbH & Co. KGaA, Weinheim)

	Monomer **4** ratio	Monomer **5** ratio (x)	Monomer **6** ratio (y)	M_n (kDa)	M_w (kDa)	PDI	EA (Calcd/Found)		
							C	H	N
ECP-1	1	0.6	0.4	9.7	15.5	1.6	67.08/66.79	9.51/9.22	1.48/1.39
ECP-2	1	0.7	0.3	10.9	15.2	1.4	67.70/66.99	9.23/9.10	1.07/1.12
ECP-3	1	0.75	0.25	10.5	14.3	1.4	67.83/64.01	9.31/9.10	0.87/0.84
ECP-4	1	0.76	0.24	11.0	14.2	1.3	67.86/66.88	9.32/9.24	0.84/0.96
ECP-5	1	0.8	0.2	14.4	19.0	1.3	67.97/63.44	9.38/8.87	0.69/0.75

3.2.3 Absorption Control of Polymers by Varying the Monomer Ratios

The UV-visible absorption spectra of the polymers in chloroform are shown in Figure 3-6a. A broad spectral absorption is evident ranging from approximately 400 nm to greater than 700 nm for each polymer. Unlike the spectra of typical donor-acceptor polymers, which generally have two distinct absorption bands, the spectra of polymers **ECP-1** to **ECP-5** show a “merging” of the short- and long-wavelength optical transitions, and no obvious peak-to-peak window is observed. As expected, **ECP-1** exhibits the lowest intensity of the short-wavelength absorption at 461 nm due to its relatively low concentration of electron-rich moiety. Considering the reduced absorption of blue and green light (400-580 nm), as well as an absence of far-red light absorption from 700 to 750 nm, it is reasonable that the solution of **ECP-1** gives a midnight blue color.

By increasing the relative amount of ProDOT-$(CH_2OEtHx)_2$ repeat unit, the difference in intensity between the two absorption bands is reduced. At a specific point where the donor/acceptor ratio is approximately 7 to 1, the intensities of the two bands are balanced, and homogenous absorptions across most of the visible spectrum (450-650 nm) are observed for **ECP-3** and **ECP-4**. Not surprisingly, solutions of **ECP-3** and

ECP-4 show a similar dark-purple-black color due to the lack of absorption in the far blue and red regions. Accordingly, the absorption of **ECP-5** shows a higher intensity of the high energy transition (530 nm) than the low energy transition (572 nm) as the increase of the donor concentration, and the solution of **ECP-5** exhibits a bright purple color due to the increased reflection/transmission of red light.

a)

b)

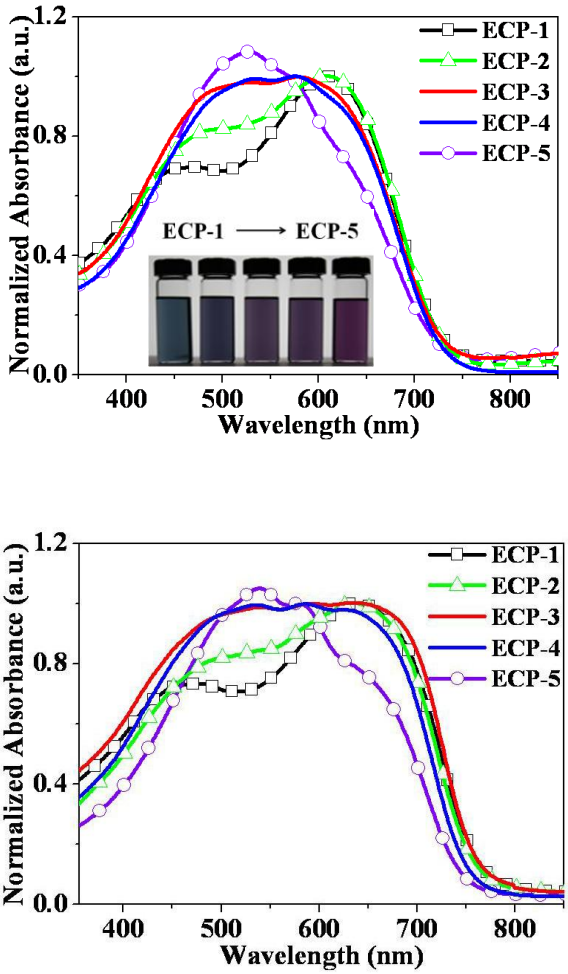

Figure 3-6. Uv-vis absorption spectra of polymers. a) Solution absorption of Polymer **ECP-1** (monomers ratio: x=0.6, y=0.4), **ECP-2** (x=0.7, y=0.3), **ECP-3** (x=0.75, y=0.25), **ECP-4** (x=0.76, y=0.24) **ECP-5** (x=0.8, y=0.2) in chloroform. The inset shows the various colors obtained across the polymer series. b) Normalized film absorption of Polymer **ECP-1**, **ECP-2**, **ECP-3**, **ECP-4** and **ECP-5**. (Adapted with permission from Ref. 202 Copyright 2010 WILEY-VCH Verlag GmbH & Co. KGaA, Weinheim)

Thin films of each polymer were then spray-cast onto indium tin oxide (ITO) coated glass slides from toluene solution (2 mg mL^{-1}). The visible absorption spectra of the films shown in Figure 3-6b exhibit a broadening of the long wavelength absorption with little to no change at the higher energy end in the solid state compared to solutions for all five polymers. The significant extension of absorption into the far red region is important, as it leads to a more pure black color of the films. As determined from the onset of their neutral-state lower-energy optical transitions, the polymers have relatively low band gaps ranging from 1.6-1.7 eV.

From these results, we observe that the absorptions of the polymers are sensitive to small changes in the donor-acceptor ratios. For example, by lowering the acceptor ratio from 0.25 to 0.24, **ECP-4** shows a slightly narrowed absorption with an observable increase in the intensity of the high energy transition compared to **ECP-3** in both the polymer solution and the solid film. However, this change can be detected only by a UV-Vis spectrophotometer and it is not distinguishable by the human naked eye.

3.2.4 Polymerization Repeatability

The importance of polymerization repeatability has been discussed in Chapter 2. A detailed study on the repeatability of the synthesis of the black-to-transmissive ECPs was carried out. The GPC results in Table 3-2 show that all the polymers had similar molecular weights, a crucial parameter related to the polymer solution viscosity. Considering the applications of these polymers, which require the polymers to be processed from a solution into solid films by printing or spray casting, it is important to reproduce polymers in batches with minimal deviations in molecular weights and with similar solution viscosities. Furthermore, it is worth mentioning that the polymerization is also scalable. For example, 3.3 g of **ECP-4-s2** was prepared successfully in our lab,

and our collaborators in BASF were able to reproduce polymers with the same monomer ratio as **ECP-3** in a 30 g scale (Chapter 2, Section 2.2 for more details).

Table 3-2. GPC estimated molecular weights of reproduced polymers.

	Monomer **4** ratio	Monomer **5** ratio (x)	Monomer **6** ratio (y)	M_n (kDa)	M_w (kDa)	PDI	Yield (%)
ECP-3	1	0.75	0.25	10.5	14.3	1.4	50
ECP-3-s1	1	0.75	0.25	11.1	14.4	1.3	65
ECP-3-s2	1	0.75	0.25	10.2	13.7	1.3	67
ECP-3-s3	1	0.75	0.25	10.5	15.0	1.4	83
ECP-4	1	0.76	0.24	11.0	14.2	1.3	80
ECP-4-s1	1	0.76	0.24	12.7	18.2	1.4	72
ECP-4-s2	1	0.76	0.24	12.0	19.0	1.6	83
ECP-6	1	0.735	0.265	18.0	29.0	1.6	83
ECP-7	1	0.74	0.26	12.0	17.1	1.5	89

Polymers **ECP-3-s1**, **ECP-3-s2** and **ECP-3-s3**, which share the same monomer feed ratio with **ECP-3**, are consistent with **ECP-3** in terms of number average molecular weight (M_n) and PDI. More importantly, no obvious difference was detected for the polymer solution absorption by either the spectrophotometer or the human eye (Figure 3-7a). In another example, polymers **ECP-4-s1** and **ECP-4-s2** were synthesized utilizing the same monomer ratio as polymer **ECP-4**. As expected, the three polymers showed the same solution absorption in the visible region (Figure 3-7b).

Moreover, two additional random copolymers **ECP-6** and **ECP-7** were prepared with a small variation in the monomer feed ratio (Table 3-2). In Figure 3-7c, the absorption of **ECP-6**, which has a lower concentration of donor moieties, shows a lower intensity for the high energy transition (530 nm) compared the low energy transition (600 nm). By increasing the donor/acceptor ratio from 1.735:0.265 to 1.74:0.26 (the donor ratio here is the sum of monomer **4** and monomer **5** ratios), polymer **ECP-7** showed relatively higher absorption intensity in the high energy transition. The results

here confirmed the observation that the polymer absorption feature is really sensitive to a small change in the polymer structure (Section 3.2.3).

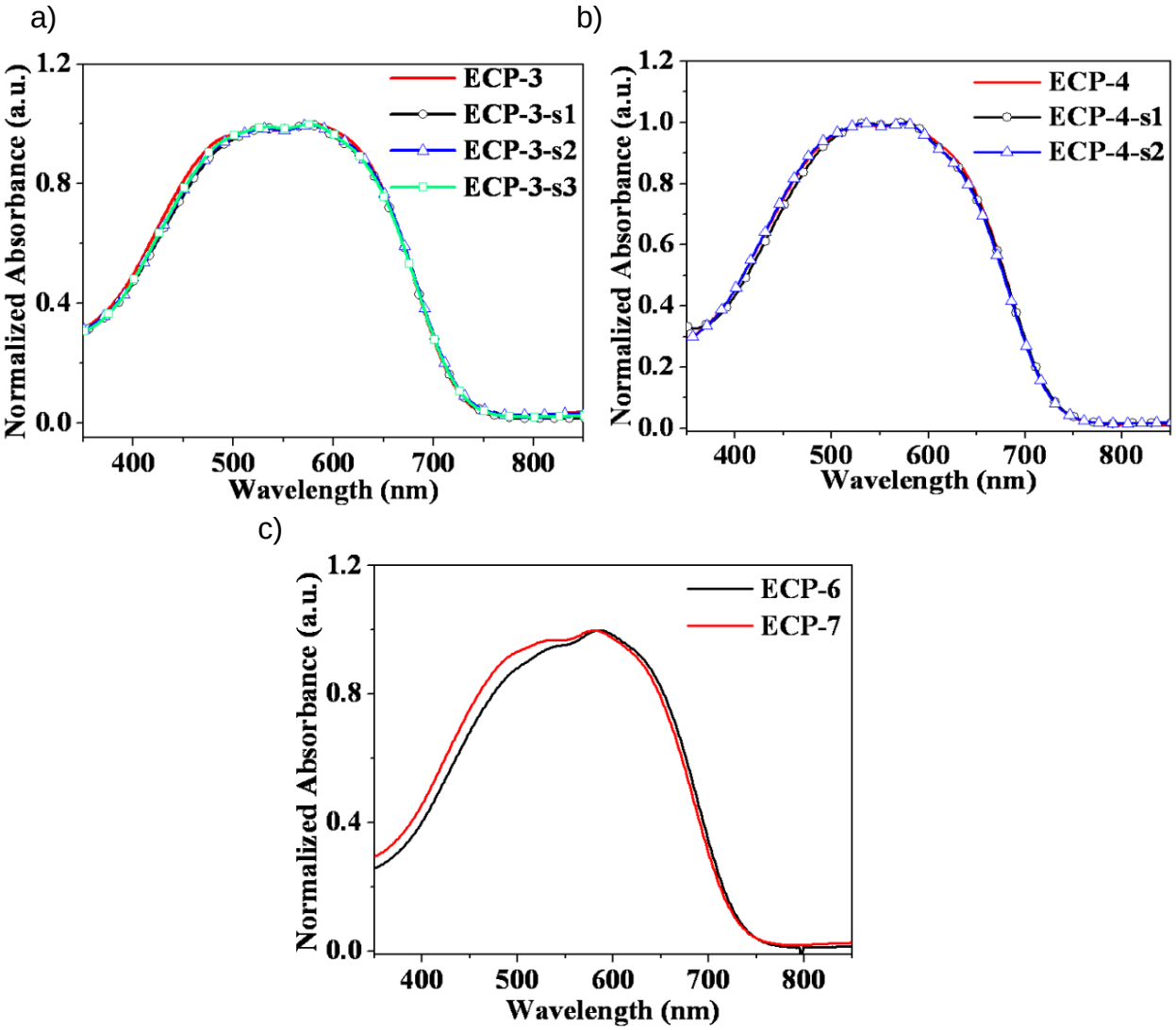

Figure 3-7. Normalized solution absorption of polymers in chloroform a) **EPC-3**, **EPC-3-s1**, **EPC-3-s2** and **EPC-3-s3** (x=0.75, y=0.25). b) **ECP-4**, **ECP-4-s1** and **ECP-4-s1** (x=0.76, y=0.24), c) **ECP-6** (x=0.735, y=0.265) and **ECP-7** (x=0.74, y=0.26).

3.2.5 Polymer Thermal Analysis

The thermal stability of **ECP-3** and **ECP-4** was studied by TGA in a nitrogen atmosphere. The thermograms displayed in Figure 3-8 show that the polymers exhibit a high thermal stability until the temperature reaches 330°C, and then a drastic

degradation process occurs from this temperature up to around 600°C. Moreover, the two polymers processed the same thermal profile, indicating that the thermal stability is not affected by changing the polymer donor-acceptor ratio.

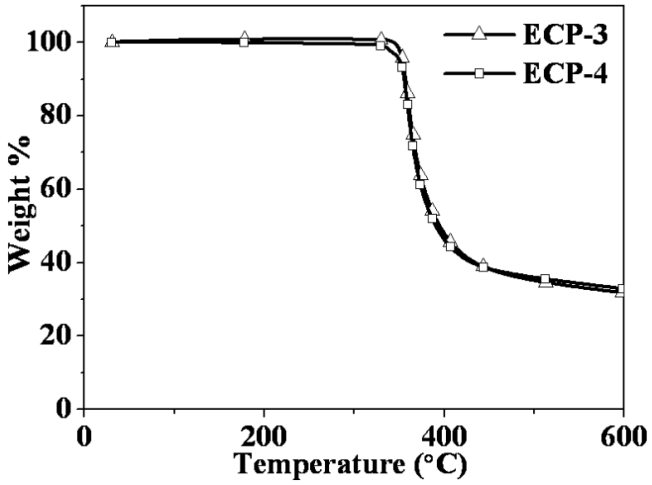

Figure 3-8. Thermogravimetric analysis of polymer **ECP-3** and **ECP-4**. The experiments were carried out using high-resolution dynamic scans under nitrogen atmosphere.

3.3 Polymer Electrochemistry and Spectroelectrochemistry

3.3.1 Electrochemistry Studies

The redox properties of **EPC-3** were studied by electrochemistry. The polymer was deposited on a Pt button electrode by drop-casting from a dilute toluene solution. Differential pulse voltammetry (DPV) was recorded in 0.1 M $TBAPF_6$/propylene carbonate (PC) electrolyte solution with a Pt foil counter electrode and a Ag/Ag^+ reference electrode. An onset of oxidation ($E_{onset,ox}$) of -0.04 V and reduction ($E_{onset,red}$) of -1.64 V *vs.* Fc/Fc^+ were determined (Figure 3-9). According to the results, the polymer has a HOMO energy level of about -5.1 eV, a LUMO energy level of -3.5 eV and a band gap (E_g) of 1.6 eV, which agrees well with the optical band gap (1.6 eV) determined from the onset of the polymer film neutral-state lower-energy optical transition (Section 3.2.3).

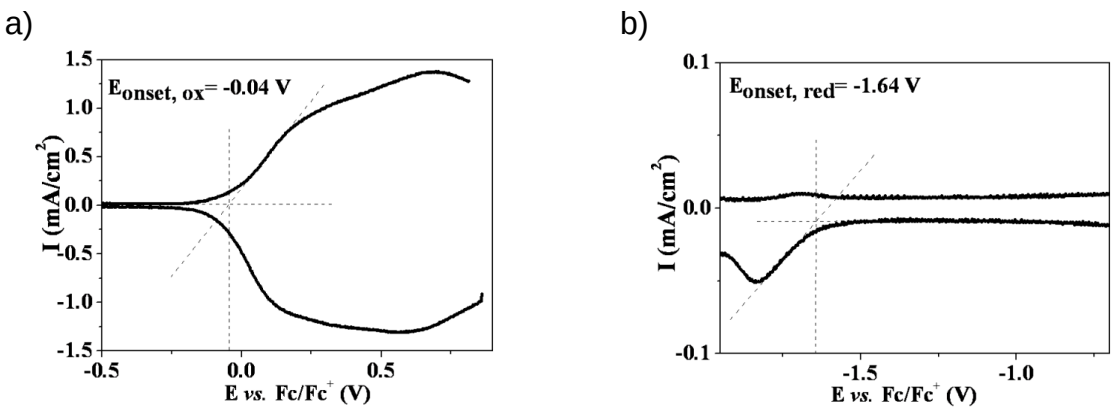

Figure 3-9. Differential pulse voltammetry of **ECP-3** drop-cast from toluene solution onto platinum button electrode (A= 0.02 cm^2). Measurements were performed in 0.1 M $TBAPF_6$/propylene carbonate (PC) with a Pt foil counter electrode and a Ag/Ag^+ reference electrode calibrated *vs.* Fc/Fc^+ ($E_{Fc/Fc+}$ = 0.087 V *vs.* Ag/Ag^+). a) Oxidation. b) Reduction. (Adapted with permission from Ref. 202 Copyright 2010 WILEY-VCH Verlag GmbH & Co. KGaA, Weinheim)

3.3.2 Spectroelectrochemistry Studies

Spectroelectrochemical behavior of an **ECP-3** thin film is shown in Figure 3-10a. The spray-cast film was redox cycled to a stable and reproducible switch prior to the analysis, and then electrochemically oxidized from -0.25 to +0.35 V *vs.* Fc/Fc^+ (in 25 mV steps) using a silver wire as a quasi reference electrode (calibrated against Fc/Fc^+) and a platinum wire as the counter electrode. Upon oxidization of the polymer, the broad absorption in the visible region is depleted, and a polaronic transition in the near-IR (800-1200 nm) arises, and then falls and merges into a bipolaronic transition, which appears further into the NIR region. When fully oxidized, the generated bipolaronic absorption peaks beyond 1600 nm, which allows effective bleaching of the visible absorption and a remarkably high level of transmissivity to the human eye.

In order to further accentuate the optical changes that occur upon oxidation, the electrochromic response is shown in terms of transmissivity across only the visible region in Figure 3-10b from 350 nm to 750 nm. For a film of **ECP-3** in its neutral state, a

nearly flat transmittance profile at 20% from 450 nm to 700 nm is observed. A small range of visible blue light (400- 450 nm) and red light (700-750 nm) are not absorbed as strongly as the other parts of the visible region. On the other hand, when the film is fully oxidized, the transmittance increases to above 60% through most of the visible region. The electrochromic contrast (as percent transmittance change, $\Delta\%T$) is as high as 48% at 555 nm, the wavelength at which the human eye has greatest sensitivity. However, the bleaching of the film leaves an uneven transmittance in the visible region; more blue and green light (400-500 nm) is transmitted compared to the remainder of the visible region, giving the film a faint residual color.

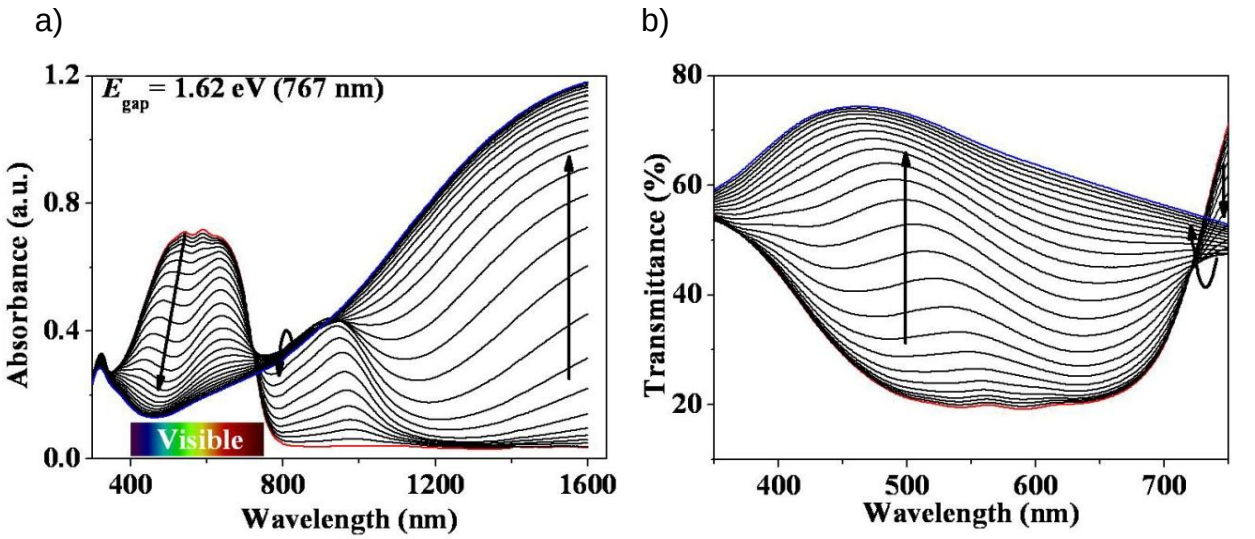

Figure 3-10. Spectroelectrochemical behavior of an **ECP-3** thin film. a) Spectroelectrochemistry of **ECP-3**. The films were spray-cast onto ITO-coated glass from toluene (2 mg mL^{-1}). Electrochemical oxidation of the films was carried out in 0.1 M LiBTI/PC, supporting electrolyte using a silver wire as a quasi reference electrode (calibrated against Fc/Fc^{+}), and a platinum wire as the counter electrode. The applied potential was increased in 25 mV steps from -0.25 to + 0.35 V *vs.* Fc/Fc^{+}. b) Electrochromic response in terms of transmissivity in the visible region (replotted from Figure 3-10a). (Adapted with permission from Ref. 202 Copyright 2010 WILEY-VCH Verlag GmbH & Co. KGaA, Weinheim)

3.4 Polymer Colorimetric Analysis

To evaluate the color changes of the ECPs occurring on electrochemical switching (on the basis of the “Commission Internationale de l’Eclairage” 1976 *L*a*b** color standards), three **ECP-3** films with varying thicknesses were subjected to colorimetric analysis. Here, *L** represents the lightness of the color (0= black, 100= diffuse white), *a** represents how much red versus green (red for +*a** values and green for -*a** values), and b* represents how much yellow versus blue (yellow for +*b** values and blue for-*b** values). Figure 3-11a shows the determined CIE 1976 *L** values as a function of applied voltage. This gives an indication of relative brightness of the film as it is oxidized while illuminated from behind (transmission mode) with a standard D50 simulated daytime light source. In their neutral state, the polymer films exhibit *L** values from 46 for the thickest film to 75 for the thinnest film. Importantly, the film with absorption maximum of 1.1 a.u. displays a deep black color with *a** and *b** values as low as 3 and -11. This observation is consistent with the visible absorption spectra of the **ECP-3** thin film as a small amount of red and slightly more blue light is transmitted by the polymer. In comparison, the fully oxidized polymer films exhibit high *L** values from 82 to 92 with smaller *a** and *b** values, demonstrating that this polymer is able to reach a highly transmissive near-colorless state as defined by the *L*a*b** color coordinates. Moreover, based on the trace of the *L** change, all the films start to be oxidized at around -0.1 V *vs.* Fc/Fc^{+}, which agrees well with the polymer onset of oxidation (Section 3.3.1). Also, the films reach their high transmissive state in a 0.6 V window.

a)

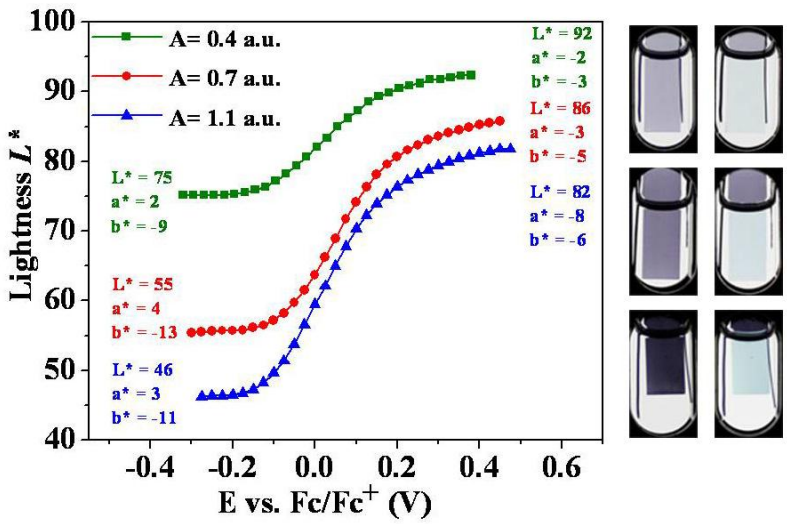

b)

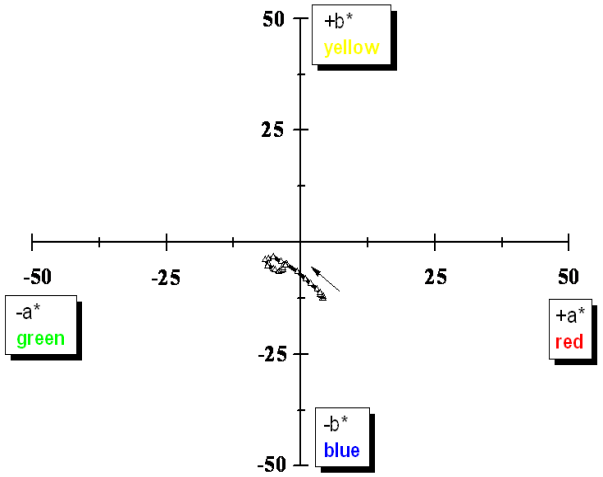

c)

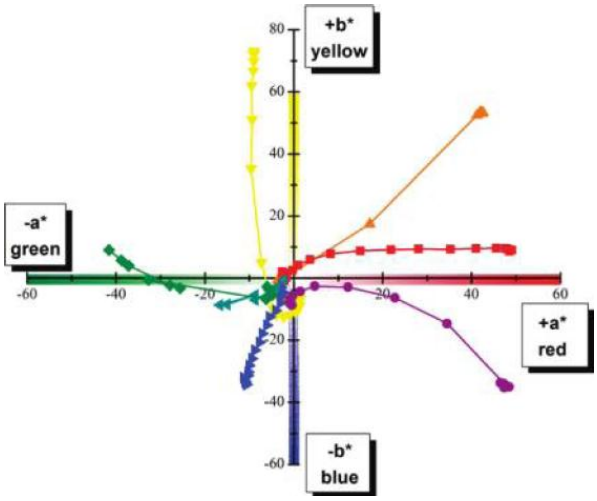

Figure 3-11. Colormetric analysis of **ECP-3** thin films. a) Lightness (*L**) as a function of applied potential for spray-coated **ECP-3**. *L*a*b** values of fully neutral and oxidized states are reported for the films. Photographs are of the fully neutral (left) and fully oxidized films (right). (Adapted with permission from Ref. 202 Copyright 2010 WILEY-VCH Verlag GmbH & Co. KGaA, Weinheim) b) Plot of CIE 1976 *a*b** color coordinates showing calculated values of **ECP-3** as a function of applied potential. c) CIE 1976 *a*b** color coordinates showing calculated values of the seven vibrantly colored ECPs (orange triangle, ECP-orange; red square, ECP-red; purple circle, ECP-magenta; blue right-facing triangle, ECP-blue; teal left-facing triangle, ECP-cyan; green, diamond, ECP-green; and yellow downward-facing triangle, ECP-yellow) as a function of applied potential. The polymer neutral states are furthest from the origin and the values track toward the origin as the polymer is oxidized to the bleached state. (Adapted with permission from Ref. 136 Copyright 2011 American Chemical Society)

Figure 3-11b shows a typical *a** and *b** color track of **ECP-3** film during oxidation (A= 0.7 a.u.). As we can see, the color of the neutral polymer film falls into a red-blue region, which presents a dark purple color (*a**= 4, *b**= -13). As the polymer is oxidized, the *a** and *b** values decrease, indicating a loss of color, with the fully oxidized state having a highly transmissive faint blue green tint (*a**= -3, *b**= -5). It is worth mentioning that *a***b** values of **ECP-3** are changed in a rather small range, which is close to the achromatic point (*a**= 0, *b**= 0), while *a***b** values of electrochromic polymers ECP-orange, ECP-red, ECP-magenta, ECP-blue, ECP-cyan, ECP-green and ECP-yellow are reduced in magnitude as the saturation of the color is switched to a bleached state. (Figure 3-11c).[136]

3.5 Polymer Switching Study

3.5.1 Polymer Switching Rate

Given that the speed at which electrochromic materials change color states is important in display-type devices, the film switching rate was examined by monitoring the transmittance change at a single wavelength (EC contrast, $\Delta\%T$) as a function of time by applying square-wave potential steps for periods of 10, 2 and 1 s. As shown in Figure 3-12a, a transmittance change (monitored at 540 nm) as high as 47% is recorded at the longer switch time (10 s). By decreasing the switch time to 1 s, the transmittance change is reduced to 42% with a 5% contrast lost.

Moreover, the switching rate was limited by the diffusion and migration of charge balancing counter ions within the polymer films because the electronic and ionic effects are strongly coupled. Thus the largest fraction of the redox process usually occurs within the first portion of the voltage pulse. Considering this, the switching times to reach anywhere from 90 to 95 or 98% of the full optical contrast, which can be

considerably shorter than that of the full optical switch, are also reported in many display characterizations. In this case, by taking a close look at the feature of a 10 s switching time cycle, it takes only 1.6 s to reach a 95% contrast (ΔT = 45%) when the polymer is switched from its colored state to bleached state. Interestingly, the time for a 95% switching contrast from fully bleached state to colored state is much less than the time for the reverse process (0.8 s compared to 1.6 s), which is possibly due to the repulsion from the polymer network on the counter ions. Clearly, it is much easier to eliminate the counter ions than to absorb them.

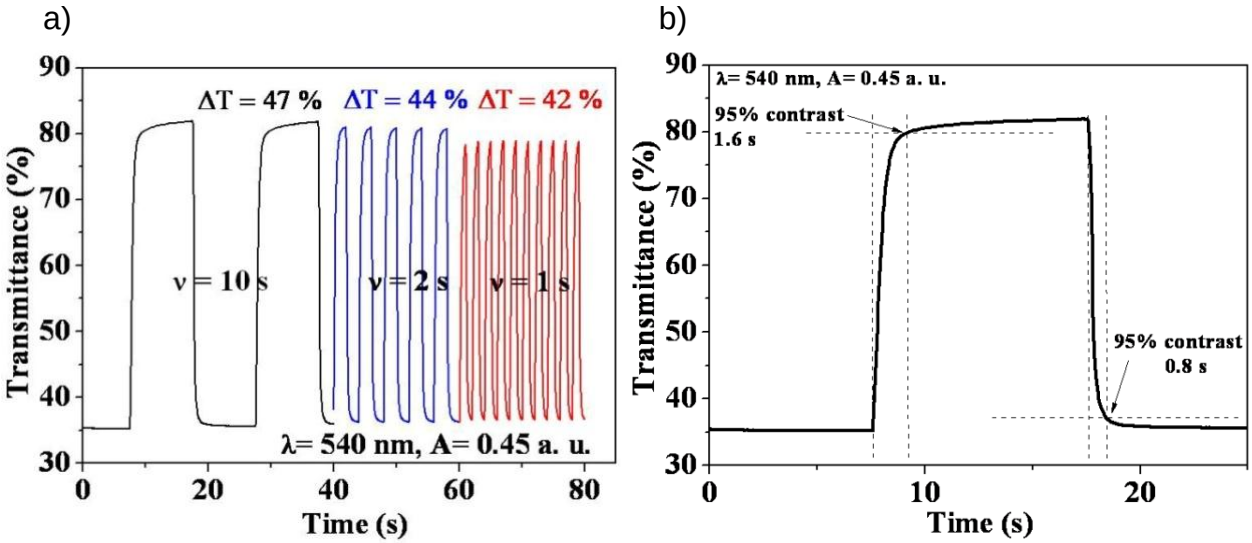

Figure 3-12. Switching speed study of polymer **ECP-3**. a) Square-wave potential-step chronoabsorptometry of **ECP-3** spray-coated on ITO (monitored at 540 nm, -0.72 to +0.48 V *vs.* Fc/Fc^+ in 0.1 M LiBTI/PC electrolyte solution). The step times (10 s, 2 s and 1 s) are indicated on the figure. b) Percent transmittance and time to reach 95% of the full optical contrast. (Adapted with permission from Ref. 202 Copyright 2010 WILEY-VCH Verlag GmbH & Co. KGaA, Weinheim)

3.5.2 Polymer Switching Stability

The long-term stability to repeated redox switching is essential to the practical utilization of these materials in EC devices. Therefore, the EC contrast ($\Delta\%T$ at 540 nm) of a film was monitored while repeated square-wave potential steps of 1.5 s (complete

cycle is 3 s, switching between -0.72 to +0.48 V *vs.* Fc/Fc^{+}) for 18,000 cycles were applied. As shown in Figure 3-13, polymer **ECP-3** exhibits a continuous switching stability with a decrease of only 8% in electrochromic contrast over this time period, most of which happening in the beginning of the experiment. Moreover, it is necessary to point out that the stability study was performed in a LiBTI/PC solution and the system was not properly sealed. The stability of the polymer will possibly improve by keeping oxygen and water out of the system.

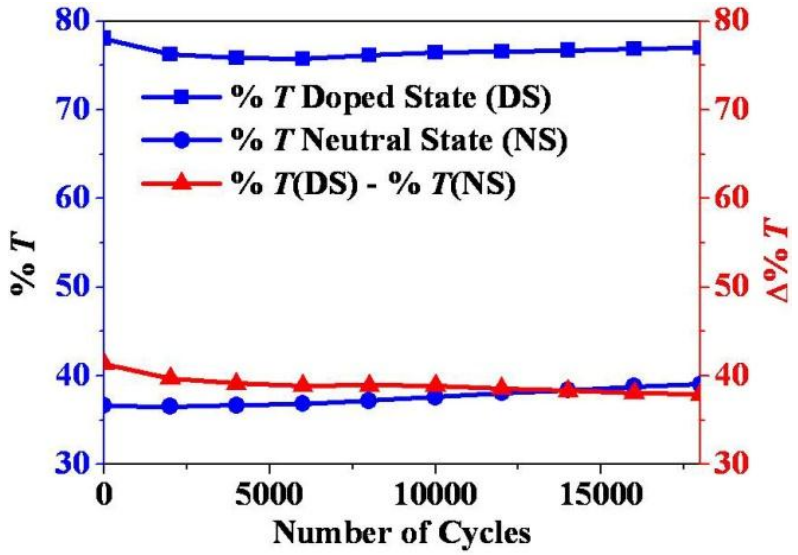

Figure 3-13. Long-term stability study via square-wave potential stepping while monitoring electrochromic switching of **ECP-3** at 540 nm in 0.1 M LiBTI/propylene carbonate solution switching between -0.72 to +0.48 V (*vs.* Fc/Fc^{+}), and with a switch time of 18,000 cycles (1.5 s step). In blue: %*T* of oxidized and reduced states, and in red: Δ%*T*, as a function of the number of cycles. (Adapted with permission from Ref. 202 Copyright 2010 WILEY-VCH Verlag GmbH & Co. KGaA, Weinheim)

3.6 Electrochromic Devices

3.6.1 Black-to-Transmissive Electrochromic Window

To further reinforce the utility of these polymers, we have demonstrated black-to-transmissive switching in an absorptive/transmissive window-type electrochromic device. Using the device structure as detailed in Chapter 1 (Section 1.6.1, Figure 1-

16a), the polymer **ECP-3** was utilized as the active switching material at the working electrode, and a minimally color-changing polymer (N-alkyl substituted poly(3,4-propylenedioxypyrrole)), which is similar to that previously described by our group,[150] was used as the charge-balancing material at the counter electrode. As shown in Figure 3-14a, the transmittance spectra of the device in both the dark state and transmissive state were measured across the visible region from 400 to 750 nm. Higher transmittance in the blue region is observed when the polymer is in the oxidized state, giving a highly transmissive light blue color. Conversely, when the polymer is neutralized at a device cell potential of -0.6 V, the transmittance decreases to a near featureless spectral profile. The device contrast is about 40% at 555 nm.

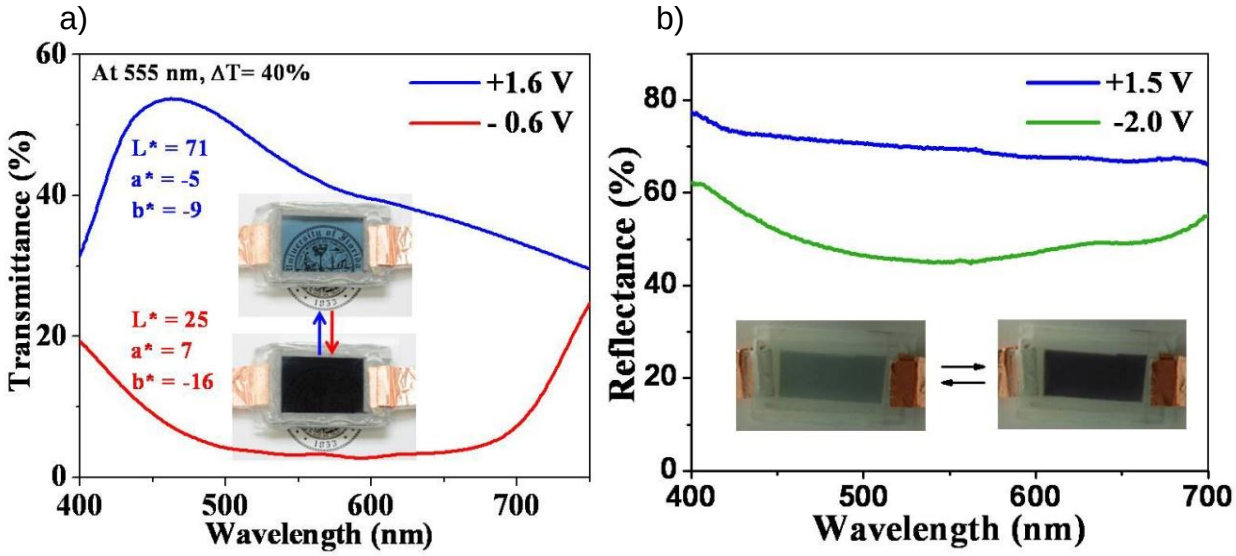

Figure 3-14. Window type and display type electrochromic devices using **ECP-3** as an active layer. a) Transmittance spectra of ECD in extreme states of highly absorptive (at an applied cell voltage of -0.6 V) and highly transmissive (at an applied cell voltage of +1.6 V). The insets show photographs of the same device in both states. b) Reflectance spectra of ECD in extreme states of highly absorptive (at an applied cell voltage of -2.0 V) and highly reflective (at an applied cell voltage of 1.5 V). The insets show photographs of the same device in both states. (Adapted with permission from Ref. 202 Copyright 2010 WILEY-VCH Verlag GmbH & Co. KGaA, Weinheim)

3.6.2 Black-to-Transmissive Electrochromic Display

Additionally, an absorptive/reflective display-type device was constructed utilizing polymer **ECP-3** as the active electrochrome (Figure 3-14b). When oxidizing potentials are applied across the device, the reflectance in the visible region begins to increase as the polymer becomes faded, which allows more light to pass through the film and be reflected by the TiO_2 layer. A reflectance change of 25% was observed at 555 nm.

3.7 Chapter Summary

The incorporation of the donor-acceptor theory with the random Stille polymerization method allows precise control of the absorption spectra of conjugated polymers. By varying monomer feed ratios, black-to-transmissive ECPs with broad and uniform visible absorptions were synthesized and characterized. More importantly, this type of polymerization was proved to be an efficient way to produce ECPs with highly reproducible M_n, optical and electronic properties between different runs. The resulting polymer showed a high optical contrast (> 40%), rapid redox switching (1 s for $\Delta\%T$= 42%) and long-term redox stability (>18,000 cycles). The performance of the polymers was further evaluated through the construction of a series of ECDs and showed promising results.

While the project described in this chapter was underway, the synthesis of a new black-to-transmissive ECP was reported by Önal and coworkers.[198] The polymer was afforded via electrochemical polymerization of two donor–acceptor systems, 2-decyl-4,7-bis(3,3-didecyl-3,4-dihydro-2H-thieno[3,4-b][1,4]dioxepin-6-yl)-2H-benzotriazole and 2-decyl-4,7-bis(3,3-didecyl-3,4-dihydro-2H-thieno[3,4-b][1,4]dioxepin-6-yl)-2,1,3-benzoselenadiazole in a 1:4 feed ratio (Figure 3-15). Surprisingly, the polymer did not show encouraging EC properties. Although the polymer could be switched from a dark

black neutral state to a dark gray oxidized state, the transmittance change was only 15.3% (*T*% from 7.8% to 23.1%) when fully oxidized.

From a chemistry point of view, it is difficult to achieve homogenous polymers via electropolymerization. For instance, there are always unreacted monomers, small oligomers as well as electrolytes and solvents, trapped in the polymer networks. Moreover, control of the polymerization process is difficult, and thus conjugated polymers with defects, cross-linked sites and large PDIs are usually generated. All these drawbacks may be the main reason that the material prepared by Önal *et al.* did not perform well in the switching study.[198]

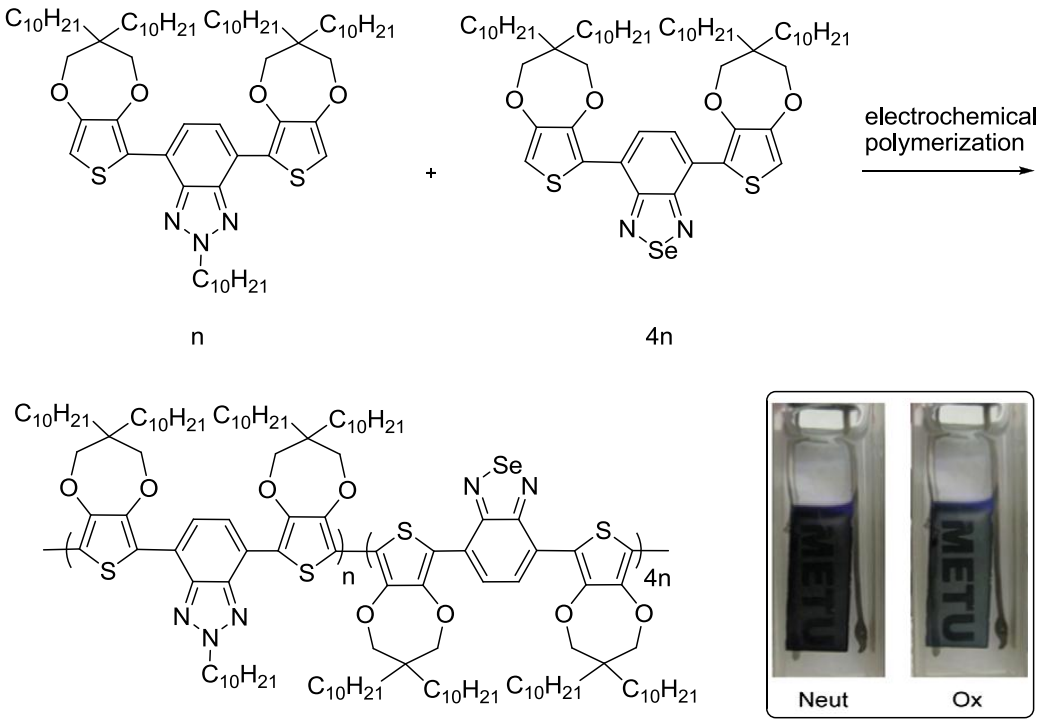

Figure 3-15. Synthesis of copolymer via electrochemical polymerization. Photographs are of the fully neutral (left) and fully oxidized films (right). (Adapted and modified with permission from Ref.198)

However, this report also leads to a new idea for making perfect black-to-transmissive ECPs. Considering the absorption of **ECP-3**, which failed to cover part of

the blue light (380- 450 nm) and the red light (690-750 nm), it was logical that the polymer films showed a noticeable black purple hue. How to fill the absorption gaps has become an issue for the next generation ‘random black’. By taking a close look at the polymer structure demonstrated in the report discussed above, the authors coordinated two different acceptors (benzotriazole and benzoselenadiazole) and one donor (ProDOT) in the polymer backbone to achieve a broad absorption. According to the structure of ‘random black’, an extra stronger acceptor (for example thienopyrazine) is expected to expand the low energy absorption band to a much higher wavelength, while an extra weaker donor (for example dioxythiophene) will lower the high energy absorption band wavelength. The random Stille polymerization introduced in this chapter is expected to be an optimal route towards achieving such a system.

With regard to tuning the absorption band, the modification of polymer side chains is another interesting direction. By putting different side chains on polymers, the polymer solubility properties are changed, as well as its optoelectronic properties. One particular example is affording polymers with water solubility by grafting water soluble functional groups such as sulfonate, carboxylate, phosphonate and ammonium. This strategy will be investigated more thoroughly in Chapter 4.

3.8 Experimental Details

3,3-Bis(bromomethyl)-3,4-dihydro-2H-thieno[3,4-b][1,4]dioxepine (ProDOT($CH_2Br)_2$, 2) 3,4-dimethoxythiophene (9.52 g, 66 mmol), 2,2-bis(bromomethyl)propane-1,3-diol (35.5 g, 136 mmol), *p*-toluenesulfonic acid (1.26g, 6.6 mmol), and 300 mL toluene were combined in a 500 mL flask equipped with a soxhlet extractor with molecular sieves in a cellulose thimble. The solution was refluxed for 1 day. The reaction mixture was cooled, and after dilution with ether (100 mL), the

organic phase was washed with water and dried over anhydrous magnesium sulfate. The solvents were removed under vacuum, and the crude product was purified by column chromatography with hexane/ methylene chloride (4:1) as an eluent to obtain compound **2** as a white crystalline solid (22.5 g, yield: 80%). ^{1}H NMR ($CDCl_3$) δ 6.49 (s, 2H), δ4.10 (s, 4H), δ3.61 (s, 4H). ^{13}C NMR ($CDCl_3$) δ148.84, 105.95, 74.33, 46.37, 34.62. HRMS: *m/z* calcd for $C_9H_{10}Br_2O_2S$ (M^+): 339.8768 found: 339.8796. Anal. calcd for $C_9H_{10}Br_2O_2S$: C 31.60, H 2.95, found C 31.78, H 2.90.

3,3-Bis((2-ethylhexyloxy)methyl)-3,4-dihydro-2H-thieno[3,4-b][1,4]dioxepine (ProDOT(CH_2OEtHex)$_2$, 3) To a 250 mL flame dried round-bottom flask filled with 120 mL of DMF, 2-ethylhexan-1-ol (15.3 g, 117 mmol), and compound **2** (10 g, 29.2 mmol), NaH (5.3 g, 131 mmol) was added in portion. The reaction mixture was then heated at 110°C for overnight. After completion, the mixture was cooled and added into ice water slowly and extracted three times with ethyl ether. The organic layer was then washed three times with water and dried over magnesium sulfate, and the solvent was removed by rotary evaporation under reduced pressure. The resulting crude product was purified by flash column chromatography with hexane as an eluent to obtain compound **3** as colorless oil (10 g, yield: 78%). ^{1}H NMR ($CDCl_3$): δ 6.43 (s, 2H), δ4.02 (s, 4H), δ3.50 (s, 4H), δ3.31 (d, 4H, *J*= 5.7 Hz), δ1.58-0.86 (m, 30H). ^{13}C NMR ($CDCl_3$): δ149.95, 105.06, 74.46, 73.91, 70.10, 48.11, 39.90, 30.97, 29.40, 24.30, 23.36, 14.35, 11.40. HRMS: *m/z* calcd for $C_{25}H_{45}O_4S$ ($M+H^+$): 441.3033 found 441.3049. Anal. Calcd for $C_{25}H_{44}O_4S$: C 68.14, H 10.06, found C 68.50, H 10.17.

6,8-Bis(tributylstannyl)-3,3-bis((2-ethylhexyloxy)methyl)-3,4-dihydro-2H-thieno[3,4-b][1,4]dioxepine (4) A solution of n-butyllithium (16.0 mL, 20.4 mmol, 1.28

M in hexane) was added slowly to diisopropylamine (2.06 g, 20.4 mmol) in ether (50.0 mL) at -78°C. After stirring for 1 h at -78°*C*, the solution was warmed to room temperature and then cooled to 0°*C* in an ice bath. Compound **3** (3 g, 6.81 mmol) was added, and the mixture was warmed to room temperature and stirred overnight. After the reaction mixture was cooled to 0°*C* again, tributylchlorostannane (6.64 g, 20.4 mmol) was added. The mixture was stirred for 3 h at 0°*C*. After dilution with ether (100 mL), the organic phase was washed with water and dried over anhydrous magnesium sulfate. The solvent was evaporated and the residue was yellow oil and purified by flash chromatography with hexane as an eluent on treated silica gel (washed the silica gel with neat triethylamine, then hexane) to give 6.56 g (95%) of the title compound as colorless oil. ^{1}H NMR ($CDCl_3$): δ 3.89 (s, 4H), δ 3.46 (s, 4H), δ 3.30 (d, 4H, *J*= 5.4 Hz), δ 1.60-0.87 (m, 84H). ^{13}C NMR ($CDCl_3$): δ 156.59, 122.64, 74.42, 73.56, 70.40, 47.91, 39.84, 30.91, 29.37, 29.28, 27.48, 24.23, 23.33, 14.34, 13.94, 11.33, 10.80. Anal. calcd for $C_{49}H_{96}O_4SSn_2$: C 57.77, H 9.50, found C 58.04, H 9.62.

6,8-Dibromo-3,3-bis((2-ethylhexyloxy)methyl)-3,4-dihydro-2H-thieno[3,4-b][1,4]dioxepine (5) Compound **3** (2.0 g, 4.54 mmol) and NBS (2.02 g, 11.35 mmol) were added into a round-bottom flash and then degassed and refilled with argon 3 times. DMF (20 mL) was then added. The reaction mixture was stirred at room temperature for overnight, diluted with ethyl acetate (50 mL), and washed with water (2 times with 200 mL). The organic layer was dried with $MgSO_4$. After the solvent was evaporated, the residue was purified by column chromatography with hexane as an eluent to obtain compound **5** as colorless oil (2.44 g, yield: 90%). ^{1}H NMR ($CDCl_3$): δ 4.08 (s, 4H), δ 3.48 (s, 4H), δ 3.29 (d, 4H, *J*= 5.7 Hz), δ 1.56-0.86 (m, 30H). ^{13}C NMR

($CDCl_3$): δ 147.23, 91.03, 74.55, 74.50, 69.94, 48.21, 39.82, 30.86, 29.34, 24.20, 23.31, 14.33, 11.37. HRMS (ESI–FTICR): *m/z* calcd for $C_{25}H_{42}Br_2KO_4S$ ($M+K^+$) 635.0802 found 635.0798. Anal. calcd for $C_{25}H_{42}Br_2O_4S$: C 50.17, H 7.07, found C 50.47, H 7.20.

4,7-Dibromobenzo[c][1,2,5]thiadiazole (**6**)[203] In a 500 mL three-neck round bottom flask with benzothiadiazole (19.6 g, 144 mmol) and 150 mL of HBr (47%), a 100 mL of HBr solution containing Br_2 (68.9 g, 432 mmol) was added dropwise. After total addition of the Br_2, the solution was refluxed for 6 h. Precipitation of an orange solid was noted. After cooling to room temperature, the mixture was filtered under vacuum and washed with saturated solution of $NaHSO_3$ for 3 times (100 mL solution per time) and then water for 5 times. The solid was then dried under reduced pressure and purified by column chromatography with hexane as an eluent affording compound **6** as a white crystalline solid (31.5 g, yield: 75%). ^{1}H NMR ($CDCl_3$): δ 7.73 (s, 1H).

General polymerization procedure. Polymer ECP-1: A solution of compound **4** (0.509 g, 0.5 mmol), compound **5** (0.180 g, 0.3 mmol), compound **6** (0.059 g, 0.2 mmol), tris(dibenzylideneacetone)dipalladium (0) (9 mg, 0.01 mmol) and tri(o-tolyl)phosphine (12 mg, 0.04 mmol) in toluene (20 mL) was degassed three times by successive freeze-pump-thaw cycles and heated at 100°*C* for 36 h in an oil bath. The solution was then precipitated into methanol (300 mL). The precipitate was filtered through a cellulose thimble and purified via Soxhlet extraction for 24 hours with methanol and then 48 hours with hexane. The polymer was extracted with chloroform, concentrated by evaporation, and then precipitated into methanol again (300 mL). The collected polymer was a black solid (0.29 g, 76 %). ^{1}H NMR (300 MHz, $CDCl_3$) δ 8.34-8.20 (m, 2H), 4.17-4.00 (m, 16H), 3.55 (bs, 16H), 3.27 (bs, 16H), 1.45-1.05 (m, 72H), 0.84 (bs, 48H). GPC analysis:

M_n = 9,700, M_w = 15,500, PDI = 1.6. Anal. Calcd. for **ECP-1**: C 67.08, H 9.51, N 1.48, found C 66.79, H 9.22, N 1.39.

General procedure of using 'Slurry' (Millipore stirred cell): first, unscrew the locks, disassemble the device by removing the stainless steel top, the glass cylinder wall and the o-ring on the bottom. Second, put a right size Nylon filter paper on the bottom and reassemble the device. The polymer solid as well as the solvents can be added through the hole with a cap on the steel top. After stirring the polymer suspension for 1-2 hours, filter the mixture under high pressure gas (do not exceed the pressure limit). Then add more solvent for the next cycle.

CHAPTER 4
WATER SOLUBLE BLUE- AND BLACK-TO-TRANSMISSIVE SWITCHING ELECTROCHROMIC POLYMERS

4.1 Motivations for Water Soluble Electrochromic Polymers

The utilization of π-conjugated polymers is significantly influenced by their optoelectronic properties as well as their solution processability. In this regard, the fine-tuning of the desired properties by synthetic modification of the polymer backbones and the nature of the pendant groups is perhaps the most widely used tool.[15] Despite there being a large number of conjugated polymers with diverse material properties, which have been synthesized and evaluated for applications such as OLEDs,[209-211] OPVs,[167,171,212] FETs[213,214] and ECDs[7,15,202,215], only poly(3,4-ethylenedioxythiophene): poly(styrene sulfonate) (PEDOT:PSS) has been particularly commercially successful. This is largely due to its highly processable nature, which affords it the ability to be processed from an aqueous solution yielding thin films with a high conductivity.[117,216,217] In addition, the high contrast between a deep blue neutral state and a highly transmissive oxidized state makes PEDOT:PSS an excellent candidate for electrochromic applications.[151,218] Combination of the water processable features of PEDOT/PSS with the optoelectronic properties of the electrochromic polymers (ECPs) is necessary to produce water soluble ECPs for fabrication of ECDs with minimal processing costs and environment impact.

Water-soluble conjugated polymers (WS-CPs), which are also referred to as conjugated polyelectrolytes (CPEs), were first introduced by Wudl and Heeger *et al.*[219] in the synthesis of polythiophene with sulfonate derivatives, and also by our group for polypyrroles.[220] Considering the unique hydrophilicity of these materials, a combination of a fully conjugated polymer backbone and ionic pendant groups such as sulfonate (-

SO_3^-), carboxylate ($-CO_2^-$), phosphonate ($-PO_3^-$) and ammonium ($-NR_3^+$) must be achieved. In parallel, like most of the organic soluble CPs, WS-CPs can be made via a variety of existing polymerization reactions, which, including electrochemical polymerization,[221,222] oxidative polymerization[223,224] and transition-metal mediated polymerization such as Suzuki and Sonogashira polymerizations.[225-227] Although a large number of WS-CPs have been prepared, the investigation of such polymers has been mainly focused on applications in chemical and biological sensors due to the high water solubility and high optical sensitivity.[228-230] Unfortunately, the use of WS-CPs in optoelectronic devices such as PLEDs and ECDs, has gained limited success. Within these contributions, several polymers have been proved as excellent materials for electron injection layers (EILs) in making multi-layer PLEDs.[231-233] For example, conjugated polyelectrolyte $PF_{PEO}CO_2Na$ was synthesized and used as an EIL in PLEDs by Nguyen *et al*.[234] A luminance response time of microseconds was achieved by a combination of thermal and voltage treatments, aiming to control the ion motion at the EIL interface. Furthermore, water soluble poly(4,4'-diphenylene vinylene) and its rotaxinated derivatives have been shown to attain a high degree of alignment in stretched PVA films, and to emit highly polarized light when they were excited by a pulsed diode laser.[235]

In this contribution, we focus on the preparation of water processable conjugated polymers which transmit or reflect between two or more different color states upon redox activity. More specifically, we are in pursuit of polymer electrochromes with the following properties: 1) can be processed from an aqueous solution into solid films by existing print or spray technologies; 2) can be switched form a strongly colored neutral

state to a highly transmissive oxidized state; 3) exhibit short switching time (sub-second) without losing contrast when employed into electrochromic displays. To fulfill these three requirements, several approaches have been proposed. In a previous paper, our group presented the layer-by-layer (LbL) deposition of alkoxy-sulfonated poly(*p*-phenylene) (PPP-$OPSO_3$) in conjunction with multiple types of conjugated or non-conjugated polyelectrolytes.[236] Combining the optoelectronic properties and the advantages of LbL deposition, which promotes uniform thin films with a molecular level thickness control, the polymer has been demonstrated to be a good candidate for PLEDs. Subsequently, a detailed study of alkoxy-sulfonated PEDOT polyelectrolyte was reported by our group.[188,237] Multilayer films based on the polymer and poly(allylamine hydrochloride) (PAH) were prepared by the LbL method and the electrochromic properties of the films were extensively characterized. Furthermore, a regioregular water-soluble polymer based on 3,4-propylenedioxythiophene (ProDOT) was synthesized by Kumar *et al*.[238] It is worth mentioning that the solid state electrochromic devices consisting of PProDOT-sultone/PAH bilayer films demonstrated fast switching times due to the rapid movement of ions in and out of the films, in agreement with the same observation in our group's research mentioned above.

This chapter describes the synthesis of a new ProDOT monomer bearing four carboxylate ester groups (Figure 4-1). Incorporation of the ProDOT monomer and BTD units has successfully yielded two electrochromic polymers: **ECP-Blue** (a donor-acceptor alternating copolymer) and **ECP-Black** (a donor-acceptor random copolymer). Subsequent deprotection of the ester group afforded polymer carboxylate salts with high

water solubility. The electrochromic properties of the neutralized films were evaluated and showed promising sub-second switching times.

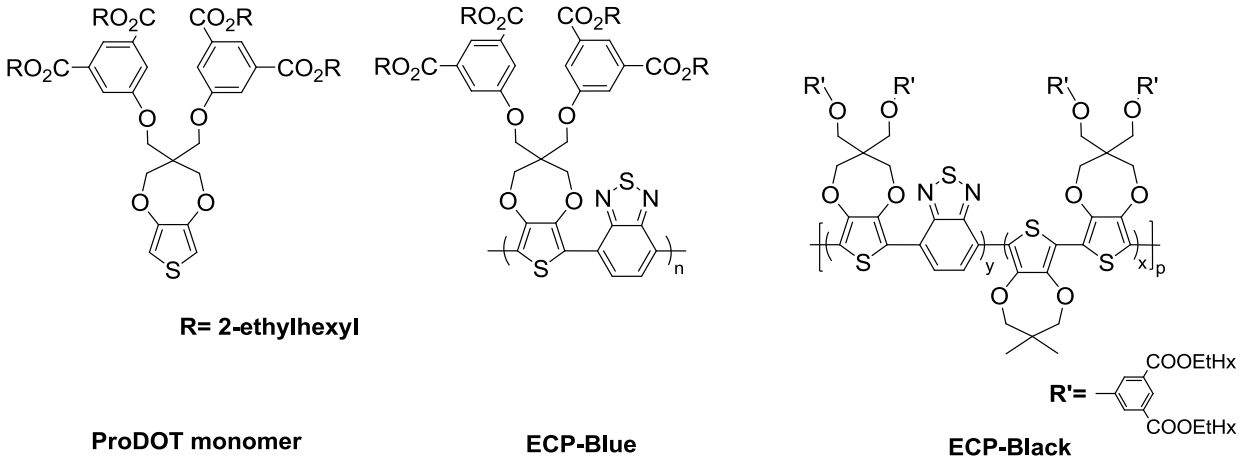

Figure 4-1. Structures of ProDOT monomer, organic soluble precursors **ECP-Blue** and **ECP-Black**.

4.2 Concept and Design of Carboxylic-Acid Functionalized CPEs from Chemically Cleavable Esters

Recently, our group reported the synthesis of a new polyProDOT (ECP-Magenta) bearing cleavable carboxylate ester functional groups (Figure 4-2).[239] In this study, the use of a side-chain defunctionalization approach yielded a PProDOT-salt homopolymer (WS-ECP-Magenta) that can be dissolved and processed in water. Upon neutralization of the spray-cast thin films, the formed polymer acid became insoluble in both organic solvents and water. Importantly, the resulting film, which was switched in a KNO_3/water supporting electrolyte, showed a very small loss in contrast (less than 3%) on going from a switching time of 0.5 s to 0.25 s, as compared with a contrast loss of around 13% from the toluene sprayed PProDOT-ester film switched in a LiBTI/PC electrolyte. It is worth mentioning that the synthesis of the organic soluble polymer ester is necessary in this approach, since the polymer can be easily purified (precipitation and Soxhlet extraction) and characterized (NMR, GPC *et al.*) in its organic form.

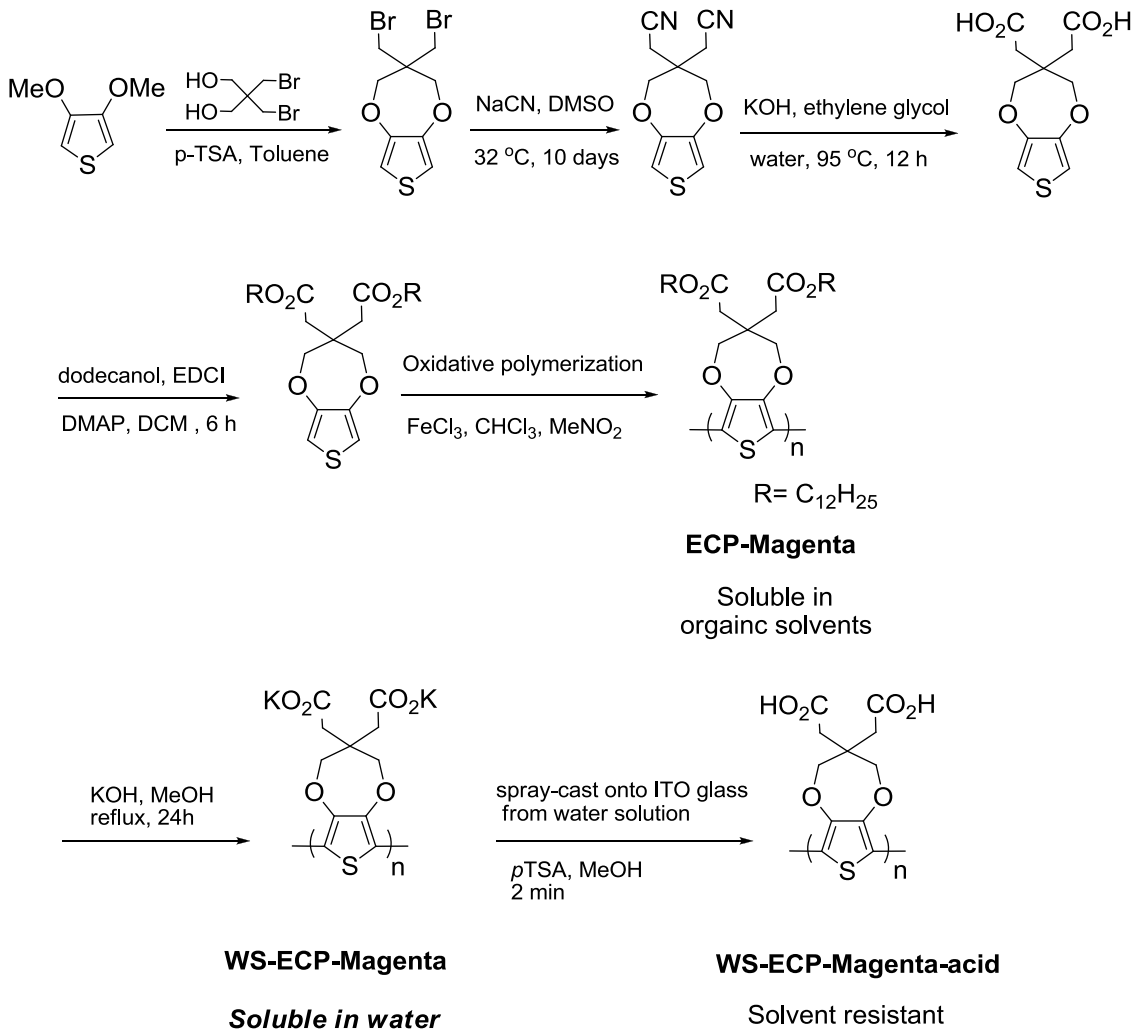

Figure 4-2. Synthesis of ECP-Magenta. Side-chain defunctionalization yields the polymer carboxylate salt, which can be dissolved in water and spray-cast onto ITO-coated glass slides. The deposited films are then neutralized by immersion in a *p*-toluenesulfonic acid/MeOH solution to afford the polymer acid. (Adapted and modified with permission from Ref.239 Copyright 2010 WILEY-VCH Verlag GmbH & Co. KGaA, Weinheim)

However, we also found that it was difficult to extend this synthetic procedure to the preparation of other colored ECPs, which need a secondary repeat unit for fine tuning of the absorption spectra.[121,126,128,197,240] Clearly, the water solubilizing groups on the ProDOT monomer were not sufficient to make a copolymer dissolve in water. Moreover, the synthesis of the repeat unit (ProDOT-diester), which involved four steps of organic synthesis, was rather complicated. In particular, the second reaction,

preparation of the nitrile compound of ProDOT, required a 10-day reaction and the use of the highly toxic compound sodium cyanide. Therefore, it was necessary to find a new ProDOT repeat unit with modified pendant groups, which can be synthesized easily and provide strong water solubility in the copolymer chain after being defunctionalized.

4.3 Polymer Synthesis and Characterization

4.3.1 Monomer Synthesis

The synthesis of the monomers is shown in Figure 4-3. In order to achieve organic processability of the monomers and copolymers before the defunctionalization process, 2-ethylhexyl alkyl chain was used as protecting groups in the ProDOT unit. Compounds **1** and **2** were synthesized according to the previously reported methods.[119,241] The nucleophilic substitution of **1** with **2** under basic conditions afforded compound **3** in a good yield. It is worth noting that this S_N2 reaction is much slower using traditional oil bath heating. The crude reaction mixture was predominantly the monosubstituted byproduct and the starting material (compound **1**) after 3 days' stirring at 120°C; only a small amount of the final product was found. Fortunately, by using a microwave reactor and raising the reaction mixture to 140°*C*, the reaction was accomplished with a dramatically reduced reaction time (2 hours) and an improved reaction yield (74%) after the purification. The subsequent bromination of **3** using NBS afforded compound **4** in a 90% yield, which was originally designed as one of the monomer units in the synthesis of **ECP-Black**. On the other hand, the common method in making ditin compound **5** by reacting compound **3** with *n*BuLi first and then adding Me_3SnCl also failed, because BuLi reacted with the ester groups as a strong base. Finally, ditin compound **5** was synthesized by coupling **4** with hexamethyldistannane in toluene at 115°C using $Pd(PPh_3)_4$ as the catalyst.

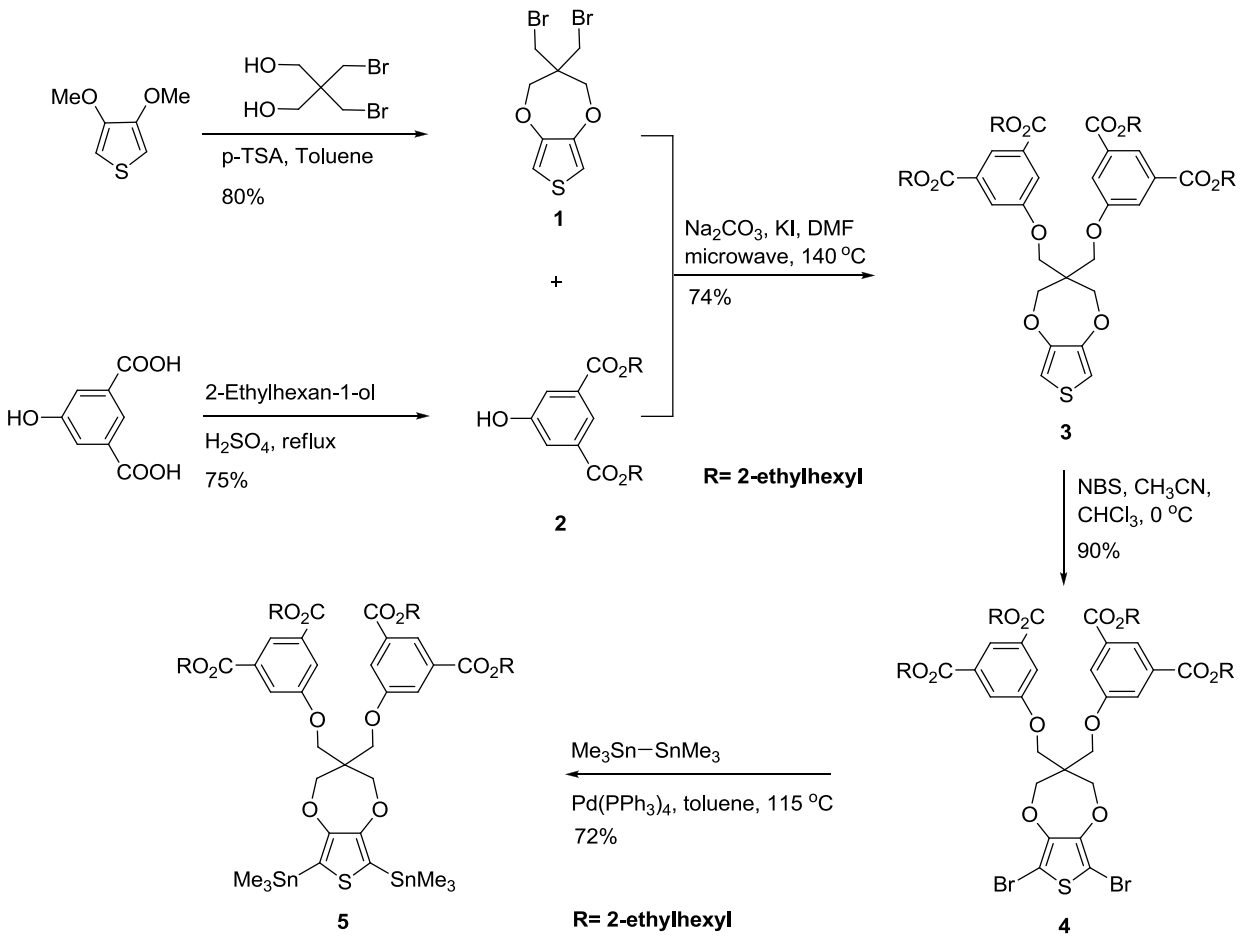

Figure 4-3. Reaction scheme for the synthesis of monomers.

4.3.2 Polymer Synthesis: A Pendant Group Modification

Alternating copolymer **ECP-Blue** (the ester precursor of **WS-ECP-Blue**) was successfully prepared by a Stille polymerization of ditin compound **5** and dibromo benzothiadiazole **8** (Figure 4-4). After the Soxhlet extraction and re-precipitation, the organic soluble polymer **ECP-Blue** presented a satisfactory number-average molecular weight (M_n) of 25.8 kDa and PDI of 1.5 (estimated by GPC in THF), and there was good agreement of the elemental analysis results with the calculated numbers (Table 4-1). The dark blue polymer solid can be dissolved in THF, toluene and chlorinated solvents with good solubility (> 10 mg/mL).

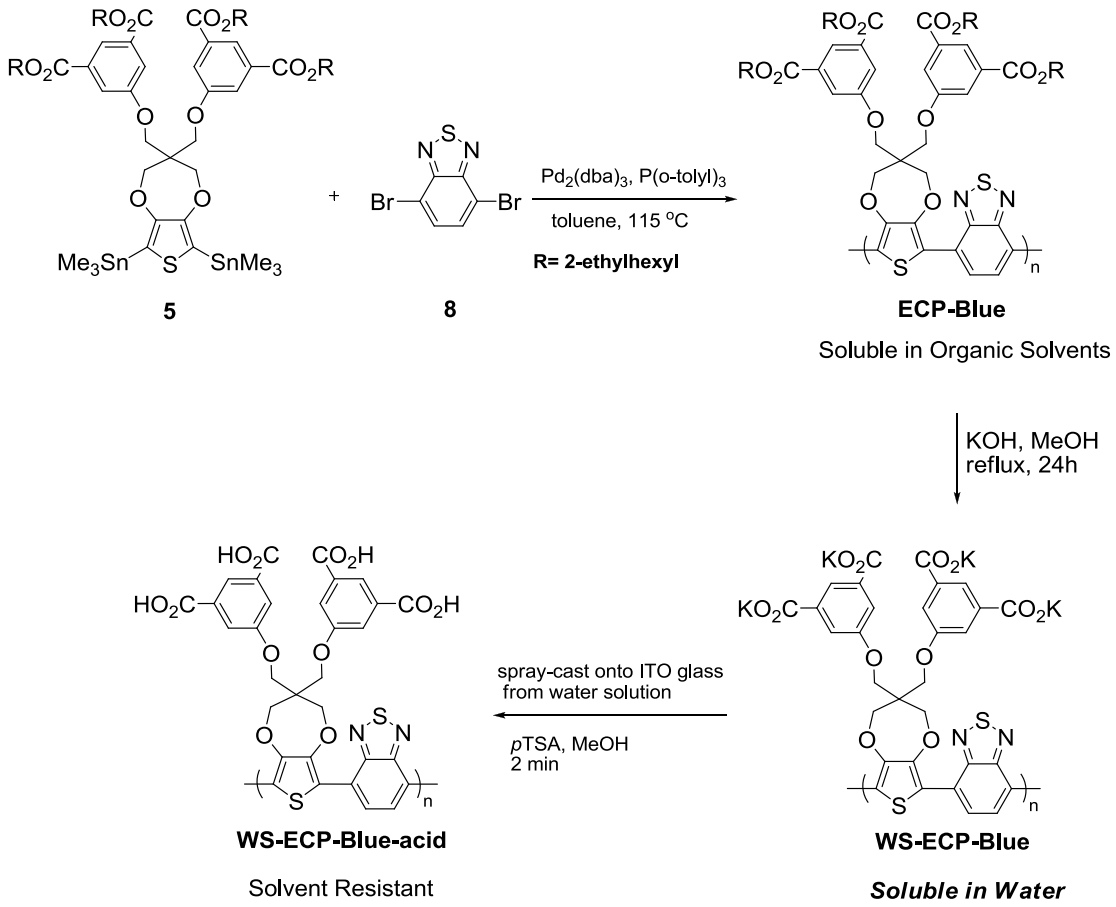

Figure 4-4. Synthesis of polymer **ECP-Blue**. Side-chain defunctionalization yields polymer carboxylate salt (**WS-ECP-Blue**), which can be dissolved in water. Further treatment of the spray-cast thin films affords **WS-ECP-Blue-acid** that is insoluble in both organic solvents and water.

However, the original plan of making **ECP-Black** by coupling compounds **4**, **5** and dibromo benzothiadiazole in a fixed monomer feed ratio failed. The steric hindrance generated from the bulky side chains on the ProDOT unit prevented a high extent of reaction in this step-growth polymerization. As a result, the polymerizations according to this methodology resulted in low reaction yields, as well as polymers with low M_n at around 7 kDa. In order to achieve high molecular weight conjugated polymers with maximized optical properties, it was necessary to reduce the size of one of the monomers. To pursure this, an alternative way was to replace monomer compound **4** by

another ProDOT unit with much smaller side chains. And thus, compound **7** was utilized in the synthesis of **ECP-Black** (Figure 4-5). In this approach, the polymer M_n was increased to 14 kDa. The polymer molecular weights and elemental analysis are summarized in Table 4-1.

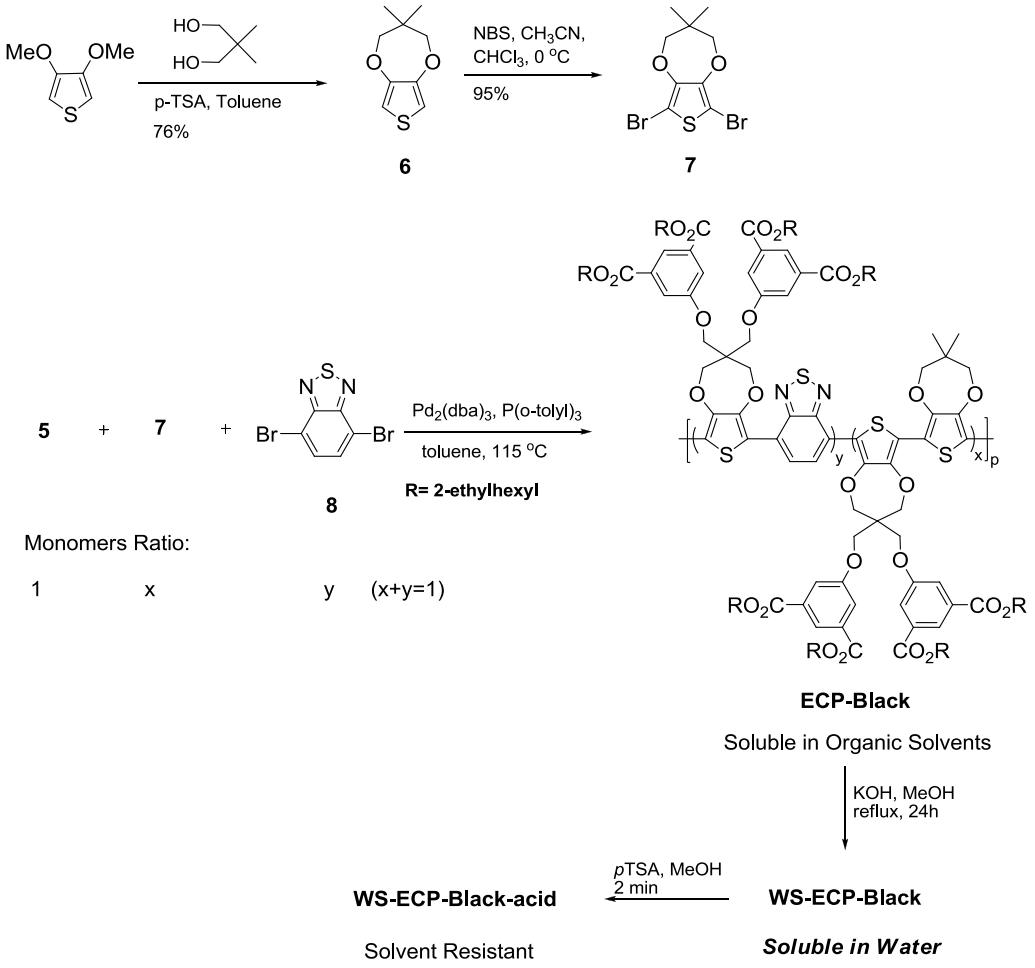

Figure 4-5. Synthesis of monomer compound **7** with reduced side chain size and random copolymer **ECP-Black**.

Table 4-1. GPC estimated molecular weights in THF and elemental analysis of the polymers.

	Monomer **5** ratio	Monomer **7** ratio (x)	Monomer **8** ratio (y)	M_n (kDa)	M_w (kDa)	PDI	EA (Calcd/Found)		
							C	H	N
ECP-Blue	1	/	1	25.8	38.5	1.5	67.23/66.94	7.52/7.64	2.49/2.42
ECP-Black	1	0.7	0.3	13.9	23.3	1.7	67.46/67.11	7.79/7.89	0.73/0.68

To obtain the WS-ECPs, the organic soluble ester precursors **ECP-Blue** and **ECP-Black** were suspended separately in 1 M KOH/methanol, and the mixture was then refluxed overnight under argon. The successful deprotection of the ester group afforded **WS-ECP-blue** and **WS-ECP-Black** as fine powdery polymer salts, which were highly soluble in water at room temperature but insoluble in organic solvents such as toluene, THF and chloroform. Furthermore, the water solutions of the polymers (4 mg mL^{-1}) were spray-cast onto ITO-coated glasses to achieve homogeneous polymer thin films with varying thicknesses. By immersing the films in a *p*TSA/MeOH solution (1 mg/mL^{-1}) for 2 minutes, the polymers were finally converted into their acid forms, which cannot be dissolved in water or organic solvents.

4.3.3 Polymer Thermal Analysis

The thermal stability of the polymers was studied by TGA in a nitrogen atmosphere using high-resolution dynamic scans from 50°C to 600°C. As shown in Figure 4-6, the polymers exhibited high thermal stabilities with negligible weight loss below 340°C. And then a drastic degradation process occurred for **ECP-Black** at this temperature. Interestingly, **ECP-Blue** with a clear sign of degradation starting at 350°C, showed a slightly higher thermal stability than **ECP-Black**.

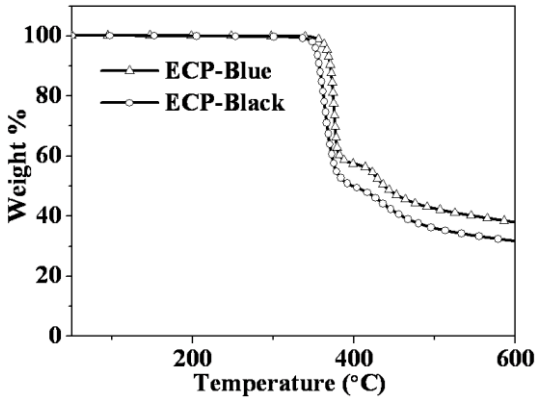

Figure 4-6. Thermogravimetric analysis of polymers **ECP-Blue** and **ECP-Black**.

4.3.4 Polymer Optical Characterization

The optical properties of the polymers were investigated by UV-vis-NIR absorption spectroscopy in dilute THF solutions and as spray-casted films on ITO glasses. As shown in Figure 4-7a, **ECP-Blue** and its salt derivative **WS-ECP-Blue** exhibit a typical two-band absorption in the UV-vis spectra with a gap in the blue and bluish green region (380-550 nm). The absorption maxima of the polymers in solutions as well as thin films fall into the wavelength range of 600-650 nm. Clearly, the deprotection of the ester group, as well as the use of a highly polar solvent, has affected the optical absorption of the chromophores in solution. The generated polymer salt **WS-ECP-Blue** demonstrates a 30 nm red shift of its long wavelength absorption peak in the water solution compared with that of **ECP-Blue** in THF. Moreover, due to a better intermolecular interaction in the solid state, the long wavelength optical transition of **ECP-Blue** thin film shows a 50 nm red shift as well as a broadening of the peak compared to its solution absorption. Interestingly, there is no dramatic change observed between the solution and film absorption of water soluble polymer **WS-ECP-Blue**. As determined from the onsets of their neutral-state lower-energy optical transitions (polymer film absorption), the optical band gaps of **ECP-Blue** and **WS-ECP-Blue** are 1.56 and 1.59 eV, respectively, in good agreement with the band gaps evaluated by differential-pulse voltammetry (Section 4.4.1).

As expected, **ECP-Black** shows a “merging” of the high- and low-energy transitions, and no obvious peak-to-peak window is observed in the visible region (Figure 4-7b). However, judging by the absorption profile of **ECP-Black**, which is unable to cover the entire visible region evenly, it is logical that the solution and the film of the polymer show a dark purple-black color due to the absorption missing in part of the blue

(350- 470 nm) and the red (650-700 nm) regions. Furthermore, the broad absorption of **ECP-Black** in THF (from 450 to 650 nm) shifts to a higher wavelength after deprotection of the ester group (see absorption spectrum of **WS-ECP-Black** in water), which is consistent with the similar observation from **ECP-Blue**. Although there is only a small λ_{max} change between **WS-ECP-Black** water solution and its film absorption, the polymer thin film does show a broadening of the absorption in the range of 500-560 nm. The optical bandgaps of **ECP-Black** and **WS-ECP-Black** are estimated to be 1.58 and 1.60 eV, which are slightly higher than the band gaps of the corresponding blue polymers, due to the reduced donor-accepter effect upon decreasing the number of electron-deficient heterocycles along the polymer backbone.

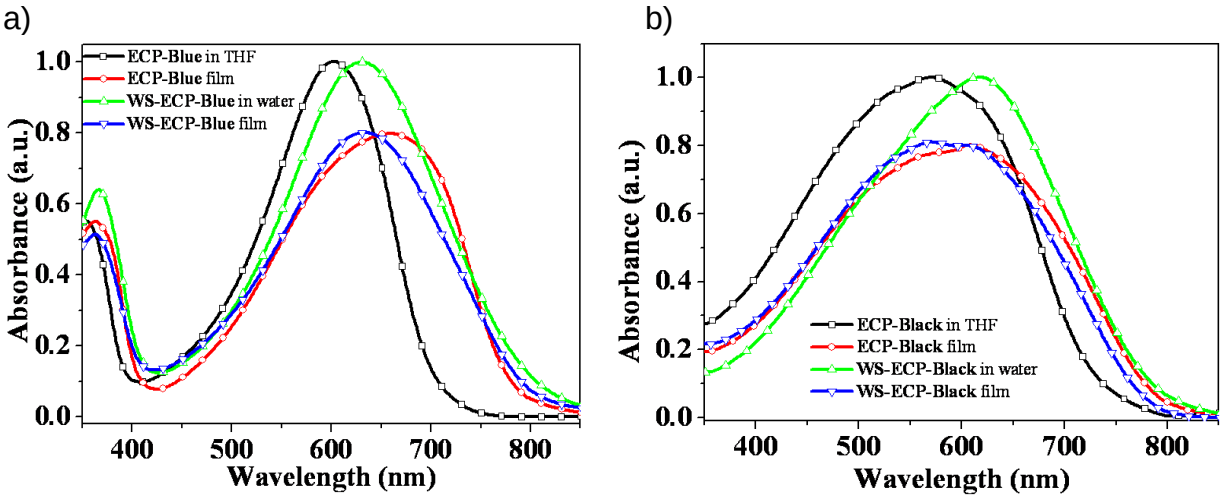

Figure 4-7. Normalized UV-vis-NIR absorption spectra of polymers. a) **ECP-Blue** and **WS-ECP-Blue** and (b) **ECP-Black** and **WS-ECP-Black** in dilute THF and water solution and thin films on ITO-coated glasses.

4.4 Polymer Electrochemistry and Spectroelectrochemistry

4.4.1 Electrochemistry Studies

For electrochromic applications it is necessary to have a good understanding of the redox properties of the polymers and to be able to estimate the oxidation and

reduction onset levels. Differential pulse voltammetry (DPV) was performed in order to characterize the accessible redox states of both **ECP-Blue** and **ECP-Black**. Figure 4-8 shows the DPV results obtained for the polymers. **ECP-Blue** exhibits onsets of oxidation and reduction at 0.24 and -1.38 V *vs*. Fc/Fc^+, respectively (Figure 4-8a). The difference between the oxidation and reduction potentials yields electrochemical band gap of 1.62 eV, which is slightly higher than the optical band gap (1.56 eV, Section 4.3.3). According to the results, the polymer has a HOMO energy level at about -5.34 eV and a LUMO energy level at -3.72 eV. The relatively low HOMO value allows the polymer to be easily handled in air without encountering undesired oxidation.

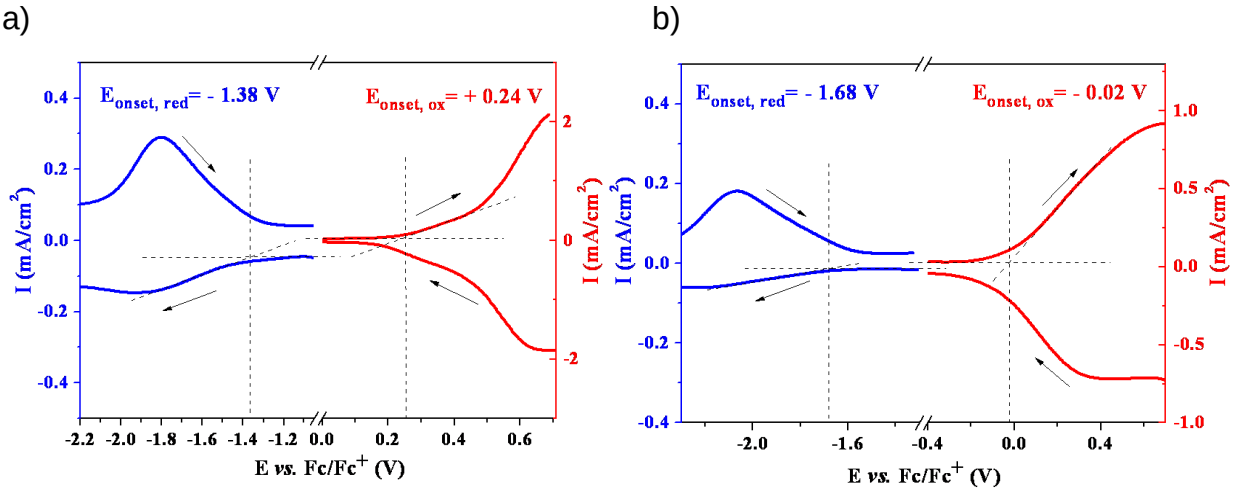

Figure 4-8. Differential pulse voltammetry of polymer esters. a) **ECP-Blue** and b) **ECP-Black** drop-cast from toluene solution onto platinum button electrode (A= 0.02 cm^2). Measurements were performed in 0.2 M LiBTI /propylene carbonate (PC) with a Pt foil counter electrode and a Ag/Ag^+ reference electrode calibrated *vs*. Fc/Fc^+ ($E_{Fc/Fc+}$ = 0.085 V *vs*. Ag/Ag^+).

On the other hand, **ECP-Black** shows much lower onsets of oxidation and reduction at -0.02 and -1.68 V *vs*. Fc/Fc^+ than those of **ECP-Blue**, which leads to less negative HOMO (-5.08 eV) and LUMO (-3.42 eV) energy levels. Clearly, as the relative amount of the electron rich units (ProDOP in this case) increases, **ECP-Black** can be oxidized more easily than the D-A alternating copolymer **ECP-Blue**. Interesting, both

polymers have almost the same energy gap, even though their energy levels and colors are different.

4.4.2 Spectroelectrochemistry Studies

The full spectroelectrochemical behavior of the polymers was evaluated by monitoring the absorption changes of the polymer thin films upon a simultaneous change of the applied external bias across the films. A film of **ECP-Blue** (λ_{max}= 655 nm, A= 0.87 a.u.) and a film of **ECP-Black** (λ_{max}= 609 nm, A= 0.76 a.u.) were spray-cast onto ITO-coated glass from their 3 mg mL^{-1} toluene solution, respectively. Electrochemical oxidation of the polymers was carried out in 0.2 M lithium bis(trifluoromethylsulfonyl)imide (LiBTI)/propylene carbonate (PC) supporting electrolyte using a Ag/Ag^{+} reference electrode (calibrated against Fc/Fc^{+}) and a platinum wire as the counter electrode. As shown in Figure 4-9a and b, when the potential increased, the two-band absorption of **ECP-Blue** (350-400 nm and 450-700 nm) and the broad absorption of **ECP-Black** (400-800 nm) in the visible region are depleted with a clear appearance of the polaronic transitions in the near-IR region from 800 to 1200 nm. As expected, the development of the polaronic transitions stops at a particular point, and then the absorption falls back and merges into a much broader bipolaronic transition due to the further increase of the oxidation potentials applied to the films. When fully oxidized, both of the polymer films show a dramatic loss of absorption in the visible region, and present a remarkably high level of transmissivity to the human eye. It is worth mentioning that a slight blue hue is observed for the transmissive oxidized films since both of the low energy bipolaronic transitions tail into in the 600 nm to NIR region, even though they peak beyond 1500 nm.

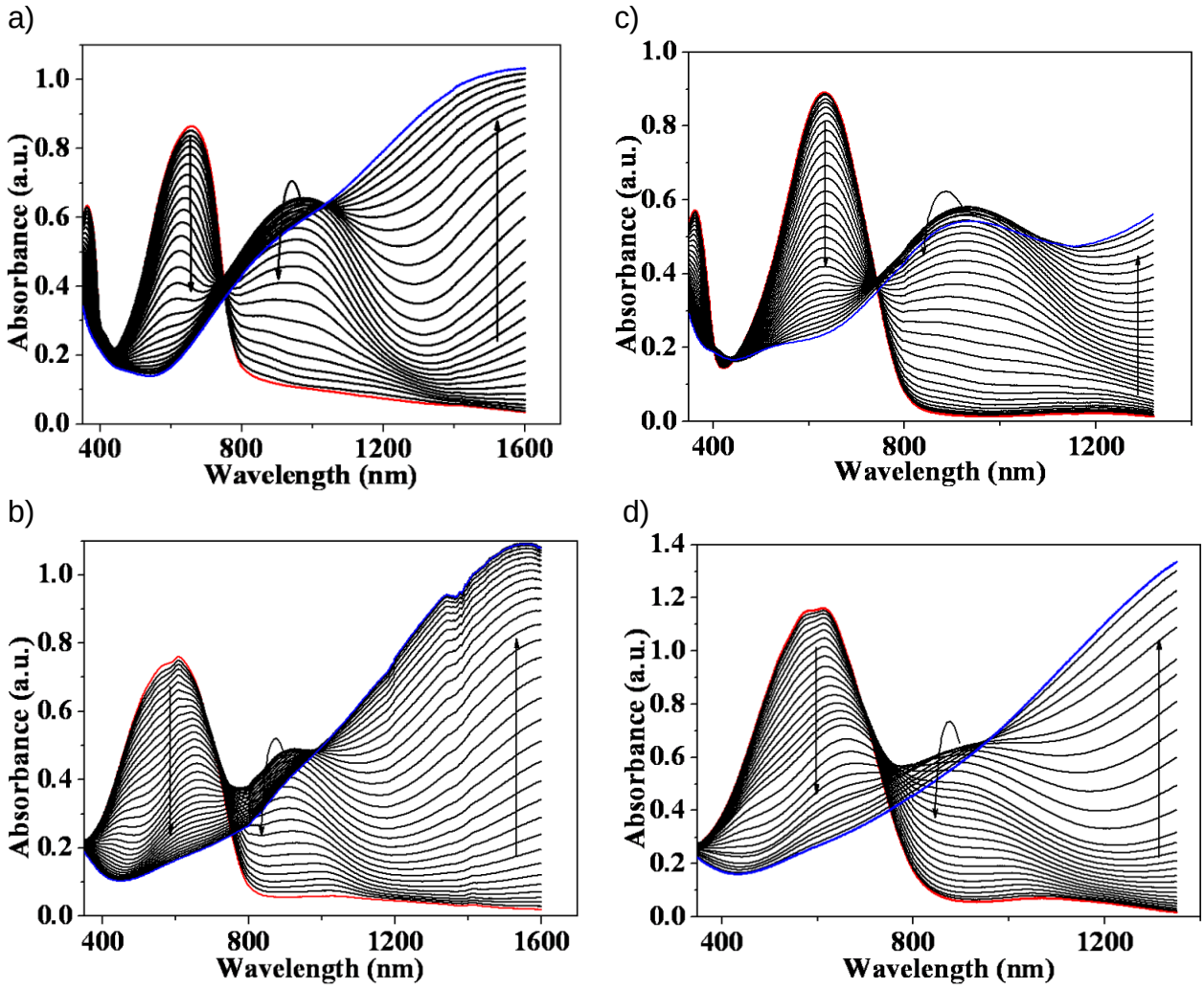

Figure 4-9. Spectroelectrochemistry of polymers. a) **ECP-Blue**, b) **ECP-Black**, c) **WS-ECP-Blue-acid** and d) **WS-ECP-Black-acid**. The films were spray-cast onto ITO-coated glass from toluene (a and b, 3 mg mL^{-1}) or from water (c and d, 4 mg mL^{-1}). Electrochemical oxidation of the films was carried out in 0.2 M LiBTI/PC supporting electrolyte using a Ag/Ag^{+} reference electrode (a and b, calibrated against Fc/Fc^{+}); or in 0.2 M KNO_3/water supporting electrolyte using a Ag/AgCl reference electrode (c and d). A platinum wire was used as the counter electrode. The applied potential was increased in 25 mV steps from (a) -0.25 to +0.35 V *vs.* Fc/Fc^{+}, (b) -0.36 to +0.47 V *vs.* Fc/Fc^{+}, (c) 0 to +0.8 V *vs.* Ag/AgCl and (d) -0.2 to +0.5 V *vs.* Ag/AgCl.

On the other hand, spectroelectrochemistry of **WS-ECP-Blue-acid** and **WS-ECP-Black-acid** (Figure 4-9c and d) was carried out in 0.2 M KNO_3/water supporting electrolyte using a Ag/AgCl reference electrode. The spray-cast polymer films were prepared from their aqueous solutions and neutralized as previously described.

Different from their ester derivatives, the absorption measurements of the polymer films are cut off at 1300 nm due to the extensive absorption of water beyond that point. In the neutral state, the film absorptions of the neutralized polymer acids show a good agreement with these of their salts, respectively, which means no further optical change upon the treatment of the films with *p*TSA/MeOH solution.

Moreover, a transmittance change ($\Delta\%T$) of 46% is estimated by examining the depletion of the long wavelength absorption maximum at 630 nm for **WS-ECP-Blue-acid**, indicating a well defined electrochromic performance. However, **WS-ECP-Black-acid** shows a transmittance change of 51% at 555 nm, the wavelength at which the human eye has greatest sensitivity. Here, it is obvious that the thin film of **WS-ECP-Black-acid** starts oxidizing at a much lower potential (-0.2 V *vs.* Ag/AgCl) than that of **WS-ECP-Blue-acid** (0 V *vs.* Ag/AgCl), which is also observed in **ECP-Black** and **ECP-Blue** (-0.36 and -0.25 V *vs.* Fc/Fc^+, respectively). This is due to the increase of donor ratio in the random **ECP-Black** polymer, thus raising the HOMO level.

4.5 Polymer Switching Study: A Comparison of Organic Soluble Polymers and Water Soluble Polymers

4.5.1 Polymer Colorimetric Measurements

Colorimetric analysis of the polymer films with varying thickness was performed in order to evaluate the color changes of the ECPs occurring on electrochemical oxidation (on the basis of the “Commission Internationale de l’Eclairage” 1976 *L*a*b** color standards). Before the test, films were spray-cast and redox-cycled several times using the same conditions for each polymer, as previously discussed in Section 4.4.2. Figure 4-10 shows the determined *L** values as a function of applied voltage. This gives an indication of relative transmission of the films as they are oxidized while illuminated from

behind (in essence a measure of the attenuation of a light's intensity) with a standard D50 simulated daytime light source.

Here, in its neutral state, films of **ECP-Blue** exhibit *L** values from 47 for the thickest film (A= 1.3 a.u.) to 78 for the thinnest film (A= 0.4 a.u.) (Figure 4-10a). Moreover, a saturated blue color at all film thicknesses, which is supported by the large negative *b** values, is also observed. As expected, a small amount of green light, as indicated by the relative small negative *a** values, also passed through the polymer films due to the partial absorption missing in the range between 500 and 600 nm. By increasing the applied potentials, the polymer films begin to increase in transmission dramatically at about 0.2 V *vs.* Fc/Fc^+. Upon full oxidation, **ECP-Blue** demonstrates *L** values ranging from 86 to 95 depending on the optical density of the thin films. In the mean time, the decreased *a** and *b** values fall into the 'colorless' range. Judging by the potential shift corresponding to the lightness change, the potential window of the polymer full switch is calculated to be 0.6 V.

Compared with **ECP-Blue**, **ECP-Black** illustrates an obvious drop of *L** value in its neutral state. For example, an **ECP-Black** film with an optical density A= 1.1 a.u. shows a *L** value at about 33 (Figure 4-10b), which is much lower than that of an **ECP-Blue** film with a even higher optical density (A=1.3 a.u., *L**= 47). Clearly, this is due to the broad absorption nature of the polymer. However, as discussed previously, the broad absorption of **ECP-Black** does not evenly cover the entire visible spectrum, and thus allows part of the red and blue light to pass through the films, as indicated by the small positive *a** values and the relative large negative *b** values. For instance, the color of the neutral polymer film (A= 0.9 a.u.) falls into a red-blue color region, which presents a

dark black purple color (*a**= 10, *b**= -27). When fully oxidized, the polymer film shows a highly transmissive faint blue green tint with *a**= -2 and *b**= -3.

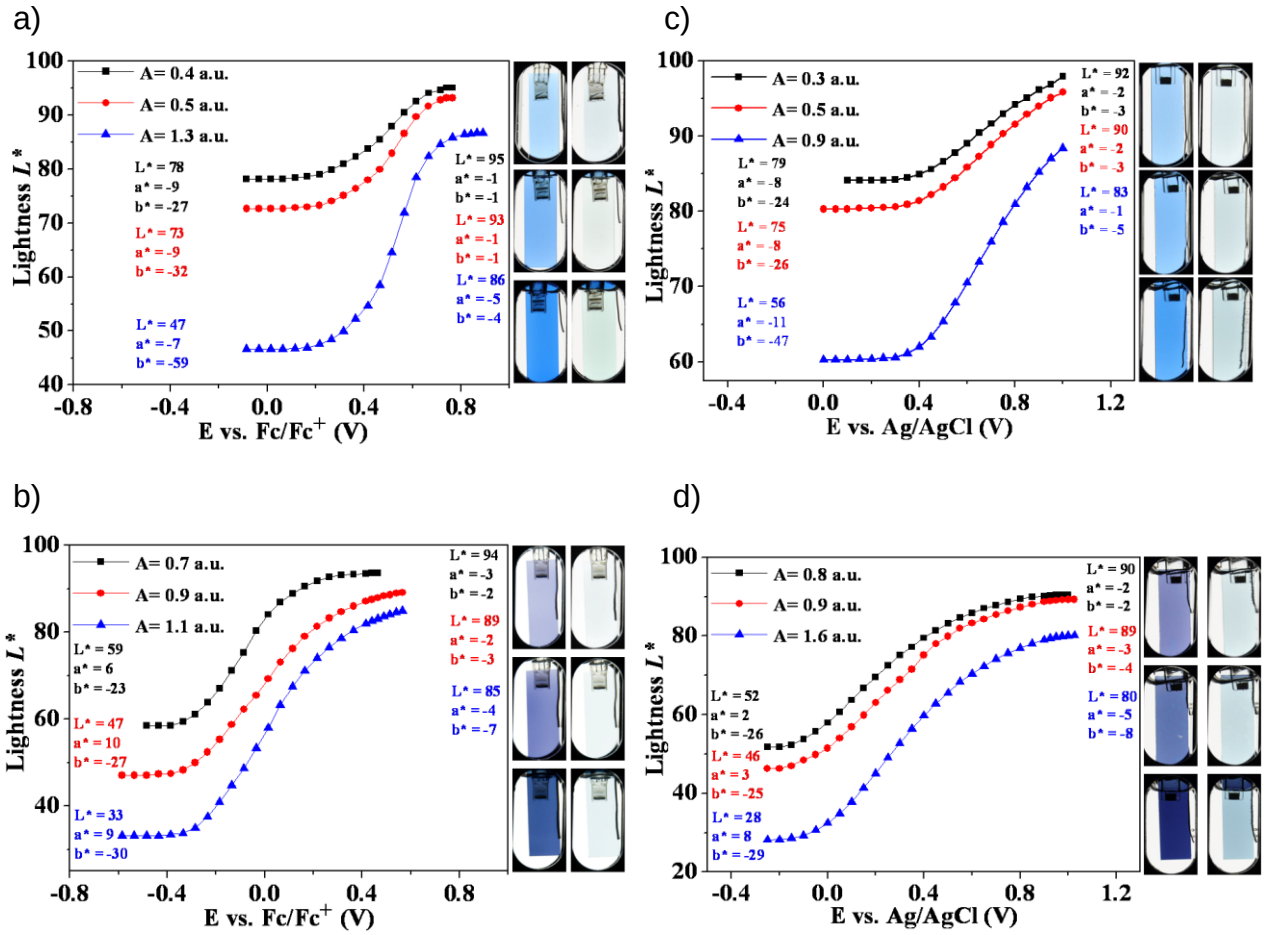

Figure 4-10. Lightness (*L**) as a function of applied potential for spray-coated polymers. a) **ECP-Blue**, b) **ECP-Black**, c) **WS-ECP-Blue-acid** and d) **WS-ECP-Black-acid**. *L*a*b** values of fully neutral and oxidized states are reported for the films. Photographs are of the fully neutral (left) and fully oxidized films (right).

In spite of changing to a KNO_3/water supporting electrolyte with Ag/AgCl as the reference electrode, **WS-ECP-Blue-acid** and **WS-ECP-Black-acid** show features in the EC performance similar to these in the corresponding polymer esters. The prominent increase of *L** values, as well as the decrease in *a** and *b** values, is a direct evidence of polymers being switched into a highly transmissive state upon oxidation of the films. It

is worth mentioning that the measurements were stopped when the potential was about 1 V *vs.* Ag/AgCl to avoid over-oxidation of the polymer films. Under these conditions, the experimental data was unable to show the track of its fully oxidized state for **WS-ECP-Blue-acid** (Figure 4-10c). Fortunately, the polymer films still present satisfactory transmissive state as defined by the *L*a*b** color coordinate. For example, an **WS-ECP-Blue-acid** film with an optical density A= 0.5 a.u. shows a *L** value of 90 with *a**= -2 and *b**= -3 in its oxidized state, which are comparable to these values of an **ECP-Blue** film with the same optical density (A=0.5 a.u., *L**= 93, *a**= -1 and *b**= -1, Figure 4-10a).

The potential window of **WS-ECP-Blue-acid** in a near full switch is 0.7 V, which is about the same as that of **ECP-Blue** (0.6 V). Due to the high HOMO level of **WS-ECP-Black-acid**, which makes it easier to be oxidized, the polymer reaches its fully oxidized state at 0.9 V *vs.* Ag/AgCl. For a thick film (A= 1.6 a.u.), **WS-ECP-Black-acid** presents an intense black purple state before being oxidized (*L**= 28) and a faint blue transmissive state when fully oxidized (*L**= 80), a lightness change higher than 50%.

4.5.2 Polymer Switching Rate

To evaluate the switching rate of the polymers, the transmittance change (EC contrast, $\Delta\%T$) at a single wavelength of the polymer films was monitored as a function of time by applying square-wave potential steps for periods of 10, 5, 2, 1, 0.5, 0.25 and 0.2 s. In Figure 4-11a, **ECP-Blue** shows a transmittance change as high as 48% at the longer switch time (10 s), which is only minimally reduced to 45% for the 2 s switch. Further decrease of the switch time causes a significant loss of contrast. For example, only 40% of the full contrast ($\Delta\%T$= 20%) remains at the 0.5 s switch, and this number drops to about 12% of the full contrast ($\Delta\%T$= 6%) at the 0.2 s switch, where the switch of the polymer can barely be detected. For an **ECP-Black** film with an optical density of

A= 1.02 a.u. (Figure 4-11b), the contrast drops from 54% to 40% when the switch time is reduced from 10 s to 2 s. This represents an earlier stage contrast loss, which is possibly due to the longer diffusion time of the counter balancing ions penetrating the thick polymer film. At the 0.2 second switch, the polymer film shows a transmittance change of 6%, corresponding a total contrast loss of around 90%.

In order to compare the switching performance, the polymer acid films were obtained with nearly identical thickness as their corresponding ester films (taking the optical density as representative of the thickness). As shown in Figure 4-11c, the **WS-ECP-Blue-acid** film, which is switched in a 0.2 M KNO_3/water electrolyte solution, exhibits a much faster EC switching speed than that of **ECP-Blue**. From 10 s to 0.5 s switch time, there is only a 5% loss of the full contrast observed compared with 60% for an **ECP-Blue** film with the same optical density. Unfortunately, the **WS-ECP-Blue-acid** film shows a bit lower contrast compared to its ester film even at the 10 s switch time, since the film is not fully oxidized as discussed in Section 4.5.1.

On the other hand, a **WS-ECP-Black-acid** film with an optical density of A=1.04 a.u. (Figure 4-11d), has a comparable contrast (52%, 10 s switch time) as its ester film, and is still able to maintain the contrast at 48% when the switch time is reduced to 1 s. The faster switching speed is possibly due to a better affinity to the electrolyte of the defunctionalized polymers, as well as the reduction of the counter ion size, and thus a faster ion diffusion process.[239] Although, the contrasts of both polymer films drop to a relative low level (20-30%) at much higher switching rates, the results still demonstrate a significant possibility of these polymers using in fast switching ECDs.

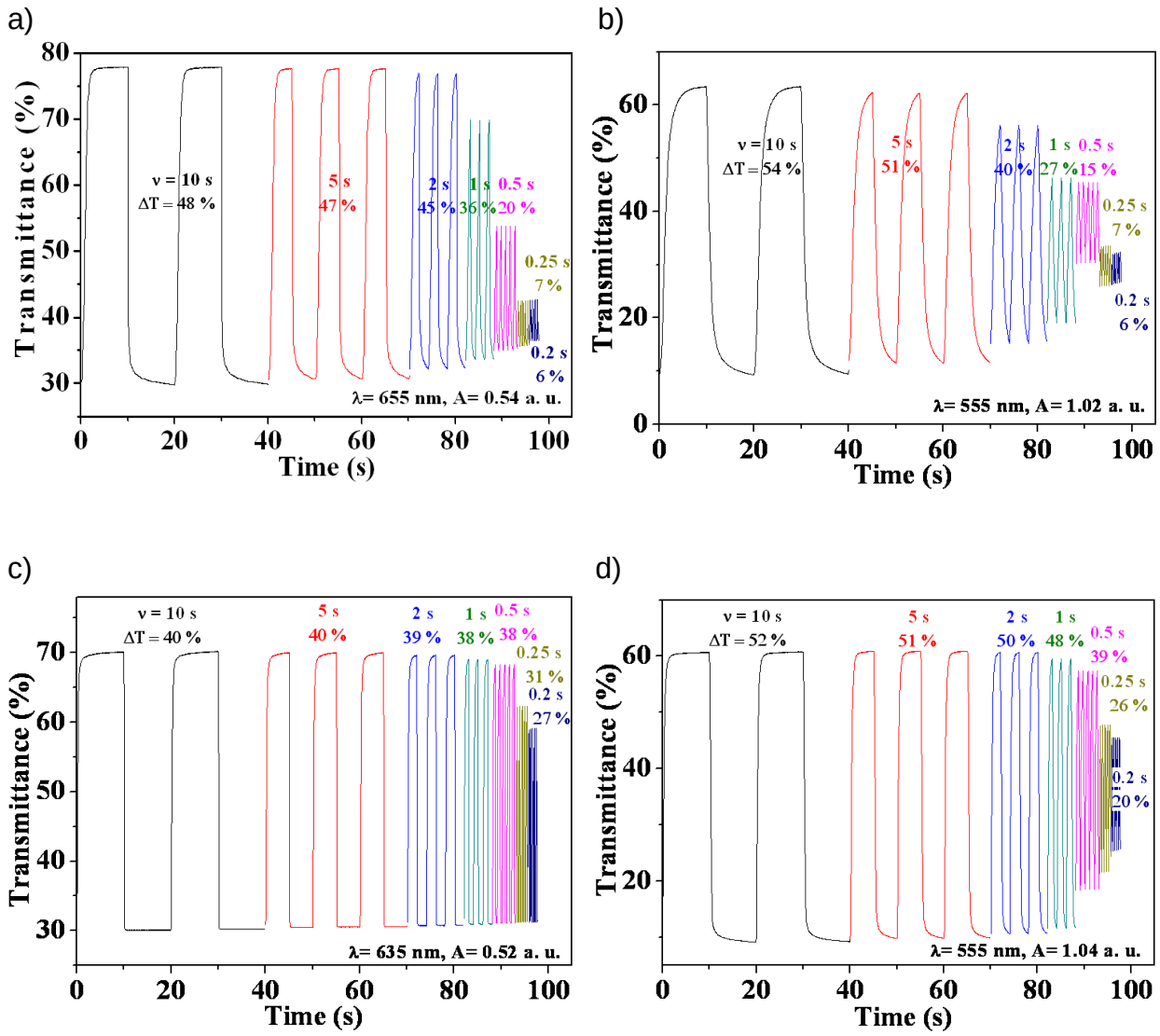

Figure 4-11. Square-wave potential-step chronoabsorptometry of polymers. a) **ECP-Blue** (monitored at 655 nm, switching potential range: -0.31 to +0.74 V *vs.* Fc/Fc^+); b) **ECP-Black** (monitored at 555 nm, switching potential range: -0.49 to +0.56 V *vs.* Fc/Fc^+) in 0.2 M LiBTI/PC electrolyte solution; c) **WS-ECP-Blue** acid (monitored at 630 nm, switching potential range: -0.1 to +0.95 V *vs.* Ag/AgCl); d) **WS-ECP-Black** acid (monitored at 555 nm, switching potential range: -0.2 to +0.95 V *vs.* Ag/AgCl) in 0.2 M KNO_3/water electrolyte solution. The switch times (10 s, 5 s, 2 s, 1 s, 0.5 s, 0.25 s and 0.2 s) are indicated on the figure.

In order to achieve an idea about how the switching performance is affected by the thickness of the film, the transmittance change (contrast) and the switching time of several films of polymer **ECP-Blue** with varied thickness were compared (Figure 4-12).

In the figure, the switching time is represented by its frequency for a better view, for example, the frequency at 0.1 Hz corresponds to a switching time of 10 s. Moreover, the film thickness is represented by its optical density monitored at 655 nm. In all cases, the contrast drops as the polymer films are switched faster (higher frequency). For instance, the contrast of the film with absorption at 1.25 a.u. drops from 45% at a frequency of 0.1 Hz to 2% at a frequency of 5 Hz. Interestingly, the contrasts of different polymer films at a fixed frequency are also related to the their thicknesses. For example, the film with the absorption at 0.54 a.u. shows the highest contrast among all the films at all switching frequencies.

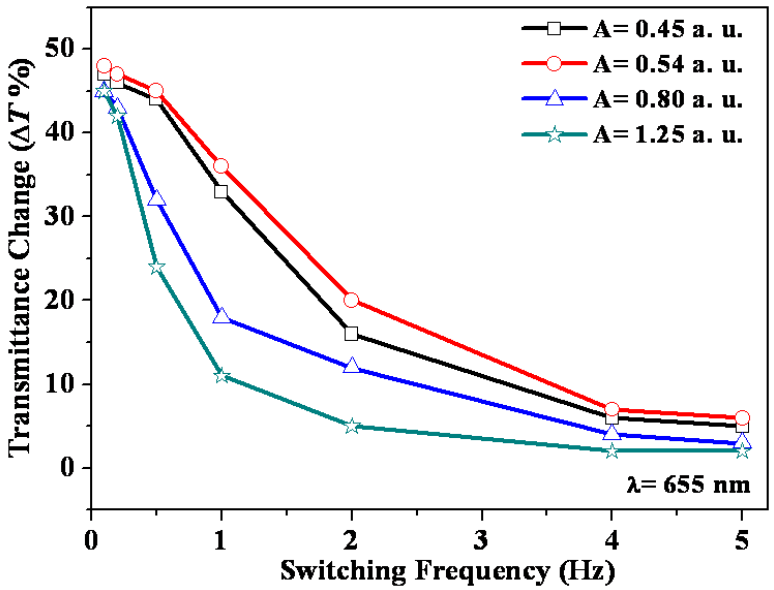

Figure 4-12. Transmittance change (contrast) as a function of switching frequency for **ECP-Blue** spray-coated on ITO (switching potential range: -0.31 to +0.74 V *vs.* Fc/Fc^+ in 0.2 M LiBTI/PC electrolyte solution). Film absorption was monitored at 655 nm, with absorption intensity of A= 0.45, 0.54, 0.80 and 1.25 a.u..

Instead of monitoring the transmittance change at one single wavelength, fast switching polymer films of **WS-ECP-Blue-acid** and **WS-ECP-Black-acid** were subjected to a novel technique, which evaluates electrochromic properties by

associating a time parameter with a specific full visible spectrum during the electrochromic transition.[242] Using a fiber-optic light source and a spectrometer containing a photodiode array detector, this measurement is capable of rapid data acquisition to track the electrochromic change in the polymer films. It is important to note that this absorption/transmission profile is not a typical spectroelectrochemical experiment in which the electrochromic film is monitored at a steady-state (*i.e.* constant applied potential). Rather, it is an in-situ measurement of the dynamic change in the film optical transitions. In this measurement, polymer films were stepped between the neutralized and the oxidized state (-0.2 and +0.8 V *vs.* Ag/AgCl) using a 2 s switch time, and the optical spectra were captured every 6 ms during the electrochromic transition period. The selected transmittance spectra in Figure 4-13 are shown at intervals of 50 ms for clarity. (A total of 41 spectra are abstracted from about 320 spectra in a 2 s switch.)

For **WS-ECP-Blue-acid**, the polymer film in the colored neutral state shows a low transmittance of 10% at λ_{max} (635 nm). Upon applying a positive potential (+0.8 V *vs.* Ag/AgCl) to the polymer film, the transmittance steadily increases to a higher level (Figure 4-13a). When the bleached state is reached, the film shows a transmittance of 46% with a transmittance contrast of 36% ($\Delta\%T$). Although the polymer shows a dual-band absorption, the high energy band with λ_{max} at 370 nm will not be discussed in this case, since the human eyes are not sensitive at that region. Moreover, the polymer film of **WS-ECP-Black-acid** demonstrates a transmittance of 12% in the neutral state and 68% in the fully bleached state at 555 nm with a transmittance contrast of 56% (Figure 4-13b).

a)

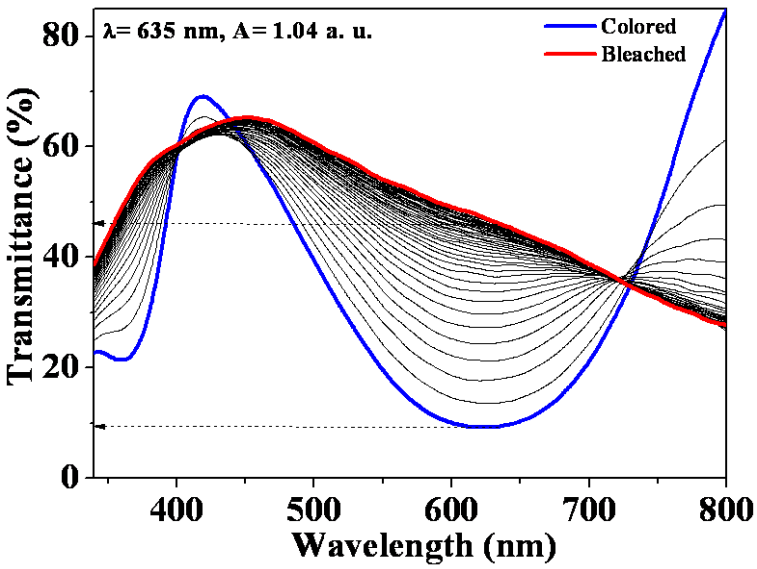

b)

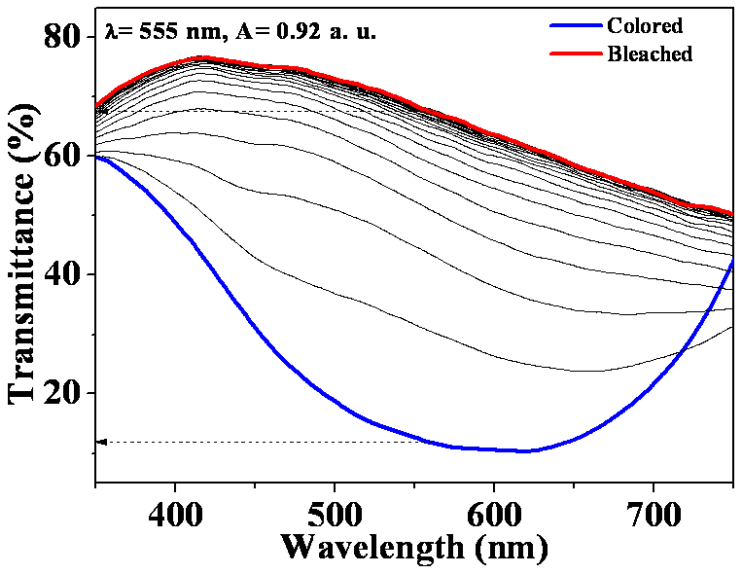

Figure 4-13. Rapid full spectrum measurement of polymers. a) **WS-ECP-Blue-acid** and b) **WS-ECP-Black-acid** film. Switching from -0.2 V to +0.8 V *vs.* Ag/AgCl with the full potential step in 0.2 M KNO_3/water electrolyte solution. Spectra are showed at 50 ms intervals for a total of 41 spectra in 2000 ms.

Another interesting aspect in this new methodology is that an estimate of the switching speed profile can be roughly observed in the absorption/transmission spectra, because each spectrum shown has a 50 ms time separation in Figure 4-13a and b. And this forms a time line in the whole spectra. In the case of **WS-ECP-Blue-acid**, the

transmission increase in the long wavelength region (500-700 nm) is relatively steady and slow, and the first 20 spectra can be clearly observed in the figure. However, the **WS-ECP-Blue-acid** shows a more pronounced transmission increase, so that the spectra after the first 10 transitions are compressed at a transmission level close to the fully bleached state, indicating a faster switching speed compared to the blue polymer.

In order to quantitatively evaluate how fast the polymers are switched, the transmittance values at a single wavelength were extracted from the collected data and plotted *vs.* their acquisition times. Figure 4-14a shows the results for **WS-ECP-Blue-acid**. Judging by the transmittance profile, which is still increasing after 2 seconds, the polymer film is unable to reach a fully transimissive oxidized state in this time frame using a potential of +0.8 V *vs.* Ag/AgCl. Although the low potential will protect the polymer film from being overoxidized, it could lower the switching speed because of insufficient driving force for ion motion, and lower the contrast as well since the polymers are not fully oxidized. In this case, 95% of the full transmittance contrast ($t_{95\%}$) for the bleaching process is achieved after 1060 ms (from transmittance of T= 9.6% to T= 45.0%), whereas the neutralization process is achieved in 190 ms (from T= 46.9% to T= 11.5%).

On the other hand, **WS-ECP-Black-acid** presents a fully bleached state in the 2 seconds time frame. This is due to the polymer‘s low oxidation potential (high HOMO level), which results in a large potential difference compared to +0.8 V *vs.* Ag/AgCl, and thus a stronger driving force for ion motion. A $t_{95\%}$ (from T= 12.9% to T= 65.4%) of 440 ms is observed for the bleaching process, which is faster than that of **WS-ECP-Blue-**

acid ($t_{95\%}$= 1060 ms). However, a slightly slower neutralization process is observed with $t_{95\%}$ of 390 ms (from T= 68.2%% to T= 15.7%).

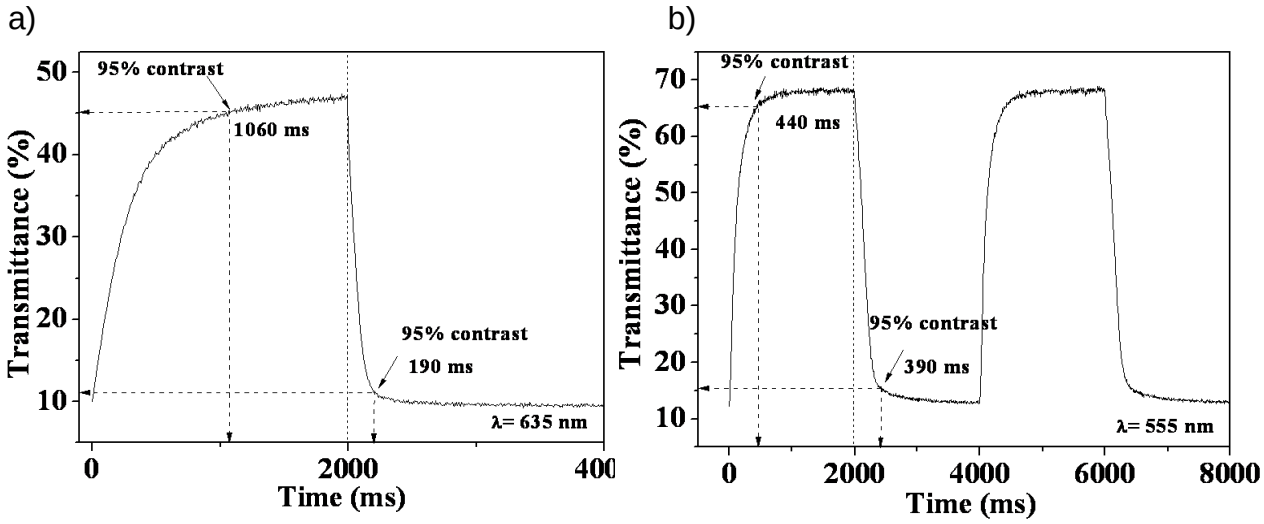

Figure 4-14. Time dependence of polymers. a) **WS-ECP-Blue-acid** at 635 nm and b) **WS-ECP-Black-acid** at 555 nm with an applied 2-second potential square-wave from -0.2 V to +0.8 V *vs.* Ag/AgCl in 0.2 M KNO_3/water electrolyte solution.

4.6 Chapter Summary

The design of conjugated electrochromic polymers (ECPs) has been driven by their excellent solution processability and rapid switching properties, as well as the growing interest in their application in non-emissive electrochromic devices (ECDs). In this chapter, we have demonstrated the synthesis of two new ECPs by Stille polymerization: a blue-to-transmissive conjugated polymer (**ECP-Blue**) and a black-to-transimissive conjugated polymer (**ECP-Black**). The structural, optical, electrochemical and electrochromic (EC) properties of both resulting polymers were characterized. Importantly, the defunctionalization of the carboxylate ester side chains affords the polymer salts with great water solubility, which can be processed from polymer/water solutions into thin films by spray-casting onto ITO glasses. Upon the subsequent neutralization of the thin-films, the resulting polymer acid films are ready to be switched

in a KNO_3/water electrolyte solution and show a dramatic improvement in the EC switching speed performance compared with their ester derivatives at the sub-second switching time scale. Moreover, a rough estimate of the effect of film thicknesses on switching performance was obtained using **ECP-Blue** as an example. The results of the electrochromic properties study indicate that these water soluble electrochromic conjugated polymers are promising candidates for rapid switching electrochromic devices.

Regardless of all the inspiring results shown in this chapter, the side-chain defunctionalization approach, as well as the following neutralization process, provides a new perspective in making multilayer devices. More specifically, a second polymer layer can be easily processed on top of the first lay with polymers that cannot be dissolved in organic solvents or water.

One major concern in this work is that the **ECP-Black** is not really black due to its lack of absorption in the range of 400 to 500 nm. To increase the 'blackness', a more bulky side chain could be used on monomer **7** (Figure 4-5) without significantly affecting its reactivity in Stille polymerization. The bulky side chain on monomer **7** will interact with the massive functional groups on the monomer **5** repeat unit, and afford a more twisted plane conformation of the backbone, resulting in an increase in the band gap and blue shift of the optical transition. Future work can also be directed toward applying this methodology to the synthesis of water soluble conjugated polymers with other saturated colors (yellow, cyan, and red *etc*.), as well as tuning the switching conditions for rapid EC switches.

4.7 Experimental Details

Bis(2-ethylhexyl) 5-hydroxyisophthalate (2) To a stirred suspension of 5-hydroxy-isophthalic acid (30 g, 165 mmol) and 2-ethylhexan-1-ol (51.5 g, 395 mmol) in 250 mL toluene, concentrated H_2SO_4 (5 drops) was added and the reaction mixture was refluxed with a Dean-Stark apparatus for 48 h. After removal of unreacted 5-hydroxy-isophthalic acid by filtration, the residue was washed with water for three times and dried over anhydrous $MgSO_4$. The solvent was evaporated and the residue was purified by flash chromatography using 8:1:1 hexane: ethyl acetate: acetone to give compound **2** as a yellow oil (50 g, 75%). ^{1}H NMR ($CDCl_3$): δ 8.22 (t, 1H, *J*= 1.2 Hz), δ 7.85 (d, 2H, *J*= 1.2 Hz), δ 7.06 (br, 1H), δ 4.27 (d, 4H, *J*= 5.7 Hz), δ 1.72 (m, 2H), δ 1.50-1.31 (m, 16H), δ 0.96-0.87 (m, 12H). ^{13}C NMR ($CDCl_3$): δ 166.52, 156.82, 132.32, 122.75, 121.23, 68.17, 39.10, 30.73, 29.18, 24.17, 23.16, 14.23, 11.28. HRMS (ESI–FTICR): *m/z* calcd for $C_{24}H_{38}NaO_5$ ($M+Na^+$) 429.2611 found 429.2618. Anal. calcd for $C_{24}H_{38}O_5$: C 70.90, H 9.42, found C 70.53, H 9.78.

Tetrakis(2-ethylhexyl) 5,5'-(3,4-dihydro-2H-thieno[3,4-b][1,4]dioxepine-3,3-diyl)bis(methylene)bis(oxy)diisophthalate (3) Compound **1** (5 g, 14.6 mmol), compound **2** (17.8 g, 43.8 mmol), K_2CO_3 (12.1 g, 87.7 mmol), KI (0.97 g, 5.9 mmol) and DMF (60 mL) were added to a 100 mL round bottom flask. And the solution was irradiated with microwaves under reflux at 150°C (maximum power 200 W) for 1 h. After removal of the extra salt by filtration, the reaction mixture was diluted with methylene chloride and washed with water. The organic phase was dried over $MgSO_4$ and the solvent was removed. The crude product was purified by column chromatography on silica gel (hexane: ethyl acetate, 9:1) to yield the desired product as a yellow oil (10.8 g,

74%). ^{1}H NMR ($CDCl_3$): δ8.26 (t, 2H, *J*= 1.2 Hz), δ7.75 (d, 4H, *J*= 1.5 Hz), δ6.52 (s, 2H), δ4.31 (s, 4H), δ4.30 (s, 4H), δ4.24 (d, 8H, *J*= 6.0 Hz), δ1.72 (m, 4H), δ1.48-1.26 (m, 32H), δ0.97-0.86 (m, 24H). ^{13}C NMR ($CDCl_3$): δ165.85, 158.75, 149.34, 132.50, 123.54, 119.82, 105.91, 72.88, 68.05, 67.12, 47.61, 39.08, 30.74, 29.18, 24.18, 23.16, 14.26, 11.27. HRMS (ESI–FTICR): *m/z* calcd for $C_{57}H_{85}O_{12}S$ ($M+H^+$) 993.5756 found 993.5740. Anal. calcd for $C_{57}H_{84}O_{12}S$: C 68.92, H 8.52, found C 68.68, H 8.74.

Tetrakis(2-ethylhexyl) 5,5'-(6,8-dibromo-3,4-dihydro-2H-thieno[3,4-b][1,4]dioxepine-3,3-diyl)bis(methylene)bis(oxy)diisophthalate (4) A solution of NBS (1.1 g, 6.3 mmol, in 15 mL acetonitrile) was added slowly to a compound **3** (3.0 g, 3.0 mmol) chloroform (15.0 mL) solution at 0°C. The mixture was stirred at the same temperature for 2 h before allowing it to warm to room temperature. After stirring at room temperature for overnight, the solution was diluted with methylene chloride and the organic phase was washed with water and dried over anhydrous $MgSO_4$. The solvent was evaporated and the residue was purified by column chromatography on silica gel (hexane: ethyl acetate, 9:1) to yield the desired product as a light yellow oil (3.1 g, 90%). ^{1}H NMR ($CDCl_3$): δ8.27 (t, 2H, *J*= 1.2 Hz), δ7.74 (d, 4H, *J*= 1.2 Hz), δ 4.38-4.25 (m, 16H), δ1.72 (m, 4H), δ1.51-1.26 (m, 32H), δ0.97-0.85 (m, 24H). ^{13}C NMR ($CDCl_3$): δ165.78, 158.53, 146.67, 132.54, 123.67, 119.75, 91.88, 73.25, 68.07, 66.80, 47.75, 39.07, 30.72, 29.17, 24.17, 23.16, 14.26, 11.27. HRMS (ESI–FTICR): *m/z* calcd for $C_{57}H_{83}Br_2O_{12}S$ ($M+H^+$) 1151.3955 found 1151.3917. Anal. calcd for $C_{57}H_{82}Br_2O_{12}S$: C 59.47, H 7.18, found C 59.68, H 7.49.

Tetrakis(2-ethylhexyl) 5,5'-(6,8-bis(trimethylstannyl)-3,4-dihydro-2H-thieno[3,4-b][1,4]dioxepine-3,3-diyl)bis(methylene)bis(oxy)diisophthalate (5) A

solution of compound **4** (5 g, 4.3 mmol), hexamethylditin (4.3 g, 13.1 mmol) and $Pd(PPh_3)_4$ (1 g, 0.9 mmol) in toluene (50 mL) was degassed three times by successive freeze-pump-thaw cycles and heated at 115°C for 3 h during which time TLC analysis indicated completion of the reaction. The reaction mixture was then cooled to room temperature and water was added. After extraction with methylene chloride, the organic phase was dried with anhydrous $MgSO_4$ and solvent was removed under vacuum. The remaining residue was then taken up in hexanes and filtered over a pad of silica gel (the gel was pre-treated with neat triethylamine and washed with hexanes), and the solvent was then evaporated to give a colorless oil (4.1 g, 72%). ^{1}H NMR ($CDCl_3$): δ 8.27 (t, 2H, *J*= 1.2 Hz), δ 7.77 (d, 4H, *J*= 1.2 Hz), δ 4.33-4.23 (m, 16H), δ 1.75 (m, 4H), δ 1.50-1.35 (m, 32H), δ 0.98-0.88 (m, 24H), δ 0.35 (s, 18H). ^{13}C NMR ($CDCl_3$): δ 165.86, 158.84, 156.28, 132.42, 124.10, 123.35, 119.79, 72.94, 67.98, 67.42, 47.34, 39.05, 30.71, 29.15, 24.16, 23.12, 14.22, 11.25, -8.35. Anal. calcd for $C_{63}H_{100}O_{12}SSn_2$: C 57.37, H 7.64, found C 57.65, H 7.73.

3,3-Dimethyl-3,4-dihydro-2H-thieno[3,4-b][1,4]dioxepine (**6**) 3,4-dimethoxythiophene (10 g. 69 mmol), 2,2-dimethylpropane-1,3-diol (14.4 g, 139 mmol), *p*-toluenesulfonic acid (1.3 g, 6.9 mmol), and 300 mL toluene were combined in a 500 mL flask equipped with a soxhlet extractor with molecular sieves in a cellulose thimble. The solution was refluxed for 1 day. The reaction mixture was cooled, and after dilution with ether (100 mL), the organic phase was washed with water and dried over anhydrous magnesium sulfate. The solvents were removed under vacuum, and the crude product was purified by column chromatography with hexane as an eluent to obtain compound **6** as a white crystalline solid (9.7 g, yield: 76%). ^{1}H NMR ($CDCl_3$) δ

6.47 (s, 2H), δ3.73 (s, 4H), δ1.03 (s, 6H). ^{13}C NMR ($CDCl_3$) δ150.23, 105.74, 80.33, 39.11, 21.91.

6,8-Dibromo-3,3-dimethyl-3,4-dihydro-2H-thieno[3,4-b][1,4]dioxepine (**7**) A solution of NBS (7.9 g, 44.4 mmol, in 50 mL acetonitrile) was added slowly to a compound **6** (3.9 g, 21.2 mmol) chloroform (50 mL) solution at 0°C. The mixture was stirred at the same temperature for 2 h before allowing it to warm to room temperature. After stirring at room temperature for overnight, the solution was diluted with methylene chloride and the organic phase was washed with water and dried over anhydrous $MgSO_4$. The solvent was evaporated and the residue was purified by column chromatography on silica gel (hexane) to yield the desired product as a white solid (6.85 g, 95%). ^{1}H NMR ($CDCl_3$): δ3.80 (s, 4H), δ1.04 (s, 6H). ^{13}C NMR ($CDCl_3$): δ147.46, 91.70, 80.53, 39.26, 21.80. HRMS (ESI–FTICR): *m/z* calcd for $C_9H_{10}Br_2O_2S$ (M^+) 341.8748 found 341.8689. Anal. calcd for $C_9H_{10}Br_2O_2S$: C 31.60, H 2.95, found C 31.77, H 2.81.

General Polymerization Procedure. Polymer ECP-Blue: A solution of compound **5** (0.9 g, 0.68 mmol), compound **8** (0.201 g, 0.68 mmol), tris(dibenzylideneacetone)dipalladium (0) (13.8 mg, 0.015 mmol) and tri(o-tolyl)phosphine (18.3 mg, 0.06 mmol) in toluene (20 mL) was degassed three times by successive freeze-pump-thaw cycles and heated at 115°C for 36 h in an oil bath. The solution was then precipitated into methanol (400 mL). The precipitate was filtered through a cellulose thimble and purified via Soxhlet extraction for 24 hours with methanol and then 48 hours with hexane. The polymer was extracted with chloroform, concentrated by evaporation, and then precipitated into methanol again (400 mL). The

collected polymer was a blue solid (0.7 g, 91 %). ^{1}H NMR (300 MHz, $CDCl_3$) δ 8.41 (s, 2H), 8.27 (s, 2H), 7.81 (d, 4H, *J*= 0.9 Hz), 4.67 (s, 4H), 4.50 (s, 4H), 4.30-4.20 (m, 8H), 1.74-1.29 (m, 36H), δ 0.95-0.85 (m, 24H). GPC analysis: M_n = 25.8 kDa, M_w = 38.5 kDa, PDI = 1.5. Anal. Calcd. for $C_{63}H_{84}N_2O_{12}S_2$: C 67.23, H 7.52, N 2.49, found C 66.94, H 7.64, N 2.42.

ECP-Black: Compound **5** (0.9 g, 0.682 mmol), compound **7** (0.163 g, 0.478 mmol), compound **8** (0.060 g, 0.205 mmol), tris(dibenzylideneacetone)dipalladium (0) (13.8 mg, 0.015 mmol) and tri(o-tolyl)phosphine (18.3 mg, 0.06 mmol), toluene (20 mL). The collected polymer was a black solid (0.66 g, 84 %). ^{1}H NMR (300 MHz, $CDCl_3$) δ 8.25 (m, 13H), 7.79 (s, 20H), 4.48-4.21 (m, 80H), 4.50 (s, 4H), 3.85 (s, 14H), 1.69-1.11 (m, 180H), δ 0.95-0.85 (m, 141H). GPC analysis: M_n = 13.9 kDa, M_w = 23.3 kDa, PDI = 1.7. Anal. Calcd. for $C_{651}H_{896}N_6O_{134}S_{20}$: C 67.46, H 7.79, N 0.73, found C 67.11, H 7.89, N 0.68.

WS-ECP-Blue: A solution of 1 M KOH in methanol (50 mL) was refluxed and simultaneously sparged with argon for two hours, and **ECP-Blue** (360 mg) was added as a solid. This suspension was refluxed for 24 hours, during which time the polymer dispersed into fine particles. The suspension was filtered on a nylon filter paper and washed with 100 mL methanol followed by 100 mL diethyl ether, and dried under vacuum to yield 260 mg of a dark solid (90%).

WS-ECP-Black: The same reaction and purification procedure as described for **WS-ECP-Blue** was followed. **ECP-Black** (395 mg) was used. Got polymer **WS-ECP-Black** 300 mg as a dark black powder, yield 92%.

WS-ECP-Black-acid and **WS-ECP-Blue-acid:** Refer to manuscript text.

CHAPTER 5
FINE ABSORPTION TUNING IN DIKETOPYRROLOPYRROLE-BASED CONJUGATED POLYMERS FOR PHOTOVOLTAIC APPLICATIONS

5.1 Improvement of the Light-Harvesting Efficiency

In Chapter 3 and 4, two polymer systems for electrochromic applications were developed. Although these two types of polymeric materials are distinct in their structures, they share the same chemistry approach, the random Stille polymerization method. In this chapter, we will focus on extending this methodology to the synthesis of conjugated polymers with efficient light harvesting properties (light absorption) as well as well-defined energy levels and band gaps; and explore their potential application in photovoltaic devices.

As mentioned in Chapter 1, due to the development of donor-acceptor conjugated polymers with low band gaps and reasonable solution processabilities, significant progress has been made in the field of OPVs. Power conversion efficiencies (PCEs) of polymer/fullerene BHJ solar cells have reached 7% in academia,[161-164] or even above 8%, a psychological barrier, in industry.[243-245] This dramatic improvement in OPV performance, along with the capability of low cost fabrication into light weight, large area and flexible devices,[138,142,146] has made them a strong competitor to the silicon based solar cells.

However, the improvement of PCEs does not occur spontaneously. It is based on several years' intense research to acquire the know-how for synthesis and characterization of conjugated polymers as efficient p-type materials for OPVs.[212] Of paramount importance is the polymers' ability to absorb sunlight. The materials should present a broad absorption (400-850 nm) across the visible and near-IR region with a high absorption coefficient, since the short-circuit current density (J_{sc}) of the solar cell is

proportional to the spectral absorption breadth and absorption probability of the polymer/PCBM active layer.[246] Second, the material should have a low-lying HOMO energy level to assure a large energy difference compared to the LUMO of PCBM, and thus a high open-circuit voltage (V_{oc}).[57,212,247-249] Third, a proper offset between the LUMO energy levels of the polymer and the fullerene derivative is necessary in order to provide sufficient driving force for charge generation. Fourth, the materials should present high hole mobilities[250,251] and a balanced charge carrier mobility in the polymer/PCBM blends, which favors charge extraction and transport, leading to an increase in fill factors.[252] Finally, the polymers must be able to mix with fullerene effectively in order to generate a nanoscale bicontinuous morphology with favored phase separation and interpenetrating network.[253-255]

For the first parameter, the improvement of the light-harvesting efficiency is usually achieved via the donor-acceptor approach,[53-55] which reduces the polymer band gap by incorporating electron-rich and electron-deficient units together. However, instead of broadening the polymer absorption profile, this approach mostly shifts the polymer absorption into the solar radiation region that has a larger fraction of solar photons; on the other hand, it diminishes the absorption in the region of 400-600 nm, which hinders the desired increase of J_{sc} and efficiency.[59,256-259] Consequently, several methods have been devised in order to fulfill the purpose of broadening the polymer absorption.

One of the most important methods here is the use of tandem bulk-heterojunction solar cells to minimize the loss of absorption. More specifically, two BHJ solar cells with different absorption characteristics are stacked in series to generate a wider range of absorption in the solar spectrum. The first tandem BHJ solar cell was reported by

Heeger and coworkers.[260] In this report, a D-A polymer PCPDTBT/$PC_{61}BM$ blend, which absorbs mainly in the range of 600-850 nm (Figure 5-1b), is used as the active layer in the front cell (Figure 5-1a), while P3HT/$PC_{71}BM$ blend, which absorbs from 450 to 650 nm in the visible region, is used as complementary light-absorbing active layer in the back cell. For comparison, the PCPDTBT/$PC_{61}BM$ single cell yields a PEC of 3.0% with J_{sc} of 9.2 mA cm^{-2}, V_{oc} of 0.66 V and *FF* of 0.5; the P3HT/$PC_{71}BM$ single cell yields a PEC of 4.7% with J_{sc} of 10.8 mA cm^{-2}, V_{oc} of 0.63 V and *FF* of 0.69; and the tandem cell shows a PEC of 6.5% with J_{sc} of 7.8 mA cm^{-2}, V_{oc} of 1.24 V and *FF* of 0.67. Clearly, the major contribution to the improvement of the tandem cell is the large open circuit voltage, which is the sum of the individual subcell voltages. The current, which is extracted from the tandem cell, is limited by the current generated from the subcell with smaller J_{sc}.

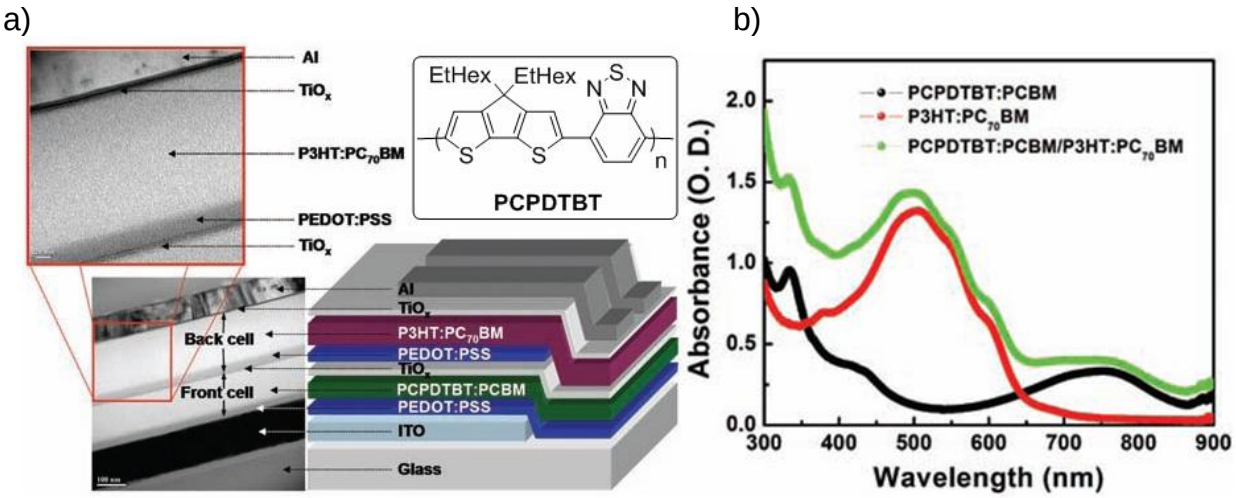

Figure 5-1. Illustration of a tandem bulk-heterojunction solar cell. a) Device structure (right) and TEM cross-sectional image (left) of the polymer tandem solar cell. Scale bars, 100 nm (lower image) and 20 nm (upper image). Structure of PCPDTBT (top right). b) Absorption spectra of a PCPDTBT:$PC_{71}BM$ bulk heterojunction composite film, a P3HT:$PC_{71}BM$ bulk heterojunction composite film, and a bilayer of the two, as relevant to the tandem device structure (O.D., optical density). (Adopted and modified with permission from Ref. 260).

Although a similar strategy has been successfully applied to other polymer systems and shows promising results,[261-264] it is also worth noting that this technique requires considerable work to optimize and balance the current in each subcell, as well as the complicated processing procedure to deposit a large number of different layers, thereby increasing the cost of production and limiting the commercial use.

An alternative way to increase the light-harvesting efficiency is by incoperating small molecule sensitizers for near-infrared absorption.[265] Generally, dye molecules, which can absorb at longer wavelengths of the solar spectrum (compared to the donor polymer P3HT), are simply blended into the polymer/PCBM mixture as additional components. These dye molecules located at the interface can contribute not only to the photocurrent generation by direct photoexcitation, but also they can harvest excitons efficiently from the donor polymer to the dye molecules through long-range energy transfer. For example, Ito *et al.* demonstrated the use of the near-infrared dye silicon phthalocyanine bis(trihexylsilyl oxide) (Figure 5-2a for structure of SiPc) in a P3HT/PCBM/SiPc ternary blend device, which showed an increased of J_{sc} from 6.5 to 7.9 mA cm^{-2}, while keeping the V_{oc} and *FF* unchanged, and thus a 20% increase of the PCE from 2.2% to 2.7% (Figure 5-2b).[266] However, this method also suffers from the formation of dye aggregates in blend films, which reduce the absorption efficiency and the charge mobility of the active layer.[267,268]

In this chapter, we discuss our efforts in the improvement of the light-harvesting efficiency of conjugated polymers by broadening their absorption spectra on the molecular level. More specifically, we use diketopyrrolopyrrole (DPP) as an acceptor, incorporate it into a random donor-acceptor polymer system by Stille polymerization,

and control the polymer absorption by tuning the monomer feed ratio. We further explore the photovoltaic prosperities of these DPP-based random copolymers by applying them in solar cells.

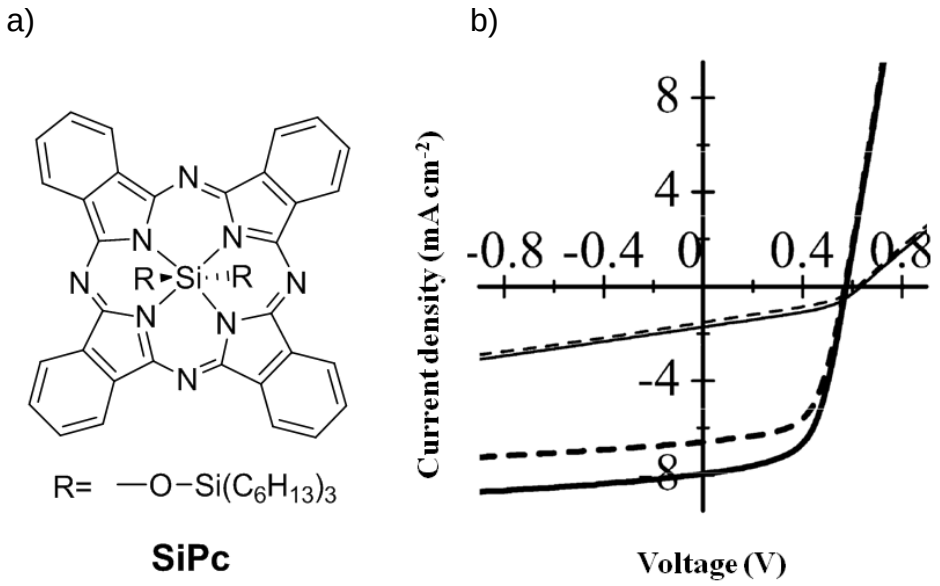

Figure 5-2. Bulk-heterojunction solar cell with SiPc as an additional component. a) Structure of SiPc. b) *J-V* characteristics of P3HT/PCBM (broken lines) and P3HT/PCBM/SiPc blend films (solid lines), both before (thin lines) and after (thick lines) annealing. (Adopted and modified with permission from Ref. 266).

5.2 Concept and Design of Broadly Absorbing Diketopyrrolopyrrole-Based Low Band Gap Polymers

Derivatives of 2,5-diketopyrrolo[3,4-c]pyrrole (DPP) have been widely used as high-performance pigments for fibers, plastics, prints and inks during the past three decades, due to their excellent photochemical and thermal stability, various color choices and high luminescence.[269] The electron-withdrawing effect of the DPP units causes the chromophore to have a high electron affinity, and DPP has become a popular acceptor used in the conjugated polymer systems for FETs, OLEDs and OPVs.[58,270-275] For example, Janssen *et al.* demonstrated the synthesis of PDPP3T for high performance OPVs with a PCE of 4.7% (also see Chapter 1).[109] As an extension of

that work, Fréchet and coworkers reported the synthesis of the copolymer PDPP2FT (a furan derivative of PDPP3T), with which the polymer/$PC_{71}BM$ BHJ solar cell achieved a PCE of 5%.[276] In this work, a series of copolymers were synthesized using DPP as an acceptor, and thiophene and dialkyloxybenzodithiophene (BDT) as donor repeat units (Figure 5-3). Fundamental understanding of the balance of polymer solubility, stacking ability, light absorption, and energy levels is key to this chapter.

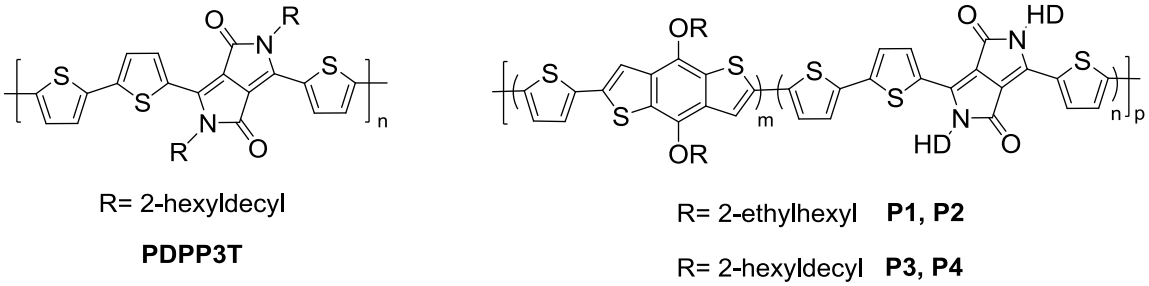

Figure 5-3. Chemical structure of **PDPP3T** and **P1**-**P4**.

During the course of our studies, two reports by Thompson[277] and Chen[278] appeared, respectively, describing a strategy similar to ours for the synthesis of DPP-based random copolymers with broad absorption spectra for OPVs. In the first report, three novel semi-random P3HT based donor-acceptor copolymers containing 5-15% of the acceptor DPP were synthesized by Stille polymerization (Figure 5-4a). For copolymers P3HTT-DPP-10% and P3HTT-DPP-15%, broad intense absorption spectra covering the range of 350 to 850 nm with absorption maxima at 685 and 703 nm were observed (Figure 5-4b). A BHJ solar cell using P3HTT-DPP-10%/$PC_{61}BM$ blend (1:1.3) as an active layer showed an efficiency of 4.94% with J_{sc} of 13.87 mA cm^{-2}, V_{oc} of 0.57 V and *FF* of 0.63.

In the second report, random donor–acceptor copolymer PDPP–T–DTT based on DPP as the acceptor unit, dithienothiophene (DTT) and thiophene as the donor units,

was synthesized by random Stille polymerization (Figure 5-5). BHJ solar cells using PDPP–T–DTT as a donor polymer and $PC_{71}BM$ as an acceptor (1:2) exhibited J_{sc} of 12.76 mA cm^{-2}, V_{oc} of 0.58 V and *FF* of 0.67 with a PCE of 5.02%.

a) b)

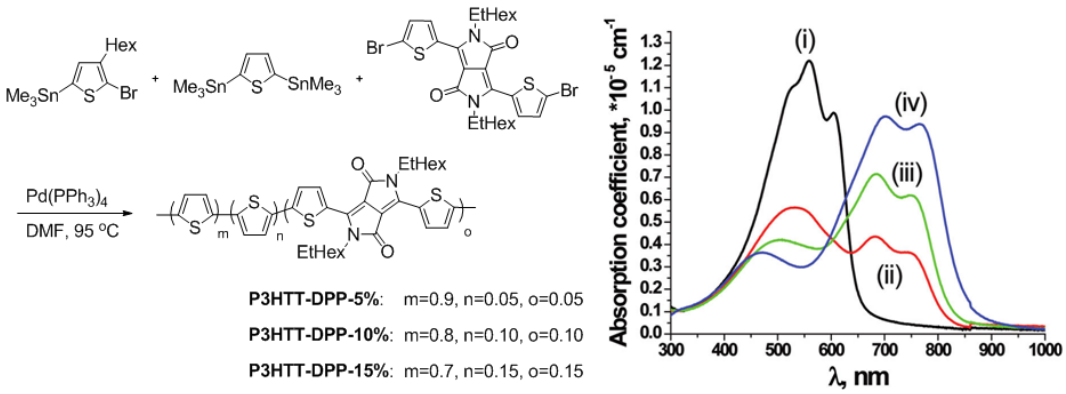

Figure 5-4. P3HTT-DPP copolymers for solar cells. a) Synthesis of P3HTT-DPP copolymers. b) Thin film (spin-coated from o-DCB) where (i) is P3HT (annealed at 150°C for 30 min for the thin films), (ii) is P3HTT-DPP-5%, (iii) is P3HTT-DPP-10% and (iv) is P3HTT-DPP-15% (thin film as-cast). (Adopted and modified with permission from Ref. 277)

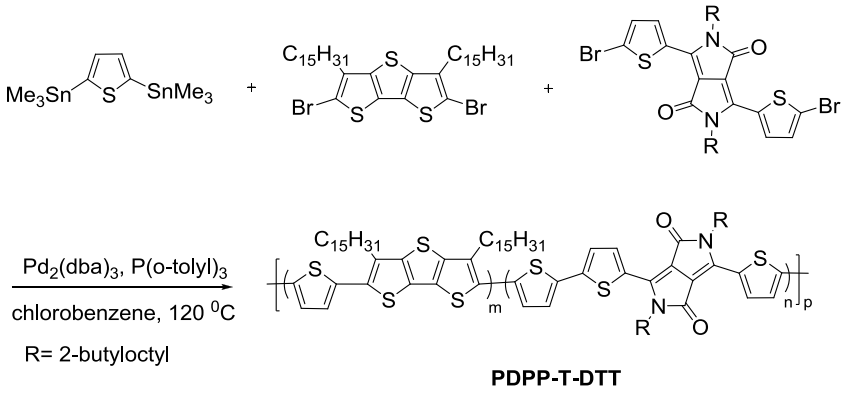

Figure 5-5. Synthesis of PDPP-T-DTT copolymer. (Adopted and modified with permission from Ref. 278)

5.3 Polymer Synthesis and Characterization

5.3.1 Monomer Synthesis

Referring to Figure 5-6, commercially available thiophene-2-carbonitrile was used to synthesize compound **1**, which was used without further purification due to the low

solubility in organic solvents caused by inter- and intramolecular H-bonding. N-alkylation of compound **1** with 7-(bromomethyl)pentadecane in the presence of potassium carbonate using DMF as solvent afforded compound **2** with a yield of 40%. Subsequent bromination of compound **2** with N-bromosuccimide in chloroform gave DPP-based monomer compound **3** in 90% yield. Instead of column chromatography, compound **3** was purified via a modified precipitation procedure by slowly adding the bad solvent (methanol) into the crude product THF solution. This slow precipitation process could extensively eliminate the impurities and afford a good yield of the reaction. It is worth mentioning that precipitation by adding the crude product THF solution into methanol (a reversed procedure) was not helpful in the purification process.

Moreover, fresh lithium diisopropylamide (LDA), which was made by reacting diisopropylamine with *n*BuLi, was used as a base in the synthesis of donor unit compound **4**. The ditin monomer is a white crystalline solid, which is believed to favor the formation of high molecular weight polymers, since solid starting material can be weighed more easily and accurately than the liquid one, affording better stoichiometric control. The synthesis procedure for making compound **5a** and **5b** was also modified in our case. Dialkyloxybenzodithiophene is commonly synthesized in aqueous solution using tetrabutylammonium bromide as a phase transfer agent and zinc powder as a reducing agent.[279,280] When this procedure was repeated in our lab, low reaction yield was observed (around 20-30%). By simply replacing water with DMF, the reaction yields were improved to 84% for **5a** and 76% for **5b**. Finally, monomer **6a** and **6b** were synthesized by bromination using NBS in a solvent mixture of chloroform and acetonitrile. Reaction yields of 74% and 69% were achieved, respectively.

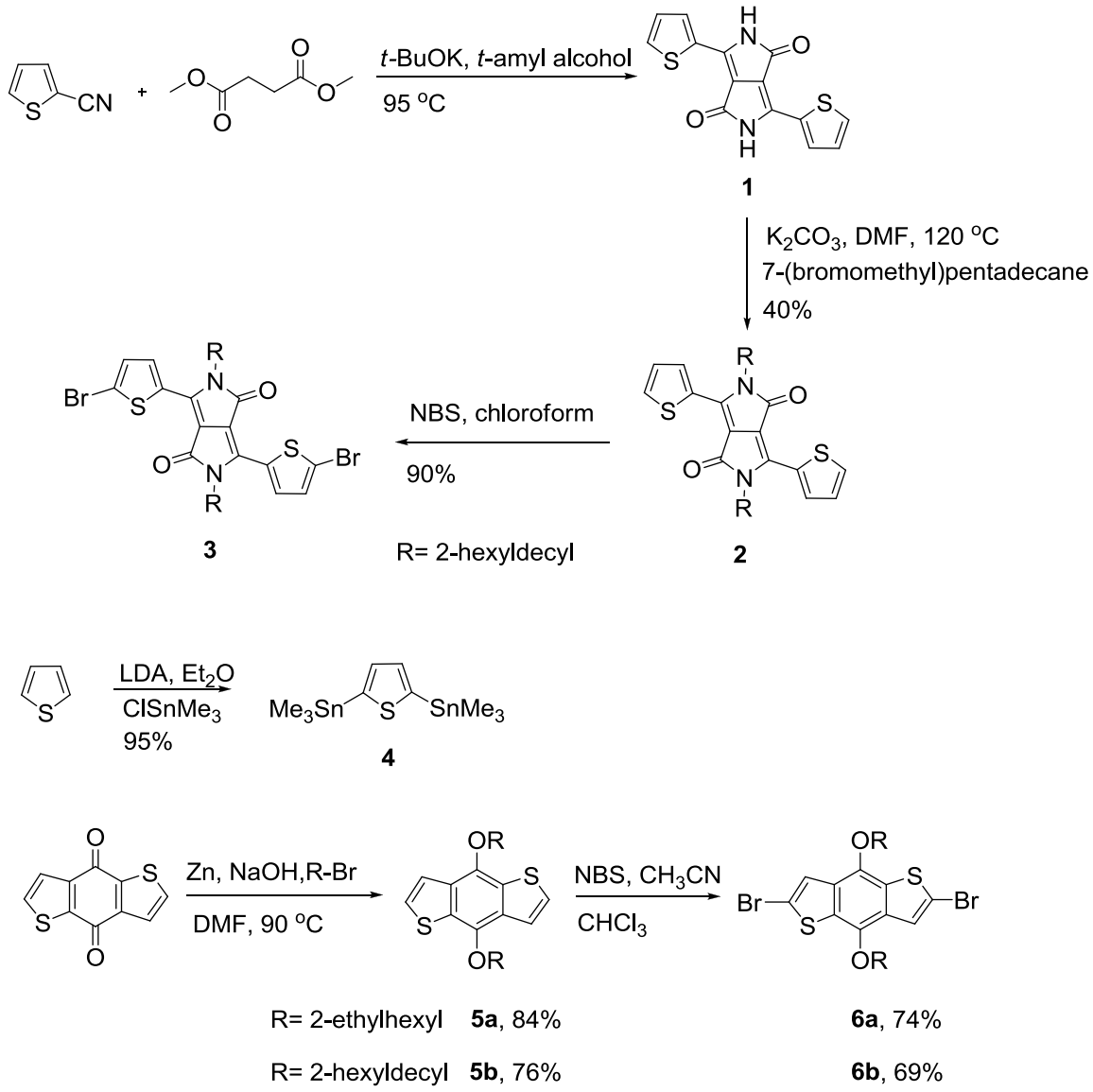

Figure 5-6. Synthesis of monomers **3**, **4**, **6a** and **6b**.

5.3.2 Polymer Synthesis: Expanding the Absorption Spectra of DPP based Donor-Acceptor Polymers

As a control polymer, alternating copolymer **PDPP3T** was successfully prepared by a Stille polymerization of dibromo compound **3** and ditin compound **4** (Figure 5-7). After Soxhlet extraction and re-precipitation, **PDPP3T** exhibited a number average molecular weight (M_n) of 124.9 kDa and PDI of 1.3 (Figure 5-8a). It is worth noting that the M_n here is much higher than that of the same polymer prepared by Suzuki

polymerization (M_n= 54.0 kDa, PDI= 3.15, estimated by GPC in ODCB at 80°C).[109] Good agreement of the elemental analysis results with the calculated numbers confirmed that the monomers were polymerized into the desired structure and the formed polymer was pure (Table 5-1). The dark green polymeric solid showed good solubility in chloroform and fair solubility in toluene and THF.

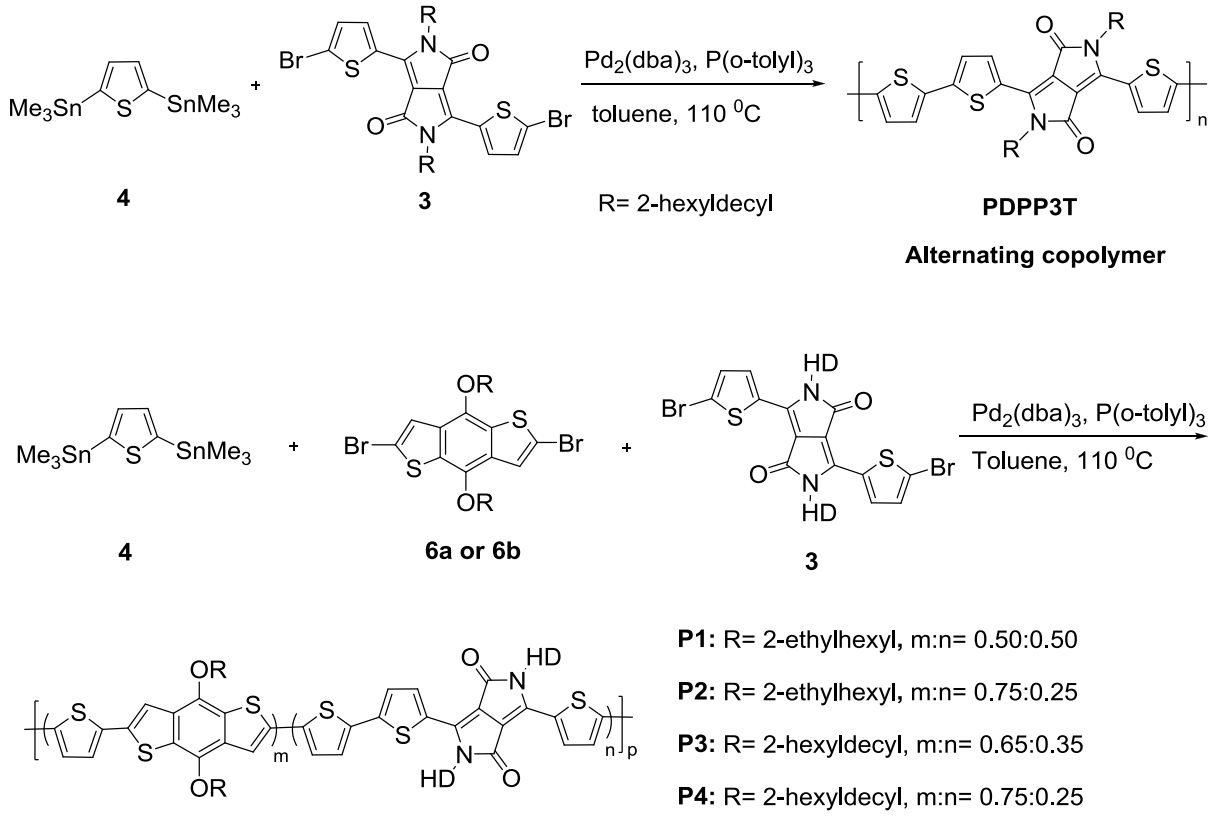

Figure 5-7. Synthesis of control polymer **PDPP3T** and random copolymer **P1**-**P4** via Stille polymerization

The synthesis of random copolymers **P1** and **P2** were carried out using the same polymerization condition as the control polymer **PDPP3T** (Figure 5-7). Copolymerization of 2,5-bis(trimethylstannyl)thiophene (**4**), 2,6-dibromo-4,8-diethylhexyloxybenzo[1,2-b:4,5-b']dithiophene (**6a**) and dibromo-bisthiophenediketopyrrolopyrrole (**3**) in a ratio of

1:0.5:0.5 and 1:0.75:0.25 yielded polymers **P1** and **P2** with M_n as high as 130.8 and 54.6 kDa, respectively (Table 5-1).

Table 5-1. GPC estimated molecular weights in THF and elemental analysis of the polymers.

	Monomer **4** ratio	Monomer **6** ratio	Monomer **3** ratio	M_n (kDa)	M_w (kDa)	PDI	EA (Calcd/Found)		
							C	H	N
PDPP3T	1	/	1	124.9	158.3	1.3	72.41/71.97	8.75/9.16	3.38/3.05
P1	1	0.50 (**6a**)	0.5	130.8	158.3	1.2	70.85/70.43	8.18/8.98	2.07/1.76
P2	1	0.75 (**6a**)	0.25	54.6	96.4	1.8	69.78/70.73	7.78/8.46	1.16/0.94
P3	1	0.65 (**6b**)	0.35	59.4	114.3	1.9	73.12/74.06	9.15/9.94	1.26/1.17
P4	1	0.75 (**6b**)	0.25	89.3	139.7	1.6	73.24/74.23	9.22/10.19	0.91/0.83

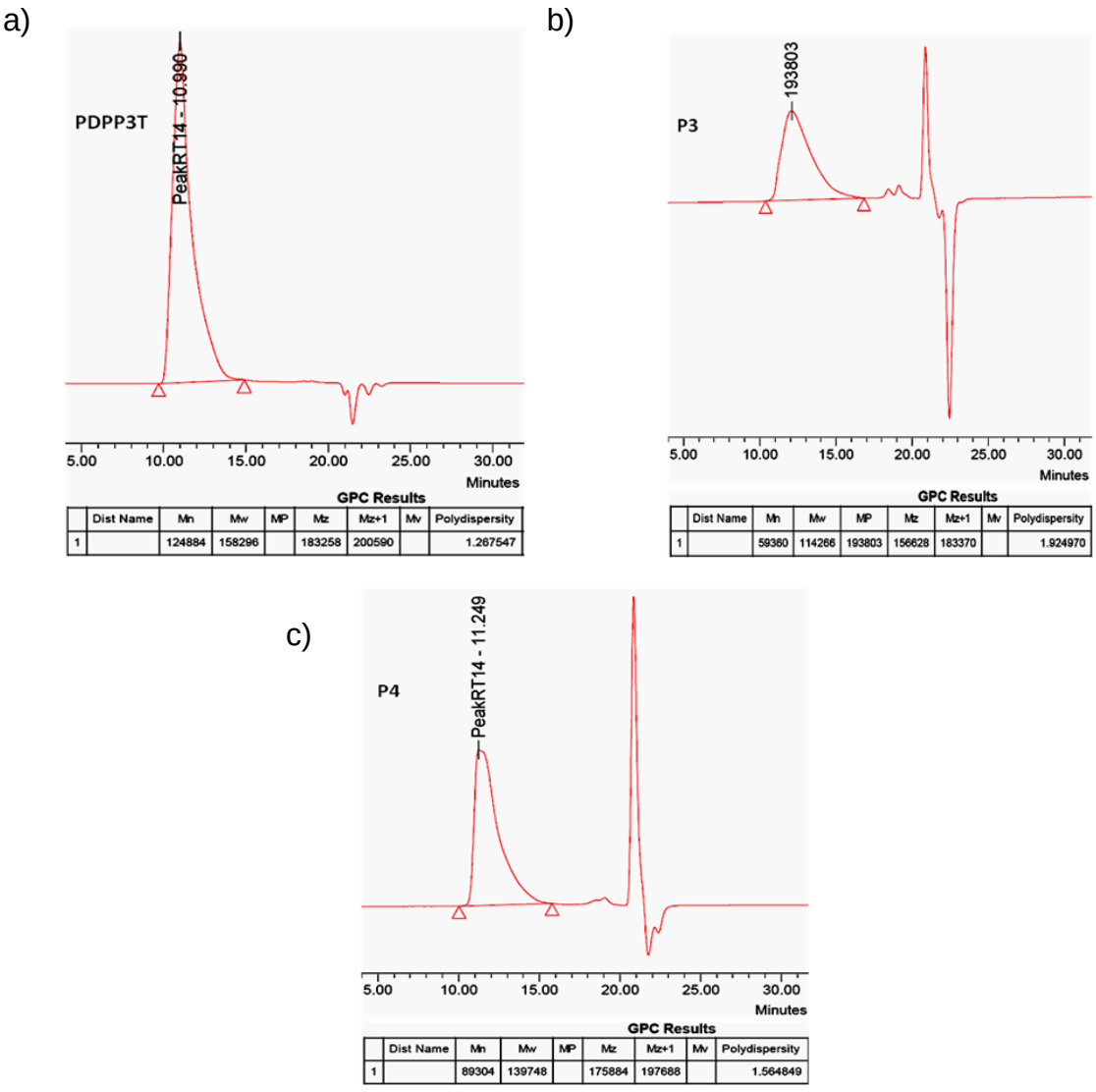

Figure 5-8. GPC trace of DPP based random copolymers. a) **PDPP3T**, b) **P3** and c) **P4** in THF solution at 40°C using polystyrene as a standard.

Polymer solution absorption spectra are shown in Figure 5-9a. Compared with **PDPP3T**, **P1** and **P2** show a blue shift of the low energy optical transition in the range of 600 to 850 nm. By increasing the relative amount of donor monomer **6a**, the difference in intensity between the two absorption bands is reduced. In the case of **P2**, the intensities of the two bands, which peak at 532 and 712 nm, are balanced. However, the broad absorption of **P2** from 350 to 850 nm is unable to cover the entire visible-NIR spectrum and leaves an absorption gap between 550 and 650 nm. Unfortunately, the solubility of **P1** and **P2** in organic solvents such as chlorobenzene, chloroform and THF is rather low, which prohibits the further utilization of these polymers in OPV application.

In order to improve the solubility of the random copolymers, monomer **6b** with 2-hexyldecyl side chains was synthesized and used in the copolymerization of polymers **P3** and **P4**. With the increased solubility, the polymerization yields were also improved to 67% for **P3** and 77% for **P4**. Importantly, the two polymers showed high molecular weights at 59.4 and 89.3 kDa with PDI of 1.9 and 1.6, respectively, which agreed well with the first three polymers. The GPC traces of **P3** and **P4** are shown in Figures 5-8b and 8c, and the results are summarized in Table 5-1. Polymer **P4** showed an absorption profile similar to **P2** in chlorobenzene solution (Figure 5-9b), which is as expected, since they shared the same monomer ratio, and thus the same polymer backbone. Compared with **P1**, **P3** with a higher benzodithiophene (BDT) ratio exhibited a relatively high intensity of the low wavelength absorption peak with an absorption maximum at 528 nm. A definite blue shift of the low energy optical transition in the range of 600 to 850 nm was also observed. Due to their good solubility in organic solvents, **P3** and **P4** were used in the subsequent characterizations.

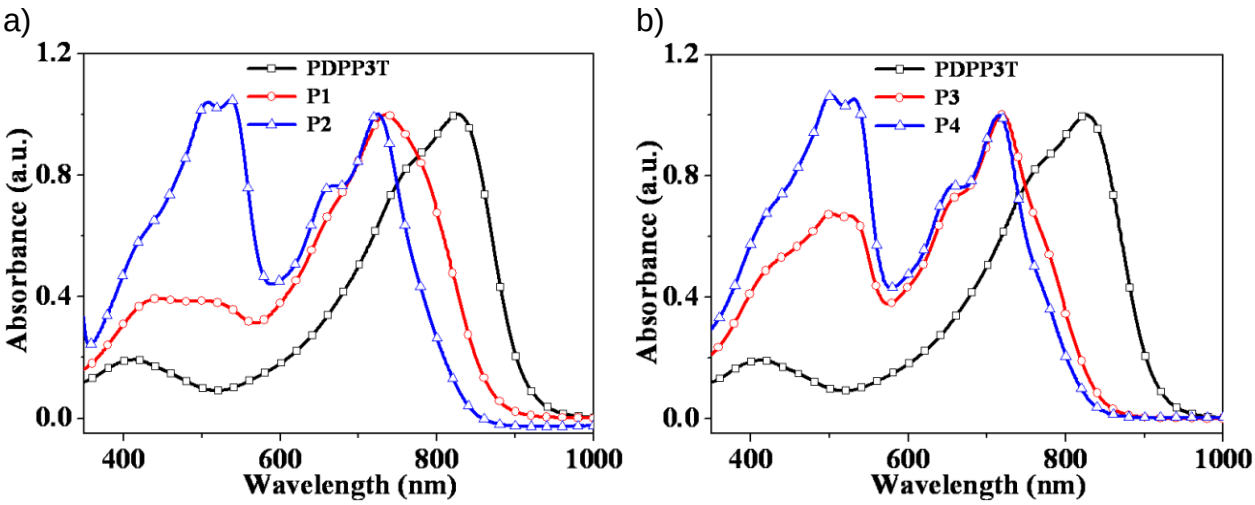

Figure 5-9. Normalized UV-vis-NIR absorption spectra of DPP based random copolymers. a) **PDPP3T, P1** and **P2** (b) **PDPP3T, P3** and **P4** in dilute chlorobenzene solution.

5.3.3 Polymer Electrochemistry and Energy Level Estimation

The HOMO and LUMO energy levels and band gaps for **PDPP3T**, **P3** and **P4** were measured by cyclic voltammetry (CV) and differential pulse voltammetry (DPV) using Ag/Ag^+ as a reference electrode calibrated *vs.* Fc/Fc^+, and converted to the vacuum scale using the approximation that the ferrocene redox couple is 5.1 eV relative to vacuum level. Figure 5-10 shows respectively the CV and DPV results obtained for the **PDPP3T**. The polymer exhibits onsets of oxidation at 0.45 and 0.18 V *vs.* Fc/Fc^+ and onsets of reduction at -1.44 and -1.38 V *vs.* Fc/Fc^+ according to the CV and DPV, respectively. Electrochemical band gaps, which were determined by the difference between the oxidation and reduction potentials, were calculated to be 1.89 and 1.56 eV (Table 5-2). Not surprisingly, there were differences between the CV and DPV results, since DPV measures a current difference, in which the major component of that difference is the faradaic current, and largely eliminates the capacitive component due to the charging of the electrode double layer. The polymer HOMO and LUMO energies

are estimated from the onsets of oxidation and reduction potential, respectively, and the results are shown in Table 5-2. The low lying HOMO level of **PDPP3T** (5.55 or 5.28 eV determined by CV or DPV) indicates that the polymer can be easily handled in air (threshold of air stability is at 5.2 eV). The LUMO level at around 3.6-3.7 eV provides a strong driving force for charge transfer from the polymer to PCBM with a LUMO at around 4.2 eV.

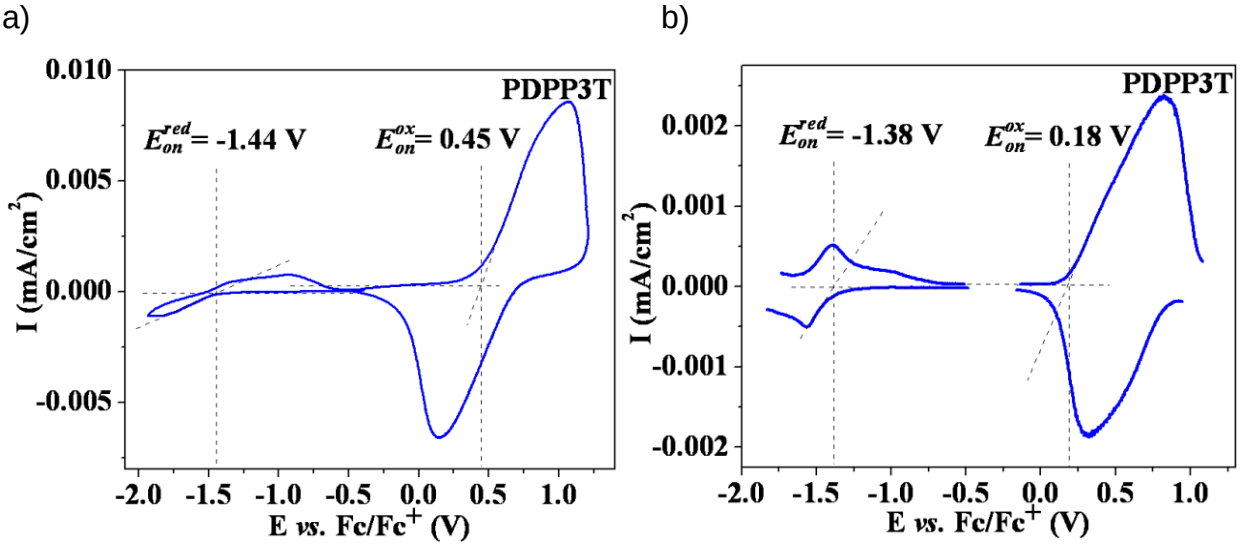

Figure 5-10. Electrochemistry results of polymer **PDPP3T**. a) Cyclic voltammograms (scan rate of 50 mV/s) and b) differential pulse voltammograms (step time of 0.1 s) of **PDPP3T** drop-cast from chlorobenzene solution onto a platinum button electrode (A= 0.02 cm^2). Measurements were performed in 0.2 M LiBTI /propylene carbonate (PC) with a Pt foil counter electrode and a Ag/Ag$^+$ reference electrode calibrated *vs.* Fc/Fc$^+$.

Incorporating the BDT unit into the polymer backbone slightly raises the oxidation and reduction potentials of the random copolymers **P3** and **P4**. For example, polymer **P3** shows onsets of oxidation and reduction at 0.22 and -1.35 V *vs.* Fc/Fc$^+$ (measured by DPV, Figure 5-11a) compared to those of 0.18 and -1.38 V *vs.* Fc/Fc$^+$ for **PDPP3T**. As expected, the potential onsets increase in proportion to the relative number of BDT units in the polymer main chain (decrease in the number of DPP units). More

specifically, polymer **P4** with a monomer ratio of 1:0.75:0.25 (monomer **4**:**6b**:**3** as indicated in Figure 5-7) shows increased oxidation and reduction onsets of 0.36 and -1.26 V *vs.* Fc/Fc$^+$ compared to these of **P3** with a monomer ratio of 1:0.65:0.35 (monomer **4**:**6b**:**3**) (Figure 5-11b).

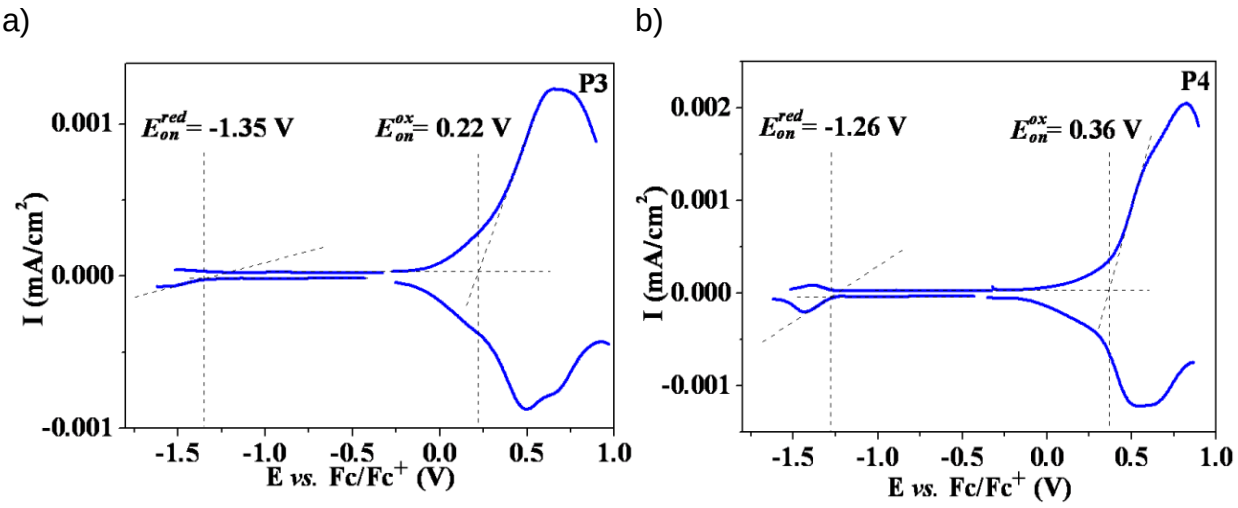

Figure 5-11. Differential pulse voltammetry of random copolymers. a) **P3**; b) **P4** drop-cast from chlorobenzene solution onto platinum button electrode (A= 0.02 cm^2). Measurements were performed in 0.2 M LiBTI /propylene carbonate (PC) with a Pt foil counter electrode and a Ag/Ag$^+$ reference electrode.

Table 5-2. Electrochemically determined HOMO energy levels, LUMO energy levels and bandgaps for **PDPP3T**, **P3** and **P4** (by CV and DPV).

	CV					DPV				
	E_{ox} (V)	HOMO (eV)	E_{red} (V)	LUMO (eV)	E_{gap} (eV)	E_{ox} (V)	HOMO (eV)	E_{red} (V)	LUMO (eV)	E_{gap} (eV)
PDPP3T	0.45	-5.55	-1.44	-3.66	1.89	0.18	-5.28	-1.38	-3.72	1.56
P3	0.49	-5.59	-1.27	-3.83	1.76	0.22	-5.32	-1.35	-3.75	1.57
P4	0.57	-5.67	-1.34	-3.76	1.91	0.36	-5.46	-1.26	-3.84	1.62

Note: Oxidation (E_{ox}) and reduction (E_{red}) onset potentials are reported *vs.* Fc/Fc$^+$. Energy levels are given based on the assumption that the energy of SCE is 4.7 eV *vs*. vacuum,[41] and Fc/Fc$^+$ is +0.38 V *vs*. SCE (i.e. 5.1 eV relative to vacuum).

Furthermore, the calculated HOMO and LUMO energy levels of **P3** and **P4** are shown in Table 5-2. Clearly, **P4** with the lowest DPP ratio has the lowest HOMO and LUMO levels at 5.46 and 3.84 eV according to the DPV measurements. Interestingly, this observation that the HOMO energy levels change according to the change in

relative donor-acceptor ratios is not consistent with the results from Thompson's work,[277] which showed that the HOMO levels were independent of the DPP content. This is possibly due to the use of benzodithiophene (BDT) unit in our case, which lowers the HOMO levels of the donor-acceptor copolymer.[279] The band gaps of **P3** and **P4** were also increased to 1.57 and 1.62 eV, respectively, which agrees well with the blue shift of the low energy optical transition in the absorption spectra (Figure 5-9b).

5.3.4 Polymer Thermal Analysis

The thermal stabilities of **P3** and **P4** were studied by TGA in a nitrogen atmosphere. The thermograms displayed in Figure 5-12 show that the polymers exhibit a high thermal stability until the temperature reaches 315°C, and then a drastic degradation process occurs from this temperature up to around 600°C.

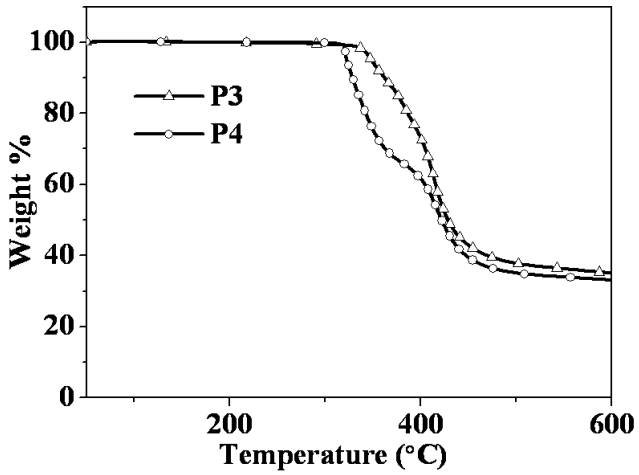

Figure 5-12. Thermogravimetric analysis of polymer **P3** and **P4**.

5.4 Photovoltaic Devices

(Experimental work was achieved and results kindly supplied by Tzung-Han Lai in Prof. Franky So's lab)

Solution processed polymer bulk-heterojunction solar cells were fabricated using **PDPP3T**, **P3** and **P4** as electron donor materials and $PC_{71}BM$ as an electron acceptor

material in a device configuration ITO/ZnO/polymer:PCBM/MoO_3/Ag. Here, due to the mobility difference between electrons and holes of **PDPP3T** (μ_h= 0.05 $cm^2V^{-1}s^{-1}$, μ_e= 0.008 $cm^2V^{-1}s^{-1}$),[109] a higher ratio of $PC_{71}BM$ was needed. **PDPP3T** solution was made with $PC_{71}BM$ in a 1:3 weight ratio with 5% 1,8-diiodoctane (DIO) by volume. The device shows a PCE of 4.01% with short circuit current (J_{sc}) of 11.2 mA cm^{-2}, open circuit voltage (V_{oc}) of 0.68 V and fill factor (*FF*) of 0.525 (Figure 5-13). The enhanced absorption in longer wavelength provides a high short circuit current.

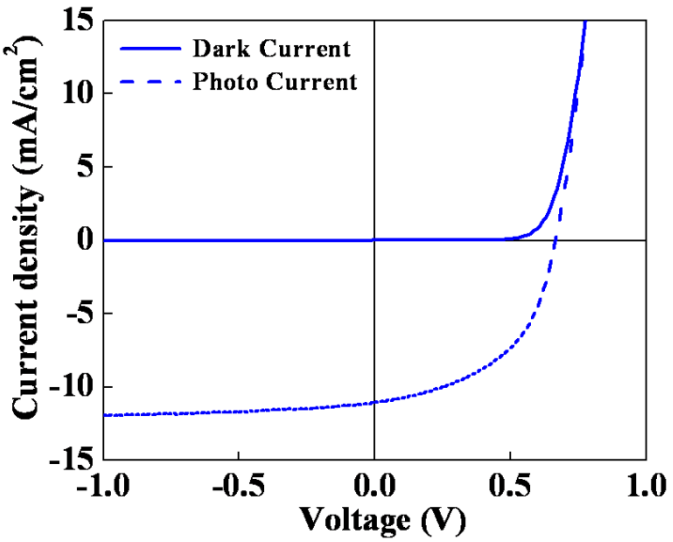

Figure 5-13. Illuminated *J-V* characteristics of **PDPP3T**:$PC_{71}BM$ solar cells using ITO/ZnO/Polymer:$PC_{71}BM$/MoO_3/Ag device architecture with DIO as a processing additive.

Random copolymer **P3** has enhanced absorption at 400-600 nm compared to **PDPP3T**, but also shows a blue shift of the onset of long-wavelength absorption from 900 to 850 nm. Higher PCE along with higher short circuit current is expected for this polymer. However, the polymer:PCBM solar cell (with 5% DIO) shows a low PCE of 2.41% with J_{sc} of 4.81 mA cm^{-2}, V_{oc} of 0.72 V and *FF* of 0.63 (Figure 5-14a). The results become even worse without DIO additive (Figure 5-14a). Moreover, copolymer **P4**, which has greater absorption in the range of 400-600 nm, shows an even lower J_{sc}

(2.69 mA cm^{-2}) than **P3**. With a V_{oc} of 0.71 V and *FF* of 0.62, the efficiency of the **P4**:$PC_{71}BM$ solar cell (with 5% DIO) is about 1.2%. Clearly, the low short circuit currents have become the limiting factor in the performance of OPVs based on **P3** and **P4**. The solar cell results of all the polymers are summarized in Table 5-3.

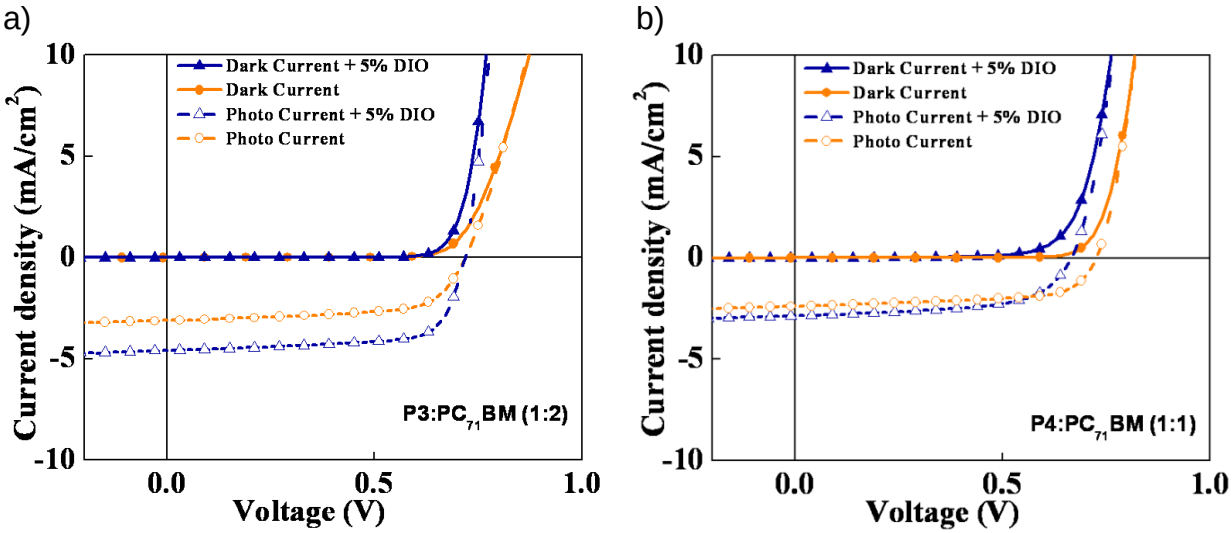

Figure 5-14. Illuminated *J-V* characteristics of polymer:$PC_{71}BM$ solar cells using ITO/ZnO/Polymer:$PC_{71}BM$/MoO_3/Ag device architecture with and without DIO as a processing additive. a) **P3**:$PC_{71}BM$ (1:2) as the active layer. b) **P4**:$PC_{71}BM$ (1:1) as the active layer.

Table 5-3. Photovoltaic Properties of **PDPP3T**, **P3** and **P4** with $PC_{71}BM$ as an acceptor.

Polymer:$PC_{71}BM$ (ratio)	Additive	J_{sc} (mA cm^{-2})	V_{oc} (V)	*FF*	η (%)
PDPP3T (1:3)	5% DIO	11.22	0.68	0.53	4.01
P3 (1:2)	5% DIO	4.81	0.72	0.70	2.41
P3 (1:2)		3.18	0.72	0.64	1.47
P4 (1:1)	5% DIO	2.69	0.71	0.62	1.19
P4 (1:1)		2.37	0.73	0.64	1.11

To understand why the enhanced absorption of **P3** and **P4** does not give a higher short circuit current, further characterizations were made using **PDTG-TPD** as a standard (see Chapter 1 for more information about this polymer).[173] Polymer **P4** was characterized and the results were compared with these of **PDTG-TPD**. Figure 5-15a shows the absorption spectra of polymer:$PC_{71}BM$ blend films. Clearly, the **P4**:$PC_{71}BM$

film demonstrates a stronger absorption in the range of 350-600 nm and an extension of the low energy optical transition to 800 nm. However, the external quantum efficiency (EQE) measurement tells another story (Figure 5-15b). From the EQE data, we can see that while the **PDTG-TPD**:$PC_{71}BM$ blend shows almost 70% of EQE at its highest, **P4**:$PC_{71}BM$ blend shows less than 20% in the polymer absorption region. The missing EQE value in the range of 600 to 800 nm, where the polymer also absorbs light, is direct evidence that the short circuit currents were mainly coming from $PC_{71}BM$.

a) b)

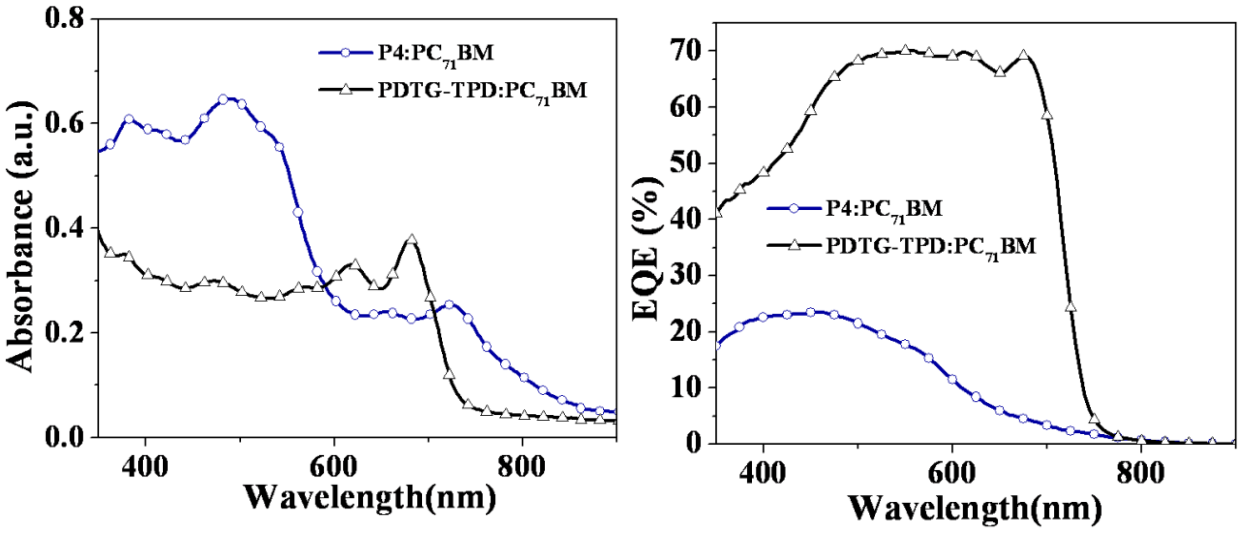

Figure 5-15. Absorption and EQE of polymer:$PC_{71}BM$ blends. a) Thin film UV-visible absorption spectra of **P4**:$PC_{71}BM$ blend and **PDTG-TPD**:$PC_{71}BM$ blend. b) EQE spectra of solar cell devices using **P4** and **PDTG-TPD**.

According to these results, it is obvious that polymer **P4** absorbs the sunlight, but there is only a small number of electrons coming out of the device, leading to low short circuit currents. In order to further understand this result, the photoluminescence (PL) quenching experiment was carried out. Figure 5-16 shows the quenching results of polymer **P4**. As we can see, the photoluminescence quenching efficiency is rather low when $PC_{71}BM$ is added, which presents low photo-induced charge transfer

efficiency.[281-284] This is possibly because most of the generated excitons did not dissociate on the polymer:PCBM interface.

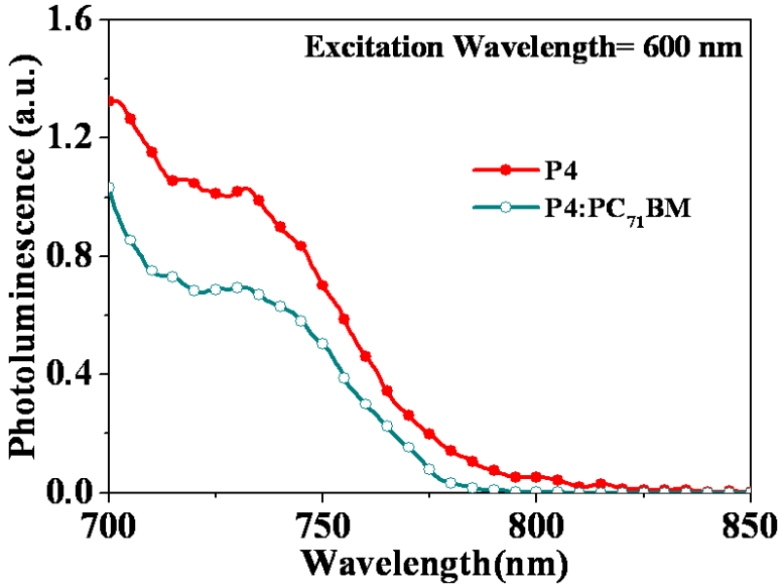

Figure 5-16. Photoluminescence spectra of **P4** and **P4**:P_{71}CBM (1:1) chlorobenzene solution shows a limited PL quenching of the **P4**:P_{71}CBM blend, compared to the PL emission from a pure **P4** solution.

From the energy level point of view, the LUMO levels of the polymers are decreased from **PDPP3T** at -3.72 eV to **P3** at -3.75 eV to **P4** at -3.84 eV as the number of DPP units is decreased. The reduced energy offsets between the LUMO energy levels of the polymers and the LUMO level of PCBM dramatically lower the driving force for exciton dissociation and charge generation, and thus decrease the photon currents. Another possible reason for the low OPV performance is the unfavorable film morphology, which will be discussed in the next section.

5.5 Polymer Morphology Studies

As with many examples found in this field, the device performance is highly dependent on the active layer thin-film morphology. A typical device of **P3**:PC_{71}BM (1:1) with 5% DIO was characterized by atomic force microscope (AFM). Figure 5-17 shows

the height images of the active layer. Clearly, even with the addition of 5% DIO, phase separation is observed to be on the order of a couple of hundred nanometers, with large aggregates of $PC_{71}BM$ or polymer observed. The coarse morphology revealed here could result from a rather pronounced phase segregation (demixing) between PCBM and the polymer, as described previously.[285,286] The lack of an interpenetrating network and the existence of large dimensions would decrease exciton harvesting, and thus the OPV performance.

The unfavorable morphology could be due to the increased bulky side (2-hexyldecyl) density of the copolymers, which prevents PCBM interpenetration into the polymer frame. Clearly, the use of side chains not only affects the solubility of the conjugated polymers, but also the molecular packing and the interaction between the polymer and acceptor molecules.

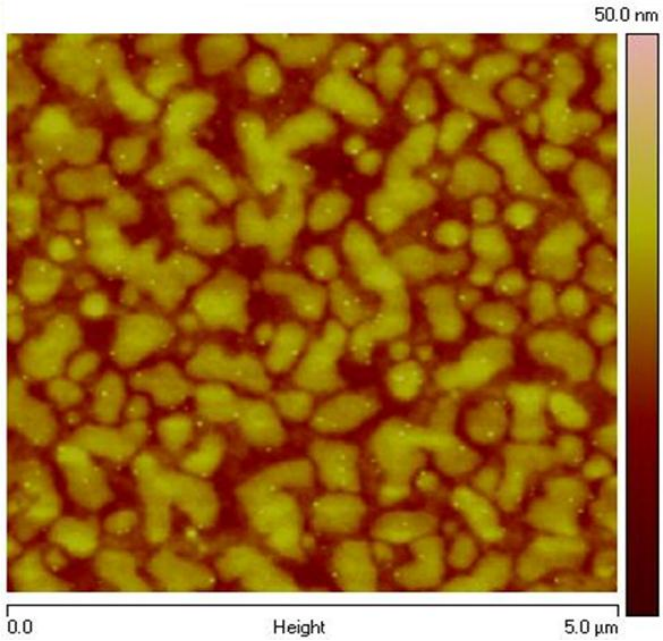

Figure 5-17. Atomic force microscope height images of **P3**:$PC_{71}BM$ (1:1) based PV cells with 5% DIO spin-coated from dichlorobenzene.

5.6 Chapter Summary

In this chapter, several DPP-based copolymers differing by the donor-acceptor ratios have been synthesized and characterized. Although polymers **P1** and **P2** with smaller alkyloxy side chains on the benzodithiophene repeat unit showed limited solubility in organic solvents, they provided insight into the control of polymer absorption by tuning the relative concentrations of electron-donating and -withdrawing substituents in the polymer backbone. With a better solubilizing group (2-hexyldecyl) on the BDT unit, random copolymers **P3** and **P4** showed considerable solubility in chlorobenzene, chloroform and THF. More importantly, **P4** with a monomer ratio of 1:0.75:0.25 (monomer **4**:**6a**:**3**) showed a broad absorption across 350 to 800 nm, except for a small absorption gap between 550 to 650 nm. This enhanced absorption profile was expected to lead to more photon-induced current and improved performance of the solar cells. However, the PCEs of **P3** and **P4** were dramatically lower than that of the control polymer **PDPP3T**. The low J_{sc} (3.87 and 2.69 mA cm^{-2} for **P3** and **P4**, respectively) is the main reason that the solar cells showed undesirable low performances.

In order to understand why enhanced absorption of **P3** and **P4** did not give expected higher short circuit currents, external quantum efficiency (EQE) and photoluminescence quenching measurements were performed using **P4** as an example. Less than 25% of EQE at all wavelengths revealed a low ratio of extracted free charge carriers to incident photons. Moreover, low charge transfer efficiency was demonstrated by the inefficient quenching of the polymer luminescence using PCBM as an acceptor. The unfavorable polymer:PCBM film morphology caused by the demixing of polymer and PCBM domains led to a lack of dissociation of excitons, and thus the low J_{sc}. The bulky side chains could be the predominant factor involved in demixing of the polymers

and PCBM. To provide further evidence for the conclusion, smaller side chains, which can provide sufficient solubility to the copolymers without blocking the interpenetration of PCBM, should be examined.

5.7 Experimental Details

3,6-Di(thiophen-2-yl)pyrrolo[3,4-c]pyrrole-1,4(2H,5H)-dione (1) Thiophene-2-carbonitrile (6.54 g, 60 mmol), *t*-BuOK (11.2 g, 100 mmol) and *t*-amyl alcohol (50 mL) were combined in a 500 mL round bottom flask and heated to 110 ºC under nitrogen. Then a solution of dimethyl succinate (2.92 g, 20 mmol) in *t*-amyl alcohol (16 ml) was added using an addition funnel. When the addition was completed, the mixture was kept at 110 ºC for another 2 h, and then cooled to 50 ºC and diluting with 100 ml methanol. After the mixture was carefully neutralized with glacial acetic acid, the suspension was filtered and washed with methanol and water. The product was obtained as a dark purple solid and used directly without further purification.

2,5-Bis(2-hexyldecyl)-3,6-di(thiophen-2-yl)pyrrolo[3,4-c]pyrrole-1,4(2H,5H)-dione (2) Compound **1** (4.5 g, 15 mmol), potassium carbonate (10.4 g, 75 mmol) and 7-(bromomethyl)pentadecane (18.3 g, 60 mmol) were dissolved in DMF (200 mL). The mixture was heated to 120 ºC and stirred for 40 h. Then the solvent was removed under vacuum. The crude material was purified by flash chromatography ($CHCl_3$) to yield purple solid of compound **2** (4.5 g, 40%). ^{1}H NMR ($CDCl_3$): δ 8.69 (d, 1H), 7.56 (d, 1H), 7.17 (d, 1H), 3.93 (d, 2H), 1.85 (m, 1H), 1.30-1.25 (m, 24H), 0.85 (m, 6H).

3,6-Bis(5-bromo-2-thienyl)-2,5-dihydro-2,5-di(2-hexyldecyl)-pyrrolo[3,4-c]pyrrolo-1,4-dione (3) Compound **2** (2.0 g, 2.67 mmol) and NBS (1 g, 5.6 mmol) were added into a round-bottom flash and then degassed and refilled with argon 3 times.

Chloroform (50 mL) was then added. The reaction mixture was stirred at room temperature for overnight, diluted with chloroform (100 mL), and washed with water. The organic layer was dried with $MgSO_4$. After the solvent was evaporated, the residue was dissolved in 30 mL THF. And then MeOH was added into the THF solution until the crude product was precipitated. After filtration, the crude product was dissolved in 30 mL THF again, and two more precipitation cycles were applied. Then the product was obtained as a dark red solid (2.18 g, 90%). ^{1}H NMR ($CDCl_3$): δ 8.62 (d, 1H), 7.21 (d, 1H), 3.91 (d, 2H), 1.86 (m, 1H), 1.29-1.22 (m, 24H), 0.86 (m, 6H). ^{13}C NMR ($CDCl_3$): δ 161.57, 139.58, 135.52, 131.62, 131.37, 119.17, 108.19, 46.52, 37.94, 32.09, 31.96, 31.36, 30.18, 29.85, 29.71, 29.50, 26.34, 22.88, 22.84, 14.33, 14.30. HRMS (ESI–FTICR): *m/z* calcd for $C_{46}H_{71}Br_2N_2O_2S_2$ ($M+H^+$) 907.3303 found 907.3325. Anal. calcd for $C_{46}H_{70}Br_2N_2O_2S_2$: C 60.91, H 7.78, N 3.09 found C 61.32, H 8.05, N 3.00.

2,5-Bis(trimethylstannyl)thiophene (4) A solution of n-butyllithium (16.5 mL, 35.65 mmol, 2.165 M in hexane) was added slowly to diisopropylamine (3.61 g, 35.65 mmol) in ether (70.0 mL) at -78°C. After stirring for 1 h at -78°C, the solution was warmed to room temperature and then cooled to 0°C in an ice bath. Thiophene (1 g, 11.88 mmol) was added, and the mixture was warmed to room temperature and stirred overnight. After the reaction mixture was cooled to 0°C again, trimethylchlorostannane (7.1 g, 35.65 mmol) was added. The mixture was stirred for 3 h at 0°C. After dilution with ether (100 mL), the organic phase was washed with water and dried over anhydrous magnesium sulfate. The solvent was evaporated and the residue was purified by flash chromatography with hexane as an eluent on treated silica gel (washed the silica gel with neat triethylamine, then hexane) to give 4.6 g (95%) of compound **4**

as a white solid. ^{1}H NMR ($CDCl_3$): δ 7.39 (s, 1H), δ 0.38 (s, 9H). ^{13}C NMR ($CDCl_3$): δ 143.25, 136.03, -7.96. Anal. calcd for $C_{10}H_{20}SSn_2$: C 29.31, H 4.92, found C 29.04, H 5.11.

4,8-Diethylhexyloxybenzo[1,2-b:4,5-b']dithiophene (5a) Benzo[1,2-b:4,5-b']dithiophene-4,8-dione (4.4 g, 20 mmol), zinc dust (3.92 g, 60 mmol), NaOH (16 g, 400 mmol) and 2-ethylhexyl bromide (15.5 g, 80 mmol) were added into a 250 mL round bottom flask and degassed. After DMF 150 mL was added, the reaction mixture was bubbled with argon and stirred at room temperature for 20 min, then heated at 90°C for overnight. At room temperature, the mixture was quenched with MeOH and diluted with ether. The organic phase was washed with water and dried over anhydrous magnesium sulfate. The crude product was purified by chromatography with hexane to obtain compound **5a** as colorless oil (7.5 g, yield: 84%). ^{1}H NMR ($CDCl_3$): δ 7.50 (d, 2H, *J*= 5.4 Hz), δ 7.38 (d, 2H, *J*= 5.4 Hz), δ 4.20 (d, 4H, *J*= 5.4 Hz), δ 1.82-1.38 (m, 18H), δ 1.05-0.92 (m, 12H). ^{13}C NMR ($CDCl_3$): δ 144.87, 131.71, 130.16, 126.14, 120.47, 76.26, 40.89, 30.69, 29.43, 24.08, 23.33, 14.36, 11.53. HRMS (ESI–FTICR): *m/z* calcd for $C_{26}H_{38}O_2S_2$ (M^+) 446.2308 found 446.2328. Anal. calcd for $C_{26}H_{38}O_2S_2$: C 69.91, H 8.57, found C 70.07, H 8.85.

4,8-dihexyldecyloxybenzo[1,2-b:4,5-b']dithiophene (5b) The same reaction and purification procedure as described for **5a** was followed. Benzo[1,2-b:4,5-b']dithiophene-4,8-dione (1.5 g, 6.81 mmol), zinc dust (1.34 g, 20.5 mmol), NaOH (5.45 g, 136.2 mmol), 2-ethylhexyl bromide (8.32 g, 27.24 mmol) and DMF 50 mL. Compound **5b** was collected as light yellow oil (3.5 g, 76%). ^{1}H NMR ($CDCl_3$): δ 7.50 (d, 1H, *J*= 5.4 Hz), δ 7.38 (d, 1H, *J*= 5.4 Hz), δ 4.19 (d, 2H, *J*= 5.1 Hz), δ 1.88-1.31 (m, 25H), δ 0.92-0.87

(m, 6H). ^{13}C NMR ($CDCl_3$): δ144.89, 131.71, 130.15, 126.09, 120.48, 76.60, 39.45, 32.14, 31.57, 30.31, 29.98, 29.87, 29.60, 27.22, 27.20, 22.93, 14.36. HRMS (ESI–FTICR): *m/z* calcd for $C_{42}H_{71}O_2S_2$ ($M+H^+$) 671.4890 found 671.4882. Anal. calcd for $C_{42}H_{70}O_2S_2$: C 75.16, H 10.51, found C 75.44, H 11.07.

2,6-Dibromo-4,8-diethylhexyloxybenzo[1,2-b:4,5-b']dithiophene (6a) A solution of NBS (1.67 g, 9.4 mmol, in 15 mL acetonitrile) was added slowly to a compound **5a** (2.0 g, 4.48 mmol) chloroform (15.0 mL) solution at 0°C. The mixture was stirred at the same temperature for 2 h before allowing it to warm to room temperature. After stirring at room temperature for overnight, the solution was diluted with methylene chloride and the organic phase was washed with water and dried over anhydrous $MgSO_4$. The solvent was evaporated and the residue was purified by column chromatography on silica gel (hexane) to yield the desired product as a light yellow oil (2 g, 74%). ^{1}H NMR ($CDCl_3$): δ7.41 (s, 1H), δ4.10 (d, 2H, *J*= 5.4 Hz), δ1.79-1.38 (m, 9H), δ1.03-0.93 (m, 6H). ^{13}C NMR ($CDCl_3$): δ142.90, 131.11, 130.95, 123.31, 115.11, 76.52, 40.82, 30.56, 29.38, 24.00, 23.30, 14.35, 11.50. HRMS (ESI–FTICR): *m/z* calcd for $C_{26}H_{37}Br_2O_2S_2$ ($M+H^+$) 605.0577 found 605.0589. Anal. calcd for $C_{26}H_{36}Br_2O_2S_2$: C 51.66, H 6.00, found C 51.27, H 6.02.

2,6-Dibromo-4,8-dihexyldecyloxybenzo[1,2-b:4,5-b']dithiophene (6b) The same reaction and purification procedure as described for **6a** was followed. NBS (1.12 g, 6.26 mmol), acetonitrile (15 mL), compound **5b** (2.0 g, 2.98 mmol) and chloroform (15.0 mL). Compound **6b** was collected as light yellow oil (1.7 g, 69%). ^{1}H NMR ($CDCl_3$): δ7.41 (s, 1H), δ4.09 (d, 2H, *J*= 5.4 Hz), δ1.82-1.26 (m, 25H), δ0.91-0.83 (m, 6H). ^{13}C NMR (Benzene-d6): δ143.76, 131.86, 131.70, 124.03, 115.86, 76.99, 39.92,

32.74, 32.69, 32.01, 30.87, 30.53, 30.48, 30.21, 27.77, 27.73, 23.53, 14.79. HRMS (ESI–FTICR): *m/z* calcd for $C_{42}H_{71}O_2S_2$ (M-2Br+3H$^+$) 671.4890 found 671.4870. Anal. calcd for $C_{42}H_{68}Br_2O_2S_2$: C 60.86, H 8.27, found C 61.19, H 8.55.

General Polymerization Procedure. Polymer PDPP3T: A solution of compound **4** (0.1024 g, 0.25 mmol), compound **3** (0.2267 g, 0.25 mmol), tris(dibenzylideneacetone)dipalladium (0) ($Pd_2(dba)_3$) (4.6 mg, 0.005 mmol) and tri(o-tolyl)phosphine (P(o-tolyl)$_3$) (6.1 mg, 0.02 mmol) in toluene (10 mL) was degassed three times by successive freeze-pump-thaw cycles and heated at 115°C for 72 h in an oil bath. After the reaction was cooled to 50°C, large spatula tip of diethylammonium diethyldithiocarbamate (D-DDC) was added into the polymer solution, and then the solution mixture was stirred for 1 h at 50°C under argon atmosphere. The mixture was then precipitated into methanol (200 mL). The precipitate was filtered through a cellulose thimble and purified via Soxhlet extraction with methanol (1 day), acetone (1 day) hexanes (1 day). The polymer was extracted with chloroform, concentrated by evaporation, and then precipitated into methanol again (200 mL). The collected polymer was a dark green solid (157 mg, 76 %). ^{1}H NMR ($CDCl_3$): δ 8.89 (b, 1H), 7.36 (b, 1H), 7.07 (b, 1H), 4.10 (b, 2H), 1.80-1.00 (b, 25H), 0.80 (b, 6H). GPC analysis: M_n = 124.9 kDa, M_w = 158.3 kDa, PDI = 1.3. Anal. Calcd. for $C_{50}H_{72}N_2O_2S_3$: C 72.41, H 8.75, N 3.38, found C 71.97, H 9.16, N 3.05.

P1: The same polymerization and purification procedure as described for **PDPP3T** was followed. Compound **4** (0.1024 g, 0.25 mmol), compound **6a** (0.0756 g, 0.125 mmol), compound **3** (0.1134 g, 0.125 mmol), $Pd_2(dba)_3$ (4.6 mg, 0.005 mmol) and P(o-tolyl)$_3$ (6.1 mg, 0.02 mmol) and toluene (10 mL). The collected polymer was a dark

green solid (45 mg, 27 %). GPC analysis: M_n = 130.8 kDa, M_w = 158.3 kDa, PDI = 1.2. Anal. Calcd. for $C_{80}H_{110}N_2O_4S_6$: C 70.85, H 8.18, N 2.07, found C 70.43, H 8.98, N 1.76.

P2: Compound **4** (0.1024 g, 0.25 mmol), compound **6a** (0.1133 g, 0.1875 mmol), compound **3** (0.0567 g, 0.0625 mmol), $Pd_2(dba)_3$ (4.6 mg, 0.005 mmol) and P(o-tolyl)$_3$ (6.1 mg, 0.02 mmol) and toluene (10 mL). The collected polymer was a dark green solid (60 mg, 40 %). GPC analysis: M_n = 54.6 kDa, M_w = 96.4 kDa, PDI = 1.8. Anal. Calcd. for $C_{140}H_{186}N_2O_8S_{12}$: C 69.78, H 7.78, N 1.16, found C 70.73, H 8.46, N 0.94.

P3: Compound **4** (0.1024 g, 0.25 mmol), compound **6b** (0.0756 g, 0.125 mmol), compound **3** (0.1134 g, 0.125 mmol), $Pd_2(dba)_3$ (4.6 mg, 0.005 mmol) and P(o-tolyl)$_3$ (6.1 mg, 0.02 mmol) and toluene (10 mL). The collected polymer was a dark green solid (130 mg, 67 %). GPC analysis: M_n = 59.4 kDa, M_w = 114.3 kDa, PDI = 1.9. Anal. Calcd. for $C_{474}H_{707}N_7O_{20}S_{30}$: C 73.12, H 9.15, N 1.26, found C 74.06, H 9.94, N 1.17.

P4: Compound **4** (0.1318 g, 0.322 mmol), compound **6b** (0.2 g, 0.241 mmol), compound **3** (0.0729 g, 0.0804 mmol), $Pd_2(dba)_3$ (5.9 mg, 0.0064 mmol) and P(o-tolyl)$_3$ (7.9 mg, 0.026 mmol) and toluene (15 mL). The collected polymer was a dark green solid (189 mg, 77 %). ^{1}H NMR (500 MHz, $CDCl_3$) δ 8.92 (b, 2H), 7.16 (b, 16H), 4.20 (b, 16H), 1.82-1.00 (b, 248H). GPC analysis: M_n = 89.3 kDa, M_w = 139.7 kDa, PDI = 1.6. Anal. Calcd. for $C_{188}H_{282}N_2O_8S_{12}$: C 73.24, H 9.22, N 0.91, found C 74.23, H 10.19, N 0.83.

CHAPTER 6
CONCLUSIONS AND PERSPECTIVES

This dissertation has focused on the utilization of random Stille polymerization as a tool for the synthesis of donor-acceptor conjugated copolymers, and an understanding of structural parameters in controlling the optoelectronic properties of these materials. A variety of methods was used to characterize the resulting conjugated polymers and investigate their structure-property relationships. As described in Chapters 2 and 3, other significant accomplishments of this work were refinement of the synthesis and purification procedures and reproducible preparation of polymers with consistent optoelectronic properties.

Chapter 3 presented the synthesis and characterization of random black-to-transmissive conjugated polymers for electrochromic applications. A series of broadly absorbing copolymers was produced with number average molecular weights ranging from 10 to 18 kDa and polydispersities ranging from 1.3 to 1.6 after Soxhlate extraction. Polymer **ECP-3** was utilized as an example for the subsequent electrochromic property study and showed a transmittance contrast as high as 42% at the 1 s switch time and a high continuous switching stability (18,000 cycles). However, this polymer was not ideally black, because it failed to cover part of the blue (380-450 nm) and red (690-750 nm) regions. According to the structure of this polymer, an extra stronger acceptor (for example thienopyrazine) is expected to extend the low energy absorption band to a much longer wavelength, while an extra weaker donor (for example dioxythiophene) will enhance absorption at the shot-wavelength end. The random Stille polymerization introduced in this chapter is expected to be an optimal route towards achieving such systems.

Chapter 4 demonstrated a facile approach to synthesize two electrochromic polymers **ECP-Blue** and **ECP-Black**, bearing alkyl ester side chains, which were converted into water-soluble and processable polymer salts after subsequent defunctionalization of the ester groups. Further neutralization of the polymer salt films (spray-cast from water solution) yielded **WS-ECP-Blue-acid** and **WS-ECP-Black-acid** films with a dramatic improvement in the electrochromic switching speed performance compared to their ester derivatives. Future work can be directed toward applying this chemistry in the synthesis of water soluble conjugated polymers with other saturation colors (yellow, cyan, and red *et al.*). Another aspect from this side-chain defunctionalization approach, as well as the following neutralization process, is that multilayer electrochromic devices can be easily achieved by depositing a second polymer layer on top of the first lay, which cannot be dissolved in organic solvents or water. The investigation of the utilities of these water soluble conjugated polymers in other applications such as OLEDs, chemical and biochemical sensors could also be another interesting direction.

In Chapter 5, attention was turned to making a new type of diketopyrrolopyrrole-based random conjugated copolymer for organic solar cells based on the success in extending polymer absorption spectra for efficient light-harvesting. The resulting polymers were expected to improve the photocurrents and power conversion efficiencies. However, reduced performance was observed for the new polymers compared with the control polymer. Subsequent experiments (EQE, photoluminescence quenching and film morphology studies) revealed that the decreased performance could be attributed to a lack of dissociation of excitons caused by the demixing of polymer and

PCBM blend. “While energy levels and band gaps are important, morphology is still key to device success.”

Over the past 40 years, significant research effort has been conducted in the field of *π*-conjugated polymers. By now, the success in applying these materials in optoelectronic devices has gained great attention not only in academia but also in industry. In this work, the understanding of structure-property relationship is an ultimate goal in this field. However, it should also be pointed out that chemistry is the foundation of the development of this course.

This dissertation demonstrates a fundamental chemical approach- random polymerization, which is used to combine multiple monomers, adjust their relative ratio and fine-tune the optoelectronic properties of polymers. The essentials of this method are now established. With further development, this method can be extended to a much broader family of conjugated polymers.

LIST OF REFERENCES

1. Günes, S.; Neugebauer, H.; Sariciftci, N. S. *Chem. Rev.* **2007**, *107*, 1324.

2. Cheng, Y.-J.; Yang, S.-H.; Hsu, C.-S. *Chem. Rev.* **2009**, *109*, 5868.

3. Murphy, A. R.; Fréchet, J. M. J. *Chem. Rev.* **2007**, *107*, 1066.

4. Ortiz, R. P.; Facchetti, A.; Marks, T. J. *Chem. Rev.* **2010**, *110*, 205.

5. Lo, S.-C.; Burn, P. L. *Chem. Rev.* **2007**, *107*, 1097.

6. Grimsdale, A. C.; Leok Chan, K.; Martin, R. E.; Jokisz, P. G.; Holmes, A. B. *Chem. Rev.* **2009**, *109*, 897.

7. Beaujuge, P. M.; Reynolds, J. R. *Chem. Rev.* **2010**, *110*, 268.

8. Groenendaal, L.; Zotti, G.; Aubert, P.-H.; Waybright, S.; Reynolds, J. R. *Adv. Mater.* **2003**, *15*,855.

9. McQuade, D. T.; Pullen, A. E.; Swager, T. M. *Chem. Rev.* **2000**, *100*, 2537.

10. Roncali, J. *J. Mater. Chem.* **1999**, *9*, 1875.

11. Dyer, A. L. Conjugated Polymer Electrochromic and Light-Emitting Devices. Ph.D. Thesis, University of Florida, Gainesville, FL, **2007**.

12. Unur, E. Application of Conjugated Polymers to Multi-Electrode Electrochromic Devices. Ph.D. Thesis, University of Florida, Gainesville, FL, **2008**.

13. Argun, A. A.; Cirpan, A.; Reynolds, J. R. *Advanced Materials* **2003**, *15*, 1338.

14. Wu, Z.; Chen, Z.; Du, X.; Logan, J. M.; Sippel, J.; Nikolou, M.; Kamaras, K.; Reynolds, J. R.; Tanner, D. B.; Hebard, A. F.; Rinzler, A. G. *Science* **2004**, *305*, 1273.

15. Robinson, N. D.; Berggren, M. *Handbook of Conducting Polymers*; Third ed.; Skotheim, T. A.; Reynolds, J. R. Eds.; CRC Press: Boca Raton, FL, **2007**; Vol. 1.

16. Shirakawa, H.; Louis, E. J.; MacDiarmid, A. G.; Chiang, C. K.; Heeger, A. J. *J. Chem. Soc. Chem. Commun*. **1977**, 578.

17. Chiang, C. K.; Fincher, C. R.; Park, Y. W.; Heeger, A. J.; Shirakawa, H.; Louis, E. J.; Gau, S. C.; MacDiarmid, A. G. *Phys. Rev. Lett.* **1977**, *39*, 1098.

18. Chiang, C. K.; Druy, M. A.; Gau, S. C.; Heeger, A. J.; Louis, E. J.; MacDiarmid, A. G.; Park, Y. W.; Shirakawa, H. *J. Am. Chem. Soc.* **1978**, *100*, 1013.

19. Chiang, C. K.; Fincher, C. R.; Park, Y. W.; Heeger, A. J.; Shirakawa, H.; Louis, E. J.; Gau, S. C.; MacDiarmid, A. G. *Phys. Rev. Lett.* **1978**, *40*, 1472.

20. Su, W. P.; Schireffer, J. R.; Heeger, A. J. 1980. *Phys. Rev.* **1980**, *B22*, 2099.

21. Suzuki, N.; Ozuki, M.; Etemad, S.; Heeger, A. J.; MacDiarmid, A. G. *Phys. Rev. Lett.* **1980**, *45*, 1209.

22. Lin-Liu, Y. R. *Phys. Rev. B*, **1982**, *25*, 5540.

23. Anslyn, E.V.; Dougherty, D.A. *Modern Physical Organic Chemistry*, University Science, **2006**.

24. Salzner, U.; Lagowski, J. B.; Pickup, P. G.; Poirier, R. A. *Synth. Met.* **1998**, *96*, 177.

25. Torsi, L. A.; Tafuri, N.; Cioffi, M. C.; Gallazzi, A.; Sassella, L.; Sabbatini, L.; Zambonin, P.G. *Sens. Actuators B* **2003**, *93*, 257.

26. Roncali, J. *Chem. Rev.* **1992**, *92,* 711.

27. Liu, J.; Tanaka, T.; Sivula, K.; Alivisators, A. P.; Frechet, J. M. J. *J. Am. Chem. Soc.* **2004**, *126*, 6550.

28. Street, G. B.; Clarke, T. C.; Krounbi, M.; Kanazawa, K.; Lee, V.; Pfluger, P.; Scott, J. C.; Weiser, G. *Mol. Cryst. Liq. Cryst.* **1982**, *83*, 253.

29. Micaroni, L.; Nart, F. C.; Hummelgen, I. A. *J. Solid State Electrochem.* **2002**, *7*, 55.

30. Kaufman, J. H.; Colaneri, N.; Scott, J. C.; Street, G. B. *Phys. Rev. Lett.* **1984**, *53*, 1005.

31. Xing, K. Z.; Fahlman, M.; Chen, X. W.; Inganas, O.; Salaneck, W. R. *Synthetic Metals* **1997**, 161.

32. Brown, T. M.; Kim, J. S.; Friend, R. H.; Cacialli, F. Daik, R.; Feast, W.J. *Appl. Phys. Lett.* **1999**, *75*, 1679.

33. Pei, Q.; Zuccarello, G.; Ahlskog, M.; Inganäs, O. *Polymer* **1994**, *35*, 1347.

34. Kumar, A.; Welsh, D. M.; Morvant, M. C.; Piroux, F.; Abboud, K. A.; Reynolds, J. R. *Chem. Mater.* **1998**, *10*, 896.

35. Chen, T.-A.; Rieke, R. D. *J. Am. Chem. Soc.* **1992**, *114*, 10087.

36. McCullough, R. D.; Lowe, R. D.; Jayaraman, M.; Anderson, D. L. *J. Org. Chem.* **1993**, *58*, 904 .

37. McCullough, R. D.; Tristram-Nagle, S.; Williams, S. P.; Lowevt, R. D.; Jayaramant, M. *J. Am. Chem. Soc.* **1993**, *115*, 4910.

38. Loewe, R. S.; Khersonsky, S. M.; McCullough, R. D. *Adv. Mater.* **1999**, *11*, 250.

39. Loewe, R. S.; Ewbank, P. C.; Jinsong Liu, L. Z.; McCullough, R. D. *Macromolecules* **2001,** *34*, 4324.

40. Onoda, M.; Tada, K.; Zakhidov, A. A.; Yoshino, K. *Thin Solid Films* **1998**, *331*, 76.

41. Bard, A. J.; Faulkner, L. R. *Electrochemical Methods:Fundamentals and Applications*, 2nd Ed.; Wiley: New York, **2001**, p.54.

42. Yamamoto, T.; Sanechika, K.; Yamamoto, A. *J. Polym. Sci., Polym. Lett. Ed.* **1980**, *18*, 9.

43. Kaneto, K.; Kohno, Y.; Yoshino, K.; Inuishi, Y. *J. Chem. Soc., Chem. Cornmun.* **1983**, 382.

44. Sato, M.; Tanaka, S.; Kaeriyama, K. *J. Chem. Soc., Chem. Commun.* **1985**, 713.

45. Sato, M.; Tanaka, S.; Kaeriyama, K. *J. Chem. Soc., Chem. Commun*. **1986**, 837.

46. Jen, K.-Y.; Miller, G. G.; Elsenbaumer, R. L. *J. Chem. Soc., Chem. Commun*. **1986**, 1346.

47. Elsenbaumer, R. L.; Jen, K.-Y.; Oboodi, R. *Synth. Met.* **1986**, *15*, 169.

48. Naarrmann, H.; Theophilou, N. *Synth. Met.* **1987**, *22*, 1.

49. Nogami, Y.; Pouget, J.; Ishiguro, T. *Synth. Met.* **1994**, *62*, 257.

50. Roncali, J. *Chem. Rev.* **1997**, *97*, 173.

51. Roncali, J. *Macromol. Rapid Commun.* **2007**, *28*, 1761.

52. Brédas, J. L.; Heeger, A. J.; Wudl, F. *J. Chem. Phys.* **1986**, *85*, 4673.

53. Havinga, E. E.; Hoeve, W.; Wynberg, H. *Polym. Bull.* **1992**, *29*, 119.

54. Havinga, E. E.; Hoeve, W.; Wynberg, H. *Synth. Met.* **1993**, *55*, 299.

55. van Mullekom, H. A. M.; Vekemans, J. A. J. M.; Havinga, E. E.; Meijer, E. W. *Mater. Sci. Eng.* **2001**, *32*, 1.

56. Dhanabalan, A.; van Dongen, J. L. J.; van Duren, J. K. J.; Janssen, H. M.; van Hal, P. A.; Janssen, R. A. J. *Macromolecules* **2001**, *34,* 2495.

57. Blouin, N.; Michaud, A.; Gendron, D.; Wakim, S.; Blair, E.; Neagu-Plesu, R.; Belletête, M.; Durocher, G.; Tao, Y.; Leclerc, M. *J. Am. Chem. Soc.* **2008**, *130*, 732.

58. Zhou, E.; Yamakawa, S.; Tajima, K.; Yang, C.; Hashimoto, K. *Chem. Mater.* **2009**, *21*, 4055.

59. Chen, H.-Y.; Hou, J.; Hayden, A. E.; Yang, H.; Houk, K. N.; Yang, Y. *Adv. Mater.* **2010**, *22*, 371.

60. Kono, T.; Kumaki, D.; Nishida, J.-I.; Sakanoue, T.; Kakita, M.; Tada, H.; Tokito, S.; Yamashita, Y. *Chem. Mater.* **2007**, *19*, 1218.

61. Ponce Ortiz, R.; Facchetti, A.; Marks, T. J.; Casado, J.; Zgierski, M. Z.; Kozaki, M.; Hernández, V.; López Navarrete, J. T.; *Adv. Funct. Mater.* **2009**, *19*, 386.

62. Beaupré, S.; Boudreault, P.-L. T.; Leclerc, M.; *Adv. Mater.* **2010**, *22*, E1.

63. Schopf, G.; Koßmehl, G. *Adv. Polym. Sci.* **1997**, *129*, 1.

64. Niemi, V. M.; Knuuttila, P.; Osterholm, J. E.; Korvola, J. *Polymer* **1992**, *33*, 1559.

65. Kossmehl, G. *Makromol. Chem., Macromol. Symp.* **1986**, *4*, 45.

66. Jikei, M.; Katoh, J.; Sato, N.; Yamamoto, K.; Nishide, H.; Tsuchida, E. *Bull. Chem. Soc. Jpn.* **1992**, *65*, 2029

67. Ruiz, J. P.; Dharia, J. R.; Reynolds, J. R.; Buckley, L. J. *Macromolecules* **1992**, *25,* 849.

68. Wu, C.-G.; Lin, Y.-C.; Wu, C.-E.; Huang, P.-H*. Polymer* **2005**, *46*, 3748.

69. Cheng, Y.-J.; Luh T.-Y.; *J. Organomet. Chem.* **2004**, *689*, 4137.

70. Milstein, D.; Stille, J. K. *J. Am. Chem. Soc.* **1978**, *100*, 3636.

71. Stille, J. K. *Angew. Chem. Int. Ed. Engl.* **1986**, *25*, 508.

72. Bao, Z.; Chan, W. K.; Yu, L. *J. Am. Chem. Soc.* **1995***,117,* 12426.

73. Carsten, B.; He, F.; Son, H. J.; Xu, T.; Yu, L. *Chem. Rev.* **2011**, *111*, 1493.

74. Bourderioux, A.; Routier, S.; Bénéteau, V.; Mérour, J.-Y. *Tetrahedron Lett.* **2005**, *46*, 6071.

75. Loewe, R.S.; McCullough, R.D. *Chem. Mater*. **2000**, *12*, 3214.

76. Lu, G.; Usta, H.; Risko, C.; Wang, L.; Facchetti, A.; Ratner, M. A.; Marks, T. J. *J. Am. Chem. Soc.* **2008**, *130*, 7670.

77. Farina, V.; Krishnan, B. *J. Am. Chem. Soc.* **1991**, *113*, 9585.

78. Mishra, S. P.; Palai, A. K.; Sirvastava, R.; Kamalasanan, M. N.; Patri, M. *Journal of Polymer Science: Part A: Polymer Chemistry* **2009**, *47*, 6514.

79. Vanormelingen, W.; Van den Bergh, K.; Verbiest, T.; Koeckelberghs, G. *Macromolecules* **2008**, *41*, 5582.

80. McCullough, R. D.; Ewbank, P. C.; Loewe, R. S. *J. Am. Chem. Soc.* **1997**, *119*, 633.

81. Zhang, Q.; Tour, J. M. *J. Am. Chem. Soc.* **1997**, *119*, 5065.

82. Zhang, Q. T.; Tour, J. M. *J. Am. Chem. Soc.* **1998**, *120*, 5355.

83. Devasagayaraj, A.; Tour, J. M. *Macromolecules* **1999**, *32*, 6425.

84. Hodgson, D. M.; Witherington, J.; Moloney, B. A.; Richards, I. C.; Braver. J. L. *Svnlett.* **1995**, 32.

85. Echavarren, A. M.; Stille, J. K. *J. Am. Chem. Soc.* **1987**, *109*, 5478.

86. Zhan, X.; Tan, Z.; Domercq, B.; An, Z.; Zhang, X.; Barlow, S.; Li, Y.; Zhu, D.; Kippelen, B.; Marder, S. R. *J. Am. Chem. Soc.* **2007**, *129*, 7246.

87. Liang, Y.; Feng, D.; Guo, J.; Szarko, J. M.; Ray, C.; Chen, L. X.; Yu, L. *Macromolecules* **2009**, *42*, 1091.

88. Bundgaard, E.; Krebs, F. C. *Macromolecules* **2006**, *39*, 2823.

89. Kimbrough, R. D. *Environmental Health Perspectives* **1976**, *14*, 51.

90. Miyaura, N.; Suzuki, A. *Chem. Rev.* **1995**, *95*, 2457.

91. Suzuki, A.; Brown, H. C. *Suzuki Coupling, Organic Syntheses via Boranes*. Aldrich Chemical Company: Milwaukee, **2003**; Vol. 3.

92. Suzuki, A. *J. Organomet. Chem.* **1999**, *576*, 147.

93. Iverson, C. N.; Smith, M. R. *J. Am. Chem. Soc.* **1999,** *121*, 7696.

94. Gronowitz, S.; Peters, D. *Heterocycles* **1990**, *30*, 645.

95. Brookins, R. N. Synthetic Routes to Novel Conjugated Polymers Based on Fluorene and Synthetic Analogues of Fluorene. Ph.D. Thesis, University of Florida, Gainesville, FL, **2008**.

96. Maryanoff, B. E.; Reitz, A. B.; Duhl-Emswiler, B. A. *J. Am. Chem. Soc.* **1985**, *107*, 217.

97. Vedejs, E.; Marth, C. F. *J. Am. Chem. Soc.* **1988**, *110*, 3940.

98. Yamataka, H.; Nagase, S. *J. Am. Chem. Soc.* **1998**, *120*, 7530.

99. Boucard, V.; Adès, D.; Siove, A.; Romero, D.; Schaer, M.; Zuppiroli, L. *Macromolecules* **1999**, *32*, 4729.

100. Thomas, C. A.; Zong, K.; Abboud, K. A.; Steel, P. J.; Reynolds, J. R. *J. Am.Chem. Soc.* **2004**, *126*, 16440.

101. Thompson, B. C.; Kim, Y.-G.; McCarley, T. D.; Reynolds, J. R. *J. Am. Chem. Soc.* **2006**, *128*, 12714.

102. Thompson, B. C.; Kim, Y.-G.; Reynolds, J. R. *Macromolecules* **2005**, *38*, 5359.

103. Galand, E. M.; Kim, Y.-G.; Mwaura, J. K.; Jones, A. G.; McCarley, T. D.; Shrotriya, V. S.; Yang, Y. Reynolds, J. R. *Macromolecules* **2006**, *39*, 9132.

104. Liu, J.; Zhou, Q.; Cheng, Y.; Geng, Y.; Wang, L.; Ma, D.; Jing, X.; Wang, F. *Adv. Funct. Mater.* **2006**, *16*, 957

105. Liang, Y.; Xiao, S.; Feng, D.; Yu, L. *J. Phys. Chem. C* **2008**, *112*, 7866.

106. Kline, R. J.; Mcgehee, M. D.; Kadnikova, E. N.; Liu, J.; Fréchet, J. M. J. *Adv. Mater.* **2003**, *15*, 1519.

107. Kline, R. J.; McGehee, M. D. *Journal of Macromolecular Science*, *Part C: Polymer Reviews* **2006**, *46*, 27.

108. Kline, R. J.; Mcgehee, M. D.; Kadnikova, E. N.; Liu, J.; Fréchet, J. M. J.; Toney, M. F. *Macromolecules* **2005**, *38*, 3312.

109. Bijleveld, J. C.; Zoombelt, A. P.; Mathijssen, S. G.; Wienk, M. M.; Turbiez, M.; de Leeuw, D.; Janssen, R. A. J. *J. Am. Chem. Soc.* **2009**, *131,* 16616.

110. Maturová, K.; van Bavel, S. S.; Wienk, M. M.; Janssen, R. A. J.; Kemerink, M. *Nano Lett.* **2009**, *9*, 3032.

111. Hoppe, H.; Niggemann, M.; Winder, C.; Kraut, J.; Hiesgen, R.; Hinsch, A.; Meissner, D.; Sariciftci, N. S. *Adv. Funct. Mater.* **2004**, *14*, 1005.

112. Chen, L.-M.; Xu, Z.; Hong, Z.; Yang, Y. *J. Mater. Chem.* **2010**, *20*, 2575.

113. Kaneto, K.; Yoshino, K.; Inuishi, Y. *Solid State Communcations* **1983**, *46*, 389.

114. Garnier, F.; Tourillon, G.; Gazard, M.; Dubois, J. C. *J. Electroanal.Chem.* **1983**, *148*, 299.

115. Druy, M. A.; Seymour, R. J. *Org. Coat. Appl. Polym. Sci. Proc.* **1983**, *48*, 561.

116. Roncali, J.; Blanchard, P.; Frère, P. *J. Mater. Chem.* **2005**, *15*, 1589.

117. Heywang, G.; Jonas, F. *Adv. Mater.* **1992**, *4*, 116.

118. Dietrich, M.; Heinze, J.; Heywang, G.; Jonas, F. *J. Electroanal. Chem.* **1994**, *369*, 87.

119. Reeves, B. D.; Grenier, C. R. G.; Argun, A. A.; Cirpan, A.; McCarley, T. D.; Reynolds, J. R. *Macromolecules* **2004**, *37*, 7559.

120. Dyer, A. L.; Craig, M. R.; Babiarz, J. E.; Kiyak, K.; Reynolds, J. R. *Macromolecules* **2010**, *43*, 4460.

121. Amb, C. M.; Dyer, A. L.; Reynolds, J. R. *Chem. Mater.* **2011**, *23*, 397.

122. Salzner, U. *J. Phys. Chem. B* **2002**, *106*, 9214.

123. Salzner, U.; Kose, M. E. *J. Phys. Chem. B* **2002**, *106*, 9221.

124. Karalt, O.; Durdağı, S.; Salzner, U. *J. Mol. Model.* **2006**, *12*, 687.

125. Sonmez, G.; Shen, C. K. F.; Rubin, Y.; Wudl, F. *Angew. Chem. Int. Ed.* **2004**, *43*, 1498.

126. Durmus, A.; Gunbas, G. E.; Camurlu, P.; Toppare, L. *Chem. Commun.* **2007**, 3246.

127. Beaujuge, P. M.; Ellinger, S.; Reynolds, J. R. *Adv. Mater.* **2008**, *20*, 2772.

128. Beaujuge, P. M.; Ellinger, S.; Reynolds, J. R. *Nat. Mater.* **2008**, *7*, 795.

129. Beaujuge, P. M. Spectral Engineering in π-Conjugated Organic Polymers. Ph.D. Thesis, University of Florida, Gainesville, FL, **2009**.

130. Beaujuge, P. M.; Chad, A. M.; Reynolds, J. R. *Accounts of Chemical Research* **2010**, *43*, 1396.

131. Gundlach, D. J. *Nat. Mater.* **2007**, *6*, 173.

132. Tang, C. W.; VanSlyke, S. A. *Appl. Phys. Lett.* **1987**, *51*, 913.

133. Horowitz, G. *Adv. Mater.* **1998**, *10*, 365.

134. Schubert, D. W.; Dunkel, T. *Materials Research Innovations* **2003**, *7*, 314.

135. Degarmo, E. P.; Black, J. T.; Kohser, R. A. *Materials and Processes in Manufacturing* 9th ed.; **2003**, Wiley

136. Dyer, A. L.; Thompson, E. J.; Reynolds, J. R. *ACS Appl. Mater. Interfaces* **2011**, *3*, 1787.

137. Mortimer, R. J.; Graham, K. R.; Grenier, C. R. G.; Reynolds, J. R. *ACS Appl. Mater. Interfaces* **2009**, *1*, 2269.

138. Garnier, F.; Hajlaoui, R.; Yassar, A.; Srivastava, P. *Science* **1994**, *265*, 1684.

139. Shaheen, S. E.; Radspinner, R.; Peyghambarian, N.; Jabbour, G. E. *Appl. Phys. Lett.* **2001**, *79*, 2996.

140. Holdcroft, S. *Adv. Mater.* **2001**, *13*, 1753.

141. Bao, Z.; Rogers, J. A.; Katz, H. E. *J. Mater. Chem.* **1999**, *9*, 1895.

142. Steiger, J.; Heun, S.; Tallant, N. J. *Imaging Sci. Technol.* **2003**, *47*, 473.

143. Yoshioka, Y.; Jabbour, G. E. *Synth. Met.* **2006**, *156*, 779.

144. De Gans, B.-J.; Duineveld, P. C.; Schubert, U. S. *Adv. Mater.* **2004**, *16*, 203.

145. Aernouts, T.; Aleksandrov, T.; Girotto, C.; Genoe, J.; Poortmans, J. *Appl. Phys. Lett.* **2008**, *92*, 033306.

146. Wengeler, L.; Schmidt-Hansberg, B.; Peters, K.; Scharfer, P.; Schabel, W. *Chemical Engineering and Processing* **2011**, *50*, 478.

147. Krebs, F. C.; Gevorgyan, S. A.; Alstrup, J. *Journal of Materials Chemistry* **2009**, *19*, 5442.

148. Blankenburg, L.; Schultheis, K.; Schache, H.; Sensfuss, S.; Schrödner, M. *Sol. Energy Mater. Sol. Cells* **2009**, *93*, 476.

149. Monk, P. M. S.; Mortimer, R. J.; Rosseinsky, D. R. *Electrochromism and electrochromic devices*; Cambridge University Press: Cambridge, **2007**.

150. Walczak, R. M.; Reynolds, J. R. *Adv. Mater.* **2006**, *18*, 1121.

151. Schwendeman, I.; Hwang, J.; Welsh, D. M.; Tanner, D. B.; Reynolds, J. R. *Adv. Mater.* **2001**, *13*, 634.

152. Chandrasekhar, P.; Zay, B. J.; Birur, G. C.; Rawal, S.; Pierson, E. A.; Kauder, L.; Swanson, T. *Adv. Funct. Mater.* **2002**, *12*, 95.

153. Dyer, A. L.; Grenier, C. R. G.; Reynolds, J. R. *Adv. Funct. Mater.* **2007**, *17*, 1480.

154. Tehrani, P.; Isaksson, J.; Mammo, W.; Andersson, M. R.; Robinson, N. D.; Berggren, M. *Thin Solid Films* **2006**, *515*, 2485.

155. Andersson, P.; Forchheimer, R.; Tehrani, P.; Berggren, M. *Adv. Funct. Mater.* **2007**, *17*, 3074.

156. Tehrani, P.; Hennerdal, L.-O.; Dyer, A. L.; Reynolds, J. R.; Berggren, M. *J. Mater. Chem.* **2009**, *19*, 1799.

157. Möller, M.; Asaftei, S.; Corr, D.; Ryan, M.; Walder, L. *Adv. Mater.* **2004**, *16*, 1558.

158. Chen, C.-Y.; Wang, M.; Li, J.-Y.; Pootrakulchote, N.; Alibabaei, L.; Ngocle, C.-H.; Decoppet, J.-D.; Tsai, J.-H.; Grätzel, C.; Wu, C.-G.; Zakeeruddin, S. M.; Grätzel, M. *ACS Nano* **2009**, *3*, 3103.

159. O'Regan, B.; Grätzel, M. *Nature* **1991**, *353*, 737.

160. Bach, U.; Lupo, D.; Comte, P.; Moser, J. E.; Weissörtel, F.; Salbeck, J.; Spreitzer, H.; Grätzel, M. *Nature* **1998**, *395*, 583.

161. Liang, Y. Y.; Feng, D. Q.;Wu, Y.; Tsai, S. T.; Li, G.; Ray, C.; Yu, L. P. *J. Am. Chem. Soc.* **2009**, *131*, 7792.

162. Li, G.; Shrotriya, V.; Huang, J. S.; Yao, Y.; Moriarty, T.; Emery, K.; Yang, Y. *Nat. Mater.* **2005**, *4*, 864.

163. Park, S. H.; Roy, A.; Beaupre, S.; Cho, S.; Coates, N.; Moon, J. S.; Moses, D.; Leclerc, M.; Lee, K.; Heeger, A. J. *Nat. Photonics* **2009**, *3*, 297.

164. Chu, T.-Y.; Lu, J.; Beaupr_e, S.; Zhang, Y.; Pouliot, J.-R.; Wakim, S.; Zhou, J.; Leclerc, M.; Li, Z.; Ding, J.; Tao, Y. *J. Am. Chem. Soc.* **2011**, *133*, 4250.

165. Price, S. C.; Stuart, A. C.; Yang, L.; Zhou, H.; You, W. *J. Am. Chem. Soc.* **2011**, *133*, 4625.

166. Olson, D. C.; Lee, Y.-J.; White, M. S.; Kopidakis, N.; Shaheen,S. E.; Ginley, D. S.; Voigt, J. A.; Hsu, J. W. P. *J. Phys. Chem. C* **2007**, *111*, 16640 .

167. Yu, G.; Gao, J.; Hummelen, J. C.; Wudl, F.; Heeger, A. J. *Science* **1995**, *270*, 1789.

168. Zhan, G.; He, Y.; Li, Y. *Adv. Mater.* **2010**, *22*, 4355.

169. Chen, H.-Y.; Hou, J.; Zhang, S.; Liang, Y.; Yang, G.; Yang, Y.; Yu, L.; Wu, Y.; Li, G. *Nat. Photonics* **2009**, *3*, 649.

170. Liang, Y.; Xu, Z.; Xia, J.; Tsai, S.-T.; Wu, Y.; Li, G.; Ray, C.; Yu, L. *Adv. Mater*. **2010**, *22*, E135.

171. Son, H. J.; Wang, W.; Xu, T.; Liang, Y.; Wu, Y.; Li, G.; Yu, L. *J. Am. Chem. Soc.* **2011**, *133*, 1885.

172. Zhou, H.; Yang, L.; Stuart, A. C.; Price, S. C.; Liu, S.; You, W. *Angew. Chem. Int. Ed.* **2011**, *50*, 2995.

173. Amb, C. M.; Chen, S.; Graham, K. R.; Subbiah, J.; Small, C. E.; So, F.; Reynolds, J. R. *J. Am. Chem. Soc.* **2011**, *133*, 10062.

174. Armarego, W. L. F.; Chai, C. L. L. *Purification of Laboratory Chemicals, 5th Edition*; ELSEVIER, **2003**.

175. Bard, A. J.; Faulkner, L. R. *Electrochemical Methods: Fundamentals and Applications*, 2nd Ed.; Wiley: New York, **2001**.

176. Brett, C. M. A.; Brett, A. M. O. *Electrochemistry, Principles, Methods, and Applications*; Oxford University: Oxford, **1993**.

177. Irvin, J. A. A. Low Oxidation Potential Electroactive Polymers. Ph.D. Thesis, University of Florida, Gainesville, FL, **1998**.

178. Thomas, C. A. Donor-Acceptor Methods for Band Gap Reduction in Conjugated Polymers: The Role of Electron Rich Donor Heterocycles. Ph.D. Thesis, University of Florida, Gainesville, FL, **2002**.

179. Galand, E. M. Processable Variable Band Gap Conjugated Polymers for Optoelectronic Devices Ph.D. Thesis, University of Florida, Gainesville, FL, **2006**.

180. Barry C. T. Variable Bandgap Poly(3,4-alkylenedioxythiophene)-Based Polymers for Photovoltaic and Electrochromic Applications, Ph.D. Thesis, University of Florida, Gainesville, FL, **2005**

181. Cardona, C. M.; Li, W.; Kaifer, A. E.; Stockdale, D.; Bazan, G. C. *Adv. Mater.* **2011**, *23*, **2367**.

182. Graham, K. R. Morphology Control in Polymer Light Emitting Diodes and Molecular Bulk-Heterojunction Photovoltaics Ph.D. Thesis, University of Florida, Gainesville, FL, **2011**.

183. Monk, P.M.S.; Mortimer, R.J.; Rosseinsky, D. R. *Electrochromism:Fundamentals and Applications*, VCH, Weinheim, **1995**.

184. Granqvist, C.G. *Handbook of Inorganic Electrochromic Materials*, Elsevier, Amsterdam, **1995**.

185. Habib, M. A. *Electrochem. Transition* **1992**, 51.

186. Monk, P.M.S*.; The Viologens: Physicochemical Properties, Synthesis and Applications of the Salts of 4,40-Bipyridine*, J. Wiley & Sons, Chichester, **1998**.

187. Rosseinsky, D. R.; Mortimer, R. J. *Adv. Mater.* **2001**, *13*, 783.

188. Cutler, C. A.; Bouguettaya, M.; Kang, T. S.; Reynolds, J. R. *Macromolecules* **2005**, *38*, 3068.

189. Gunbas, G. E.; Durmus, A.; Toppare, L. *Adv. Mater.* **2008**, *20*, 691

190. Sonmez, G. *Chem. Commun*. **2005**, *42*, 5251.

191. Gazard, M.; Dubois, J. C.; Champagne, M.; Garnier, F.; Tourillon, G. *J. Phys. Colloq.* **1983**, *44*, 537.

192. Aizawa, M.; Watanable, S.; Shinohara, H.; Shirakawa, H. *J. Chem. Soc., Chem. Commun.* **1985**, *5*, 264.

193. Diaz, A. F.; Castillo, J. I.; Logan, J. A.; Lee, W.-Y. *J. Electroanal. Chem.* **1981**, *129*, 115.

194. Diaz, A. F.; Castillo, J.; Kanazawa, K. K.; Logan, J. A.; Salmon, M.; Fajardo, O. *J. Electroanal. Chem.* **1982**, *133*, 233.

195. Amb, C. M.; Kerszulis, J. A.; Thompson, E. J.; Dyer, A. L.; Reynolds, J. R. *Polymer Chemistry* **2011**, *2*, 812.

196. Welsh, D. M.; Kloeppner, L. J.; Madrigal, L.; Pinto, M. R.; Thompson, B. C.; Schanze, K. S.; Abboud, K. A.; Powell, D.; Reynolds, J. R. *Macromolecules* **2002**, *35*, 6517.

197. Amb, C. M.; Beaujuge, P. M.; Reynolds, J. R. *Adv. Mater.* **2010**, *22*, 724.

198. Icli, M.; Pamuk, M.; Algi, F.; Önal, A. M.; Cihaner, A. *Org. Elec.* **2010**, *11*, 1255.

199. Delnoye, D. A. P.; Sybesma, R. P.; Vekemans, J. A. J. M.; Meijer, E. W. *J. Am. Chem. Soc.* **1996**, *118*, 8717.

200. Zou, Y.; Hou, J.; Yang, C.; Li, Y. *Macromolecules* **2006**, *39*, 8889.

201. Yue, W.; Zhao, Y.; Tian, H.; Song, D.; Xie, Z.; Yan, D.; Geng, Y.; Wang, F. *Macromolecules* **2009**, *42*, 6510.

202. Shi, P.; Amb, C. M.; Knott, E. P.; Thompson, E. J.; Liu, D. Y.; Mei, J.; Dyer, A. L.; Reynolds, J. R. *Adv. Mater.* **2010**, *22*, 4949.

203. DaSilveira Neto, B. A.; Lopes, A. S. A.; Ebeling, G. R.; Goncalves, S.; Costa, V. E. U.; Quina, F. H.; Dupont, J. *Tetrahedron* **2005**, *61*, 10975.

204. Bates, R. E.; Kroposki, L. M.; Potter, D. E. *J. Org. Chem.* **1972**, *37*, 560.

205. Clayden, J.; Yasin, S. A. *New J. Chem.* **2002**, *26*, 191

206. Tomboulian, P.; Amick, D.; Beare, S.; Dumke, K.; Hart, D.; Hites, R.; Metzger, A.; Nowak, R. *J. Org. Chem.* **1973**, *38*, 322.

207. Bartlett, P. A.; Meadows, J. D.; Ottow, E. *J. Am. Chem. Soc.* **1984**, *106*, 5304

208. Stanetty, P.; Mihovilovic, M. D. *J. Org. Chem.* **1997**, *62*, 1514.

209. Burroughes, J. H.; Bradley, D. D. C.; Brown, A. R.; Marks, R. N.; Mackay, K.; Friend, R. H.; Burn, P. L.; Holmes, A. B. *Nature* **1990**, *347*, 539.

210. Braun, D.; Heeger, A. J. *Appl. Phys. Lett.* **1991**, *58*, 1982.

211. Bernius, M. T.; Inbasekaran, M.; O'Brien, J.; Wu, W. *Adv. Mater.* **2000**, *12*, 1737.

212. Scharber, M. C.; Mühlbacher, D.; Koppe, M.; Denk, P.; Waldauf, C.; Heeger, A. J.; Brabec, C. J. *Adv. Mater*. **2006**, *18*, 789.

213. Tsao, H. N.; Cho, D.; J. Andreasen, W.; Rouhanipour, A.; Breiby, D. W.; Pisula, W.; Müllen, K. *Adv. Mater.* **2009**, *21*, 209.

214. Sonar, P.; Singh, S. P.; Li, Y.; Soh, M. S.; Dodabalapur, A. *Adv. Mater.* **2010**, *22*, 5409.

215. Balan, A.; Gunbas, G.; Durmus, A.; Toppare, L. *Chem. Mater*. **2008**, *20*, 7510.

216. Bayer AG, European Patent 339 340, **1988**.

217. Groenendaal, L. B.; Jonas, F.; Freitag, D.; Pielartzik, H.; Reynolds, J. R. *Adv. Mater.* **2000**, *12*, 481.

218. Welsh, D. M.; Kumar, A.; Meijer, E. W.; Reynolds, J. R. *Adv. Mater.* **1999**, *11*, 1379.

219. Patil, O.; Ikenoue, Y.; Wudl, F.; Heeger, A. J. *J. Am. Chem. Soc.* **1987**, *109*, 1858.

220. Sundaresan, N. S.; Basak, S.; Pomerantz, M.; Reynolds, J. R. *J. Chem. Soc.*, *Chem. Commun.* **1987**, 621.

221. Stéphan, O.; Schottland, P.; Le Gall, P.-Y.; Chevrot, C.; Carrier, M. M. *J. Electroanal. Chem.* **1998**, *443*, 217.

222. Krishnamoorthy, K.; Kanungo, M.; Ambade, A. V.; Contractor, A. Q.; Kumar, A. *Synth. Met.* **2002**, *125*, 441.

223. Zotti, G.; Zecchin, S.; Schiavon, G.; Groenendaal, L. B. *Macromol. Chem. Phys.* **2002**, *203*, 1958.

224. Ho, H. A.; Boissinot, M.; Bergeron, M. G.; Corbeil, G.; Doré, K.; Boudreau, D.; Leclerc, M. *Angew. Chem. Int. Ed.* **2002**, *41*, 1548.

225. Liu, B.; Bazan, G. C.; *J. Am. Chem. Soc.* **2004**, *126*, 1942.

226. McQuade, D. T.; Hegedus, A. H.; Swager, T. M. *J. Am. Chem. Soc.* **2000**, *122*, 12389.

227. Brookins, R. N.; Schanze, K. S.; Reynolds, J. R. *Macromolecules* **2007**, *40*, 3524.

228. Jiang, H.; Taranekar, P.; Reynolds, J. R.; Schanze, K. S. *Angew. Chem. Int. Ed.* **2009**, *48*, 4300.

229. Thomas III, S. W.; Joly, G. D.; Swager, T. M. *Chem. Rev.* **2007**, *107*, 1339.

230. Qin, C.; Wong, W.-H.; Wang, L. *Macromolecules* **2011**, *44*, 483.

231. Wu, H.; Huang, F.; Mo, Y.; Yang, W.; Wang, D.; Peng, J.; Cao, Y. *Adv. Mater.* **2004**, *16*, 1826.

232. Ma, W.; Iyer, P. K.; Gong, X.; Liu, B.; Moses, D.; Bazan, G. C.; Hegger, A. J. *Adv. Mater.* **2005**, *17*, 274.

233. Garcia, A.; Yang, R.; Jin, Y.; Walker, B.; Nguyen, T.-Q. *Appl. Phys. Lett.* **2007**, *91*, 153502.

234. Garcia, A.; Bakus II, R. C.; Zalar, P.; Hoven, C. V.; Brzezinski, J. Z.; Nguyen, T.-Q. *J. Am. Chem. Soc.* **2011**, *133*, 2492.

235. Stasio, F. D.; Korniychuk, P.; Brovelli, S.; Uznanski, P.; McDonnell, S. O.; Winroth, G.; Anderson, H. L.; Tracz, A.; Cacialli, F. *Adv. Mater.* **2011**, *23*, 1855.

236. Kim, S.; Jackiw, J.; Robinson, E.; Schanze, K. S.; Reynolds, J. R.; Baur, J.; Rubner, M. F.; Boils, D. *Macromolecules* **1998**, *31*, 964.

237. Culter, C. A.; Bouguettaya, M.; Reynolds, J. R. *Adv. Mater.* **2002**, *14*, 684.

238. Jain, V.; Sahoo, R.; Mishra, S. P.; Sinha, J.; Montazami, R.; Yochum, H. M.; Heflin, J. R.; Kumar, A. *Macromolecules* **2009**, *42*, 135.

239. Beaujuge, P. M.; Amb, C. M.; Reynolds, J. R. *Adv. Mater.* **2010**, *22*, 5383.

240. Wu, C.-G.; Lu, M.-I.; Chang, S.-J.; Wei, C.-S. *Adv. Funct. Mater*. **2007**, *17*, 1063.

241. Inouye, M.; Fujimoto, K.; Furusyo, M.; Nakazumi, H. *J. Am. Chem. Soc.* **1999**, *121,* 1452.

242. Liu, D. Y.; Chilton, A. D.; Shi, P.; Craig, M. R.; Miles, S. D.; Dyer, A. L.; Ballarotto, V. W.; Reynolds, J. R. *Adv. Funct. Mater*. **2011**, accepted.

243. Green, M. A.; Emery, K.; Hishikawa, Y.; Warta, W. *Prog. Photovoltaics* **2011**, *19*, 84.

244. http://www.konarka.com

245. http://www.solarmer.com

246. Bundgaard, E.; Krebs, F. *Sol. Energy Mater. Sol. Cells* **2007**, *91*, 954.

247. Schlinsky, P.; Waldauf, C.; Brabec, C. J. *Appl. Phys. Lett.* **2002**, *81*, 3885.

248. Svensson, M.; Zhang, F.; Veenstra, S. C.; Verhees, W. J. H.; Hummelen, J. C.; Kroon, J. M.; Ingana¨s, O.; Andersson, M. R. *Adv. Mater.* **2003**, *15*, 988.

249. Wang, E.; Wang, L.; Lan, L.; Luo, C.; Zhuang, W.; Peng, J.; Cao, Y. *Appl. Phys. Lett.* **2008**, *92*, 033307.

250. Mihailetchi, V. D.; Koster, L. J. A.; Blom, P. W. M.; Melzer, C.; deBoer, B.; van Duren, J. K. J.; Janssen, R. A. J. *Adv. Funct. Mater.* **2005***, 15,* 795*.*

251. Ong, K.-H.; Lim, S.-L.; Tan, H.- S.; Wong, H.-K.; Li, J.; Ma, Z.; Moh, L. C. H.; Lim, S.-H.; de Mello, J. C.; Chen, Z.-K. *Adv. Mater.* **2011**, *23*, 1409.

252. Mihailetchi, V.; Wildeman, J.; Blom, *P. Phys. Rev. Lett.* **2005**, *94*, 126602.

253. Lee, J. K.; Ma, W. L.; Brabec, C. J.; Yuen, J.; Moon, J. S.; Kim, J. Y.; Lee, K.; Bazan, G. C.; Heeger, A. J. *J. Am. Chem. Soc.* **2008**, *130*, 3619.

254. van Bavel, S.; Veenstra, S.; Loos, J. *Macromol. Rapid Commun.* **2010**, *31*, 1835.

255. Moulé, A. J.; Meerholz, K. *Adv. Funct. Mater.* **2009**, *19*, 3028.

256. Peet, J.; Kim, J. Y.; Coates, N. E.; Ma, W. L.; Moses, D.; Heeger, A. J.; Bazan, G. C. *Nat. Mater.* **2007**, *6*, 497.

257. Zhou, E.; Nakamura, M.; Nishizawa, T.; Zhang, Y.; Wei, Q.; Tajima, K.; Yang, C.; Hashimoto, K. *Macromolecules* **2008**, *41*, 8302.

258. Zhu, Z.; Waller, D.; Gaudiana, R.; Morana, M.; Muehlbacher, D.; Scharber, M.; Brabec, C. *Macromolecules* **2007**, *40*, 1981.

259. Piliego, C.; Holcombe, T. W.; Douglas, J. D.; Woo, C. H.; Beaujuge, P. M.; Fréchet, J. M. J. *J. Am. Chem. Soc.* **2010**, *132*, 7595.

260. Kim, J. Y.; Lee, K.; Coates, N. E.; Moses, D.; Nguyen, T.-Q.; Dante, M.; Heeger, A. J. *Science* **2007**, *317*, 222.

261. Chou, C. H.; Kwan, W. L.; Hong, Z. R.; Chen, L. M.; Yang, Y. *Adv. Mater.* **2011**, *23*, 1282.

262. Yang, J.; Zhu, R.; Hong, Z. R.; He, Y. J.; Kumar, A.; Li, Y. F.; Yang, Y. *Adv. Mater.* **2011**, *23*, 3465.

263. Gilot, J.; Wienk, M. M.; Janssen, R. A. J. *Adv. Funct. Mater.* **2010**, *20*, 3904.

264. Yang, J.; You, J.; Chen, C.-C.; Hsu, W.-C.; Tan, H.-R.; Zhang, X. W.; Hong, Z.; Yang, Y. *ACS Nano*, **2011**, *5*, 6210.

265. Peet, J.; Tamayo, A. B.; Dang, X.-D.; Seo, J. H.; Nguyen, T.-Q. *Appl. Phys. Lett.* **2008**, *93*, 163306.

266. Honda, S.; Nogami, T.; Ohkita, H.; Benten, H.; Ito, S. *ACS Appl. Mater. Interfaces*, **2009**, *1*, 804.

267. Dastoor, P. C.; McNeill, C. R.; Frohne, H.; Foster, C. J.; Dean, B.; Fell, C. J.; Belcher, W. J.; Campbell, W. M.; Officer, D. L.; Blake, I. M.; Thordarson, P.; Crossley, M. J.; Hush, N. S.; Reimers, J. R. *J. Phys. Chem. C* **2007**, *111*, 15415.

268. Kaulach, I.; Muzikante, I.; Gerca, L.; Plotniece, M.; Roze, M.; Kalnachs, J.; Shlihta, G.; Shipkovs, P.; Kampars, V.; Tokmakov, A. *Eur. Phys. J. Appl. Phys.* **2007**, *40*, 169.

269. Hao, Z.; Iqbal, A. *Chem. Soc. Rev.* **1997**, *26,* 203.

270. Tieke, B.; Rabindranath, A. R.; Zhang, K.; Zhu, Y. *Beilstein J. Org. Chem.* **2010**, *6,* 830.

271. Zhu, Y.; Heim, I.; Tieke, B. *Macromol. Chem. Phys.* **2006**, *207, 2*206.

272. Kanimozhi, C.; Baljaru, D.; Sharma, G. D.; Patil, S. *J. Phys. Chem. C* **2010**, *114,* 3287.

273. Zhou, E.; Wei, Q.; Yamakawa, S.; Zhang, Y.; Tajima, K.; Yang, C.; Hashimoto, K. *Macromolecules* **2010**, *43,* 821.

274. Li, Y.; Singh, S. P.; Sonar, P. *Adv. Mater.* **2010**, *22*, 4862.

275. Cho, S.; Lee, J.; Tong, M.; Seo, J. H.; Yang, C. *Adv. Funct. Mater.* **2011**, *21*, 1910.

276. Woo, C. H.; Beaujuge, P. M.; Holcombe, T. W.; Lee, O. P.; Fréchet, J. M. J. *J. Am. Chem. Soc.* **2010**, *132*, 15547.

277. Khlyabich, P. P.; Burkhart, B.; Ng, C. F.; Thompson, B. C. *Macromolecules*, **2011**, *44*, 5079.

278. Li, J.; Ong, K.-H.; Lim, S.-L.; Ng, G.-M.; Tan, H.-S.; Chen, Z.-K. *Chem. Commun.* **2011**, *47*, 9480.

279. Hou, J.; Park, M.-H.; Zhang, S.; Yao, Y.; Chen, L.-M.; Li, J.-H.; Yang, Y. *Macromolecules* **2008**, *41*, 6012.

280. Kroon, R.; Lenes, M.; Hummelen, J. C.; Blom, P. W. M.; Boer, B. *Polym. Rev.* **2008**, *48*, 531.

281. Dyakonov, V.; Zoriniants, G.; Scharber, M.; Brabec, C. J.; Janssen, R. A. J.; Hummelen, J. C.; Sariciftci, N.S. *Phys. Rev. B* **1999**, *59*, 8019.

282. Al-Ibrahim, M.; Roth, H. K.; Schroedner, M.; Konkin, A.; Zhokhavets, U.; Gobsch, G.; Scharff, P.; Sensfuss, S. *Org. Electron.* **2005**, *6*, 65.

283. Trotzky, S.; Hoyer, T.; Tuszynski, W; Lienau C; Parisi, J. *J. Phys. D: Appl. Phys.* **2009**, *42*, 055105.

284. Wang, J.; Wang, D.; Moses, D.; Heeger, A. J. *J. Appl. Polym. Sci.* **2011**, *82*, 2553.

285. Zhang, F.; Jespersen, K. G.; Björström, C.; Svensson, M.; Andersson, M. R.; Sundström, V.; Magnusson, K.; Moons, E.; Yartsev, A.; Inganäs, O. *Adv. Funct. Mater.* **2006**, *16*, 667.

286. Wienk, M. M.; Kroon, J. M.; Verhees, W. J. H.; Knol, J.; Hummelen, J. C.; Hal, P. A. V.; Janssen, R. A. J. *Angew. Chem. Int. Ed.* **2003**, *42*, 3371.

BIOGRAPHICAL SKETCH

Pengjie Shi was born in Changchun, China, in 1980. He graduated with his B.S. in chemistry from the University of Science and Technology of China in 2004, where he worked in the research group of Prof. Caiyuan Pan in the field of living free-radical polymerization and block copolymers design. In 2005, Pengjie moved to Gainesville, Florida to pursue his Ph.D. under the guidance of Prof. John R. Reynolds. His research has been focused on the synthesis and characterization of discrete π-conjugated oligomers and polymers for optoelectronic devices. Pengjie earned his doctoral degree from the University of Florida in the fall 2011. He will work as a R&D scientist (polymer synthesis) at Sigma-Aldrich.